

IIT RESEARCH INSTITUTE
Technology Center
Chicago, Illinois 60616

AD 636048

Summary of Research Report
IITRI Project No. M6064 (3)

ENTRANCEWAYS AND EXITS FOR BLAST-RESISTANT
FULLY-BURIED PERSONNEL SHELTERS

Distribution of this document is unlimited.

This report has been reviewed in the Office of Civil Defense and approved for publication. Approval does not signify that the contents necessarily reflect the views and policies of the Office of Civil Defense.

by

J. D. Stevenson
J. A. Havers

for

Office of Civil Defense
Department of the Army - OSA
Under
Contract No. OCD-PS-64-50
Subtask 1152-E

September 1965

IITRI Project No. M6064 (3)
Final Report

Contract No. OCD-PS-64-50 Subtask 1152-E
ENTRANCEWAYS AND EXITS FOR BLAST-
RESISTANT FULLY-BURIED PERSONNEL
SHELTERS

Distribution of this document is unlimited.

for

Office of Civil Defense - Washington 25, D. C.

ENTRANCEWAYS AND EXITS FOR BLAST-RESISTANT
FULLY-BURIED PERSONNEL SHELTERS

SUMMARY

INTRODUCTION

The work reported in this study is a continuation of the Total Shelter Design Optimization series which, under OCD sponsorship, is currently in progress at the IIT Research Institute. These studies have developed the design requirements and identified in-place costs for single-purpose, fully-buried personnel shelters of 100, 500 and 1000-man capacities. The attack environment, for analytical purposes, is described by a megaton yield ($W = 1$ to 100 MT) nuclear explosion and by side-on surface overpressures of 10 to 200 psi. Reports issued to date in this series have included the following:

- (1) "Structural Materials for Hardened Personnel Shelters," by John A. Havers, Contract No. OCD-PS-62-66, Subtask 1151-A, IIT Research Institute, December 1963.
- (2) "Structural Cost Studies for Hardened Shelters," by John A. Havers and Jerry J. Lukes, Contract No. OCD-PS-64-50, Subtask 1152-E, IIT Research Institute, January 1965.
- (3) "Entranceways and Exits for Blast-Resistant Fully-Buried Personnel Shelters," by John D. Stevenson, and John A. Havers, Contract No. OCD-PS-64-50, Subtask 1152-E, IIT Research Institute, September 1965.
- (4) "An Investigation of Minimal Equipment Needs in Personnel Shelters," by John A. Havers, Claire B. Monk, Jr. and Erich H. Koeller, Contract No. OCD-PS-64-50. Subtask 1216-A, (in publication).

In the two earlier studies of this series, structural design and cost data were developed for fully-buried personnel shelters of 100-man, 500-man and 1000-man capacities. These related studies supplied the in-place structural cost for each shelter capacity as a function of the design over-pressure, but did not include any detailed consideration of suitable entranceways to serve the shelters. This report extends the scope of the earlier studies by investigating the design requirements and structural costs for shelter entranceways.

IIT RESEARCH INSTITUTE

The possible types of shelter entranceways and exits include various stairways, ramps, slides, elevators, etc. The preferred type of entranceway and exit for each shelter is influenced by the operational requirements (physical condition of shelterees and permissible time for loading the shelters, etc.) the availability of real estate, excavation costs, location of shelter relative to the ground surface and the natural topography. The entranceway layout examined in this study consists of conventional stairways and connecting corridors. Assuming its survival following a nuclear explosion, such a layout would obviously be equally suitable as an exit. Consideration is also given to an emergency type of exit, where a vertical tube is used to connect the shelter with the ground surface. This exit would be protected from surface explosion effects by a removable cover and by a layer of soil.

The fully-buried shelter configurations which were examined in the earlier optimization studies have included the rectangular cubicle, the 180 deg arch and the 360 deg cylinder, the 180 deg dome and the 360 deg sphere. Each such shelter is designed to protect its occupants from all anticipated adverse effects associated with the postulated level of nuclear explosion. Table S-1 lists those features of the optimum shelters which are pertinent to the layout and radiation design of their associated entranceway structures.

The entranceways and exits are designed to service these minimum structural-cost shelters and must similarly be able to withstand the destructive effects of 1-100 MT explosions at ground ranges characterized by surface overpressures of 10 to 200 psi. The capacity of an entranceway must also be consistent with the shelter size and with the time available for loading the shelter. This latter requirement dictates the number of traffic lanes and/or entranceway structures. Table S-2 lists the minimum dimensional requirements, excluding minor provisions for doorways and jambs, which are considered to be applicable to interior portions of the entranceway.

Table S-1

**PARAMETERS OF OPTIMUM SHELTERS WHICH ARE PERTINENT
TO ENTRANCEWAY DESIGN**

Capacity	Static Equivalent Design Pressure (psi)	Type*	Length (ft)	Width (ft)	Depth to Entrance Level (ft)	Effective Depth of Earth Cover (ft)
100 Man	10	1 St. Cubicle	40	23	12.1	3.5
	50	1 St. Cubicle	30	30	13.3	4.5
	100	1 St. Cubicle	30	30	15.0	5.5
	200	1 St. Cylinder	65	15	17.8	7.5
	325	1 St. Cylinder	65	15	20.3	10.0
500 Man	10	1 St. Cubicle	74	60	12.1	3.5
	50	1 St. Cubicle	74	60	13.3	4.5
	100	2 St. Cylinder	155	20	14.5	5.5
	200	2 St. Cylinder	155	20	16.5	7.5
	325	2 St. Cylinder	155	20	19.0	10.0
1000 Man	10	1 St. Cubicle	111	78	12.1	3.5
	50	1 St. Cubicle	96	90	13.3	4.5
	100	2 St. Cylinder	289	20	14.5	5.5
	200	2 St. Cylinder	289	20	16.5	7.5
	325	2 St. Cylinder	289	20	19.0	10.0

* Note: The 10 psi level shelters are structural steel frames. All other shelters consist of reinforced concrete construction. "St." refers to "story."

Table S-2
DIMENSIONAL CRITERIA FOR ENTRANCEWAY TRAFFIC LANES

Entranceway Element	One-Lane		Two-Lane		Four-Lane	
	Width	Height	Width	Height	Width	Height
Stairway	2'-6"	7'-0"	3'-8"	7'-0"	7'-4"	8'-0"
Door	1'-10"	6'-6"	3'-8"	6'-6"	7'-4"	6'-6"
Corridor	2'-6"	7'-0"	3'-8"	7'-0"	7'-4"	8'-0"

Stairway riser and run dimensions are limited to a maximum of 7 3/4 in. for the riser and a minimum of 9-1/2 in. for the run. The maximum elevation difference between landings is limited to 8 ft-6 in. except where blast attenuation requirements necessitate a greater height difference. Landing widths are restricted to a minimum of 1 ft-7 in.

The major design emphasis is given to prestressed and reinforced concrete structural elements. Structural steel plate is used in design applications where large plastic deformation is permitted or where structural integrity between elements is desired without the transferral of large bending stresses. Structural steel shapes are used in such functional applications as the support channels for the blast door, and are also proposed in instances where weight or dimensional limitations require the substitution of structural steel for a reinforced concrete member. Prestressed concrete elements are used extensively in the blast-resistant portions of the entranceway, since this composite material has the capability of carrying both tension and compression loading in a stress reversal cycle.

FINDINGS

For both blast and nonblast-resistant structures, the total cost of the entranceway systems can be subdivided into three basic areas. The percentage of total entranceway cost which is represented by each of these areas will then be found to remain fairly constant for all entranceway configurations and for all pressure ranges. The first of these cost areas, which is associated with the basic requirement for blast protection will account for 55 to 60 percent of the total entranceway cost. System components in this area will include the transition and blast sections as well as the blast door, door hardware and door

IIT RESEARCH INSTITUTE

support items. The second cost area which can be correlated with ionizing radiation protection, will represent some 22 to 27 percent of the total cost. Included items in this category are the radiation sections themselves plus any supplementary barrier shielding. Finally, the remaining 15 to 20 percent of the total entranceway cost can be allocated to site preparation, including excavation and slope stabilization, and to such necessary functional elements as stairs and emergency exits.

The explicit findings of this study are summarized by plotting in-place structural cost as a function of design pressure. The resulting plots are shown in Fig. S-1 and S-2. In general, the tension cubicle represents the least-cost entranceway design in the low pressure loading range ($p_{go} < 25$ psi), while the compression cylinder dominates in the middle and high overpressure ranges. The actual cross-over point between the cubicle and cylinder seems to be dependent on the requirements for entranceway capacity. In most cases, the compression sphere costs closely parallel the compression cylinder costs.

With this information, together with the data presented in Table S-1, the optimum shelter entranceway system can be matched with the corresponding optimum shelter for a particular shelter capacity and design pressure. Fig. S-3 presents the cost per sheltered occupant of the optimum entranceway system for least-structural-cost shelters of 100-500-1000 man capacity. In preparing this figure, the combination of entranceway lane designs which is used with each particular shelter is based on a rated traffic capacity of 250 persons per lane. A 1000 -man shelter capacity would thus require four one-lane entranceway structures or two two-lane entranceways. It is further postulated that shelter systems with capacities greater than 500 persons will require a minimum of two separate entranceways in addition to any emergency exits which may be provided.

The results of this study indicate that entrance systems which are adequate for buried shelters of 100-500 and 1000-man capacities and for overpressure ranges of 10 to 200 psi can be provided at an additional cost of between 25 to 40 percent of the structural cost of the basic shelter. It has also been established that an a priori knowledge of the shelter which is to be serviced is necessary input if optimum entranceway designs are to be realized.

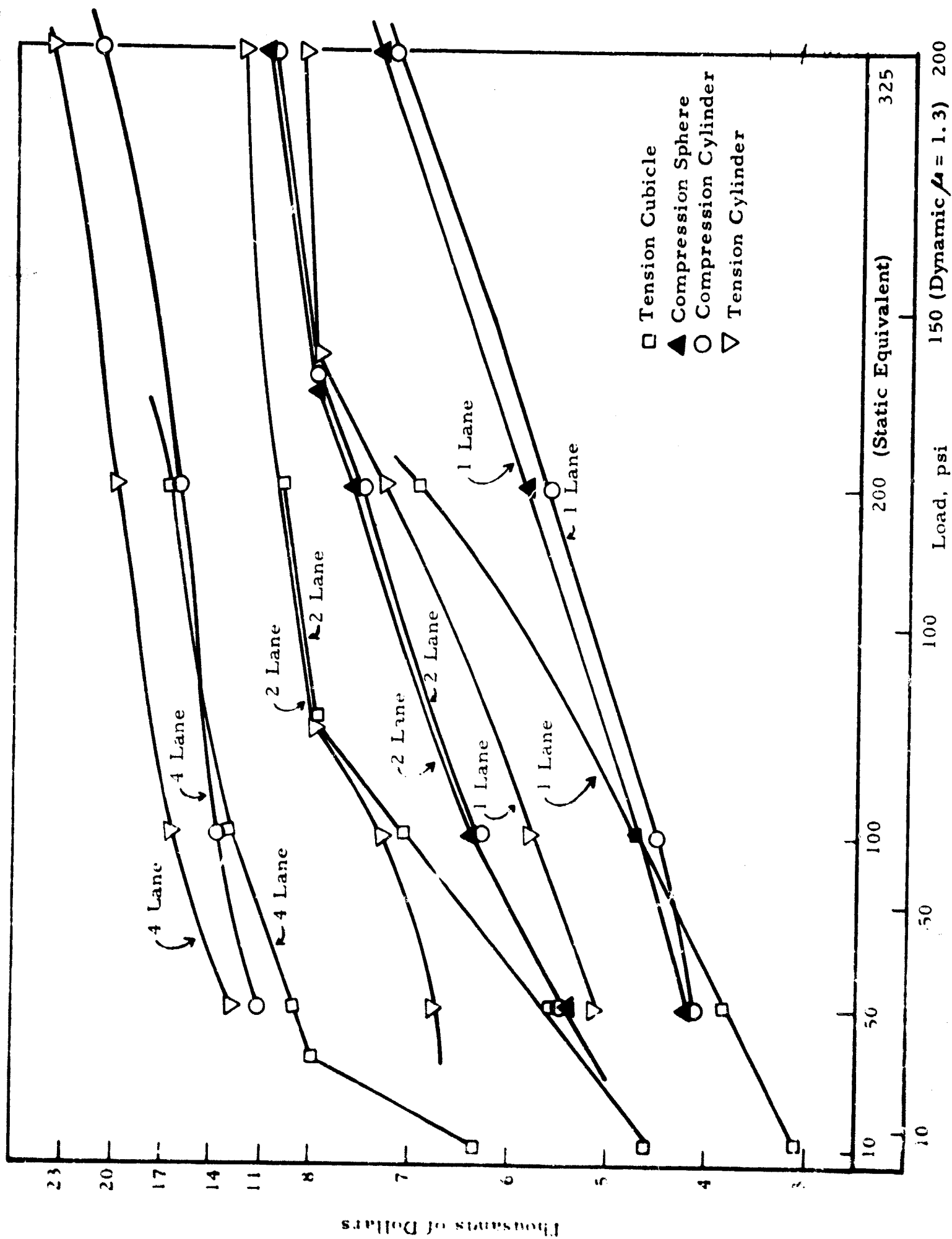


Fig. S-1 IN-PLACE COST FOR BLAST-RESISTANT ENTRANCEWAYS

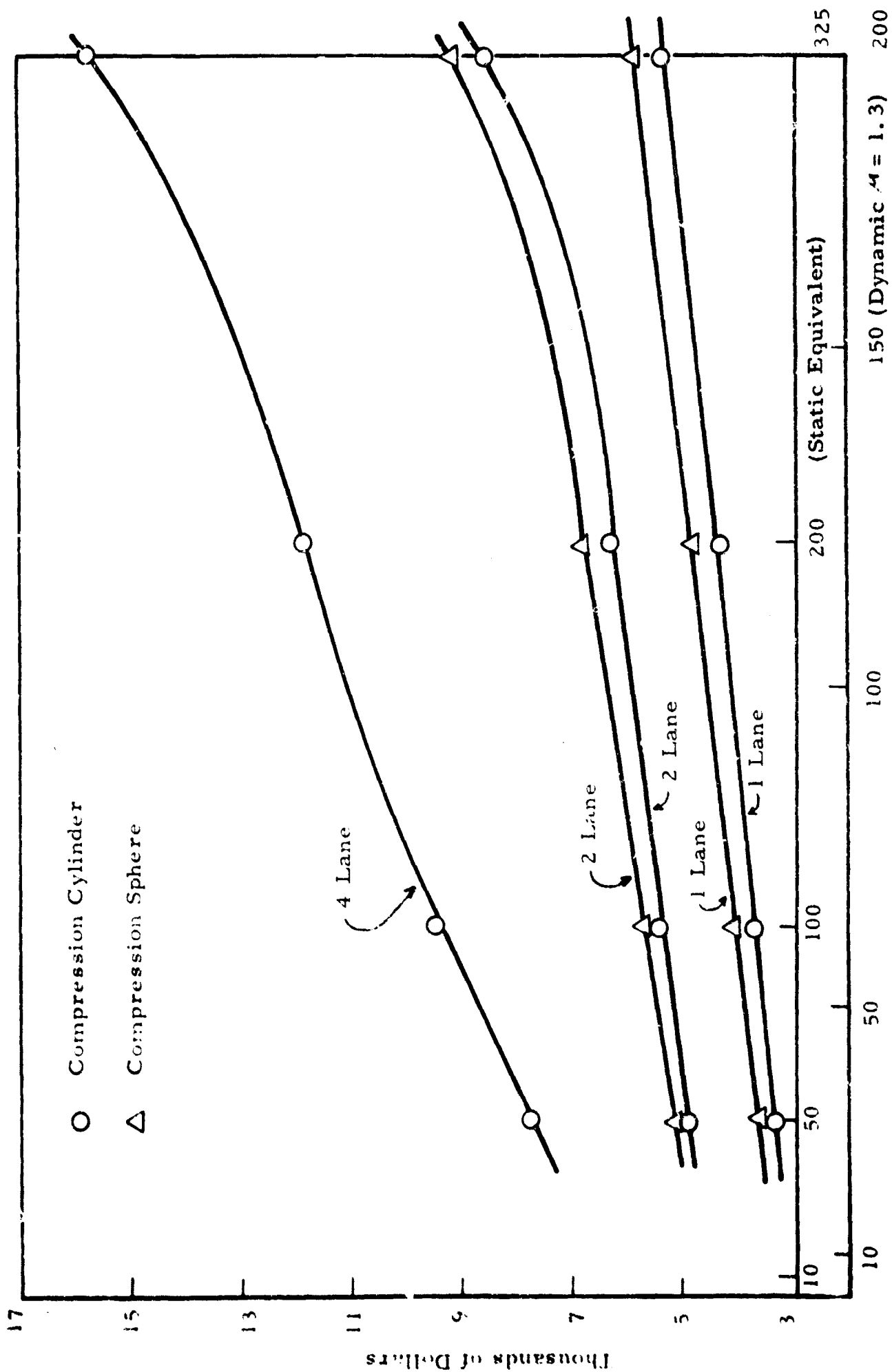


Fig. S-2 IN-PLACE COST FOR NONBLAST-RESISTANT ENTRANCEWAYS

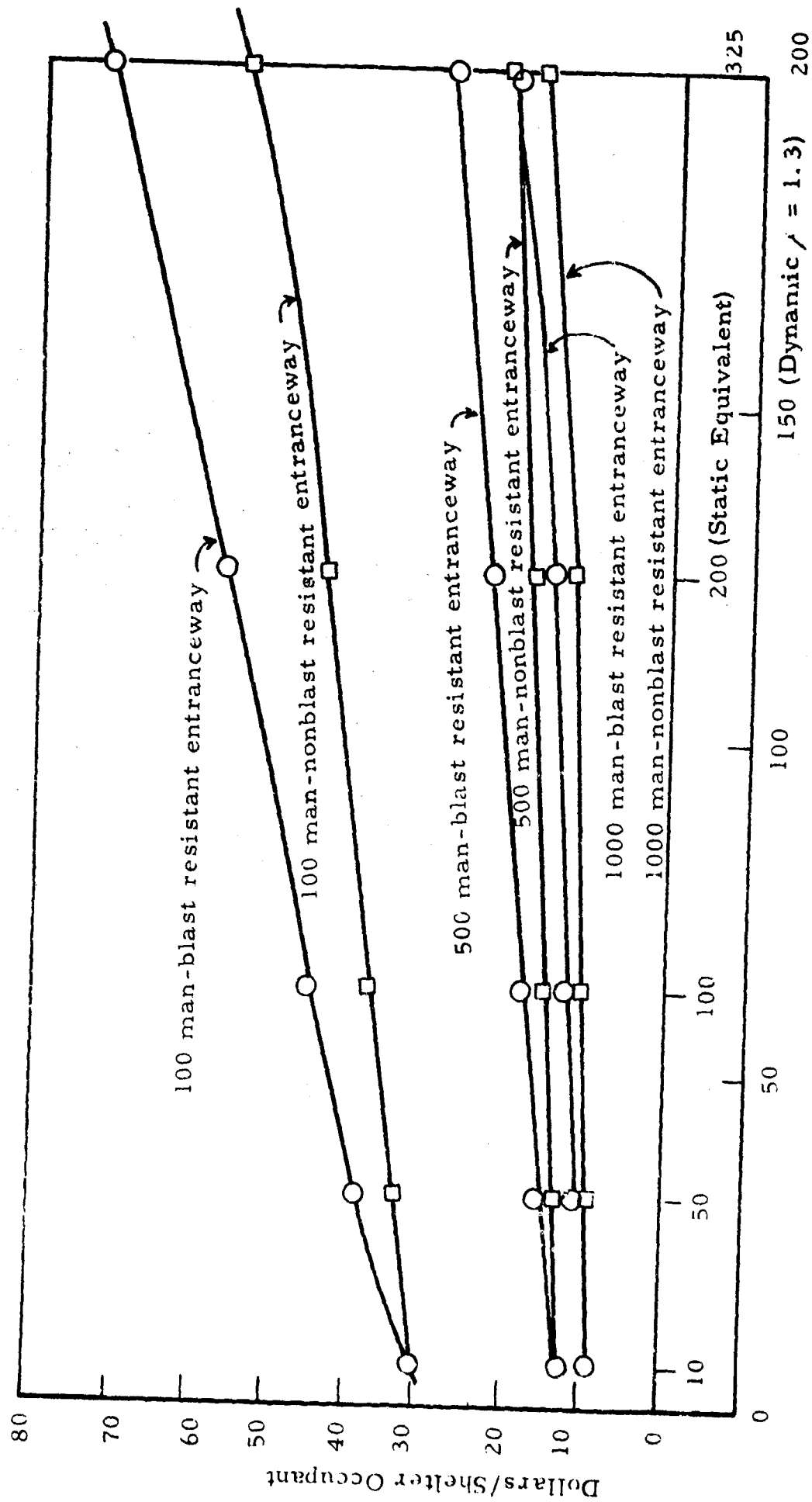


Fig. S-3 MINIMUM IN-PLACE ENTRANCEWAY STRUCTURAL COSTS

An increase in the design capacity of the entranceway is shown to effect a marked decrease in the system cost-per-entrant. Of the entranceway lane capacities studied in detail, it appears that the optimum two-lane system can accommodate traffic at approximately 30 percent less cost than can an equivalent one-lane system. A two-lane system is slightly less expensive (< 5 percent) than an equivalent four-lane system in the higher overpressure range ($p_{s0} > 50$ psi), but the reverse is true in the lower overpressure design region.

IIT RESEARCH INSTITUTE
Technology Center
Chicago, Illinois 60616

IITRI Project No. M6064 (3)
Final Report

ENTRANCEWAYS AND EXITS FOR BLAST-RESISTANT
FULLY-BURIED PERSONNEL SHELTERS

Distribution of this document is unlimited.

This report has been reviewed in the Office of Civil Defense and approved for publication. Approval does not signify that the contents necessarily reflect the views and policies of the Office of Civil Defense.

by

J. D. Stevenson
J. A. Havers

for

Office of Civil Defense
Department of the Army - OSA
Under
Contract No. OCD-PS-64-50
Subtask 1152-E

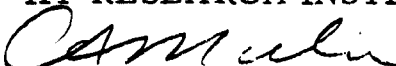
September 1965

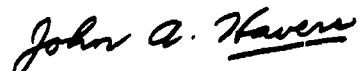
FOREWORD

This final report describes an investigation which was performed as a portion of Subtask 1152-E of Contract OCD-PS-64-50, IITRI Project No. M6064, "Total Shelter Design Optimization." The research reported herein has consisted of blast analyses, radiation analyses, traffic studies, and structural evaluations of entranceway and exit systems for fully-buried personnel shelters. Attention is directed to shelters of 100, 500 and 1000-man capacities, extending the earlier structural and economic studies of IITRI Projects M254 (Subtask 1151-A) and M6064 (1). The total in-place cost of the fully-buried shelter structure and of its entranceway system can now be estimated, as a function of design overpressure level in the 10-200 psi range, by combining the findings of these three studies.

Respectfully submitted,

IIT RESEARCH INSTITUTE

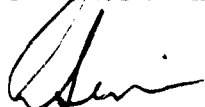

for John D. Stevenson
Structures Research



John A. Havers
Senior Research Engineer
Structures Research

JAH/gm

APPROVED BY:



E. Sevin, Director
Solid Mechanics Research Division

ENTRANCEWAYS AND EXITS FOR BLAST-RESISTANT FULLY-BURIED PERSONNEL SHELTERS

ABSTRACT

The work reported in this study is a continuation of the Total Shelter Design Optimization series which, under OCD sponsorship, is currently in progress at the IIT Research Institute. These studies have developed the design requirements and identified in-place costs for single-purpose, fully-buried personnel shelters of 100, 500, and 1000-man capacities. The attack environment, for analytical purposes, is described by a megaton ($W = 1$ to 100 MT) nuclear explosion and by side-on surface overpressures of 10 to 200 psi. Reports issued to date in this series have included the following:

- (1) "Structural Materials for Hardened Personnel Shelters," by John A. Havers, Contract No. OCD-PS-62-66, Subtask 1151-A, IIT Research Institute, December 1963.
- (2) "Structural Cost Studies for Hardened Shelters," by John A. Havers and Jerry J. Lukes, Contract No. OCD-PS-64-50, Subtask 1152-E, IIT Research Institute, January 1965.
- (3) "Entranceways and Exits for Blast-Resistant Fully-Buried Personnel Shelters," by John D. Stevenson, and John A. Havers, Contract No. OCD-PS-64-50, Subtask 1152-E, IIT Research Institute, May 1965 (draft).
- (4) "An Investigation of Minimal Equipment Needs in Personnel Shelters," by John A. Havers, Claire B. Monk, Jr. and Erich H. Koeller, Contract No. OCD-PS-64-50, Subtask 1216-A, May 1965 (draft).

By combining the findings of these separate studies, it is possible to perform rapid evaluations of specific attack environments, composite performance requirements, alternative analytical solutions and estimated in-place costs as a basis for the preliminary design of this particular type of shelter. It is found that structural per-occupant costs are strongly related to the design capacity of the shelter, and exhibit a decrease as the shelter capacity is increased. The structural costs are also found to increase with increasing levels of design overpressure, although this latter correlation becomes decidedly weaker as the overpressure level is increased.

CONTENTS

<u>Chapter</u>		<u>Page</u>
1.	INTRODUCTION	
	1.1 Study Objective	1-1
	1.2 Scope	1-2
	1.3 Design Considerations	1-3
	1.3.1 Description of Entranceways and Exits	1-3
	1.3.2 Operational Aspects of Design	1-5
	1.3.3 Protective Aspects of Design	1-7
	1.4 Known Limitations of the Study	1-11
	1.5 Possible Uses for Study Findings	1-12
2.	STRUCTURAL MATERIALS	
	2.1 Introduction	2-1
	2.2 Structural Steels	2-2
	2.2.1 Strength Properties	2-2
	2.2.2 Cost of Rolled Structural Shapes	2-3
	2.2.3 Cost of Uniform-Thickness Plates, Curved	2-4
	2.2.4 Cost of Corrugated Steel Plate, Single Curvature	2-4
	2.3 Steel Reinforcing Rod	2-5
	2.3.1 Strength Properties	2-5
	2.3.2 Cost	2-7
	2.4 Prestress Steel	2-7
	2.4.1 Strength Properties	2-7
	2.4.2 Cost	2-9
	2.5 Structural Concrete	2-9
	2.5.1 Strength Properties	2-9
	2.5.2 Cost	2-10
	2.6 Concrete Forms	2-11
	2.7 Earthwork	2-12
	2.8 Miscellaneous	2-12
	2.8.1 Stairs	2-12
	2.8.2 Roller Supports for Blast Doors	2-12
	2.8.3 Blast Door Latch	2-13
	2.8.4 Emergency Exit	2-13
	2.8.5 Flexible Metal Section Joints	2-13

CONTENTS (Cont'd)

<u>Chapter</u>		<u>Page</u>
3.	TRAFFIC CAPACITIES OF SHELTER ENTRANCEWAYS	
	3.1 Introduction	3-1
	3.2 Traffic Rates	3-2
	3.3 Dimensional Criteria	3-4
	3.4 Entranceway Capacity Related to Shelter Capacity	3-5
4.	DESIGN CRITERIA FOR BLAST LOADING	
	4.1 Introduction	4-1
	4.2 Blast Loading on Structures	4-2
	4.3 Criteria for Entranceway Design	4-9
5.	DESIGN CRITERIA FOR RADIATION SHIELDING	
	5.1 Introduction	5-1
	5.2 Radiation Units (Exposure dose, Absorbed dose, and Biological response)	5-2
	5.3 Initial Nuclear Radiation	5-4
	5.3.1 Significance in Shelter Entranceway Design	5-4
	5.3.2 Free-Field Characteristics of Initial Radiation	5-5
	1. Yield-Range-Dose Relationships	5-5
	2. Angular Distribution of Radiation Energies (Energy Spectrum)	5-7
	5.3.3 Correlation Between Free-Field Levels of Overpressure and Initial Radiation	5-15
	5.4 Residual Nuclear Radiation	5-20
	5.5 Barrier Shielding	5-25
	5.5.1 Entranceway Wall Attenuation of Neutron Flux	5-29
	5.5.2 Gamma Attenuation by Corridor Bends	5-34
	5.6 Overhead Contribution to Total Shelter Dose	5-34
	5.7 Contribution of Entranceway Streaming to Total Shelter Dose	5-37
	5.8 Composite Analysis of the Shelter and Entranceway	5-38
6.	DESIGN OF STRUCTURAL ELEMENTS	
	6.1 Introduction	6-1
	6.2 Rectangular Cubicle (Monolithic Reinforced Concrete)	6-3
	6.2.1 Design	6-3
	6.2.2 Unit Cost	6-7

CONTENTS (Cont'd)

<u>Chapter</u>	<u>Page</u>
6.3 Thick-Wall Cylinder (Prestressed Concrete)	6-11
6.3.1 Design	6-11
6.3.2 Unit Cost	6-18
6.4 Thin-Wall Cylinder	6-20
6.4.1 Reinforced Concrete (Compression Loading)	6-20
1. Design	6-20
2. Unit Cost	6-22
6.4.2 Reinforced Concrete (Tension Loading)	6-22
1. Design	6-22
2. Unit Cost	6-25
6.4.3 Structural Steel (Tension or Compression Loading)	6-25
1. Design	6-25
2. Unit Cost	6-26
6.5 Thin-Wall Sphere	6-27
6.5.1 Reinforced Concrete (Compression Loading)	6-27
1. Design	6-27
2. Unit Cost	6-38
6.5.2 Structural Steel (Compression Loading)	6-39
1. Design	6-39
2. Unit Cost	6-40
6.5.3 Structural Steel (Tension Loading)	6-40
1. Design	6-40
2. Unit Cost	6-43
6.6 Support Rings for Openings in Spheres	6-44
6.6.1 Analysis	6-44
6.6.2 Ring No. 1 (Reinforced Concrete, Compression Sphere)	6-46
1. Design	6-46
2. Unit Cost	6-50
6.6.3 Ring No. 1 (Structural Steel, Compression Sphere)	6-50
1. Design	6-50
2. Unit Cost	6-51

CONTENTS (Cont'd)

<u>Chapter</u>	<u>Page</u>
6.6.4 Ring No. 1 (Structural Steel, Tension Sphere)	6-52
1. Design	6-52
2. Unit Cost	6-52
6.6.5 Ring No. 2 (Reinforced Concrete, Compression Sphere)	6-53
1. Design	6-53
2. Unit Cost	6-56
6.6.6 Ring No. 2 (Structural Steel, Compression Sphere)	6-57
1. Design	6-57
2. Unit Cost	6-58
6.6.7 Ring No. 2 (Structural Steel, Tension Sphere)	6-58
1. Design	6-58
2. Unit Cost	6-59
6.7 Blast-Resistant Door	6-59
6.7.1 Discussion	6-59
6.7.2 Flat Plate	6-60
1. Analysis	6-60
2. Prestressed Concrete	6-64
(a) Design	6-64
(b) Unit Cost	6-67
3. Structural Steel	6-67
(a) Design	6-67
(b) Unit Cost	6-68
6.7.3 Single-Curvature Surface	6-68
1. Analysis	6-68
2. Prestressed Concrete	6-74
(a) Design	6-74
(b) Unit Cost	6-77
3. Structural Steel	6-78
(a) Design	6-78
(b) Unit Cost	6-79
6.7.4 Double-Curvature Surface	6-79
6.8 Channel Guides for Blast-Resistant Door	6-81

CONTENTS (Cont'd)

<u>Chapter</u>	<u>Page</u>
6.9 Supports for Blast-Resistant Door	6-83
6.9.1 Discussion	6-83
6.9.2 Door Supports, Cubicle Structure	6-84
1. Design	6-84
2. Unit Cost	6-90
6.9.3 Door Supports, Cylindrical Structure	6-91
1. Support Rings	6-91
(a) Design	6-91
(b) Unit Cost	6-95
2. Beam Members Between Support Rings	6-96
(a) Design	6-96
(b) Unit Cost	6-100
6.9.4 Circular Slab, Spherical Structure	6-100
1. Design	6-100
2. Unit Cost	6-102
7. STRUCTURAL DESIGN OF ENTRANCEWAYS FOR 100-500-1000 MAN SHELTERS	
7.1 Introduction	7-1
7.2 Design Configurations	7-2
7.2.1 Discussion	7-2
7.2.2 Blast-Resistant Structures	7-2
1. Compression Sphere Blast Section	7-3
2. Tension Cylinder Blast Section	7-5
3. Compression Cylinder Blast Section	7-7
4. Tension Cubicle Blast Section	7-7
7.2.3 Nonblast-Resistant Structures	7-10
1. Compression Cylinder or Cubicle	7-11
2. Compression Sphere	7-11
7.3 Input Parameters for Entranceway Designs	7-11
7.3.1 Dimensional Elements	7-11
7.3.2 Static Design Equivalent of Dynamic Blast Pressure	7-16
7.3.3 Tension Cubicle Design and Cost Factors	7-17

CONTENTS (Cont'd)

<u>Chapter</u>	<u>Page</u>
7.3.4 Compression Cubicle Design and Cost Factors	7-17
7.3.5 Supplemental or Emergency Exits	7-20
7.4 Blast-Resistant Entranceway Design	7-21
7.4.1 Compression Sphere (Sample Analysis and Cost Evaluation)	7-21
1. Blast Analysis	7-23
2. Radiation Analysis	7-37
3. Total Cost	7-47
7.4.2 Tension Cylinder (Sample Analysis and Cost Evaluation)	7-53
1. Blast Analysis	7-55
2. Radiation Analysis	7-62
3. Total Cost	7-69
7.4.3 Compression Cylinder (Sample Analysis and Cost Evaluation)	7-73
1. Blast Analysis	7-75
2. Radiation Analysis	7-81
3. Total Cost	7-86
7.4.4 Tension Cubicle (Sample Analysis and Cost Evaluation)	7-90
1. Blast Analysis	7-92
2. Radiation Analysis	7-97
3. Total Cost	7-103
7.5 Nonblast-Resistant Entranceway Design	7-107
7.5.1 Compression Cylinder (Sample Analysis and Cost Evaluation)	7-107
1. Blast Analysis	7-108
2. Radiation Analysis	7-114
3. Total Cost	7-121
7.5.2 Compression Sphere (Sample Analysis and Cost Evaluation)	7-125
1. Blast Analysis	7-126
2. Radiation Analysis	7-126
3. Total Cost	7-132

CONTENTS

<u>Chapter</u>		<u>Page</u>
8.	OPTIMUM ENTRANCEWAY DESIGN	
	8.1 Introduction	8-1
	8.1.1 Optimization Techniques	8-1
	8.1.2 Cost Allocation by Functional Area	8-2
	8.2 Materials	8-3
	8.3 Minimum-Structural-Cost Entranceways	8-4
	8.4 Conclusions	8-9
	8.5 Recommendations for Further Study	8-9
	BIBLIOGRAPHY	8-11

LIST OF ILLUSTRATIONS

<u>Figure</u>		<u>Page</u>
4-1	Effect of Initial-Peak Triangular Force Pulse on an Elasto-Plastic System	4-7
4-2	Surface Overpressure Versus Transmitted Overpressure Within Ducts With Open Ends	4-11
5-1	Values of Solid Angle Fraction, ω	5-13
5-2	Entranceway-Mouth Reduction Factors, R_{fc} , for Streaming of Gamma (γ) and Neutron (N) Fractions of Initial Radiation in Shelter Entranceways, As Functions of ω and β_B	5-14
5-3	Relationships Between Burst Height ($R_s \cos \gamma_B$), Distance from Ground Zero ($R_s \sin \gamma_B$) and Peak Side-On Surface Overpressure (p_{so}) for a 1 KT Explosion Yield ($R_s = R_{so}$)	5-18
5-4	Barrier Reduction Factors for Initial Gamma Radiation (≈ 6.5 Mev) As Functions of Barrier Mass Thickness and Incident Angle, β_S	5-28
5-5	Barrier Reduction Factors for Fallout Gamma Radiation (≈ 2 Mev) As Functions of Barrier Mass Thickness and Shielding Position Relative to Contaminated Plane	5-30
5-6	Barrier Reduction Factors for Fission-Yield Neutrons (≈ 2.5 Mev) As Functions of Barrier Mass Thickness and Incident Angle, β_S	5-31
5-7	Barrier Reduction Factors for Fusion-Yield Neutrons (≈ 14 Mev) As Functions of Barrier Mass Thickness and Incident Angle, β_S	5-32
5-8	Entranceway-Mouth Reduction Factors, R_{fc} , for Fallout-Radiation Streaming in Shelter Entranceways. As Functions of ω and Position of Entranceway Mouth Relative to Contaminated Plane	5-36
6-1	Thick Cylinder Wall Stresses	6-14
6-2	Thin-Wall Sphere, Meridian Section, Single-Opening Analysis (Loading Assumptions as Illustrated)	6-30
7-1	Entranceway Configuration with Compression Sphere Blast Section	7-4
7-2	Entranceway Configuration with Tension Cylinder Blast Section	7-6
7-3	Entranceway Configuration with Compression Cylinder Blast Section	7-8

LIST OF ILLUSTRATIONS (Cont'd)

<u>Figure</u>		<u>Page</u>
7-4	Entranceway Configuration with Tension Cubicle Blast Section	7-9
7-5	Entranceway Configuration with Nonblast-Resistant Cubicle	7-12
7-6	Entranceway Configuration with Nonblast-Resistant Cubicle and Compression Sphere	7-13
7-7	Design Chart for Tension Cubicle Roof and Wall Sections	7-18
7-8	Sectional View of Compression Sphere	7-22
7-9	Detail of Entrance Ring and Blast Door Layout	7-26
7-10	Plan View of Radiation Barrier Shield	7-47
7-11	Sectional View of Tension Cylinder	7-54
7-12	Sectional View of Compression Cylinder	7-74
7-13	Sectional View of Tension Cubicle	7-91
7-14	Plan View of Revised Entranceway Layout, Nonblast-Resistant Cubicle and Cylinder	7-118
7-15	Plan View of Revised Entranceway Layout, Nonblast-Resistant Compression Sphere	7-131
8-1	In-Place Cost for Blast-Resistant Entranceways	8-5
8-2	In-Place Cost for Nonblast-Resistant Entranceways	8-6
8-3	Percentage Cost Advantage, Nonblast Versus Blast-Resistant Entranceways	8-7
8-4	Minimum In-Place Entranceway Structural Costs	8-8

LIST OF TABLES

<u>Table</u>	<u>Page</u>
1-1 Values of Ductility Ratio Frequently Proposed for Blast-Resistant Design	1-8
2-1 Grouping of Typical Structural Steels According to Dynamic Yield Strength	2-3
2-2 In-Place Cost of Rolled Structural Steel Shapes, Dollars Per Pound	2-3
2-3 In-Place Cost of Uniform-Thickness Curved Steel Plate, Dollars Per Square Foot of Curved Surface	2-4
2-4 In-Place Cost of Single-Curvature Corrugated Steel Plate, Dollars Per Square Foot of Curved Surface	2-4
2-5 Kinds and Grades of Reinforcing Bars as Specified in ASTM Standards	2-6
2-6 In-Place Cost of Steel Reinforcing Rod, Dollars Per Cubic Foot of Steel	2-7
2-7 Sizes and Grades of Prestress Strand and Bar	2-8
2-8 In-Place Cost of Prestress Steel	2-9
2-9 In-Place Cost of Ready-Mix Concrete, Dollars Per Cubic Foot of Concrete	2-11
2-10 In-Place Cost of Forms for Concrete, Dollars Per Square Foot of Concrete Surface	2-11
2-11 In-Place Cost of Earthwork, Dollars Per Cubic Foot	2-12
3-1 Dimensional Criteria for Entranceway Traffic Lanes	3-4
3-2 Required Number of Entranceway Lanes As a Function of Shelter Capacity	3-7
5-1 Peak Pressures (Dynamic and Static, for $\mu = 1.30$); Slant Ranges, R_s ; and Initial Radiation Components γ_w , N_w	5-21
6-1 Values of $K_{\phi 1}$ and $K_{\phi 2}$ for Use in Cost Eq. (6-4)	6-8
6-2(a) Minimum In-Place Cost for One-Way Reinforced Concrete Rectilinear Elements Which Are Subjected to Tensile Loading in Their Axial Plane, Plus Uniformly-Distributed Transverse Loading in a Second Plane	6-9
6-2(b) Minimum In-Place Cost for One-Way Reinforced Concrete Rectilinear Elements Which Are Subjected to Compressive Loading in Their Axial Plane, Plus Uniformly-Distributed Transverse Loading in a Second Plane	6-10
6-3 Coefficients for Central Flat-Plate Bending Moments in Simply-Supported, Rectilinear, Reinforced Concrete Slabs ($\nu = 0.16$) Which Are Subjected to Uniformly-Distributed Transverse Loading	6-62

LIST OF TABLES (Cont'd)

<u>Table</u>		<u>Page</u>
6-4	Coefficients for Central Flat-Plate Bending Moments in Simply-Supported, Rectilinear Steel Plates ($\nu = 0.30$) Which Are Subjected to Uniformly-Distributed Transverse Loading	6-63
7-1	Minimum Dimensions for Selected Entranceway Elements	7-14
7-2	Parameters of Optimum Shelters Which are Pertinent to Entranceway Design	7-15
7-3	Relationships Between Values of Static Equivalent Load and Long-Duration Dynamic Load ($\mu = 1.3$)	7-16
7-4	Static Equivalent Design Pressures	7-17
7-5	Compression Cubicle Design and Cost Parameters	7-19

NOMENCLATURE

A	cross-sectional area, (sq in.)
A_1	plan area of entranceway section (sq ft)
A_2	projected plan area of entranceway section at ground level, assuming a 1:1 side slope (sq ft)
A_s	total area of reinforcing steel in one principal direction of a concrete member, (sq in.)
$\sum A_s$	total area of reinforcing steel, summed for the principal directions of a concrete member, (sq in.)
A_{sL}	area of reinforcing steel on the left side of the centroidal longitudinal axis of a concrete member, (sq in.)
A_{sR}	area of reinforcing steel on the right side of the centroidal longitudinal axis of a concrete member, (sq in.)
A_{te}	area of temperature reinforcing steel in a concrete member, (sq in.)
A_T	total area of surface, (sq ft)
A_v	area of diagonal tension reinforcement steel in a concrete member, (sq in.)
A_w	net area of steel beam web, (sq in.)
b	width of beam, column, slab or wall, (in.)
B	center-to-center spacing of similar structural members, (ft)
B_p	short dimension of projected area of entranceway mouth, used in radiation streaming investigations, (ft)
B_T	total width of rectangular structure, (ft)
c/d	distance from extreme compressive fiber to neutral axis of a bending reinforced-concrete member, expressed as a ratio of the effective depth of the section
C	general term for cost factor
C_c	cost factor per unit of structural element for concrete, (\$/ft or \$/sq ft)
C_{dr}	drag coefficient for dynamic pressure-loading evaluation of a specific structural member
C_f	cost factor per unit of structural element for form work, (\$/ft or \$/sq ft)
C_g	cost factor per unit of structural element for gunite cover over externally-wrapped prestress steel, (\$/sq ft)
C_s	cost factor per unit of structural element for main reinforcing steel, (\$/ft or \$/sq ft)

IIT RESEARCH INSTITUTE

NOMENCLATURE (Cont'd)

C_{sp}	cost factor per unit of structural element for prestressing steel, (\$/ft or \$/sq ft)
C_{st}	cost factor per unit of structural element for temperature reinforcing steel, (\$/ft or \$/sq ft)
C_t	factor for composite cost per unit of a structural element, (\$/ft or \$/sq ft)
C_v	cost factor per unit of structural element for shear reinforcement steel, (\$/ft or \$/sq ft)
C_{vt}	cost factor per unit of structural element for torsion reinforcement steel, (\$/ft or \$/sq ft)
C_C	total cost of concrete in structural element, (\$)
C_F	total cost of form work for structural element, (\$)
C_G	total cost of gunite cover for externally-wrapped prestress steel in structural element, (\$)
C_S	total cost of main reinforcing steel in structural element, (\$)
C_{SP}	total cost of prestressing steel in structural element, (\$)
C_{ST}	total cost of temperature steel in structural element, (\$)
C_T	composite cost of entire structural element, (\$)
C_V	total cost of shear reinforcement steel in structural elements, (\$)
C_{VT}	total cost of torsion reinforcement steel in structural element, (\$)
d	distance from compression face of reinforced concrete beam or slab to center of gravity of tension reinforcement, (in.). Also known as "effective depth."
d'	distance from tension face of reinforced concrete beam or slab to center of gravity of tension reinforcement, $d' = D - d$, (in.)
d''	distance from compression face of reinforced concrete beam or slab to center of gravity of compression reinforcement, (in.)
d_w	net depth of web in steel beams, (in.)
D	total depth or thickness of a member, (in.)
e	ratio of short dimension to long dimension for projected area of entranceway mouth (used in radiation streaming investigations, with $e = B_p/H_p$). Also base for Napierian system of logarithms.
e_d	eccentricity, referenced to geometric centroid, of dynamic axial thrust applied to reinforced concrete section, (in.)
E	modulus of elasticity, (psi)
f'_c	unit static compressive strength of concrete, based on standard 28-day cylinder test, (psi)
f'_{dc}	unit dynamic compressive strength of concrete, (psi)

IIT RESEARCH INSTITUTE

NOMENCLATURE (Cont'd)

f_{dv}	dynamic yield stress of steel in shear (psi)
f_{dy}	dynamic yield stress of steel in tension or compression, (psi)
f_r	unit stress, acting in the radial direction, in the wall of a loaded cylinder, (psi)
f_t	unit stress, acting in the tangential (circumferential) direction, in the wall of a loaded cylinder, (psi)
f_v	static yield stress of steel in shear, (psi)
f_y	static yield stress of steel in tension or compression, (psi)
F_{sp}	manufacturer's recommended design load per prestressing cable, (lb)
h	depth from ground surface to top of structure, (ft)
h_{av}	average depth of earth cover, (ft)
H	height of column or wall, (ft)
H_p	height of projected area of entranceway mouth, (ft)
i	summation index
I	moment of inertia, (lb/in. ⁴)
j	summation index
k	general term for a defined constant
k'_f	composite unit cost of form work in roof slabs and beams, $k'_f = X_f + 0.012 D$, (\$)
k_h	ratio of horizontal to vertical soil pressure
K	general term for a defined constant
KT	kilotons, TNT equivalent in explosion yield
L	span length of beam or slab, (ft)
$L_{1/2}$	neutron half-length for entranceway corridor, (ft)
L_{sp}	required length of prestressing strand for concrete member, (ft/sq ft)
L_L	length of long span for rectangular flat-plate element, (ft)
\widehat{L}_L	arc length of curved (long) span for rectangular singly-curved plate element, (ft)
L_S	length of short span for rectangular plate element, (ft)
L_T	total length of structure, (ft)
M	general term for applied or resisting moment (in. -lb) or (in. -lb/in.)
M_{10}	moment in central portion of long span of uniformly-loaded, rectangular-plan structural element, with hinged edge-support, (in. -lb/in.). In the case of a cylindrical-surface element, the curved span is taken as the long span.

NOMENCLATURE (Cont'd)

M_{20}	moment in central portion of straight span of uniformly-loaded, rectangular-plan structural element, with hinged edge-support, (in. - lb/in.)
M_{1e}	value of moment at curved edge of cylindrical-surface blast door, assuming fixed-edge support, (in. - lb/in.)
M_{du}	dynamically-applied ultimate moment, acting singly or in combination with an axial thrust N_{du} , which develops the ultimate bending resistance of a reinforced concrete member, (in. - lb)
M_{ev}	million electron volts, measure of energy of radiation from a nuclear burst
MT	megaton, tri-nitro toluene (TNT) equivalent in explosion yield
n	$2Z/H_p$ (used in solid angle calculations for radiation streaming)
$n_{1/2}$	number of neutron half-lengths, related to attenuation of neutron radiation energy
n_o	integrated neutron flux in air at slant range, R_{so} ft from a 1 KT fission explosion (neutrons/sq cm)
n_w	integrated neutron flux in air at slant range R_s from a W MT fission explosion, (neutrons/sq cm)
n_L	required number of traffic lanes in a shelter entranceway
N	total design population of a shelter (persons); also, general term for absorbed neutron dose (rad)
N_{du}	dynamically-applied thrust, which acting singly or in combination with moment M_{du} , develops the ultimate resistance of a reinforced concrete member, (lb/in.)
N_o	absorbed dose (rad) resulting from unshielded exposure to the neutron flux produced at range R_{so} by a 1 KT fission yield. (Based on relationship that one neutron/sq cm $\approx 1.8 \times 10^{-9}$ rad for fission neutrons with energies in excess of 200 electron volts and for $R_s > 1500$ ft.)
N_w	absorbed dose (rad) resulting from unshielded exposure to the neutron flux produced at range R_s by a W MT fission yield (Same assumptions as for N_o)
N_{10}	circumferential equilibrium force in the wall of a cylindrical shell, (lb/in.)
N_{20}	longitudinal equilibrium force in the wall of a cylindrical shell, (lb/in.)
N_0	latitudinal equilibrium force in wall of spherical shell, (lb/in.)

NOMENCLATURE (Cont'd)

N_{ψ}	meridional equilibrium force in wall of spherical shell, (lb/in.)
p_a	ambient atmospheric pressure at the ground surface, (psi)
p_d	peak intensity of dynamic pressure at the ground surface, (psi)
p_{dr}	peak intensity of the "drag" pressure on an above-ground structural member due to the peak dynamic pressure, p_d , (psi)
p_m	peak intensity of dynamically-applied loading on a buried structure, (psi)
p_r	peak intensity of pressure due to reflection of the free-field blast wave, (psi)
p_{ri}	peak intensity of reflected pressure wave inside an entranceway structure, (psi)
p_{so}	peak intensity of side-on overpressure at the ground surface, (psi)
p_t	prestressing strand pitch, (in.)
p_{to}	peak intensity of transmitted overpressure within an entranceway structure, (psi)
P_{L1}	unit line loading due to external forces on support ring of second (circular) opening in a spherical structure. Loading is taken as acting normal to plane of ring curvature, (lb/in.)
P_{L2}	unit line loading due to external forces on support ring of second (circular) opening in a spherical structure. Loading is taken as acting normal to plane of ring curvature, (lb/in.)
q	general term for static-equivalent, uniformly-distributed unit loading which by implication, develops the yield or ultimate resistance of the loaded member in one or more of its possible failure modes, (psi). With this definition, the notation "q" will be applied both to an applied loading and to the yield or ultimate resistance which is developed in a member by such loading.
q_c	unit compression mode resistance, (psi)
q_d	ratio of $p f_{dy} / f'_{dc}$ for reinforced concrete member
$q_{dL} =$	$\frac{A_s L f_{dy}}{b d f'_{dc}}$
$q_{dR} =$	$\frac{A_s R f_{dy}}{b d f'_{dc}}$

NOMENCLATURE (Cont'd)

q_f	unit flexural mode resistance, (psi)
q_{sc}	unit diagonal tension or shear compression mode resistance, (psi)
q_t	unit tensile mode resistance, (psi)
q_u	unit ultimate resistance, (psi)
q_v	unit shear mode resistance, (psi)
$\sum q_E = q_{Ep} + q_{Es} + q_{Ed}$	
q_{Ep}	inwardly-directed radial component of prestressing force T_{sp} , acting on prestressed shell structure, (psi)
q_{Es}	conventional dead and live loadings acting on a buried shell structure, approximated as a radial inwardly-directed loading, (psi)
q_{Ed}	static equivalent representation of earth-transmitted overpressure-loading on the exterior surfaces of a buried structure, considered to act as a radial inwardly-directed loading, (psi)
q_I	static equivalent representation of interior reflected pressure, psi, within a structure open to blast-wave penetration. This pressure is assumed to act as a radial outwardly-directed loading, (psi)
r	radius, measured on a right transverse section, from center of cylinder to interior point within the cylinder wall, (ft)
rad	unit of absorbed dose of any nuclear radiation
rem	unit which describes the effect of any nuclear radiation on human tissue
r_m	mean radius of projection of entranceway mouth on plane normal to longitudinal axis of entranceway leg, (ft)
R	roentgen, measure of exposure dose of gamma nuclear radiation
RBE	relative effect of one rad of absorbed dose of nuclear radiation on biological dose, referenced to observed effect of one rad of some "standard" radiation
R_{fb}	barrier reduction factor for nuclear radiation
R_{fc}	bend reduction factor for nuclear radiation
R_{fe}	entrance mouth reduction factor for nuclear radiation
R_{fw}	wall reduction factor for nuclear radiation
R_{H1}	exposure dose rate for fallout gamma radiation at one hour following the explosion, (R/hr)
R_s	slant range between explosion center and location considered, (ft)
R_{so}	slant range which, for a weapon yield of 1 KT, corresponds to a specified value of the peak overpressure, (ft)

NOMENCLATURE (Cont'd)

R_t	exposure dose rate for fallout gamma radiation at time t hours following the explosion, (R/hr)
S	elastic section modulus of beam, (in. ³)
S_L	span of singly-curved or doubly-curved structure or structural member, (ft)
t	thickness of steel plate, (in.), elapsed time since explosion, (hr)
t_d	effective duration of blast loading, (seconds)
t_f	thickness of steel beam flange, (in.)
t_r	rise time of pressure pulse, (seconds)
t_w	thickness of steel beam web, (in.)
T	natural period of vibration of structure or structural member, (seconds)
T_{sp}	effective value of prestressing force applied to a concrete member, (lb/in.)
TNT	tri-nitro toluene, high explosive
V	total shear, (lb)
V_p	total shear causing full plastification of net web area of rolled steel beam, (lb) or of the section of a steel plate, (lb/in.)
V_u	ultimate shearing resistance of cross section of reinforced concrete member, (lb) or reinforced concrete slab, (lb/in.)
w	weight per unit of structural element, (lb/ft, lb/sq ft or lb/ft ³)
W	equivalent nuclear explosion yield, expressed in megatons (MT) of TNT
W'	scaling factor for initial gamma radiation flux, corresponding to a fission yield of W MT
x	coordinate axis in rectilinear Cartesian system
X	general term for cost coefficient
X_c	unit cost of concrete, (\$/ft ³)
X_f	unit cost of form work, (\$/sq ft)
X_g	unit cost of gunite coating, (\$/sq ft)
X_p	unit cost of prestressing strand, (\$/ft)
X_s	unit cost of steel, excluding shear and torsional reinforcement, expressed as (\$/ft ³) for reinforcing tie and temperature steel, (\$/lb) for rolled steel shapes and (\$/sq ft) for steel plate
X_v	unit cost of shear and torsional reinforcement steel, (\$/ft ³)
y	coordinate axis in rectilinear Cartesian system

IIT RESEARCH INSTITUTE

NOMENCLATURE (Cont'd)

- z depth below ground surface, (ft), coordinate axis in rectilinear Cartesian system
- Z distance from radiation detector to projected plane of entranceway mouth, (ft)
- α ratio of short to long spans for flat rectangular plates and slabs
- β_B angular orientation of burst relative to line-of-sight for a specified entranceway leg, (deg)
- β_S angular orientation of radiation shielding, measured relative to line-of-sight to explosion center, (deg)
- $\beta_z = \tan^{-1} \frac{r_m}{Z}$ (deg)
- γ general term for absorbed dose due to gamma radiation, (rad)
- γ_o absorbed dose due to unshielded gamma radiation at slant range, R_{so} from a 1 KT explosion, (rad)
- γ_w absorbed dose due to unshielded gamma radiation at slant range, R_s from a W MT explosion, (rad)
- θ angle measured in horizontal plane, (deg)
- θ' ratio of negative to positive reinforcement percentages in concrete member
- θ_B angular orientation of burst center relative to x-axis, projected in horizontal plane, (deg)
- θ_E angular orientation of specified entranceway leg relative to x-axis, projected in horizontal plane, (deg)
- λ ratio of straight-edge length L_S to curved-edge length \hat{L}_L for rectangular-plan element of a cylindrical surface. Note that λ approaches α as cylinder radius becomes infinite.
- μ ductility factor representing ratio of maximum permissible deflection of a structural member to its deflection at yield, also a defined term
- $$\left[\mu = \frac{6912 (1 - \nu^2) L_S^4}{\pi^4 S_L^2 D^2} \right] \text{ in studies of cylindrical shells}$$
- ν Poisson's ratio, value dependent upon specific material considered
- ρ_m effective mass density of radiation shielding, (lb/ft²)
- ϕ symbol for diameter of a circular cross section
- ϕ general term for percentage of tensile steel reinforcement in concrete member, referred to net section area normal to direction of reinforcement

NOMENCLATURE (Cont'd)

ϕ'	general term for percentage of compressive steel reinforcement in concrete member, referred to net section area normal to direction of reinforcement
ϕ_c	effective percentage of tensile steel reinforcement at midspan of concrete member, referred to net section area normal to direction of reinforcement
ϕ_{cL}	effective percentage of tensile steel reinforcement at midspan in the long direction of a two-way reinforced, rectangular concrete slab. Referenced to net section area normal to direction of reinforcement
ϕ_e	effective percentage of tensile steel reinforcement at end support of concrete member, referred to net section area normal to direction of reinforcement.
ϕ_t	total percentage of main reinforcing steel in one principal direction of a concrete member, referred to gross section area normal to direction of reinforcement
$\sum \phi_t$	summed percentages of main reinforcing steel in the principal directions of a concrete member, referred to gross section areas normal to each direction of reinforcement
ϕ_{te}	percentage of temperature reinforcing steel and/or tie steel in concrete member, referred to gross section area normal to direction of reinforcement
ϕ_{tL}	percentage of reinforcing steel which resists those tensile membrane forces acting in latitudinal direction, referred to gross area of section normal to direction of reinforcement
ϕ'_{tL}	percentage of reinforcing steel which resists those compressive membrane forces acting in latitudinal direction of spherical shell, referred to gross area of section normal to direction of reinforcement
ϕ_{tM}	percentage of reinforcing steel which resists those tensile membrane forces acting in meridional direction of spherical shell, referred to gross area of section normal to direction of reinforcement
ϕ'_{tM}	percent of reinforcing steel which resists those compressive membrane forces acting in meridional direction of spherical shell, referred to gross area of section normal to direction of reinforcement
ϕ_v	percentage of web reinforcing steel in concrete member, supplied as vertical stirrups and referred to net section area in plane of stirrups
ϕ_{vt}	percentage of torsional vertical stirrup steel in concrete member, referred to total surface area of member in plane normal to stirrups
ϕ_L	$= \frac{A_{sL}}{b d}$

NOMENCLATURE (Cont'd)

- ψ general symbol for vertical angle measured in any z, θ plane of a spherical coordinate system, commencing at the z axis. Also specified as a particular coordinate in the spherical blast-exclusion structure, where it is referenced to the radial bisector of the first (circular) opening in the structure, (deg)
- ψ' vertical angle, used as a particular coordinate in the spherical blast-exclusion structure, where it is referenced to the radial bisector of the second (circular) opening in the structure, (deg)
- ψ_B vertical angle to explosion center, as observed at some specified location and measured from the z coordinate axis, (deg)
- ψ_E vertical angle to longitudinal axis of inclined entrance section of shelter entranceway, as observed at a detector station within the entranceway and measured from the z coordinate axis, (deg)
- ψ_o one-half of the central angle, measured in a transverse sectional plane through a cylindrical-element blast doorway, which is subtended by the (long) curved edge of the door, (deg)
- ψ_{01} one-half of the central angle subtended by the principal diameter of the first (circular) opening in a spherical structure, (deg)
- ψ_{02} one-half of the central angle subtended by the principal diameter of the second (circular) opening in a spherical structure, (deg)
- ψ_R vertical angle between radial bisectors of first and second (circular) openings in a spherical structure, (deg)
- ψ_T vertical angle, referenced to radial bisector of a single (circular) opening in a concrete spherical structure, at which the tensile latitudinal membrane forces due to loads on the shell and at the opening can be satisfied with $\phi_{tL} = 0.50$
- ω solid angle fraction (solid radians)
- ω' reduced solid angle fraction for gamma radiation, as a function of bend effects (solid radians)

ENTRANCEWAYS AND EXITS FOR BLAST-RESISTANT FULLY-BURIED PERSONNEL SHELTERS

CHAPTER 1 INTRODUCTION

1.1 STUDY OBJECTIVE

In two earlier studies, performed by the IIT Research Institute under the authorization of the Office of Civil Defense, structural design and cost data were developed for fully-buried personnel shelters of 100-man, 500-man and 1000-man capacities.^{1, 2*} These related studies developed in-place structural costs for each shelter capacity as a function of the design overpressure, but did not include any detailed consideration of suitable entranceways to serve the shelters. Exploratory projections,¹ however, indicated that entranceway costs could represent a significant fraction of the total structural costs of a shelter system. In recognition of this economic importance, this report extends the scope of the earlier studies by investigating the design requirements and structural costs for shelter entranceways.

1.2 SCOPE

The entranceways and exits which are examined in this study are specifically intended to service those shelters whose design capacities, interior layouts, structural materials, structural systems and basic configurations are described in earlier reports.^{1, 2} It is recommended that direct reference be made to these studies, since their initial postulates and subsequent findings have established certain design constraints which are used in this entranceway study. For the benefit of the casual reader, however, several pertinent features of these references are summarized.

The shelter capacities are set at 100-man, 500-man and 1000-man. All shelters are designed for significant resistance to blast loadings characterized by overpressures ranging from 10 psi to 200 psi at the ground surface. The design weapons are considered to be in the megaton range, with yields (W) ranging from 1 MT to 100 MT. The shelter is assumed to be fully buried and located above the permanent ground water table. It is designed to protect its occupants from all adverse effects, considered both singly

*Superscript numerals identify reference sources, as listed in the bibliography contained in the last section of this report.

and in combination, which may result from the postulated explosion. From a practical standpoint, this normally means that the buried shelter is first designed for adequate structural resistance to the overpressure-induced loading, using simplified loading and response theory.¹ Subsequently, the barrier shielding supplied by the shelter against the effects of ionizing radiation is examined. Direct thermal emissions, due to the thermal shielding of the earth cover over the shelter, do not influence the structural design.

The shelter configurations of interest include the rectangular cubicle, the 180 deg arch and the 360 deg cylinder, the 180 deg dome and the 360 deg sphere. When cost minimization techniques are applied to shelters with fixed capacities and with efficient interior layouts, strong cost-interactions are identified between shelter configuration, structural materials and systems, and design magnitude of overpressure loading. The pertinent features of the least-structural-cost shelter, as would be expected, are found to vary as the conditions of loading are changed. The cubicle configuration is associated with least-structural-cost at low levels of loading, but is successively replaced by the 180 deg arch and the 360 deg cylinder as loading levels are increased. The relationship between shelter configuration and minimum-structural-cost, as is apparent from Fig. 6.3, of Ref. 2 is also influenced by the design capacity of the shelter. The structural material normally associated with the least-structural-cost shelter is identified, for various shelter configurations and for a broad range of design loadings, as reinforced concrete. At the lower end of the study range, characterized by overpressures in the vicinity of 10 psi, the structural steel and structural timber designs appear to have some economic advantages.

The entranceways and exits, since they are designed to service the minimum-structural-cost shelters,^{1, 2} must similarly be able to withstand the destructive effects of 1-100 MT explosions at ground ranges characterized by surface overpressures of 10 to 200 psi. The interactions between these explosion effects and the entranceway structure will, however, differ somewhat from those analyzed for the shelter proper. These factors, which will be discussed subsequently in Chapters 4 and 5, will influence the geometry of the shelter entranceway or exit. The entranceway capacity must also be consistent with the shelter size and with the time available for loading the shelter. This latter requirement will dictate the number of traffic lanes and/or entranceway structures, and is discussed in Chapter 3.

The shelter analyses, ^{1, 2} have identified reinforced concrete as the least-cost structural material for all but the lower pressure ranges. It will subsequently be shown (Chapter 4) that the peak loading on an entranceway structure is typically much more severe than that imposed on the adjoining buried shelter. These factors suggest that minimum-cost studies of entranceway structures should be focused on the use of structural concrete, both prestressed and conventionally reinforced. Structural steel is also of obvious interest and, as in the shelter studies, will be examined as an alternative structural material. While these two materials will be considered exclusively in this study, it is recognized that certain others (such as aluminum) may be suitable for specific application in appropriate entranceway designs.

1.3 DESIGN CONSIDERATIONS

1.3.1 Description of Entranceways and Exits

The possible types of shelter entranceways and exits include various stairways, ramps, slides elevators etc. These are discussed in some detail in Ref. 3, where evaluations of their relative effectiveness and cost are supplied. The preferred type of entranceway and exit for each shelter is influenced by the operational requirements (physical condition of shelterees and permissible time for loading the shelters, etc.), the availability of real estate, excavation costs, location of shelter relative to the ground surface and natural topography. However, it has been concluded that an entranceway layout which includes conventional stairways and connecting corridors will generally prove the most satisfactory for personnel shelters. ^{3, 4} This type of entranceway will be considered exclusively in the following analyses, and, assuming its survival following a nuclear explosion, would obviously be equally suitable as an exit. Consideration is also given to an emergency type of exit which would consist of a vertical tube connecting the shelter with the ground surface. Such an exit would be protected from surface explosion effects by a removable cover and by a layer of soil.

The functional components of a shelter entranceway can be categorized as follows:

- (a) Surface transition section; consists of an open U-shaped portion which leads from the ground surface to the mouth of the entranceway proper.
- (b) Depth transition section; provides all or a major part of the required change in elevation between the entranceway mouth

IIT RESEARCH INSTITUTE

and the elevation at which the shelter itself is entered. This section is designed to withstand both internal and external blast loading, unless it is specifically intended to collapse under blast loading. In this latter case, it is designed only for conventional loading. Obviously, the depth transition section can be structurally integrated with the surface transition section. The magnitude of the elevation change which the depth transition section must accommodate is related to such factors as the surface topography, the shelter configuration and interior layout, the exterior dimensions of the shelter, and the depth of earth cover over the shelter. In this study, the natural topography is assumed to be approximately level.

(c) Blast-exclusion section; includes the blast door and its supporting structure. Its function is to shield the downstream portions of the entranceways, as well as the shelter itself, from the effects of the interior reflected blast wave. The door will also provide some degree of barrier protection from ionizing radiation. A portion of the required elevation change can be obtained in this section if so desired.

(d) Blast-resistant corridor section; provides separation in plan between the blast-exclusion section and the shelter. The blast wave does not enter this section, although earth-transmitted overpressure loading will act against its exterior. The section is oriented to provide attenuation of any ionizing radiation which streams along the passage. Again, a portion of any required elevation change can be accomplished in this section.

(e) Nonblast-resistant corridor section; also provides plan and/or elevation separation between the entranceway mouth and the blast-exclusion section. It may be designed to be integral with the transition section, however, it is not designed to resist either interior or exterior blast loading.

(f) Interlock section; this optional fixture permits late arrivals to enter the shelter without the risk that a blast wave

will also penetrate the entranceway. Thus, the primary feature of an interlock is two blast-resistant doors with a holding space between them.

(g) Decontamination section; some provision for a decontamination facility may be desirable for a large shelter complex. However, this optional feature will not be included in this study.

1.3.2 Operational Aspects of Design

The preliminary geometric layout of a shelter entranceway is largely controlled, both in plan and in elevation, by the relative locations of the surface transition section and the shelter proper. Analyses of blast and radiation penetration into the entranceway may subsequently lead to modifications of this basic layout, frequently in the form of additional corridor bends or lengthened corridor sections. The sectional dimensions within the entranceway are dictated by the shelter capacity and the required rate of loading. These considerations are used to establish corridor and stairway widths, head-room clearances, and the number and dimensions of stair treads and risers. The design alternatives for the entranceway can be analyzed and estimates can be made of their respective in-place costs, leading to minimum-cost solutions similar to those obtained for the basic shelter structures.^{1,2} However, there are still other design considerations which, while certainly affecting the final cost of an entranceway, should properly be evaluated in terms of their operational features as well as on the basis of their estimated costs. Several items in this general class are discussed in the following paragraphs.

An immediate question arises as to whether, from the standpoint of reliability, it is acceptable to provide a single entranceway for any or all capacities of shelters. A single entranceway can be sized for the required rate of traffic flow, even for the 1000-man capacity shelters, and it is not unlikely that cost studies would identify this as the least costly arrangement. (For a single entranceway and large shelters, attention should also be focused on the traffic flow as people move to areas within the shelter.) Giving recognition to the directional characteristics of a blast wave and to such indeterminant problems as debris accumulation in the entranceway, it can

be argued that a single entranceway is undesirable. Our understanding of the risk and survival probabilities is insufficient to permit a meaningful cost analysis of the alternatives, and we can only proceed on the basis of our best judgment. For purposes of this study, the single entranceway is considered as acceptable only for shelters with design capacities of 500 or less.

In much the same vein, the justification for a separate exit can be explored. An entranceway structure, if designed to withstand the blast and related effects associated with a specified level of overpressure, can be expected to be adequate as a post-attack exit if this design overpressure has not been exceeded. However, there are obvious dangers that transported debris will block the entranceway or that the blast door mechanism may fail to function. It would certainly seem futile for the sheltered occupants to survive the attack but subsequently perish through their inability to leave the shelter. An emergency exit requirement can be satisfied at relatively low cost, since there should be no comparable urgency in the rate of shelter unloading. Such an exit, consisting essentially of a vertical cylinder which contains a ladder, has been assumed as a basic requirement for each of the three shelter capacities considered herein.

There is a question as to whether a single-locking system of blast closure is adequate for the shelter entranceway, or whether a double-locking feature should be incorporated. In this usage, a single-locking system describes an entranceway which contains a single blast door. Since this door must be closed before the shelter occupants are protected from blast effects, a difficult decision rests with the shelter manager as to when to seal the shelter and thus, in order to protect those persons who are already within, deny access to any late arrivals. This situation becomes of particular importance when brief warning times are postulated as a design condition for the shelter system. A double-locking system, in contrast, will contain two blast-resistant doors with some travel distance between them. Late arrivals can thus be brought into the shelter system by opening the first blast door, holding them in the intervening space until this door has been closed, and then opening the second blast door and passing them into the shelter proper. While such a system is obviously more costly than

a single locking system, it contains the potential for a fuller usage of shelter space. However, for this study, only the single-locking system is considered.

There are also basic questions as to whether the entranceway should be designed to resist the design level of overpressure, or whether all or a part of it should be permitted to collapse under such loading. In the latter case, full reliance must be placed on the emergency exits as a means of egress. Certain design complications may arise if the collapsed entranceway is also intended for some dual form of usage, such as an air intake or an equipment room. However, if the rate of collapse can be controlled so that unduly large blast loadings are not reflected at the blast door, this type of design has a definite appeal. It is considered in this study as an alternative possibility.

1.3.3 Protective Aspects of Design

The primary criterion for the structural design of a fully-buried shelter has been shown to be the peak intensity of the dynamic loading, p_m , which is imposed on the structure by the peak value of the overpressure, p_{so} , acting at the ground surface.^{1, 2} For shallow-buried structures which satisfy certain postulated requirements for full-burial, the peak dynamic loading on the shelter roof, p_m , is frequently considered to be numerically equal to the peak value of the side-on surface overpressure, p_{so} .^{5, 15} This assumption merits further study, since limited studies suggest that actual value for p_m may range from somewhat greater than p_{so} to a small fraction of p_{so} .¹ Any final resolution of this matter will involve a much better understanding of combined soil-structure response to earth-transmitted dynamic loading.

The dynamic loading imposed on a structure by a megaton explosion can thus be characterized by its peak magnitude, p_m . The duration of this blast-initiated dynamic loading is long in comparison with the natural periods of vibration of typical structural members. Its rise time, by way of contrast, is frequently of the order of a few milliseconds. These relationships have been recognized and incorporated into an approximate design method, whereby the permissible elasto-plastic yielding of an idealized structure or structural member is analytically related to peak values of a step loading

IIT RESEARCH INSTITUTE

with zero rise time.⁵ Using this simplified approach a dynamic loading of peak intensity p_m is replaced, when analyzing the structural requirements for a fully-buried structure, by a statically-applied uniform load, q , of "equivalent" magnitude.¹ As a further simplifying assumption, considered reasonably valid for long-duration loading from megaton yields, the relation between the magnitudes of q and p_m is considered to be a unique function of the ductility ratio, μ , of a structural element.⁵ The maximum permissible value for μ , considering each structural element, is related to its material properties, its dimensions, and its type of restraint. Limiting values for this ductility are still under investigation,¹ but are frequently represented by the following:^{1, 5}

Table 1-1
VALUES OF DUCTILITY RATIO FREQUENTLY PROPOSED
FOR BLAST-RESISTANT DESIGN

Ductility Ratio μ	Structural Parameters	q/p_m
1.0	timber	2.0
1.3	reinforced concrete in compressive or shearing modes	1.6
3.0	reinforced concrete in flexural mode	1.2
10-30	ductile structural steel	1.0

It is also a requirement that the shelter be designed to furnish its occupants with adequate protection from ionizing radiation (initial radiation and fallout). It would be an acceptable design objective to provide a shelter with consistent levels of protection from all explosion effects, whereby (in a statistical sense, at least) the probabilities of blast-survival and radiation-survival for the sheltered occupants would be the same for all attack environments whose lethal effects do not exceed those levels assumed in the shelter design. This is not possible, since the yield-range relationships for overpressure and for ionizing radiation are considerably different. An alternative would be to design for "balanced" protection from these two effects when the shelter is just at the point of "failure;" this still presents a difficult problem. Factors of weapon yield, weapon makeup, burst height and atmospheric conditions, must be specified in considerable detail. This leads to

unworkable complexities when extended to any generalized analyses.

From the standpoint of economic studies, it is fortunate that additional radiation shielding can be provided in a fully-buried shelter at rather nominal structural cost. For this reason, it is usually acceptable for the structural evaluations of the shelter proper to assume that the "worst case" radiation field which corresponds to each specified level of overpressure will exist at the location of interest.¹ This radiation field, in earlier studies^{1, 2} was considered to consist of the maximum intensity of initial radiation (gamma rays, γ , and neutrons, n) associated with a specified level of overpressure and with any nuclear yield in the 1-100 MT range, plus a fallout gamma radiation field whose flux intensity one hour after the explosion is the free-field equivalent of 10,000 rad per hour for all cases of interest. As a final step, since the shelter designs in these studies were prepared for a statically-applied equivalent load, q , rather than for a dynamically-applied load, p_m , a constant value of the ductility ratio ($\mu = 1.3$, $q/p_m = 1.6$) was assumed in order to express the "worst case" radiation field in terms of the equivalent uniform load.¹ This was recognized as a rather crude approximation, but since it almost invariably predicted a radiation environment in excess of that which could reasonably be expected, was considered to be an acceptable approximation for generalized analyses. It is obvious, however, that such a design is not "balanced" in the sense of providing the sheltered occupants with consistent levels of protection from all adverse explosion effects. Such an objective, even if accepted as desirable, does not appear possible of fulfillment.⁴

Much of this same argument can be applied to the design of the shelter entranceway. Once the operational requirements have indicated its basic geometry, the entranceway must be designed to withstand the blast loadings and to furnish acceptable shielding from ionizing radiation. However, while the structural cost of the shelter proper^{1, 2} was found to be rather insensitive to the requirement for barrier radiation shielding (and hence to the initial postulates of the design radiation environment), this will not be equally true for entranceways. Radiation shielding for the basic shelter is in the form of a barrier, consisting of the shelter roof and the overlying soil, and a moderate increase in this barrier thickness is sufficient to effect a large decrease in the radiative energies which penetrate

within the shelter. In the entranceway, radiation streaming down the entranceway must be recognized in addition to direct radiation penetration through the earth cover and the entranceway structure. In this situation it is generally found that bends and specific corridor lengths must be deliberately introduced into the entranceway design, obviously at increased cost, in order to reduce the radiation to an acceptable level at the entranceway-shelter interface. Consequently, in order to identify minimum cost designs for entranceways, it becomes necessary to examine the pertinent features of the radiation field in considerably more detail than was justified in the studies of basic shelter structures. These aspects are reviewed in a subsequent section of this report (Chapter 5).

The maximum structural loading, p_m , which is imposed on a fully-buried shelter by a specified peak value, p_{so} , of surface overpressure, was approximated very simply in the studies of the basic shelter.^{1,2} For shallow burial and for megaton weapons, as previously stated, p_m and p_{so} were considered to be numerically equal for horizontal and curved surfaces. For vertical surfaces, such as exterior walls, this relationship was modified to the form $p_m = k_h p_{so}$. Here k_h is a constant which is related to the strength properties of the surrounding earth, and has a value ranging between zero and unity.⁵ For all conditions of loading, p_m was considered to act in a direction normal to the shelter surfaces.

The loading conditions are considerably more complex when a shelter entranceway is considered. First, at least a portion of the entranceway projects above the ground surface, and thus is directly exposed to the advancing blast wave. For such conditions, the peak loading on the projecting portions will be considerably larger than is implied by the peak values of the free-field pressures at the blast front. Next, except for those cases where a blast door at the ground surface seals the entire entranceway, the blast wave will advance into the entranceway and will produce large reflected pressures within the interior of this structure. As a consequence, there will be both direct and reflected pressures acting on above-ground portions of the structure, earth-transmitted pressures acting inwardly on below-ground portions of the entranceway structure, and multiple pressure-reflections acting outwardly from within the structure. The relative time-

sequencings of these several pressure applications may be of considerable importance in specific structural evaluations, but are not amenable to the generalized type of analysis considered herein. It should also be noted that, in the upper portions of the entranceway structure at least, the criteria for full-burial⁵ are not satisfied and a possibility of nonuniform loading and consequent localized structural failures (buckling, etc.), may exist. Again, this situation cannot be treated with precision in a generalized analysis. Blast loading design criteria, as used in this study, are discussed in detail in a subsequent section of the report (Chapter 4).

1.4 KNOWN LIMITATIONS OF THE STUDY

This study is intended to supply a generalized evaluation of design and cost alternatives for entranceways to fully-buried personnel shelters, giving particular emphasis to entranceways which can service those shelter structures considered previously.² The investigative technique used in this study requires initial postulates as to the operational and service requirements for the entranceway, which will include a description of pertinent features of the attack environment. Once these have been supplied, repetitive applications of preliminary designs and cost estimates can be used to identify "minimum cost" solutions. While these will subsequently be considered as "optimum" solutions, it is readily conceded that the practical necessity of adopting a generalized (hence considerably simplified) analytical approach, coupled with a very rudimentary state-of-the-art knowledge of many of the load-time-response relationships which are involved, can result in designs which are not truly "optimum." Recognition must also be given to the well-known uncertainties of the cost estimating process which are inherent in any "minimum cost" analysis. These become particularly troublesome as structural materials and shapes are grouped in classes for analytical simplicity. These are admitted shortcomings, and appear unavoidable in a study of this nature. Despite them, it is believed that this cost-minimization process will yield data which can be used subsequently, with appropriate regional and temporal modifications, to obtain valid preliminary estimates of entranceway costs.

In addition, since the choices of entranceway configurations for this study are admittedly arbitrary, there remains the possibility that some optimum combinations of structural materials and configurations have not been considered. There could conceivably be other entranceway configurations where, within some finite range of design conditions, the structural materials considered in this study could be utilized more economically. There could also be other structural materials which, either for the configurations considered herein or for some entirely different configuration, would be economically preferable. It seems unlikely, however, that the primary conclusions reached in this study would be significantly altered.

1.5 POSSIBLE USES FOR STUDY FINDINGS

The obvious use of the entranceway cost data to be developed in this study will be in conjunction with the cost data supplied^{1, 2} for the structural portions of the basic shelter. (In this regard, it should be carefully noted that the entranceway costs to be supplied herein will refer only to the structural portions of the entranceways and exits, to include blast doors and their supporting devices.) The relationships between cost, configuration and design loading, which will subsequently be developed in this study, should be of value in making preliminary studies of entranceway alternatives for a particular shelter location and function. As detailed design of the entranceway proceeds, it may also be helpful to make reference to the analytical equations which will be supplied herein for the critical structural elements. These analytical equations are accompanied by cost equations or expressions, which, when translated into current local costs, should serve as excellent guides to the proper combination of materials for minimum structural costs.

CHAPTER 2

STRUCTURAL MATERIALS

2.1 INTRODUCTION

In this study, the estimated in-place costs of the constitutive structural elements are summed to obtain comparative estimates of in-place cost for each of the entranceway structures. The in-place structural cost, in this usage, is defined as the estimated contract cost of obtaining the necessary material, labor, and equipment. The unit prices for these cost components have been compiled from various sources.^{7, 8, 9, 10} Their validity in the Chicago metropolitan area has been checked, insofar as this is possible, by contacting local contractors and fabricators.

The assumptions used in developing estimates of in-place structural cost are described in detail elsewhere,¹ and will be restated here only in summary form. First, the estimated costs of fabrication, treatment, odd-lot ordering, transportation and erection costs are added to the basic material cost. An additional 40 percent is arbitrarily added to this cumulative total as an allowance for job overhead, general overhead and profit. The total thus obtained will hereafter be referred to as the in-place cost, although it should be recognized that it excludes many real items which can affect the final cost of the shelter structure. It does not, for example, include any allowance for Architect-Engineer services in preparing preliminary designs, developing working drawings, preparing bidding documents, and supplying any general construction supervision. Neither does it provide for the costs of site acquisition and preparation, allocated charges by various government agencies during the implementation and performance of the construction, or any contract expenses not directly assignable to the structural portion of a shelter. It should also be recognized that the total in-place shelter costs which are derived in this study relate only to the basic structural portions of the shelter, which are considered to include the blast doors and their operating mechanisms.

2.2 STRUCTURAL STEELS

2.2.1 Strength Properties

The structural steels considered in this study are classified into two distinct groups; plates and heavy structural shapes. The rolled plates are designed to resist axial stress as load-supporting elements, either as a singly-curved surface in a semicircular arch or the barrel of a cylindrical shell, or as a doubly-curved surface in a sphere or in the dome ends of a cylindrical shell. The heavy structural shapes are those normally available as standard items from steel suppliers,¹¹ and include rolled beams and column sections. Such sections can function under direct or flexural loading as individual structural members, or can be combined to form rectangular and segmented bents. However, because of the myriad combinations which become possible, this study does not include an investigation of built-up or "sandwich" sections.

Yield strengths and primary failure modes, rather than deflection or stability criteria, are assumed to govern the design of the steel elements. Earlier investigations have indicated that the yield stress of a structural steel becomes greater at increased rates of load application.^{12, 13} This relationship becomes of particular significance when blast loadings are considered. In this study, the dynamic yield strength (f_{dy}) of a low-carbon steel in flexure and in direct tension or compression is postulated to be approximately 1.25 times its yield strength under a comparable static loading (f_y).^{1, 14, 15, 16} This postulate of a dynamic strength increase is not extended to the high-strength, heat-treated steels. For such steels, typified by 60,000 psi rolled shapes and 100,000 psi plates, the relationship $f_{dy} = f_y$ is assumed. The same shear-strength relationship ($f_{dy} = 0.60 f_{dy}$) is proposed for the dynamic loading of all types of structural steel. Table 2-1 supplies a grouping of typical structural steels, based on the dynamic yield strengths adopted for this study.

Table 2-1

GROUPING OF TYPICAL STRUCTURAL STEELS
ACCORDING TO DYNAMIC YIELD STRENGTH

Structural Category	Identification	Minimum Static Yield Strength (f_y , psi)	Assumed Dynamic Yield Strength (f_{dy} , psi)
Heavy Shapes	ASTM A-7, A-36	33,000-36,000	44,000
Heavy Shapes	ASTM A-242, A-440*, A-441	42,000-50,000	52,000
Heavy Shapes		60,000	60,000
Plates	ASTM A-7, A-36	33,000-36,000	44,000
Plates	ASTM A-242, A-440, A-441	50,000	60,000
Plates	Heat Treated	100,000	100,000

*ASTM A-440 is not recommended for welding.

2.2.2 Cost of Rolled Structural Shapes

Table 2-2

IN-PLACE COST OF ROLLED STRUCTURAL STEEL SHAPES,
DOLLARS PER POUND
($X_s = \$/\text{lb}$)

ASTM Designation	Dynamic Yield Stress, f_{dy} , psi	In-Place Cost, \$/lb	
		Wide-Flange Sections	I-Beam Sections
A-7, A-36	44,000	0.183	0.188
A-242, A-440, A-441	52,000	0.199	0.204
	60,000	0.202	0.207

2.2.3 Cost of Uniform-Thickness Plates, Curved

Table 2-3

IN-PLACE COST OF UNIFORM-THICKNESS CURVED STEEL PLATE,
DOLLARS PER SQUARE FOOT OF CURVED SURFACE
($X_s = \$/\text{sq ft}$)

Thickness of Steel Plate, in.	In-Place Cost, $\$/\text{sq ft}$					
	Singly-Curved Plate			Doubly-Curved Plate		
	$f_{dy} =$ 44,000 psi	$f_{dy} =$ 60,000 psi	$f_{dy} =$ 100,000 psi	$f_{dy} =$ 44,000 psi	$f_{dy} =$ 60,000 psi	$f_{dy} =$ 100,000 psi
3.00	55.00	59.50	-	-	-	-
2.50	42.75	46.00	-	-	-	-
2.00	33.00	35.50	-	-	-	-
1.50	22.95	25.50	-	-	-	-
1.25	18.55	20.50	-	-	-	-
1.00	14.35	15.75	20.60	20.00	21.65	25.70
0.75	10.20	11.25	14.45	13.37	14.60	18.20
0.50	6.08	6.70	8.90	8.22	8.95	11.40
0.25	3.21	3.53	4.45	4.45	4.84	5.90

2.2.4 Cost of Corrugated Steel Plate, Single-Curvature

Table 2-4

IN-PLACE COST
SINGLE-CURVATURE CORRUGATED STEEL PLATE,
DOLLARS PER SQUARE FOOT OF CURVED SURFACE ($X_s = \$/\text{sq ft}$)

Gage No. of Steel Plate	In-Place Cost, $\$/\text{sq ft}$	
	$f_{dy} =$ 44,000 psi	$f_{dy} =$ 60,000 psi
12	2.84	3.30
10	2.94	3.43
8	3.18	3.70
7	3.33	3.88
5	3.75	4.40
3	4.10	4.80
1	4.32	5.05

2.3 STEEL REINFORCING ROD

2.3.1 Strength Properties

The requirements for structural steels in blast-loading applications are, in general, equally applicable to concrete reinforcing steels. Table 2-5 lists the standard types of reinforcing bars and their corresponding static yield stresses, as set forth in ASTM standards.¹⁷ Four levels of dynamic yield strengths, - 44,000, 52,000, 60,000 and 75,000 psi, - are considered in this study. The 44,000 and 52,000 levels correspond to reinforcing steels with static yield strengths of 36,000-40,000 psi and 40,000-50,000 psi, respectively. No dynamic increase in yield strength is assumed for reinforcing steels with $f_y = 60,000$ psi (ASTM 432) and $f_y = 75,000$ psi (ASTM 431), since the limited ductility of these steels may affect their plastic behavior. All types of reinforcing steel should have their full continuity ensured by provisions for adequate lapping and by welding. Members with both top and bottom steel, adequately tied, will have greater ductility than singly-reinforced members with an equivalent quantity of tension reinforcement, hence are favored for blast-resistant design. For such members, which are described as "doubly reinforced", the quantities of reinforcement steel in top and bottom need not be the same. Shear reinforcement for flexural members, where required, should be placed normal to the bending axis.

Table 2-5

**KINDS AND GRADES OF REINFORCED EARS
AS SPECIFIED IN ASTM STANDARDS**

Type of Steel and ASTM Specification No.	Size Nos. Inclusive	Grade Designation	Static Yield Point Min., psi	Elongation in 8", Min. Percent (1)	Cold Bend Test (2)
Billet Steel A-15	2 to 11	Structural	33,000	$\frac{1,200,000}{\text{Tens.Str.}}$ Min. 16%	Under Size No. 6 - 180°, d = 2t Nos. 6, 7, 8 - 180°, d = 3t Nos. 9, 10, 11 - 180°, d = 4t
		Intermediate	40,000	$\frac{1,100,000}{\text{Tens.Str.}}$ Min. 12%	Under Size No. 6 - 90°, d = 3t Nos. 6, 7, 8 - 90°, d = 4t Nos. 9, 10, 11 - 90°, d = 5t
		Hard	50,000	$\frac{1,000,000}{\text{Tens.Str.}}$	Under Size No. 6 - 90°, d = 4t Nos. 6, 7, 8 - 90°, d = 5t Nos. 9, 10, 11 - 90°, d = 6t
Billet Steel A-408	14S, 18S	Structural		13	None
		Intermediate		10	None
		Hard		7	None
Billet Steel 60,000 psi Yield Point A-432	3 to 11	(3)	60,000	$\frac{1,000,000}{\text{Tens.Str.}}$	Under Size No. 6 - 90°, d = 4t Nos. 6, 7, 8 - 90°, d = 5t Nos. 9, 10, 11 - 90°, d = 6t
	14S, 18S	(3)	60,000	7	Nos. 14S, 18S - None
High Strength Billet Steel A-431	3 to 11 14S, 18S	(3)	75,000	Varies with bar size, 5% to 7 1/2%	Size Nos. 3, 4, 5 - 90°, d = 4t Nos. 6, 7 - 90°, d = 5t Nos. 8, 9 - 90°, d = 6t Nos. 10, 11 - 90°, d = 8t Nos. 14S, 18S - None
Rail Steel A-16	2 to 11	Regular	50,000	$\frac{1,000,000}{\text{Tens.Str.}}$ Min. 5%	None
	3 to 11	Special	60,000	$\frac{1,000,000}{\text{Tens.Str.}}$ Min. 5%	None
Axle Steel A-160	2 to 11	Structural	33,000	$\frac{1,200,000}{\text{Tens.Str.}}$ Min. 16%	Under Size No. 6 - 180°, d = 2t No. 6 and over - 180°, d = 4t
		Intermediate	40,000	$\frac{1,100,000}{\text{Tens.Str.}}$ Min. 12%	Under Size No. 6 - 180°, d = 6t No. 6 and over - 90°, d = 6t
		Hard	50,000	$\frac{1,000,000}{\text{Tens.Str.}}$	Under Size No. 6 - 90°, d = 6t No. 6 and over - 90°, d = 6t

(1) For base sizes of deformed bars. See specifications for adjustment for small and large sizes and for values for plain bars.

(2) d diameter of pin around which specimen is to be bent, and t nominal diameter of specimen. Values shown are for deformed bars. See specifications for values for plain bars.

(3) Designated by specification title and number.

2.3.2 Cost

Table 2-6

IN-PLACE COST OF STEEL REINFORCING ROD,
DOLLARS PER CUBIC FOOT OF STEEL
($X_s = \$/\text{ft}^3$)

Structural Element	Flexural and Temperature Steel		Shear Reinforcement (Vertical Stirrups)	
	$f_{dy} = 44,000$ to 60,000 psi	$f_{dy} =$ 75,000 psi	$f_{dy} = 44,000$ to 60,000 psi	$f_{dy} =$ 75,000 psi
Slabs, beams, columns, walls, foundations	78.8	85.8	92.5	100.5
Shells	85.8	100.5	Not Applicable	Not Applicable

2.4 PRESTRESS STEEL

2.4.1 Strength Properties

The initial stress in prestress steel is applied during the construction period and subsequently affects the concrete as a long-term static loading. This is true even in blast-resistant structures, since any dynamic loading less than the design load will only act to relieve the initial loading due to the prestressing forces. It is obvious that a dynamic increase in material strength is not justified when the maximum loading is the long-term prestressing load. Prestress steel is available in both strand and bar shapes. In addition, several strands can be woven into large tendons when required. Strand is particularly suited for use with shell elements, since its flexibility allows it to be readily developed into curved shapes. Table 2-7 lists representative prestress strand and bar sizes, as well as the ultimate and allowable strengths recommended by manufacturers and by the current code of practice.^{18, 19, 20}

Table 2-7

SIZES AND GRADES OF PRESTRESS STRAND AND BAR

Grade Designation	Size (in.)	Weight (lb/ft)	Strand		
			Ultimate* Strength (lb)	Initial Load 70% of Ultimate (lb)	Design Load (lb)
Standard ASTM 416 250K	1/4	0.122	9,000	6,300	5,040
	5/16	0.198	14,000	10,150	8,120
	3/8	0.274	20,000	14,000	11,200
	7/16	0.373	27,000	18,900	15,120
	1/2	0.494	36,000	25,000	20,160
270K	3/8	0.288	23,000	16,100	12,900
	7/16	0.395	31,000	21,700	17,350
	1/2	0.525	41,300	28,900	23,150
Bars					
Regular 145 ksi	1/2	0.67	28,400	19,900	17,000
	5/8	1.04	44,500	31,200	26,700
	3/4	1.50	64,100	44,900	38,500
	7/8	2.04	87,100	61,000	52,300
	1	2.67	113,800	79,700	68,300
	1-1/8	3.38	144,100	100,900	86,500
	1-1/4	4.17	177,900	124,500	106,700
	1-3/8	5.05	215,300	150,700	129,200
	1/2	0.67	31,400	22,000	18,800
	5/8	1.04	49,100	34,400	29,500
	3/4	1.50	70,700	49,500	42,400
	7/8	2.04	96,200	67,300	57,700
	1	2.67	125,600	87,900	75,400
Special 160 ksi	1-1/8	3.38	159,000	111,300	95,400
	1-1/4	4.17	196,300	137,400	117,800
	1-3/8	5.05	237,600	166,300	142,600

* Lacking specific test data, yield strength can be taken as 80 percent of ultimate strength.

2.4.2 Cost

The in-place unit costs of prestress steel are based on the assumption that material purchases are made in greater than 40,000 pound lots for single shipment to a single destination. Costs of prestress steel are related to strand size, and may vary by as much as 30 percent over the size-ranges cited in Table 2-8. However, this wide cost variation is a function of current demand rather than of inherent limitations in the manufacturing process.

Table 2-8

IN-PLACE COST OF PRESTRESS STEEL (X_{sp})

Size	Strand (\$/ft)	
	ASTM Standard	K-270
1/4	0.060	--
5/16	0.089	--
3/8	0.110	0.111
7/16	0.144	0.145
1/2	0.178	0.190
Bar (\$/lb)		
Regular (145 ksi)		Special (160 ksi)
all sizes	0.32	0.36

All prestress steel is assumed to be uncoated. When used as an external wrap, strand protection is provided by a 2 in. thickness of gunite at a cost of 0.30 \$ per sq ft.

2.5 STRUCTURAL CONCRETE

2.5.1 Strength Properties

Expressions for flexural and shearing resistances of reinforced concrete members are included in the design equations of this study. The ultimate compressive strength of reinforced concrete, for conditions of dynamic blast loading, is taken as 1.25 times its ultimate static strength

($f'_{dc} = 1.25 f'_c$).^{15, 16, 21} Lacking substantiating data, no dynamic strength increase is assumed where shearing modes become of critical significance. Walls, columns and shells are thus designed on the basis of an ultimate dynamic concrete strength, f'_{dc} , while flexural members are designed by equating the ultimate static strength f'_c to the static-loading shearing strength. The design values of f'_c used in this study (and any correspondingly derived values of f'_{dc}), are intended to be representative of the results of standard cylinder tests. The reduction factor of 0.85, which is conventionally introduced when equating cylinder test strengths to the in-place strengths of structural members, has been accepted and is incorporated in the design equations of this report. The unit bond strength, on the assumption that deformed bars with full anchorage will be used, is taken as $0.15 f'_c$ for all concretes.

The prestressing loads are applied to the concrete as a working load during the construction period. These loads will continue throughout the entire life of the structure, and blast loadings of lesser magnitude will only serve to reduce them. However, the long-term effects of creep, plastic flow and corrosion on initial prestressing requirements must be taken into consideration. Since the governing load is statically-applied and is of long duration, the conventional compressive design strength of $0.45 f'_c$ is used as the limiting value for compressive stress in all prestressed concrete elements.²⁰ Some tensile stress is considered as permissible in the concrete itself, if due to blast loading, but is limited to a maximum value of $3\sqrt{f'_c}$. Future experience and test data may eventually indicate the use of higher stresses in prestressed concrete but, for the moment, the rather conservative approach outlined herein appears to be advisable.

2.5.2 Cost

The estimated in-place costs for structural concrete are based on a ready-mix concrete which is hauled within the radius of the Chicago Metropolitan Area. If bucket placement is required for all structural elements, the costs shown for chuted concrete should be increased by five cents per cubic foot.

Table 2-9

IN-PLACE COST OF READY-MIX CONCRETE,
DOLLARS PER CUBIC FOOT OF CONCRETE
($X_c = \$/\text{ft}^3$)

Ultimate Strength of Concrete, psi		Chute Placed		Bucket Placed
Static, f'_c	Dynamic, f'_{dc}	Slabs and Beams	Foundation	Walls, Columns and Shells
2000	2500	1.09	0.95	1.00
3000	3750	1.14	1.00	1.05
4000	5000	1.21	1.08	1.13
5000	6250	1.29	1.16	1.21
6000	7500	1.37	1.25	1.30

2.6 CONCRETE FORMS

Form work costs, at their best, are still the least dependable of the values quoted in this section. The cost of form work may vary more than 200 percent on identical structures, depending on the contractor's ingenuity and ability to organize and supervise this phase of construction. The unit costs for forms, as indicated in Table 2-10, are based on a minimum of two uses of the form material.

Table 2-10

IN-PLACE COST OF FORMS FOR CONCRETE,
DOLLARS PER SQUARE FOOT OF CONCRETE SURFACE
($X_f = \$/\text{sq ft}$)

Description of Member	In-Place Cost of Form Work
Slabs and Beams	0.88
Walls and Rectangular Columns	1.00
Circular Columns	1.10
Shells	
Barrel Arch	1.05
Domes and Cylinders	1.40
Sphere	1.75
Foundations	0.75
Slab Poured on Ground	0.60

IIT RESEARCH INSTITUTE

2.7 EARTHWORK

It is assumed that open-cut excavation, with 1:1 side slopes, will be accomplished by scraper and tractor units. If conditions are such that shovel excavation is required, the unit costs listed herein should be increased by 40 percent.

Table 2-11

IN-PLACE COST OF EARTHWORK,
DOLLARS PER CUBIC FOOT
($X_e = \$/\text{ft}^3$)

Earthwork Item	In-Place Cost of Item
Excavation	0.036
Backfill	0.033
Haul of Waste	<u>0.026</u>
Total	0.095

2.8 MISCELLANEOUS

2.8.1 Stairs

The cost of entranceway stairs is expressed in terms of the cost per step, for stairways providing one to four traffic lanes (Chapter 3).

One lane - \$18.00 per step

Two lane - \$30.00 per step

Four lane - \$35.00 per step

2.8.2 Roller Supports for Blast Doors

<u>Door Material</u>	<u>Cost, \$/Door</u>
Steel	$n_L (50 + 30 t)$
Concrete	$30 n_L D$

where

t = thickness of steel plate, in.

D = thickness of concrete slab, in.

n_L = required number of traffic lanes

2.8.3 Blast Door Latch

<u>Door Material</u>	<u>Cost, \$/Door</u>
Steel	$n_L^{1/2} (50 + 10t)$
Concrete	$n_L^{1/2} (25 + 10D)$

2.8.4 Emergency Exit

The emergency exit consists of a 4 ft-0 in. inside diameter vertical pipe made of longitudinally prestressed concrete and containing a steel ladder. The installed unit cost of this exit is taken as 14.00 \$ per ft.

2.8.5 Flexible Metal Section Joints

Flexible shelter entranceway section joints are constructed of No. 10 gage steel plate in the form of a cold spring. These joints are to be designed to accommodate an 18 in. relative displacement between sections. The installed unit cost is taken as 2.90 \$ per sq ft.

CHAPTER 3

TRAFFIC CAPACITIES OF SHELTER ENTRANCEWAYS

3.1 INTRODUCTION

A comprehensive review³ of pedestrian flow rates, both observed and predicted, was prepared by this organization, in 1958, for situations which are physically analogous to those occurring in shelter entranceways (stairs, ramps, corridors, etc.). A subsequent report by Newmark⁴ utilized this earlier study, supplementing findings by more recent experimental data (the applicable provisions of the current National Fire Codes²²) proposed specific recommendations for use in traffic analyses of shelter entranceways. These two studies are the major sources of the dimensional and traffic criteria discussed in this chapter, and the reader is referred to them for additional detail.

The unit-of-exit-width concept, as developed in the National Fire Codes, is immediately applicable to the geometric analysis of a shelter entranceway. Here the unit of exit width is defined as the width necessary for the free movement of a single file of persons. The stipulated dimensional requirements of the unit of exit width will vary with the specific details of the exit passageway (railings, headroom), and are also related to the total number of exit units which are contained in each passageway.²² The theoretical maximum capacity of the unit of exit width, while not defined, would correspond to some optimum combination of pedestrian velocity and of pedestrian concentration. These optimum values will vary with the details and physical forms of the stairway, ramp and level corridor.

Maximum permissible design rates (persons per min) are specified in the National Fire Codes for each major traffic element of an exit system. This automatically suggests a design procedure whereby alternative arrangements of stairway, corridor and doorway units of exit width are examined. That combination is then selected which, when all design aspects are evaluated is considered to best satisfy a specified requirement for total exit capacity. With the exception of half-units, fractional units of exit width are not recognized in such analyses.²² There has been

some interest in exploring the relationships between "peak" and "average" pedestrian rates in both entranceway and exit facilities.^{3,4}

3.2 TRAFFIC RATES

For the shelter entranceways considered herein the basic traffic elements will consist of stairs, doorways, and corridors. The last of these elements may be level, or, where small changes in elevation are required between entranceway components, may be inclined and thus function as a ramp. All of these traffic elements, assuming that the specified dimensional criteria can be satisfied, are physically analogous to those normally considered for fire exits. For this reason, it is logical to postulate an entranceway layout whereby each traffic element contains one or more units of exit width. The elements of the entranceway, following the general procedure described for the fire exit design, would then be sized to accommodate the anticipated traffic flow.

Even conceding the validity of the unit of exit width approach, it should be recognized that the traffic criteria accepted for fire exit design may not be entirely applicable when shelter entranceways are considered. The traffic capabilities of the entranceway should be such that, within the obvious limits set by the capacity of the shelter itself, all people who arrive at the shelter location prior to sealing of the blast door are able to enter. It follows that the details of the entranceway design should facilitate the passage of a single person in as brief a time as possible. Its total capacity requirements will be established by the shelter size, the warning time, and the time-distributions of the arrivals at the shelter location. This situation is somewhat different from that considered for the typical fire exit, where the design population is concentrated near the exit system and where all exit movements must be completed within a few minutes following the alarm.

The implicit requirement for minimum travel time through a shelter entranceway can be recognized, but is largely beyond the control of the designer. The geometric layout of the entranceway will be established by the location of the shelter and by the need for attenuating blast loadings and radiation streaming. Obviously, a minimum of one unit of

exit width should be supplied in each traffic element of a shelter entranceway. The requirement for total entranceway capacity is much more difficult to assess, since only the shelter capacity will be known with any certainty. However, a rational determination of shelter design capacity will itself include prior considerations of population location and of warning time. The criteria used in establishing the entranceway capacity should obviously be consistent with those used in specifying the shelter capacity.

It is appropriate at this time to examine the conclusions reached by other investigators as to suitable design traffic rates for entranceways and exits. These rates, in all cases, are related to the standard unit of exit width. The National Fire Codes²² recommend design rates (presumably a weighted average) of 60 persons per minute for level exits and 45 persons per minute for stairs. The Armour Research Foundation³ (now IIT Research Institute) has analyzed pedestrian-movement data, and as a result has proposed average and peak rates of 50 and 70 persons per minute for level corridors. A possible peak rate of 80 persons per minute was computed for stairs, while ramps of less than 10 percent slope were found to have about the same capacity as level corridors. Newmark,⁴ after evaluating these and subsequent findings, proposed average and peak rates of 40 and 50 persons per minute for stairs, 50 and 70 persons per minute for level corridors, and 50 to 70 persons per minute for ramps with slopes below 10 percent.

These data, despite their admitted deficiencies, indicate rather minor spreads between the average traffic capacities of each traffic element. An examination of their peak traffic capacities leads to a similar conclusion. Further, it can be postulated that rather similar relationships exist between the predicted average and peak traffic rates for each traffic element. When appropriate recognition is given to the many uncertainties involved in any estimates of population movement under attack-threat conditions, plus the inherent differences between the fire exit and shelter entrance situations, there appears to be a reasonable justification for still further generalization of these design criteria. Therefore, it is proposed that a design capacity of 50 persons per minute, per unit of exit width, be assigned to all portions of a shelter entranceway without further consideration

of the specific traffic elements involved. This automatically leads to the concept of an entranceway traffic lane, whereby the several traffic elements (stairs, corridors, doorways and ramps) are series-connected to provide a uniform design capacity of 50 persons per minute per traffic lane or unit of exit width.

3.3 DIMENSIONAL CRITERIA

It now becomes possible to list the controlling dimensional requirements for various lane-widths in entranceways, which, in effect, merely involves a listing of the code requirements²² defining single and multiple units of exit for each entranceway element. Table 3-1 lists the minimum dimensional requirements, excluding minor provisions for doorways and jambs, which are applicable to interior portions of the entranceway.^{4, 22}

Table 3-1

DIMENSIONAL CRITERIA FOR ENTRANCEWAY TRAFFIC LANES

Entranceway Element	One-Lane		Two-Lane		Four-Lane	
	Width	Height	Width	Height	Width	Height
Stairway	2'-6"	7'-0"	3'-8"	7'-0"	7'-4"	8'-0"
Door	1'-10"	6'-6"	3'-8"	6'-6"	7'-4"	6'-6"
Corridor	2'-6"	7'-0"	3'-8"	7'-0"	7'-4"	8'-0"

Stairway riser and run dimensions are limited to a maximum of 7-3/4 in. for the riser and a minimum of 9-1/2 in. for the run. The maximum elevation difference between landings is limited to 8 ft-6 in. except where blast attenuation requirements, as discussed in Chapter 4, necessitate a greater height difference. Landing widths are restricted to a minimum of 1 ft-7 in.

Further research, probably of an experimental nature, could be used to establish the velocity-capacity distribution functions for traffic elements of an entranceway. For example, additional studies could be made of representative population dispersions adjacent to prospective

shelter locations, and pedestrian mobilities could be examined in simulated attack situations. The findings of these studies would then be used in establishing the probable time-accumulation functions, both within the entrance-way and exterior to it. Nevertheless, estimates of warning time will always remain conjectural, and may extend from a few minutes to several hours or days. A lower estimate of probable warning time is conservative from the standpoint of shelter utilization, since actual warning time in excess of that postulated for design purposes should not be detrimental. However, since there is obviously a relationship between warning time, loading time and the required entranceway capacity, an under-estimate of probable warning time may lead to greater entranceway costs. Intuitively, we may feel that there is adequate justification for providing a generous degree of entranceway capacity. This approach, admittedly, is uncertain at best and becomes meaningless in any rigorous economic study.

3.4 ENTRANCEWAY CAPACITY RELATED TO SHELTER CAPACITY

In this section an attempt is made to relate the entranceway capacity requirements, expressed in terms of required number of traffic lanes, to the theoretical capacity of each shelter. In Section 3.2 it was suggested that both the average and the peak pedestrian traffic rates obtainable in an entranceway could be considered as singular functions of the units of exit width, without further examination of the traffic elements which contain these width units. A constant traffic rate of 50 persons per minute lane was also proposed for design purposes, and this would then be considered as the practical capacity of a width unit. Therefore, it is of interest to explore the implications which are introduced by this assumption of a constant design rate.

A plot of arrivals versus arrival-times would, for any shelter, assume some form of a distribution curve. The elapsed time prior to the first arrival would be dictated by the travel time required for the closest person to reach the shelter. Subsequent arrivals would be distributed over some finite time period, which would end either when the explosion occurred or when the last person reached the shelter. For intermediate times, the arrival-accumulation would vary somewhere between a uniform and a peaked distribution.

Two different conditions can thus be identified, and should be recognized when establishing the requirements for entranceway capacity. If the duration of warning time appears critical, the entranceway capacity could be sized to allow each person to pass directly into the shelter without queuing or any similar delay. A precise design solution for this situation would require estimates of the time-accumulation distributions of shelter arrivals. Also, the lane capacity of the shelter entranceway should then be expressed as a time-density function rather than as a single design rate. The second condition arises when the elapsed time from first warning to the arrival of the last occupant is significantly less than the total warning time. In this latter situation, by controlling queuing outside the shelter and enforcing an orderly movement of people into the entranceway, the entranceway capacity could be sized to accommodate the average rate of arrivals rather than the peak rate.

For purposes of this study, a shelter loading period of five minutes will be assumed to be adequate for all designs of interest. This represents, when used in this context, a weighted estimate of the effective elapsed time between the first and last arrivals at the shelter location. The assumption of a five minute loading period, if combined with an estimated requirement of ten minutes prior to the arrival of the first person, is compatible with a 15-minute total warning time. Next, it will be assumed that the derived design rate of 50 persons per minute per lane can be applied as an average rate over this five minute period. By implication, this suggests that the unknown distribution function for the time-arrivals at the shelter location would be similar to the unknown velocity-capacity function which would describe pedestrian movement within the entranceways. While this last assumption has no adequate verification, it does supply a convenient basis for design. We can thus state,

$$n_L = \frac{N}{250} \quad (3-1)$$

where

n_L = required number of traffic lanes

N = design population of shelter.

Extension of Eq. (3.1) to the three shelter capacities considered in this study yields the entranceway lane requirements listed in Table 3-2.

Table 3-2

REQUIRED NUMBER OF ENTRANCEWAY LANES
AS A FUNCTION OF SHELTER CAPACITY

(assuming a loading time of 5 min and an average
traffic rate of 50 persons/min/lane)

Design Capacity of Shelter, N Persons	Required Number of Entranceway Traffic Lanes
100	1
500	2
1000	4

CHAPTER 4

DESIGN CRITERIA FOR BLAST LOADING

4.1 INTRODUCTION

The detonation of a nuclear weapon, unless occurring at a considerable distance below the natural ground surface, is accompanied by the formation of an air blast wave. Within a fraction of a second after such an explosion is initiated, a high-pressure wave is rapidly propagated outward from the fireball. In its ideal form, this pressure wave advances with a sharply-rising pressure front, known as the shock front, which exhibits a decreasing pressure gradient in the direction of its propagation center. The initial velocity of the travelling front is many times that of a sound wave in air. Both the wave velocity and the peak pressure in the wave front exhibit a time-dependent decay as the blast wave advances.⁶

At some distance removed from ground zero, the exact value of which is related to the burst height, the ground-reflected pressure wave induced by the shock front will merge with the direct pressure wave. This combined pressure wave is characterized by a near-vertical wave front and by peak pressures which may be two or more times those which would occur without ground reflection. It is this Mach region which is of primary interest to the designers of blast-resistant structures. The blast condition which it represents can conceivably be present throughout all or most of a region of blast destruction, and will then represent the worst-case loading condition for structural analyses.^{6, 16}

An actual blast environment may constitute less-severe loading conditions than those implied by an assumption that the structure is located in an idealized Mach region. A structure designed for a specified range-yield relationship may actually be located in the regular reflection region of a high-level burst. The peak loadings on the structure would then be substantially less than the Mach region loading which is assumed for design purposes. Also, while the ideal blast wave provides a severe structural loading condition because of its nearly-instantaneous rise time, an actual shock front may advance in a "nonideal" form with a significantly-delayed

III RESEARCH INSTITUTE

rise time.⁶ These or similar modifying conditions could exist in an actual attack situation and would result in appreciable departures from the structural loading conditions implied by the ideal blast wave assumption. There appears to be no way of incorporating these nonquantifiable probabilities into a generalized structural analysis, other than to note that their usual effect would be to reduce the actual loading on a structure.

4.2 BLAST LOADING ON STRUCTURES

There are three aspects of the blast wave which are of primary interest in structural analyses. The first of these is that pressure, conventionally expressed as the excess over ambient atmospheric, which is present at the front of the blast wave. This excess pressure, commonly referred to as overpressure, is propagated as a pressure pulse. Viewed at some point removed from the explosion center, this overpressure pulse is characterized by a finite time prior to its arrival, a near-instantaneous rise to a peak value, a time-dependent decay to below ambient atmospheric pressure, and a more gradual return to ambient pressure.³ A one-parameter description of the overpressure pulse at any ground range is commonly supplied in the form of its peak pressure intensity, p_{so} , as measured by a side-on gauge. A structure in the path of the advancing overpressure pulse will experience a dynamic loading as the pulse impinges on its near face and, to some extent, is reflected from it. The magnitude of the reflected pressure on an exposed structural face is related to the face orientation with respect to the front of the advancing wave, and for specific situations can become very large. This theoretical peak pressure, p_r , due to the reflection of the blast wave can be computed from the Rankine-Hugoniot equations. These equations are based upon the conservation of mass, energy and momentum of the shock front and are applicable in the Mach region of an ideal shock front. For air of moderate temperature, the peak-reflected pressure on a vertical plane due to zero degrees incidence of the shock front is given by⁶

$$p_r = 2 p_{so} \left(\frac{7 p_a + 4 p_{so}}{7 p_a + p_{so}} \right) \quad (4-1)$$

where

p_r = peak reflected pressure for zero degrees incidence of the shock front, psi

p_{so} = peak overpressure immediately behind the advancing shock front, psi

p_a = ambient atmospheric pressure ahead of the shock front, psi

IIT RESEARCH INSTITUTE

The terms of Eq. (4-1) are valid only for zero degrees incidence, since the ratios of p_r/p_{so} will differ for other incidence angles (for example, Fig. 3.71 b of Ref. 6). The actual peak magnitude of the air blast loading on an exposed structural face is a function of the free-field overpressure and the face orientation. It is significant, however, that values of this peak reflected pressure, p_r , for zero degrees incidence can range between two and eight times the value of the peak side-on overpressure, p_{so} . The time-decay from this peak loading, since the overpressure pulse rapidly engulfs a structure of typical dimensions, is related to the shape and geometry of the exposed structural face. In an actual structure, the various elements are sequentially loaded in a time-dependent manner as the blast front is first reflected from the front face and then sweeps over and around the structure. The structural requirements are dictated by the several responses to this loading sequence.

From Eq. (4-1), it was seen that the peak value of the reflected wave can be appreciably in excess of the value of two which is theoretically associated with complete reversal of a stress wave. This excess loading is attributable to a change in momentum as moving air particles are reflected at the structural barrier. The shock wave, as it propagates outward from the explosion center, is accompanied by blast winds whose peak velocities may reach hundreds of miles per hour. An air velocity gauge at some range from ground zero will show a finite arrival time, a rapid rise to a peak velocity, and time-dependent decay characteristics which are rather similar to those described for the overpressure pulse. For an idealized blast wave in air of moderate temperature, assuming that the structure of interest is located in the Mach region, the theoretical value of the peak dynamic pressure produced by the blast wind momentum can be related to the peak overpressure through the Rankine-Hugoniot equations.⁶

$$p_d = 2.5 \left(\frac{p_{so}^2}{7p_a + p_{so}} \right) \quad (4-2)$$

where

p_d = peak dynamic pressure due to the blast winds
accompanying the shock front, psi

p_{so} = peak overpressure immediately behind the advancing
shock front, psi

III RESEARCH INSTITUTE

p_a = ambient atmospheric pressure ahead of the shock front, psi

Alternatively, Eq. (4-2) can be expressed as the ratio of peak dynamic pressure to peak overpressure

$$\frac{p_d}{p_{so}} = \left[\frac{2.5}{1 + 7 p_a / p_{so}} \right] \quad (4-3)$$

Equation (4-3) indicates that, for peak overpressure in excess of approximately 70 psi, the numerical value of the peak dynamic pressure will theoretically exceed that of the peak overpressure. There is some current experimental evidence, however, which suggests that the actual dynamic pressures associated with moderately high overpressures (perhaps in excess of 50 psi) may be significantly greater than the theoretical values predicted by the Rankine-Hugoniot equations.

In this study, the dynamic pressures produced by the blast winds are of interest only by reason of the loadings which they impose on a structure in their path. A portion of this loading is due to the reflection of moving air particles as they encounter a structural barrier, and is incorporated in the expression for peak reflected pressure (Eq. 4-1). A second component of blast wind loading results from friction or drag forces as the blast winds sweep across a structure in their path. The magnitudes of these transient loadings are related to the characteristics of the blast wind (primarily its time-variation in velocity) and to the pertinent building characteristics (shape, orientation, size). The interaction between the blast wind and a building is frequently expressed in the form of a drag pressure on a structural element, which is computed by the following equation

$$p_{dr} = C_{dr} p_d \quad (4-4)$$

where

p_{dr} = drag pressure on the structural element considered, psi

C_{dr} = drag coefficient, uniquely related to the orientation, shape and size of the exposed structural face

p_d = peak dynamic pressure due to the blast winds accompanying the shock front, psi

A third loading mechanism of design interest results from the energy transfer as the blast wave advances over the ground surface. The blast wave, as it propagates outward from the explosion center, will impose dynamic loadings on the ground surface. These loadings can be expected to initiate stress waves within the soil mass. However, the pertinent properties affecting the velocities of stress wave propagations are appreciably different for air and soil media. Near ground zero, due to its high initial velocity in the region of the fire ball, the velocity of the air shock wave is many times that of the stress waves induced in any type of soil. Eventually, depending on the distance from ground zero and on the particular type of soil, the velocities of both waves become equal. Subsequently, the induced wave in the ground will outrun the air blast which initiates it.

The air-blast induced ground loadings are of particular interest in the design of fully-buried facilities, since these structures are not directly exposed to the blast wave. Many important aspects of the load-response mechanisms of a buried structure in a stress-wave environment are still unknown. While it is customarily assumed that the transfer of blast loading through shallow depths of soil is not accompanied by significant energy losses, there are obvious possibilities that the pressure wave form, and thus the loadings imposed as the pressure wave interacts with a structure, may differ for air and earth media. Also, the load-response of a buried structure is certainly influenced by the characteristics of the surrounding earth.

Analytical studies have considered the possible orientations of the induced ground pressure wave, recognizing the various soil types and the positions of buried structures.^{14, 24} These studies have indicated a time-dependent sequence of structural loading, which is somewhat modified from the time-dependent loading sequence as projected for a similar above-ground structure. Solutions so obtained are unique for each assumption of soil properties, structural dimensions, and blast characteristics; however, their use is impracticable in a generalized analysis. When recognition is given to such unknown factors as bomb positioning relative to the shelter location, and form of combined soil-structure response to blast-induced ground-pressure waves, there appears little justification for

any elaborate analytical approach. Consequently, while recognizing that the actual structural requirements could be appreciably different from those developed in a simplified analysis, it is assumed that the loading on horizontal surfaces of a fully buried structure can be represented as a step-loading with linear decay. The step loading initial magnitude is equal to that of the peak overpressure at the ground surface. Depending on the specific soil type, the loading magnitude on vertical surfaces is generally taken as somewhat less than this. All curved surfaces are treated similarly to horizontal surfaces.²³ The loadings on all surfaces are assumed to be dynamic in nature, applied simultaneously and acting normal to the structural surface. The possibility of rigid body accelerations and displacements of a buried structure in regions of high overpressure is recognized,²³ but specific consideration of such effects is not included in this study.

There is little real understanding of the actual load response mechanisms which prevail when a buried structure is subjected to blast induced earth pressures. We have described the common assumption that the peak dynamic loading (p_m) on such a structure is related only to the surface overpressure (p_{s0}) and, through the soil type (k_h), to the orientation of each structural face relative to the ground surface. A further analytical simplification can be introduced by replacing each simplified dynamic load by an equivalent static load, (q). These static loads, as was the case for the simplified dynamic loads, are assumed to be applied uniformly over the structural member of interest. The magnitude of the equivalent static load is determined by the requirement that the response of the structure, expressed in terms of its elasto-plastic yielding, must be the same for the simplified dynamic and equivalent static loads. This introduces the concept of the ductility ratio, μ , which is defined for each structure or structural member as the ratio of its total allowable yield (elastic and plastic) prior to some defined failure, to its maximum yielding in the elastic range. (See Table I-1 for typical values of μ , as related to structural material and configuration)

Figure 4-1. (from Fig. 5D-5)¹⁶ shows the plotted response of a one-degree-of-freedom elasto-plastic system to an initial-peak triangular force pulse. Since dynamic loading is involved, it is necessary to consider both the load duration and the natural period of the system. When our interest is

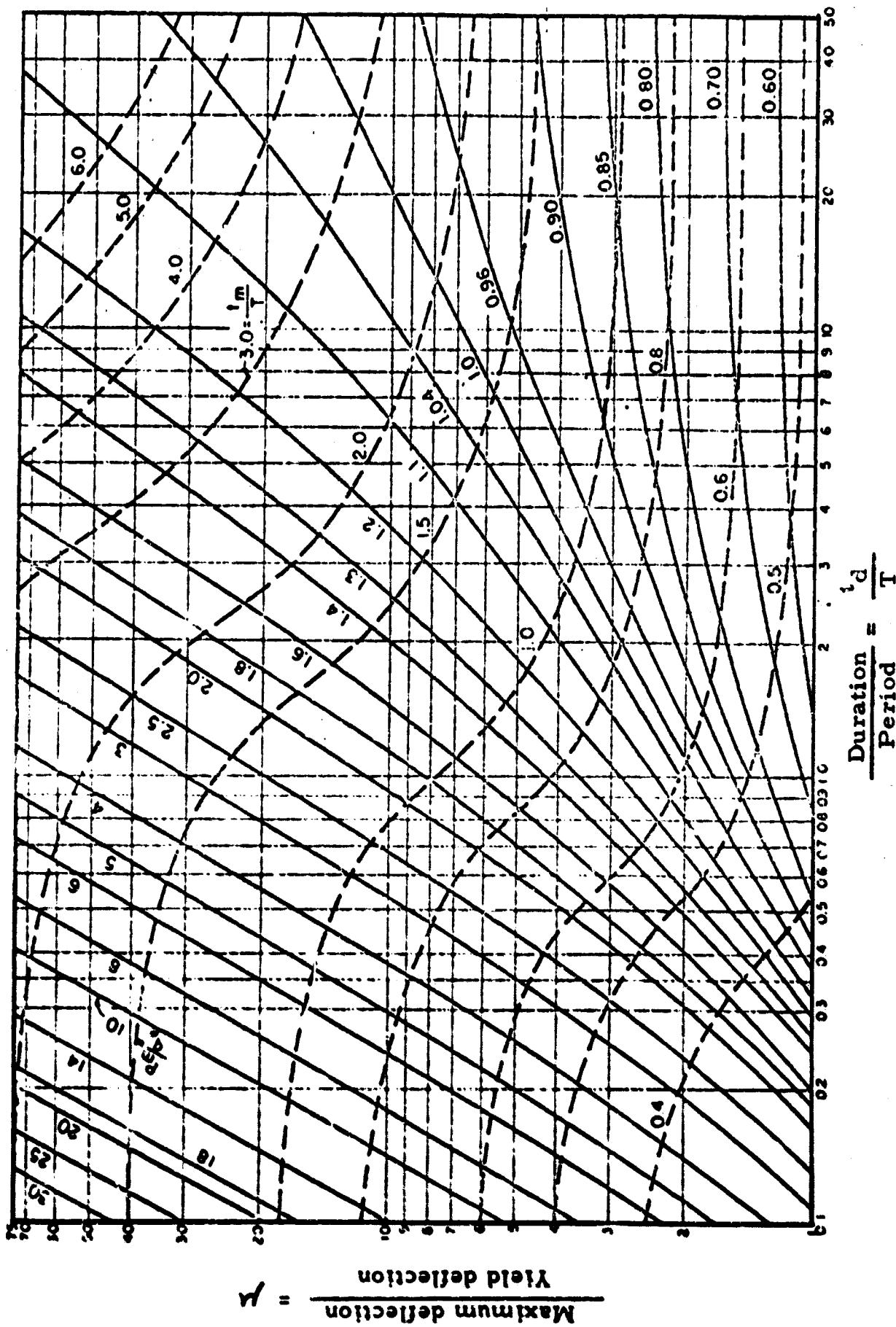


Fig. 4-1 EFFECT OF INITIAL-PEAK TRIANGULAR FORCE PULSE
ON AN ELASTO-PLASTIC SYSTEM

arbitrarily confined to those situations where the load pulse duration is much longer than the natural periods of vibration of the loaded structural members, it is reasonable to consider the loading as an infinite-duration step pulse. This is assumed to be the case for earth-transmitted loading due to the overpressure of the ground surface, since the effective load duration (for megaton weapons) may be one or more seconds. This duration is considerably longer than the natural periods of typical stiff load-resisting elements, such as are frequently considered for blast-resistant applications.

A somewhat different condition may exist when it is necessary to consider the loadings imposed on a structure by reflected dynamic pressures. Within an entranceway, for example, an advancing blast wave can be checked by a blast closure and thus be reflected back upstream. While the peak magnitude of the reflected pressure loading on the blast door may be very large, its effective duration may be appreciably less than the natural period of the loaded member. For such situations, since the loading is removed before the maximum structural response has occurred, it is unduly conservative to treat the loading as a step pulse.

In either event, by developing or postulating the limiting relationships between the effective load duration and the natural periods of vibration, it is possible to obtain unique solutions relating p_{so} , p_m , μ and q . These solutions are valid only within the limitations of the several assumptions which are incorporated in their development. Thus, once the ductility ratio μ for a member is either known or estimated, the ratio of its peak dynamic loading to an equivalent uniformly-distributed static loading ($p_m/q = p_{so}/q$ or $k_h p_{so}/q$ for earth-transmitted loading, and $p_m/q = p_{ri}/q$ for interior reflected pressure loading) can be read directly from Fig. 4-1.

A fourth type of structural loading, similar in many ways to that attributed to air-blast-induced ground pressures, can be experienced by buried structures close-in to the crater region of a surface or underground explosion. In these circumstances, there will be direct transfer of explosion energy to the surrounding soil mass. The earth pressure waves thus initiated can be of high intensity, but are considered to be of limited range.⁶ It is postulated, for purposes of this current study, that their loading effect

will not be of structural significance within the 10 psi - 200 psi overpressure range of interest. In so doing, it should be recognized that the possible effects of ground shock environments in sheltered personnel and on shelter equipment may well merit more detailed attention in the later design stages.

It is also significant to note that it is conventional design practice in a generalized blast loading analysis to assume that worst case loading conditions are present for each major element of an exposed structure. In simplified form, this means that the roof and each wall of an above-ground structure are separately designed for zero degrees incidence of the reflected pressure front in the Mach region of an ideal blast wave. Since radically-different positionings of the explosion center are thus introduced, it is obvious that no single weapon would produce the design loading on all structural surfaces. Nevertheless, in order to obtain satisfactory assurance that the entire structure will always withstand an overpressure loading of the design magnitude, such an approach seems inescapable. One intuitively suspects that a probability of structural survival is thus introduced, related only to the attack conditions and totally distinct from any ancillary consideration of material variability and analytical precision. There exist finite probabilities that a single structure or a group of structures could actually withstand overpressure in excess of the magnitude assumed for design purposes. Unfortunately, there appears to be no acceptable means for describing those probability functions and incorporating them into a structural survivability analysis.

4.3 CRITERIA FOR ENTRANCEWAY DESIGN

The entranceways of interest extend from the ground surface to a shelter buried at some level below the ground. As a result, any aboveground portions will be directly exposed to the passing blast wave and thus must be designed to resist overpressure and blast wind loadings. Except for those entranceway layouts where a blast-resistant door is located immediately at the ground surface, the blast wave will penetrate into the interior of the entranceway. For these last situations, complex and time-dependent sequences of interior and exterior loading are imposed on the shelter structure. Any generalized analysis of the actual loadings lies beyond our current

capabilities, and it is necessary to introduce several approximations in order to obtain workable loading functions.

Studies at IITRI have indicated that the peak free-field values of the blast wave components are modified, to a limited extent at least, when the blast wave enters a tunnel. Figure 4-2 illustrates the experimentally-determined relationships between peak overpressure in the free-field, entranceway orientation relative to the blast front, and the fraction of the peak overpressure which is transmitted within the tunnel. Although the tunnel orientation with respect to the direction of blast wave travel is of importance, (Fig. 4-2) it is adequate for this study to assume a 45 deg incidence angle between the entranceway axis and the direction of the blast wave. A finite length of entrance tunnel is also necessary in order to obtain the blast attenuations indicated in Fig. 4-2. Again for purposes of this study, it will be assumed that this requirement is satisfied by a minimum length-to-width ratio of 1.5. In this definition the tunnel width is taken as the largest cross sectional dimension of the entranceway opening, while the tunnel length is that of the entranceway upstream from the blast door.

Since the entranceway must be designed to withstand the maximum loadings produced by an entering blast wave, it is necessary to recognize the existence of transient reflected pressures within the structure. Such reflections will occur at an interior blast door, at surfaces adjacent to bends within the structure, and at all perimeter surfaces as the blast wave penetrates and fills the entranceway. The precise natures of these pressure increases, recognizing the time-pressure variations of loading and the existence of multiple reflections, are extremely complex. Even when rigorously-defined input data are supplied for a specific weapon burst and structure, an analytical evaluation of load-response relationships is very difficult. For the generalized analysis considered herein, where ranges of attack conditions and entranceway conditions must be expressed in simplified form, certain approximations become necessary. It has been assumed that interior reflected pressures can be estimated by assuming zero degrees incidence between the pressure front and the reflection face, and by applying a modified form of the Rankine-Hugoniot equation to compute the peak reflected pressure. With these assumptions, the peak interior reflected

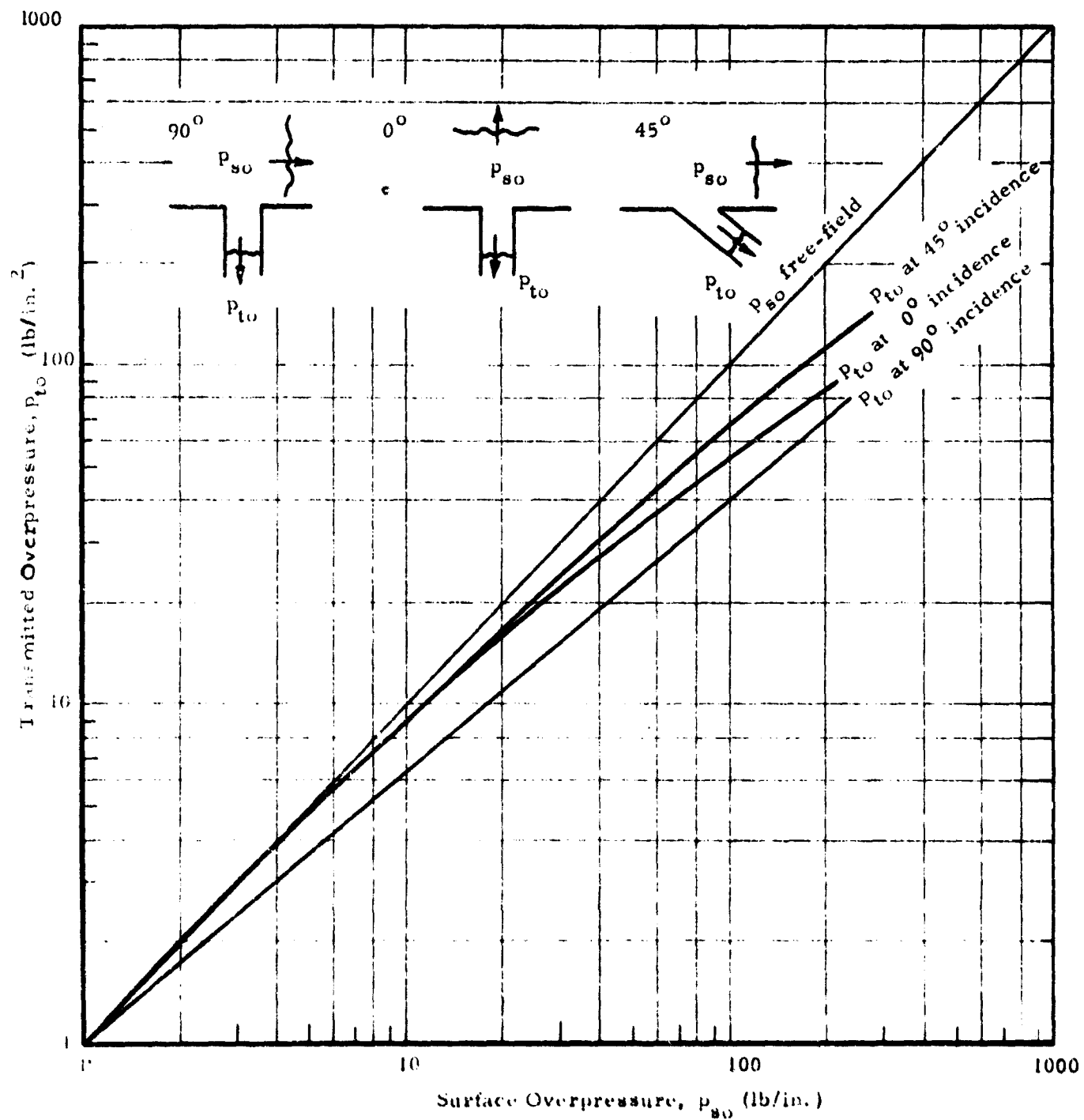


FIG. 4-2 SURFACE OVERPRESSURE VS TRANSMITTED OVERPRESSURE
WITHIN DUCTS WITH OPEN ENDS

pressure is expressed as:

$$p_{ri} = 2 p_{to} \left(\frac{7p_{to} + 4p_a}{7p_{to} + p_a} \right) \quad (4-4)$$

where

p_{ri} = peak intensity of reflected interior pressure on any structural surface within the entranceway, assuming 0 deg incidence between the overpressure front and the structural surface

p_{to} = peak intensity of transmitted overpressure within the entranceway, psi

p_a = ambient atmospheric pressure in entranceway ahead of shock front, psi

It is now possible to relate peak interior reflected pressures, which constitute a critical basis for entranceway design, to the free-field surface overpressure at the entranceway location. This is accomplished by first using Fig. 4-2 to obtain the transmitted overpressure which corresponds to a specified value of the free-field overpressure and to a known (vertical plane) entranceway orientation relative to the blast front. The peak interior reflected pressure is then computed with the aid of Eq. (4-4), and is assumed to be acting normal to all interior surfaces which are located upstream from the blast door. Interior bends are considered to have no discernible effect in reducing the peak magnitude of this interior loading.

The exterior blast loading in the entranceway structure consists of overpressure and dynamic pressure loadings on any above-ground portions, as earlier noted, plus ground-transmitted loadings on the below-ground portions. Since the entranceway provides pedestrian access between the ground surface and a fully-buried structure, the empirical requirements for full-burial^{16, 23} will not be entirely satisfied over some part of the entranceway length. The portions so excluded can be expected to be somewhat more susceptible to localized buckling and yielding, since by inference there is insufficient earth cover to ensure the existence of uniform loading conditions prior to their collapse.

The effective exterior loadings on the below-ground portions of an entranceway structure are highly indeterminate. The time-pressure characteristics of the blast induced pressure wave at the ground surface are

III RESEARCH INSTITUTE

probably modified as the pressure wave progresses downward through the soil. As a result, the rise time of the induced pressure wave and its related effect on a structure may be considerably changed from those implied by the free-field relationships. The wave front orientation as the ground pressure wave approaches a buried structure will also differ appreciably from the Mach stem conditions at an above-ground structure, further contributing to an altered loading sequence for buried structural members. It can be expected that some reflection of ground pressure will exist at the soil-structure interface, since these media have different wave-propagating properties. As the buried structure begins to deform under the ground transmitted loading, the active and passive soil resistances which mobilize adjacent to the different parts of the structure will further alter the requirements for structural load resistance.

While many or all of these effects may exist, they are not given explicit recognition in the simplified analyses. Rather, the surface overpressure is considered to be transmitted directly through any soil cover and to be applied to the structure as an instantaneous load pulse. The peak value of this normal loading is equated to the peak surface overpressure for both horizontal and curved surfaces and, for vertical surfaces, is reduced by a factor k_h whose value is primarily dependent on the soil type. Structural stresses in other loading planes are largely ignored, as are specific considerations of buckling and localized yielding. These same assumptions were used in the structural analyses of fully-buried shelters of 100-man, 500-man and 1000-man capacity.^{1, 2} In this study, however, they are extended to structural regions where the requirement for full-burial cannot be satisfied. While errors are thus introduced in estimates of structural loadings due to externally-applied pressure, it is postulated that these will not be critical if (as is usually the case for the entranceways considered herein) much larger values of internally-applied pressure are simultaneously present.

The several simplifications which are proposed for use in analyzing the effects of blast loading on entranceways to fully-buried entranceways can now be summarized. The shelter location is assumed to be in the Mach region, and critical overpressure-range-yield relationships at the ground surface are determined accordingly. The free-field characteristics of the

shock front are known to be modified when the blast wave penetrates an entranceway, and this effect is recognized in Fig. 4-2. The relationships shown on this figure are referenced to the orientation of the entranceway with respect to the blast front, and when applied to the free-field peak overpressures will predict the values of the peak overpressures within the entranceway. In applying these relationships, however, it is required that the entranceway have a minimum length-to-width ratio of 1.5.

The interior peak reflected pressure is calculated from the reduced peak overpressure, using Eq. (4-4), and is considered to be acting normal to all interior entranceway surfaces which are located upstream from the blast-resistant door. The dynamic loading which is thus imposed will determine the structural design of the door and its supporting elements, as will subsequently be discussed (Chapter 6). In addition, it will almost invariably be found that this reflected pressure loading is sufficient to control the structural design of all upstream elements of the entranceway. Any passive earth resistance which acts on the exterior surfaces of these elements, to the extent that it becomes operative during the effective duration of the reflected pressure loading, will tend to reduce the net loading and hence the structural requirement. This mitigating effect is not recognized in this generalized study, however, since the structural yieldings necessary to develop significant passive earth resistance could become intolerably large in many soil types.

The effective duration of the reflected pressure loading is related both to the velocity of the pressure wave and to the interior geometry of the entranceway passage. Any rigorous quantitative determination can become highly complex but, as noted earlier, it can be reasoned that this duration will be very brief. Commencing at approximately the same time as this reflected pressure loading, but extending for significantly-longer durations which are related primarily to the characteristics of the design weapon, all exterior portions of the entranceway structure are subjected to an inwardly-directed loading whose magnitude is directly related to the peak surface overpressure, p_{so} . This loading is applied normal to all structural surfaces, and has a magnitude of p_{so} for horizontal and for curved surfaces. For vertical surfaces the design loading is reduced to a value $k_h p_{so}$, where k_h can range between zero and unity.^{1, 23} A value of $k_h = 0.5$ is assumed for all designs considered in this study.

IIT RESEARCH INSTITUTE

The interior and exterior loadings thus act in opposing directions, and, to the extent that they act concurrently, will tend to counteract each other. Since the interior pressures are reflected to values which are at least twice that of the interior overpressure, the internal loadings are generally larger than the external loadings. However, the effective durations of the interior loadings can be significantly less than the corresponding durations of the external loadings. The external loadings from a megaton-yield weapon can be approximated as a step-loading insofar as the response of the majority of structural members is concerned, since the load-duration is considerably longer than the natural periods of such members. The interior loadings are more representative of impulsive-type loadings since their effective durations are probably comparable to the natural periods of typical structural elements.

This discussion of criteria for the blast-loading design of shelter entranceways will be concluded by noting that, for purposes of this study, the dynamic loadings resulting from the blast-wave interactions with the entranceway structure will be analytically replaced by their equivalent static loads. The equivalency between dynamic and static loading, as has been described for the shelter proper,^{1, 16} is considered to be a unique function of the ratio of effective load duration to natural period (t_d/T) and of the allowable elasto-plastic yielding (μ) for a particular structure. For overpressure-induced loading from megaton-yield weapons the ratio t_d/T becomes large, and as described for the shelter proper,^{1, 16} the equivalence between dynamic and static loading can be regarded as a unique function of the ductility ratio. A value of $\mu = 1.3$, for example, suggests little probability of damage to a ductile structure since the maximum permitted deflection is only 30 percent greater than the elastic yield deflection. For this value of μ and for larger values of t_d/T , as is apparent from Fig. 4-1, the structural member would be designed for an equivalent static load of magnitude $q = 1.6 p_m$. This corresponds to the overpressure-loading case, and typical q/p_m relationships for this situation are listed in Table 1-1. For reflected pressure loadings, lacking more precise information, it is suggested that t_d/T be taken as 1.0 and values of q/p_m determined accordingly. For example, for $t_d/T = 1.0$ and $\mu = 1.3$, Fig. 4-1 indicates that $q/p_m = 1.18$.

CHAPTER 5

DESIGN CRITERIA FOR RADIATION SHIELDING

5.1 INTRODUCTION

The several forms of ionizing radiations which can result from a nuclear explosion are commonly grouped into two broad classes. The first of these, arbitrarily considered to include those ionizing radiations which are evidenced within the first minute following the explosion, is referred to as initial radiation. This initial radiation, at least insofar as shelter design is affected, consists primarily of gamma rays and neutrons. It can be further subclassified as prompt radiation, which is emitted almost instantaneously at the time of the detonation, and the delayed radiation which is released during the remainder of the initial radiation period.⁶ While the energy components of the prompt and delayed radiations may be appreciably different, it is sufficient for purposes of this study to group them within the single classification of initial radiation.

The second major category includes those residual ionizing radiations which are present at times later than one minute after the explosion. The weapon residues from a fission weapon, along with any neutron-induced radioactivity in the soil, are typical sources of residual radiation. The situation of primary concern occurs when these sources are incorporated into large quantities of soil, as in the case of a surface or low-altitude burst. They are then raised in the ascending cloud, and subsequently may be wind-dispersed over large land areas. This dispersed radioactive material is commonly referred to as fallout, and can be further identified as early fallout or delayed fallout.

Early fallout⁶ is deposited on the earth's surface within the first 24 hours following a nuclear explosion. It can constitute a significant biological hazard, since it extends over wide areas and discharges its energy over long periods of time. Delayed fallout, which consists of any remaining portions of the fallout, is finer and more widely-dispersed. Because of the small particle sizes and slow settling rates of the delayed fallout its radioactivity has considerably diminished by the time the particles reach the ground. Several forms of residual radiation may be present following a

nuclear burst. Our primary concern is directed to the occurrence, distribution, and time-intensity decay of fallout.

5.2 RADIATION UNITS (Exposure Dose, Absorbed Dose, and Biological Response)

The intensity of a gamma radiation field is normally expressed in units of roentgens, R, and can be measured quantitatively by observing the energy release due to ion pair production as the gamma rays pass through air. The roentgen provides a useful measure of exposure dose, although it is not strictly applicable when describing neutron radiation.⁶ However, since our interest is more closely related to the absorbed dose, it is frequently preferable to introduce units of rads when describing a radiation field. Here the rad is defined for any nuclear radiation as that absorbed dose which results in the liberation of 100 ergs of energy per gram of absorbing material.⁶

Ionizing radiations, both initial and residual, are of significance in this study only by reason of their possible biological effect on shelter occupants. Since the biological effects produced by an absorbed dose are influenced by the nature of the absorbing medium and by the type of radiation, it is useful to introduce the concept of Relative Biological Effectiveness (RBE). In order to establish the RBE associated with a given form of radiation and a particular biological tissue, it is first necessary to observe the tissue response to a reference dose of gamma radiation at a specified energy level. The same tissue is then exposed to the radiation form of interest, and a determination is made of the absorbed dose which produces the same observed effect as did the reference dose. The RBE is calculated as the ratio of these two absorbed doses, both expressed in rads. Finally, when our interest is confined to those injuries produced in human tissue as a result of radiation absorption, it is convenient to introduce the concept of the rem, or roentgen equivalent man. By definition,

$$\text{Dose in rems} = \text{RBE (man)} \times \text{dose in rads}$$

The rem thus permits a quantitative prediction of the absorbed radiation dose associated with each specified level of biological injury in human tissues. Knowing the radiation energy spectrum and the RBE (man) for each associated form of ionizing radiation, it becomes possible to relate

human biological damage to the intensity of a known radiation field. In practice, since we are primarily concerned with initial and delayed gamma radiation and with neutrons, it is sufficient to know the RBE (man) for only these radiation forms. Conventionally, while recognizing that a degree of approximation exists due to the implicit averaging of radiation energies, the RBE's for both forms of gamma radiation and for neutrons are taken as 1.0. The biological dose for specific injury to humans (rem) then becomes numerically equal to that absorbed dose which releases 100 ergs of either gamma or neutron energy per gram of absorbing material (rads).

The gamma radiation exposure dose is commonly measured in roentgen units. Since the energy-release associated with the passage of one roentgen of gamma radiation through human tissue is approximately equal to 100 ergs per gram of tissue, there exists a rough numerical equivalence between the roentgen (exposure dose), the rad (absorbed dose) and the rem (human biological effect). In a neutron field, where the exposure dose is normally expressed as an integrated neutron flux, it has been found that an integrated flux of one neutron per sq centimeter is equivalent to an absorbed dose of 1.8×10^{-9} rad. This equivalence applies to neutrons from fission weapons, having energies in excess of 200 electron volts. We can thus relate fission neutron flux (exposure dose) to the rad (absorbed dose) and, since $RBE (man) = 1.0$ for neutrons, we can also relate neutron rads to neutron rems.

These relationships permit a major simplification in radiation shielding studies. Once the tolerable degree of radiation biological damage has been postulated, the effectiveness of any radiation shielding system can be explored through a numerical comparison between the tolerable dose (rem), and the sum of tissue-absorbed gamma radiation and neutron radiation (rad). If the absorbed dose does not exceed the tolerable dose, it can be concluded that the radiation shielding system is adequate.

5.3 INITIAL NUCLEAR RADIATION

5.3.1 Significance in Shelter-Entranceway Design

The initial ionizing radiations of interest in shelter entranceway design, as indicated earlier, consist of the gamma and neutron emissions during the first minute following a nuclear explosion. Their design significance can be related to two distinct processes, insofar as this analysis is concerned. First, some portion of the initial radiation energies will penetrate through the cover soil and the structural envelope of a shelter entranceway. It is this mechanism of radiation penetration which was considered in the analyses of the shelter proper,^{1,2} and it must similarly be recognized in the entranceway design. Using a simplified approach as described in these earlier studies, the cover soil and the entranceway roof can be analyzed as a thick barrier shield which is exposed to the free-field radiation. This dose contribution at any point inside the entranceway is then computed from the free-field intensities (gamma and neutron), the directional orientation and spectral energy distributions of these radiation forms as they impinge on the barrier shielding of interest, and the attenuation of their radiative energies due to passage through the shielding. The depth of earth cover thus becomes an important consideration, distinct from any full-burial requirements otherwise postulated for blast resistance. The simplified analysis suggests that the maximum radiation penetration for a given barrier and intensity of radiation field will occur when the effective barrier thickness (i. e., slant distance through the barrier) is a minimum. This condition corresponds to an overhead burst.

The second mechanism by which initial radiation may enter the system is known as radiation streaming. Here gamma and neutron radiations penetrate the entranceway mouth, passing through a barrier shield if a blast door or similar baffle is encountered, and stream along the interior of the entranceway passages. The resulting radiation hazard to shelter occupants is related to the pertinent free-field characteristics of the initial radiation, to the fraction of this flux which actually penetrates the entranceway mouth, and to its energy degradation during the streaming process. A quantitative consideration of these mechanisms requires some estimates of the directional orientation and energy distributions of the initial radiation components.

III RESEARCH INSTITUTE

Subsequently it will be shown that, as a result of the directional orientation of the initial radiation, the maximum streaming usually occurs when the axis of the entranceway depth element is directed towards the explosion center. Since the depth element is inclined at approximately 50 deg with the vertical ($\psi_E \approx 50$ deg) for the level-ground assumption used in this study, it follows that maximum radiation streaming will occur when the explosion is positioned some 40 deg above the horizon, ($\psi_B = 50$ deg). This explosion position does not coincide with the maximum barrier penetration of the entranceway and of the entranceway proper, which is instead associated with an overhead burst ($\psi_B = 0$). Obviously, the height-of-burst positioning of the bomb for worst case radiation analyses of the combined shelter system will involve tradeoffs between radiation streaming and barrier penetration.

5.3.2 Free-Field Characteristics of Initial Radiation

1. Yield-Range-Dose Relationships

The numerical value of the initial gamma radiation exposure dose, at any range of significant interest, is related to the explosion yield and to details of the bomb design. Gamma ray exposure doses have been measured at various ranges and for various yields, leading to a generalized scaling law which relates gamma flux and weapon yield. For convenience, on the basis that an exposure dose of one roentgen of gamma radiation is approximately the numerical equivalent of one rad, this scaling law will be expressed in terms of absorbed dose.

$$\gamma_w = \gamma_o W' \quad (5-1)$$

where

γ_w = absorbed (unshielded) initial gamma radiation dose (rad)
at any slant range R_s from a fission yield of W megatons

γ_o = absorbed (unshielded) initial gamma radiation dose, rad,
at the same slant range from a 1 KT fission-yield of a
similar explosion. (Fig. 8.27a for values of γ_o corresponding to a fission weapon and an above-ground burst)⁶

R_s = slant range between explosion center and point of interest, ft

W = fission yield, expressed in equivalent megatons of trinitro toluene

W' = scaling factor for initial gamma radiation, based on the specified fission yield of W MT (Fig. 8.27b of Ref. 6;

Note that W , as used herein, refers to yield in megatons rather than kilotons)

III RESEARCH INSTITUTE

If the fission yield is held constant, the absorbed dose from the initial gamma radiation will decrease with increasing R_s . This decrease is due in part to the inverse square relationship which holds for any expanding sphere, whereby the gamma flux will vary inversely as the square of the distance from the explosion center. However, there is a further decrease in the free-field flux which is attributable to scattering and attenuation as the gamma rays pass through the air. Considering an air burst, the range-yield and unshielded absorbed-dose relationships for initial gamma radiation are given by⁶

$$\mathcal{Y}_w = \left[\frac{2.9 \times 10^{10} \times W'}{R_s^2} \right] e^{-R_s/1080} \quad (5-2)$$

The attenuation of gamma radiation energy is actually related to the air density, which is in turn related to the air temperature and the burst elevation. Equation (5-2) is thus an approximate expression and, as indicated, is only applicable where the explosion occurs as an air burst. When a surface burst must be considered, it has been suggested⁶ that the corresponding values of \mathcal{Y}_0 (and hence of \mathcal{Y}_w) can be taken as two-thirds those predicted for an air burst (Fig. 8.27a).⁶ Because of major uncertainties as to the bomb makeup and the actual intensities of the resulting gamma radiation, any burst-height distinctions in the predictions of the absorbed initial-gamma doses become rather academic.

The absolute value of the neutron flux at any range distance, to an even greater extent than to that described for the initial gamma radiations, is dependent upon weapon yield and bomb makeup. Lacking any predictive understanding of bomb makeup, the neutron flux is customarily expressed as a singular function of the yield

$$n_w = 1000 n_0 W \quad (5-3)$$

where

- n_w = integrated neutron flux in air at range R_s from a W MT fission-yield explosion, neutron/cm²
- n_0 = integrated neutron flux in air, neutron/cm², at the same range from a 1 KT fission-yield explosion (Fig. 8.61 of Ref. 6 for values of n_0 corresponding to a fission weapon and an above-ground burst)

W = explosion yield in equivalent megatons of TNT

As with the initial gamma radiation, the integrated neutron flux decreases with increasing distance from the explosion center. The relationships between neutron flux and absorbed dose can be expressed in the following approximate forms for air bursts⁶

$$N_o = 1.8 \times 10^{-9} n_o \quad (a)$$

$$N_w = \left[\frac{1.4 \times 10^{14} \times W}{R_s^2} \right] e^{-R_s/630} \quad (b) \quad (5-4)$$

(Equations (5-4a) and (b) are approximately correct for fission neutrons with energies in excess of 200 electron volts, and for scaled ranges in excess of 1500 ft.)

where

N_o = absorbed (unshielded) neutron dose, expressed in rads, at slant range R_{so} (ft) from a 1 KT fission-yield explosion

N_w = absorbed (unshielded) neutron dose expressed in rads, at slant range R_s (ft) from a W MT fission-yield explosion

(N_o and N_w are obtained by assuming that an integrated flux of one neutron per cm^2 is equivalent to an absorbed dose of 1.8×10^{-9} rad for fission neutrons with energies in excess of 200 electron volts and for $R_{so} > 1500$ ft.)

2. Angular Distribution of Radiation Energies (Energy Spectrum)

The sum of the integrated gamma and neutron energies, computed for any specified set of weapon characteristics and at any range of interest, provides an estimate of the combined free-field energies of the initial radiation.

The absolute values of these energies as they exist at any specified range from the explosion center can be influenced, in considerable degree, by details in the design of the weapon and of its casing. A purely fusion weapon, for example, will emit high-energy neutrons (≈ 14 Mev) but will not emit fission-product gammas. If a layer of uranium can be used to blanket the neutron emissions from this same fission weapon, the result will be evidenced in the significant production of gamma radiations. Although all of the energy fractions of the initial radiation are degraded and absorbed to some extent due to their passage through the absorbing medium, these

changes occur in different ways. In theory, the net result for a combination of fission product and nitrogen capture gamma radiations is a general trend towards a relatively harder energy spectrum as range distances increase (i. e., the mean energy is higher than that predicted solely on the basis of range attenuation).⁶ This suggests that the energy spectrum of the initial radiation, at least insofar as it is influenced by its gamma components, will change as ground ranges are varied. While many variations in the spectrum of the range-energy relationships for the initial radiation can be recognized as possibilities, neither the probabilities of their occurrence nor their actual significance can be predicted with any confidence. The general acceptance of a representative fission-yield energy range relationship has accordingly been proposed.⁶ This would be generally applied to all initial radiation shielding analyses, unless there is known to be some specific justification for a separate consideration of individual radiation components, such as the high-energy neutron emissions from a fusion weapon.

Since any requirements for shielding are largely established by the higher-energy radiation components, it is also important to consider the spatial distribution of these energies as they may exist at any point in the free-field. As a starting point, it can be postulated that a detector will indicate the existence of an energy spectrum (or directional variation in the energy available for absorption) when the radiation components which reach it have a preferential direction of travel with respect to the radiation source. The directional distribution of radiation energies becomes of interest in the design of any facility which is not uniformly surrounded by shielding. Such a condition exists in a typical shelter entranceway, where the mouth is directly exposed to radiation penetration.

We then ask whether the line-of-sight orientation of the depth transition section, relative to the explosion center, will influence the energy characteristics of any radiation which penetrates the entranceway. In addition, will the fraction of the free-field radiation which penetrates the depth transition section of the entranceway be related to the geometry of the section (i. e., ratio of length of section to the area of the entranceway mouth, as projected on a plane normal to the longitudinal axis of the section)? Answers to these questions will involve a consideration of the directional distribution of the radiative energies released by a nuclear explosion.

IIT RESEARCH INSTITUTE

The gamma fraction of the initial radiation is attributable to several initiating sources, and as a consequence will include various energy contents. However, its major constituents are fission product gammas (≈ 2 Mev at 1 minute after the explosion) and gammas resulting from neutron capture by nitrogen nuclei in the air (≈ 6.5 Mev). Gamma radiations are electromagnetic waves which, in a vacuum, would travel in straight lines with the speed of light.⁵ In the atmosphere, these gamma radiations tend to be scattered by multiple collisions with such elements as oxygen and nitrogen. As a result, while much of the gamma radiation arrives at a target in straight lines from the source, a considerable portion (skyshine) also arrives from directions other than line-of-sight. The resulting angular distribution in the gamma exposure dose has been found to be relatively insensitive to weapon yield, assuming that the scaled value of the slant range remains constant.

While a similar tendency towards a directional distribution of radiative energy content also exists for the neutron flux, it is considerably less pronounced. Neutrons are particles of appreciable mass, and their multiple collisions with fission products and with atmospheric elements will lead to a significant amount of random scattering. As a consequence, the directions of motions for neutrons have become almost randomly distributed at those locations which are some appreciable distance from the explosion center. For this reason, the concept of an energy spectrum is not readily applicable to considerations of the neutron flux. Samplings of neutron flux at various distances have suggested that, while the total neutron flux will decrease with increasing distance from the source, there is little corresponding change in the relative distributions of its energy fractions. Until improved forecasts become available, it has been proposed⁶ that the energy spectra of both components of initial radiation be regarded as constant for all ground ranges of interest.

In evaluating the angular distribution of the initial radiation as it reaches a target, recognition should be given to the source geometries of the gamma and neutron components. The initial gamma radiations consist primarily of fission product gammas and of gammas produced by nitrogen capture of neutrons. The fission particles are released within a short distance of the explosion center, and perhaps may be considered as originating within the fireball. The nitrogen-capture gammas, which are the result of

finite neutron travel through the atmosphere, are produced within a larger space volume. Neutrons, since they are liberated at a very early explosion stage, can be assumed to originate from a point source. While a point-source representation of initial gammas and neutrons is valid when examining free-field effects at very large distances, this is certainly not true for some of the ranges considered in this study. The inaccuracies due to introducing a point-source assumption would be most pronounced at ranges close to the explosion center, and would contribute to an apparent angular distribution of the initial radiation as it reaches a shelter entranceway.

From the preceding statements, we can formulate certain hypotheses regarding the probable angular distribution of the initial radiation as measured by a collimated detector located some short distance inside an entranceway mouth. First, let us assume that the burst is positioned vertically and horizontally so that an extension of the longitudinal axis (line-of-sight) of the first entranceway leg passes through the explosion center. We have reasoned that this situation, with $\psi_B = \psi_E$, should represent the worst case for radiation streaming in the entranceway. For these burst conditions, the observed radiation energies should be a maximum when the detector axis is aligned along the line-of-sight to the explosion center. As the detector is rotated at an increasing horizontal or vertical angle to this line-of-sight, the gamma radiation would be expected to decrease. However, due to backscattering effects, significant radiation could still be recorded even after the detector axis has rotated past a limiting solid angle defined by the line-of-sight between the detector location and the periphery of the entranceway mouth. Within these same angular limits, due to its lack of directional orientation, the measured neutron flux should remain more nearly uniform than does the initial gamma radiation. The detector would thus continue to record appreciable backscattering effects at even greater angles than for the gamma radiation. The total recorded absorption of gamma and neutron energies would be influenced not only by the orientation of the detector but also by its location in relation to the geometry of the entranceway mouth. This latter dependence can conveniently be expressed in terms of the solid angle fraction subtended by the entranceway mouth. Finally, if the burst is positioned so that the entranceway line-of-sight does not pass through the explosion center, the total energies recorded by the detector will be reduced. In

IIT RESEARCH INSTITUTE

an extreme case, where the maximum fireball is not visible at the detector location, the recorded energies will be almost entirely attributable to various backscattering effects.

Having made these postulates as to the probable form of the initial radiation spectrum, the next step involves an examination of pertinent analytical and experimental findings. The available experimental data are supplied by Richie and Hurst,²⁵ and relate to relatively low-yield, fission-type weapons (10 - 20 KT) whose line-of-sight to the detector made an angle of 22 deg with the horizontal plane. The angular distribution of radiation was determined by collimators which were capable of detecting radiation within 15 deg of the direction in which the instrument axis was pointed. The collimators were placed at slant ranges of 1355, 1585, and 1825 yards from the burst. Within the scope of the experiment, no significant variation in angular distribution as a function of distance to burst or type of weapon was observed. An analytical approach has also been applied to the question of angular orientation of the radiation from a weapon burst. French and Wells²⁶ devised a mathematical model and employed a Monte Carlo procedure for detailed calculation of the radiation transport phenomenon. Results from this study have been correlated with the experimental data obtained by Richie and Hurst.

These analytical and experimental data, at least within their range of applicability, suggest that the backscattering of both gamma radiation and neutrons is sufficient to obviate any major angular dependence of the energy distribution for any radiation which reaches the entranceway mouth. All radiation which actually enters the passageway mouth, regardless of its direction of travel, might thus be considered to have essentially the same energy components. This tentative conclusion will be adopted for this study, although it undoubtedly merits more detailed investigation. There remains only the problem, related solely to geometric considerations, of computing the fraction of the free-field radiation which actually penetrates the entranceway. This calculation is conveniently expressed in relation to the solid angle defined by the lines-of-sight from within the entranceway, bounded by the periphery of the shelter mouth, and the center of the explosion based on a point-source assumption.

Consider a detector located at some point within the depth transition section of a shelter entranceway (since we are concerned with radiation streaming, the detector is usually considered to be located at the first interior bend). The point is assumed to be centrally-located in the passage-way cross section, and the reference line-of-sight is taken along the longitudinal axis of the passageway. The area of the entranceway mouth, as viewed from the detector location, is projected normal to this reference line-of-sight. The solid angle fraction, in relation to the assumed detector location, is then defined by the perimeter of this projected area.

Figure 5-1, obtained from Chart 3,³⁰ supplies solid angle fractions for rectangular openings in terms of two nondimensional parameters. The first of these, e , is defined as the ratio of the short (B_p) and long (H_p) dimensions of the entranceway mouth, as projected on a plane normal to the longitudinal axis of the entranceways. The second parameter, n , is defined by the relationship $n = 2Z/H_p$. Algebraically, Fig. 5-1 can be expressed in the following form.

$$\omega = \frac{2}{\pi} \tan^{-1} \left[\frac{e}{n\sqrt{n^2 + e^2 + 1}} \right] \quad (a) \quad (5-5)$$

where

$$e = B_p/H_p$$

$$n = 2Z/H_p$$

For a circular projection, the solid angle fraction ω can be expressed as^{4, 30}

$$\omega = 1 - \cos \beta_z \quad (b) \quad (5-5)$$

where

$$\beta_z = \tan^{-1} \frac{r_m}{Z}$$

r_m = mean radius of the entranceway mouth, projected as described, ft

Z = distance from detector to projected plane of the entranceway mouth, measured along the reference axis, ft

Figure 5-2 supplies free-field entranceway-mouth reduction factors, R_{fe} , as a function of the particular type of radiation, the angular orientation of the bomb burst with respect to the longitudinal axis of the entranceway leg, and the solid angle fraction subtended by the interior point.

IIT RESEARCH INSTITUTE

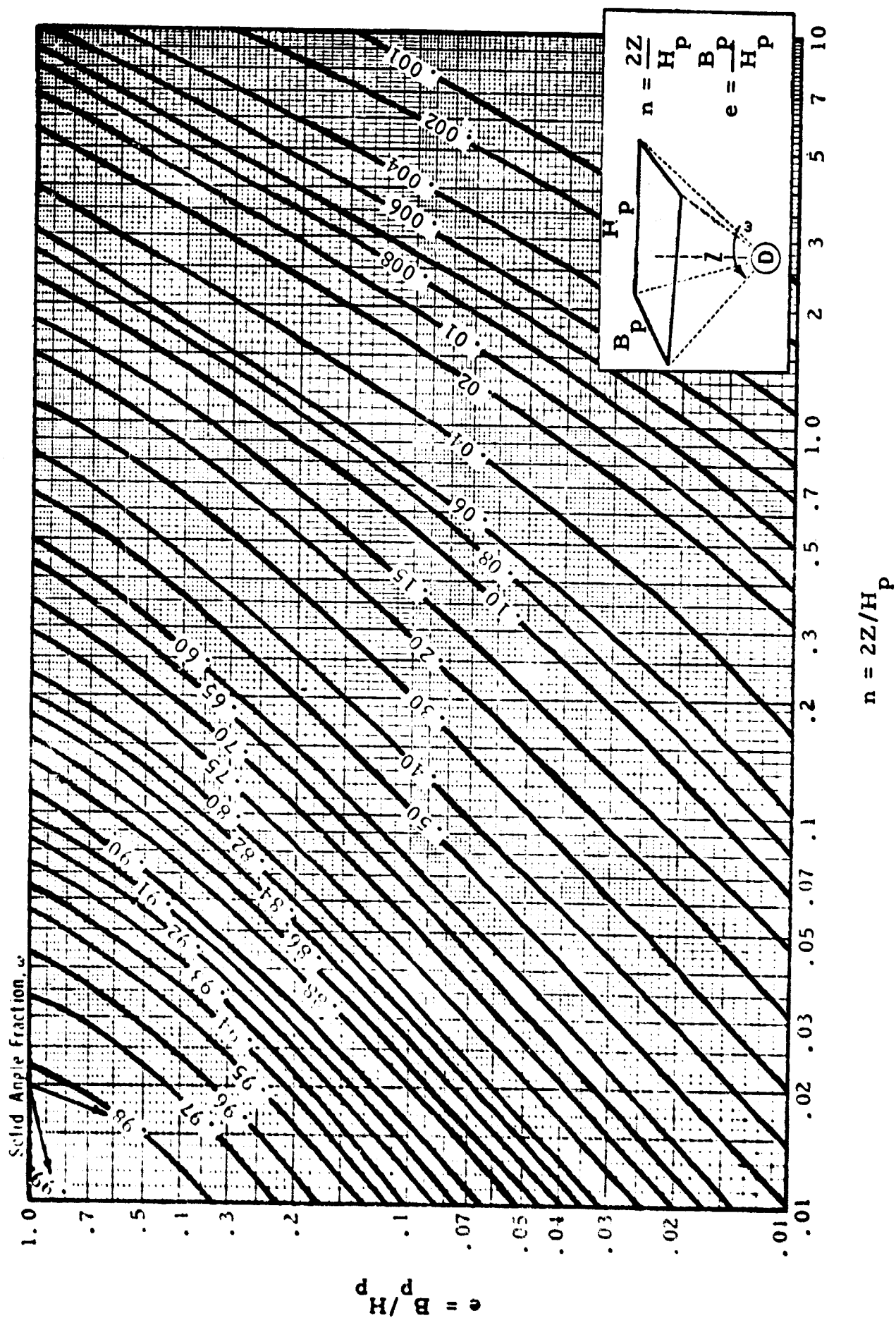


Fig. 5-1 VALUES OF SOLID ANGLE FRACTION, ω

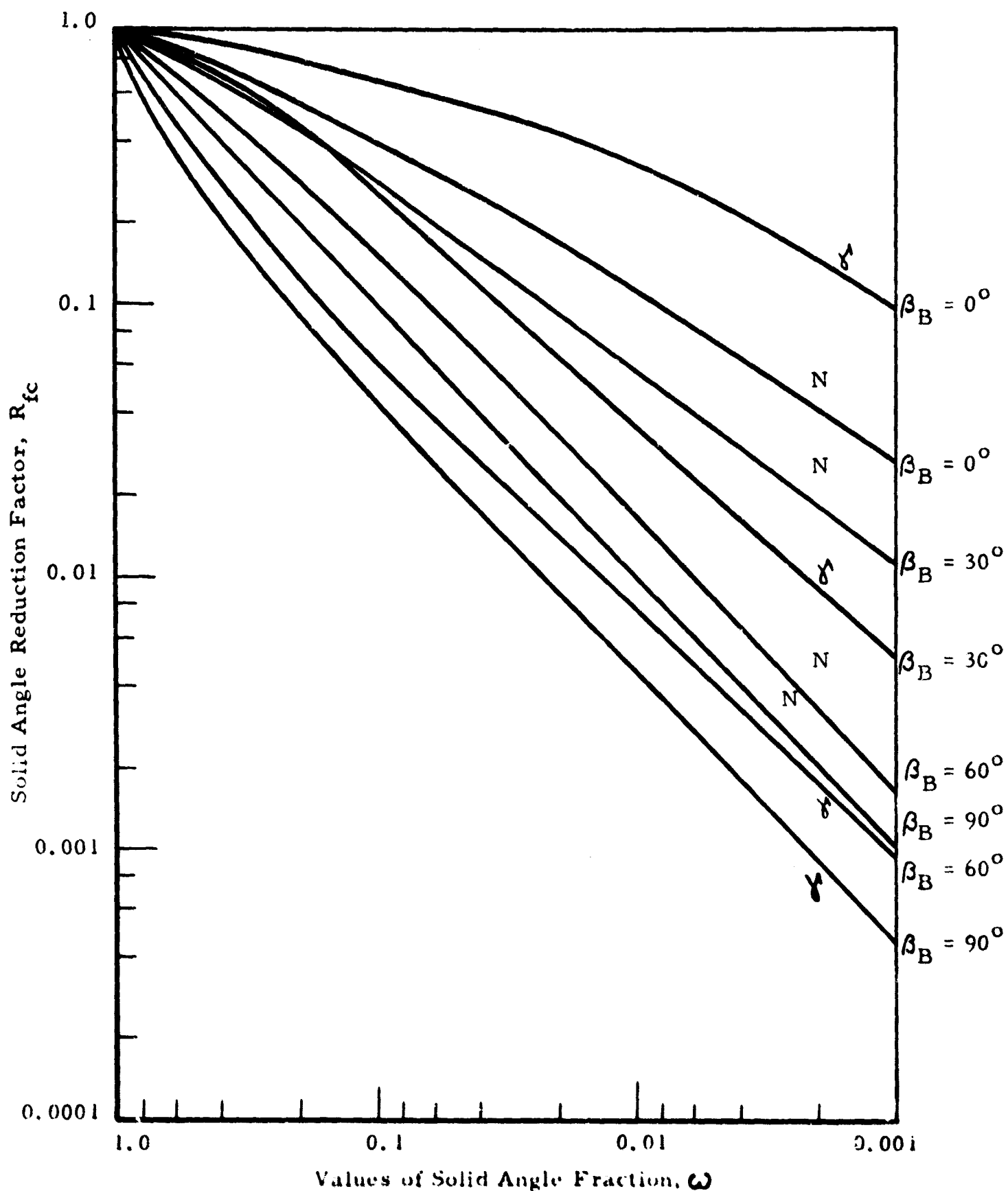


Fig. 5-2 ENTRANCEWAY-MOUTH REDUCTION FACTORS, R_{fc} , FOR STREAMING OF GAMMA (γ) AND NEUTRON (N) FRACTIONS OF INITIAL RADIATION IN SHELTER ENTRANCEWAYS, AS FUNCTIONS OF ω AND β_B

of interest and the projected perimeter of the entranceway mouth. In this manner, any effects of angular orientation for gamma and neutron radiations are combined with the geometric reduction in the radiation dose seen by an observer within an entranceway. Figure 5-2 of this report includes the basic information contained in Chart 6.01,⁴ which in turn was developed from the data presented in Reference 25. In addition, Fig. 5-2 includes several additional curves relating radiation and angular orientation. Values of R_{fe} are expressed as functions of the solid angle of the entranceway mouth (from Fig 5-1 or calculated from Eq 5-5) and the included angle β_B between the longitudinal axis of the first entranceway leg and the line-of-sight axis from the detector to the explosion center. This angle can be calculated directly from the known horizontal and vertical burst-location angles.

$$\beta_B = \cos^{-1} \left[\cos (\theta_B - \theta_E) \cos (\psi_B - \psi_E) \right] \quad (5-6)$$

where

- θ_B = angular orientation of burst center relative to an arbitrary x-axis projected in the horizontal plane, deg
- θ_E = angular orientation of the longitudinal axis of the entranceway leg, referenced to the same x-axis and projected in the horizontal plane, deg
- ψ_B = vertical angle to burst center, as observed at the detector location and measured from the z-axis, deg
- ψ_E = vertical angle to the longitudinal axis of the entranceway leg, as observed at the detector location and measured from the z-axis, deg

5.3.3 Correlation Between Free-Field Levels of Overpressure and Initial Radiation

In the earlier studies of fully-buried shelters, which have led to this investigation of entranceway requirements, it was found convenient to express all protective features of a shelter in terms of an implied resistance to peak overpressure loading.^{1,2} In order to justify this one-parameter description of shelter hardness, the shelters were designed on the assumption that their postulated overpressure loadings would also be accompanied by worst case intensities of all other destructive effects. For the buried shelters, the only other explosion effect of appreciable structural significance is ionizing radiation. The shelter effectiveness in a radiation environment was analyzed on the assumption that the shelter roof and cover soil acted together as a

IIT RESEARCH INSTITUTE

thick barrier shield.^{1, 6} The worst case radiation field resulted from an overhead positioning of the weapon ($\psi_B = 0$). With this once established, it was only necessary to explore the range-yield relationships for overpressure and for initial ionizing radiation. Once the design level of overpressure had been established for a particular shelter, all possible radiation fields associated with that specific pressure and with weapon yields in the 1-100 MT range were examined. The maximum of these radiation fields, once identified at the shelter location, was associated with its particular overpressure in all subsequent analyses. This implies that, for all anticipated attack conditions other than the extreme situation thus identified for design purposes, the relative degree of radiation protection in the shelter would exceed the protection from overpressure-induced loading.

A rather similar approach is used in specifying the protection requirements for shelter entranceways. Since it is unrealistic to expect that a detailed description of an anticipated attack will ever be made available as a factual statement of entranceway design requirements, it is reasonable to select one controlling parameter to describe the attack threat. The first step in the design is to proportion the entranceway to resist some specified level of this parameter. The next step is to examine all other destructive features which may be associated with the selected attack parameter, considering both their expected ranges and their influence on entranceway design. Conceptually, it should be possible to evaluate the probabilities that these destructive effects will occur either singly or in combination, at selected levels of intensity within their projected ranges. Since an evaluation of these distribution functions would in itself require a detailed specification of the attack threat, it is customary to assume that these related effects will always occur at their established maximum levels.

As with the shelter, and in accordance with this design philosophy, it is convenient to describe all protective features of an entranceway in terms of its resistance to blast-induced loading. All other primary destructive effects, which essentially reduce to initial and residual radiation, are once again assumed to occur at their worst case (maximum) values. It would be equally possible to design the shelter to supply a specified resistance to some other explosion effect, such as its shielding to ionizing radiation, and then to examine the requirements introduced by worst case overpressure

III RESEARCH INSTITUTE

loading. However, since the cost-overpressure interactions are considerably stronger than the cost-shielding relationships, the sensitivity of entranceway cost analyses is improved by relating entranceway design to overpressure.

In order to identify the worst case initial radiation field associated with a specified weapon yield and level of overpressure, it is necessary to examine the possible range of weapon positioning. Figure 5-3, reproduced from Fig. 3.67a,⁶ shows the loci of selected peak ground surface overpressures for a 1 KT explosion as functions of ground range $R_g \sin \psi_B$ and height of burst, $R_g \cos \psi_B$. Considering only the Mach region, which has been specified as our region of interest (Chapter 4), the ground range corresponding to a specified peak overpressure is seen to be a minimum for a contact burst and to reach a maximum at some optimum burst height. The optimum burst height is of major interest when evaluating the required structural resistance to blast wave loading, since it represents the worst case combination of ground range and a specified level of overpressure. However, when the maximum requirements for radiation shielding at the same level of overpressures are investigated, the minimum ground range becomes of interest. This conclusion is readily apparent from Eq. (5-2) and (5-4), which indicate that the free-field intensity of the initial radiation is inversely proportional to the slant range from the explosion center, raised to some power greater than unity.

The preceding argument leads to the conclusion that, with no other restrictions on bomb positioning, the worst case of initial radiation associated with each specified level of overpressure will correspond to a ground burst. As applied to the design of shelter entranceways, the geometry of the problem suggests that an additional restriction can be applied. It was initially specified (Chapter 1) that the existing ground surface at the entranceway location, for all situations examined in this study, will be considered as approximately level. Accordingly, it will be necessary to use stairs in the depth transition section of the entranceway in order to accommodate all or a major portion of the required elevation change between the ground surface and the shelter proper. As a consequence, (Section 5.3.1), the reference line-of-sight axis for a radiation detector located just at the bottom of the stairs will be inclined at approximately 40 deg to the horizontal

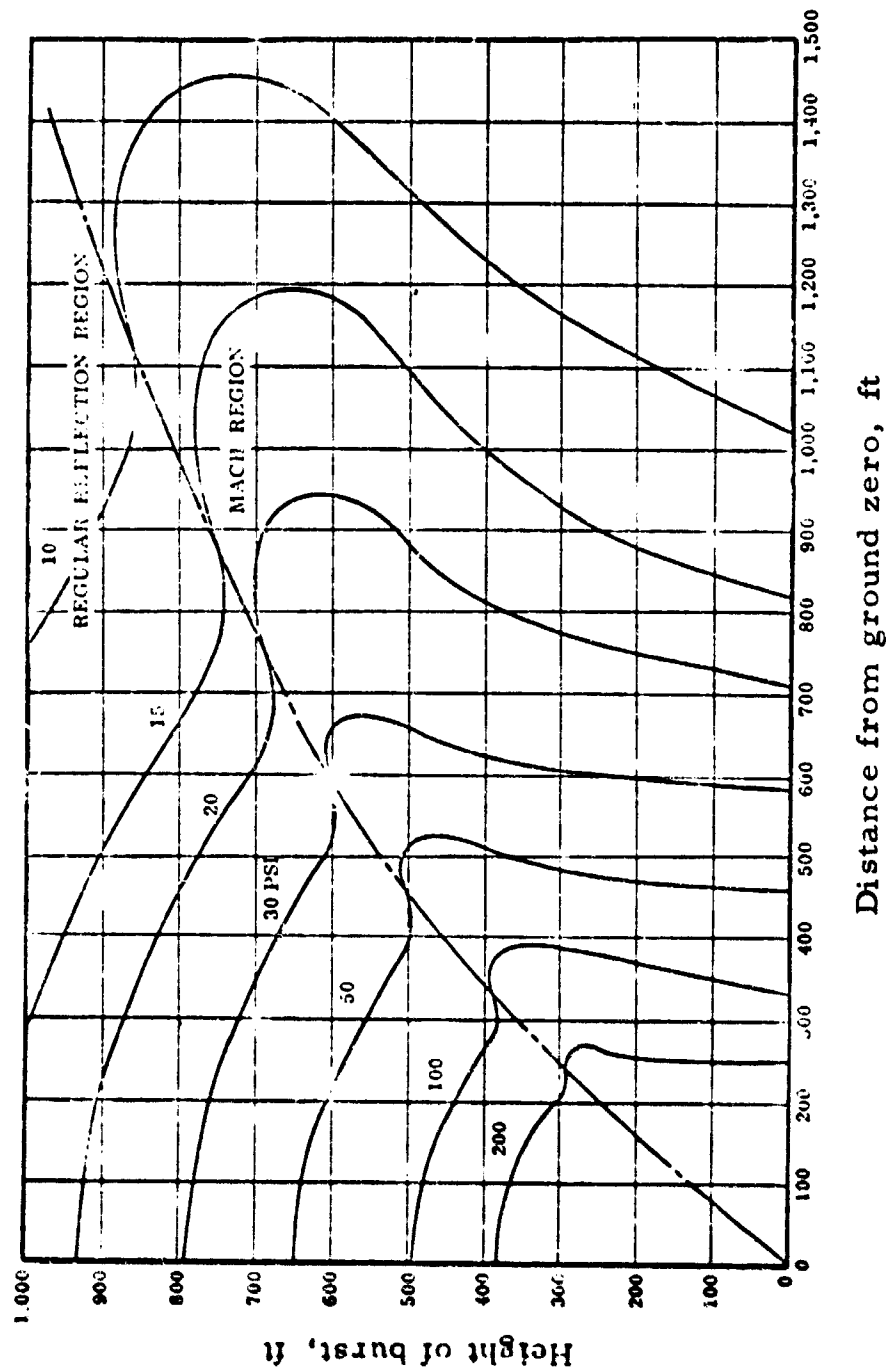


Fig. 5-3 RELATIONSHIPS BETWEEN BURST HEIGHT ($R_s \cos \psi_B$),
 DISTANCE FROM GROUND ZERO ($R_s \sin \psi_B$) AND PEAK
 SIDE-ON SURFACE OVERPRESSURE (p_{s0}) FOR A ONE-KT
 EXPLOSION YIELD ($R_s = R_{s0}$)

plane ($\psi_E = 50$ deg). The radiation recorded by this detector will, for a typical entranceway design, be a maximum when its line-of-sight axis passes through the explosion center. The slant range R_{so} (Fig. 5-3), associated with a particular value of overpressure p_{so} is a minimum for $\psi_B = 90$ deg and increases as values of ψ_B are reduced below 90 deg. The geometric layout of the entranceway can thus impose a constraint when determining the worst case radiation fields which can be associated with a specified overpressure. Where appropriate, an adjusted slant range can be determined with the aid of Fig. 5-3 and subsequently introduced into Eq. (5-2) and (5-4).

The final step in this correlation between overpressure and worst case initial radiation, as applied to entranceway design, involves an equivalent static load representation of the actual dynamic loading. Using the concepts developed in earlier studies^{1, 2} and reviewed in Chapter 4 of this report, the structural elements of a buried structure are designed to resist a statically-applied, uniformly-distributed loading of unit intensity q . The peak dynamic loads actually applied to the structural elements, p_m , are considered to be functions either of the peak overpressure at the ground surface, p_{so} , or of the peak reflected pressure within a structure. Each relationship between p_m and q is, for megaton yields and typical structures, considered to be a unique function of the ductility ratio for the structure, μ .

While this approach is quite satisfactory when establishing the requirements for structural loading resistance, it is less satisfactory when determining the requirements for radiation shielding. The earlier arguments in this section have identified a useful correlation between peak overpressure and worst case initial radiation, which is readily extended to a correlation between peak dynamic loading, p_m , and initial radiation. However, since p_m and q are related through μ , the worst case initial radiation becomes a function of μ and q , rather than a singular function of q . Expressed in another way, the structural requirements which correspond to a specified overpressure will vary according to the ductility ratio of the structure, while the radiation shielding requirements relate only to the slant range (and weapon yield) associated with that overpressure.

This difficulty, which was recognized in the earlier studies of the basic shelter,^{1, 2} is actually not a serious one. Radiation shielding is a minor cost item in a buried shelter, although perhaps it is of more significance when the entranceway alone is considered. The predictions of free-field radiation as a function of weapon yield and slant range are inaccurate at best, and may vary by an order of magnitude for yields in the megaton range.⁶ The assumption of worst case radiation as a basis for entranceway and shelter design is inherently conservative, although admittedly to an indeterminate degree. Recognizing these factors, the worst case initial radiation field for radiation analyses of the shelter proper^{1, 2} was expressed for each weapon yield as a singular function of the equivalent static load by assuming a constant value for the ductility ratio ($\mu = 1.3$). This same approximation will be extended to shelter entranceways.

Table 5-1 supplies data which relate the free-field components of initial radiation, Eq. (5-2 and (5-4), slant ranges determined from Fig. 5-3, and weapon yields in the 1 to 100 MT range. These factors are expressed as functions of the vertical angle of burst, ψ_B , for selected levels of the static equivalent load. Values of W' (Section 5.3), are obtained from Fig. 8.27b,⁶ and have been extrapolated to higher fission yields. The slant ranges for weapon yields other than 1 KT were determined from the equation⁶

$$R_s = 10 R_{so} W^{1/3} \quad (5-7)$$

where

R_s = slant range in ft which, for a weapon yield of W megatons, corresponds to a specified peak overpressure

R_{so} = slant range in ft which, for a weapon yield of 1 KT, corresponds to this same peak overpressure.

5.4 RESIDUAL NUCLEAR RADIATION

The residual radiation component of primary interest in shelter design is early fallout. It is frequently found that the anticipated fallout radiation will not influence the shielding requirements for a blast-resistant shelter, since these will be governed by considerations of blast and of initial radiation. There remains, however, the possibility that fallout radiation (particularly from multiple and distant sources) may be of significance in shelter systems which are designed for relatively-low overpressure levels.

Table 5-1

PEAK PRESSURES (Dynamic and Static, for $\mu = 1.30$): SLANT RANGES, R ,
AND INITIAL RADIATION COMPONENTS γ_w , N_w (For $0 \leq \beta_s \leq 90^\circ$ and for
Fission Yields of 1, 5, 20 and 100 MT)

γ_B Deg	Fission W MT	$q = 325 \text{ lb/in.}^2$ $P_m = 200 \text{ lb/in.}^2$					$q = 200 \text{ lb/in.}^2$ $P_m = 125 \text{ lb/in.}^2$					$q = 100 \text{ lb/in.}^2$ $P_m = 65 \text{ lb/in.}^2$					$q = 50 \text{ lb/in.}^2$ $P_m = 32 \text{ lb/in.}^2$					$q = 10 \text{ lb/in.}^2$ $P_m = 7 \text{ lb/in.}^2$					
		R_s (ft)	γ_w (rad)	N_w (rad)	R_s (ft)	γ_w (rad)	N_w (rad)	R_s (ft)	γ_w (rad)	N_w (rad)	R_s (ft)	γ_w (rad)	N_w (rad)	R_s (ft)	γ_w (rad)	N_w (rad)	R_s (ft)	γ_w (rad)	N_w (rad)	R_s (ft)	γ_w (rad)	N_w (rad)	R_s (ft)	γ_w (rad)	N_w (rad)		
0	1	2.5×10^3	3,800	1.45×10^{-5}	2.27×10^{-5}	4,700	4.15×10^{-4}	3.56×10^{-3}	7.74×10^{-3}	2.53×10^{-2}	6,600	7.74×10^{-3}	2.53×10^{-2}	7,800	8.65×10^{-2}	9.63	15,800	0	0	0	0	0	0	0	0	0	0
	5	1.5×10^4	6,500	2.46×10^{-4}	3.35×10^{-2}	8,050	3.61×10^{-3}	3.06×10^{-1}	3.67×10^{-2}	0	10,200	3.67×10^{-2}	0	13,350	1.04×10^{-1}	0	27,100	0	0	0	0	0	0	0	0	0	0
	20	3.0×10^5	10,480	5.37×10^{-3}	1.81	12,800	3.72×10^{-2}	0	6.88	0	16,400	6.88	0	21,200	0	0	43,000	0	0	0	0	0	0	0	0	0	0
	100	1.0×10^9	17,700	7.01×10^{-2}	0	21,400	9.38	0	0	0	27,000	0	0	36,300	0	0	73,500	0	0	0	0	0	0	0	0	0	0
30	1	2.5×10^3	3,720	1.67×10^{-5}	2.75×10^{-5}	4,400	6.25×10^{-4}	6.54×10^{-3}	7.45×10^{-3}	2.67×10^{-2}	6,030	7.45×10^{-3}	2.67×10^{-2}	7,800	8.65×10^{-2}	9.63	15,600	0	0	0	0	0	0	0	0	0	0
	5	1.5×10^4	6,360	2.96×10^{-4}	7.12×10^{-2}	7,540	7.02×10^{-3}	7.71×10^{-1}	2.66×10^{-2}	0.45	10,400	2.66×10^{-2}	0.45	13,350	1.04×10^{-1}	0	26,700	0	0	0	0	0	0	0	0	0	0
	20	3.0×10^5	10,100	7.27×10^{-3}	2.63	12,000	8.97×10^{-2}	0	8.68	0	16,400	8.68	0	21,200	0	0	42,500	0	0	0	0	0	0	0	0	0	0
	100	1.0×10^9	17,300	1.05×10^{-2}	0	20,500	9.50×10^{-2}	0	0	0	28,100	0	0	36,300	0	0	72,700	0	0	0	0	0	0	0	0	0	0
60	1	2.5×10^3	3,000	4.58×10^{-5}	1.29×10^{-5}	3,900	1.18×10^{-5}	1.75×10^{-4}	1.90×10^{-4}	1.36×10^{-3}	5,310	1.90×10^{-4}	1.36×10^{-3}	7,500	1.38×10^{-3}	2.08	16,370	0	0	0	0	0	0	0	0	0	0
	5	1.5×10^4	5,130	1.44×10^{-5}	7.58×10^{-3}	6,700	1.94×10^{-4}	3.67×10^{-2}	1.12×10^{-3}	2.35	9,120	1.12×10^{-3}	2.35	12,850	1.77×10^{-1}	0	28,000	0	0	0	0	0	0	0	0	0	0
	20	3.0×10^5	8,170	6.87×10^{-4}	1.05×10^{-2}	10,600	4.30×10^{-3}	0	14.450	0	14,450	6.27×10^{-1}	0	20,400	0	0	44,500	0	0	0	0	0	0	0	0	0	0
	100	1.0×10^9	13,950	4.11×10^{-5}	0	18,150	4.40×10^{-3}	0	0	0	24,700	0	0	34,900	0	0	76,200	0	0	0	0	0	0	0	0	0	0
75-90	1	2.5×10^3	2,880	6.04×10^{-5}	1.74×10^{-5}	3,810	1.45×10^{-5}	2.27×10^{-4}	2.47×10^{-4}	1.63×10^{-3}	5,100	2.47×10^{-4}	1.63×10^{-3}	7,270	1.64×10^{-3}	2.62×10^{-1}	19,800	0	0	0	0	0	0	0	0	0	0
	5	1.5×10^4	4,920	1.88×10^{-5}	1.17×10^{-4}	6,510	2.46×10^{-4}	5.35×10^{-2}	1.75×10^{-3}	8.78	8,770	1.75×10^{-3}	8.78	12,400	2.84×10^{-1}	0	39,000	0	0	0	0	0	0	0	0	0	0
	20	3.0×10^5	7,850	9.83×10^{-4}	1.77×10^{-2}	10,400	5.37×10^{-3}	1.81	1.20×10^{-2}	0	17,900	1.20×10^{-2}	0	19,750	0	0	54,000	0	0	0	0	0	0	0	0	0	0
	100	1.0×10^9	13,400	6.49×10^{-5}	0	17,750	6.80×10^{-3}	0	1.51×10^{-1}	0	23,700	1.51×10^{-1}	0	33,700	0	0	92,200	0	0	0	0	0	0	0	0	0	0
75-90	1	2.5×10^3	2,400	1.36×10^{-6}	5.37×10^{-5}	3,000	4.96×10^{-5}	1.32×10^{-5}	7.37×10^{-4}	8.36×10^{-3}	4,300	7.37×10^{-4}	8.36×10^{-3}	5,800	1.01×10^{-4}	4.24×10^{-2}	13,000	2.55	0	0	0	0	0	0	0	0	0
	5	1.5×10^4	4,100	5.69×10^{-5}	6.06×10^{-4}	5,130	1.42×10^{-5}	7.71×10^{-3}	5.18×10^{-3}	1.17×10^{-2}	7,330	5.18×10^{-3}	1.17×10^{-2}	9,900	4.60×10^{-2}	1.07	22,300	0	0	0	0	0	0	0	0	0	0
	20	3.0×10^5	6,540	4.74×10^{-5}	2.20×10^{-3}	8,160	6.70×10^{-4}	5.93×10^{-1}	1.29×10^{-3}	0	11,680	1.29×10^{-3}	0	15,750	1.62×10^{-1}	0	35,300	0	0	0	0	0	0	0	0	0	0
	100	1.0×10^9	11,150	7.52×10^{-6}	2.27	13,950	3.64×10^{-5}	0	6.87×10^{-2}	0	19,950	6.87×10^{-2}	0	27,000	0	0	60,500	0	0	0	0	0	0	0	0	0	0

For such shelters, it usually follows that the mass thicknesses of the structural elements (and thus their inherent radiation shielding, since this can be approximately related to mass thickness) are appreciably less than those required in high-overpressure regions. Also, since the ground ranges which correspond to low overpressures and megaton yields may considerably exceed the effective range of the initial radiation, such shelters may be designed without any deliberate provisions for initial radiation shielding. These same ground ranges will have little (if any) effect in reducing fallout dose rates to less than their peak values. It may then be necessary to make some deliberate provisions to ensure adequate shielding from fallout radiation.

The total release of radiative energies from fallout is difficult to predict in the general case, since it is strongly influenced by the burst location and by details of the weapon design. The residual radiation consists of fission products and unfissioned materials from the fission fraction of a nuclear weapon, plus gamma-radiations from neutron-induced activity (primarily attributable to the fusion fraction of the bomb) in casing fragments and soil elements.⁶ In addition, deliberate steps (i. e., salting) can be taken to increase the radioactivity of the weapon residuals. This has led to the popular terminology of "clean" and "dirty" for nuclear weapons, referring to their degree of residual radioactivity, although these descriptions can only be considered as relative. It has been estimated⁶ that a nuclear explosion will produce 2 ounces of fission products for each KT of fission yield. Its neutron activity will be largely determined by its fusion yield.

The occurrence of significant quantities of fallout, regardless of its energy content, is strongly dependent upon the scaled burst height. If fallout is to occur it is first necessary that soil particles and weapon residues be combined in the explosion process and subsequently incorporated in the ascending cloud. If the burst occurs at some distance below the ground surface or, alternatively, occurs as a high air burst where no earth is taken into the fireball, there will then be no fallout. In such cases, any effects of residual radiation are localized and may consist only of neutron-induced activity near ground zero. The near-surface burst represents the worst case fallout situation, since large masses of soil are then exposed to residual radiation and are subsequently incorporated within the fireball. These particles, as they later descend to earth, are deposited over large

IIT RESEARCH INSTITUTE

areas as a layer of slowly-decaying radioactivity. The early fallout fraction (occurring within 24 hours), which is of interest to us in this study, is believed to contain between 50 and 70 percent of the total radioactivity of the weapon residues.⁶

Gamma radiations from the early fallout particles are emitted by a variety of isotopes. Thus, as observed at any specified time after the explosion, they include a wide range of radiative energies. These energies are appreciably less than those evidenced by the gamma contributions to the initial radiation. For this reason, the shielding requirements are less severe for delayed gammas. Commencing at the time when early fallout deposition is complete and extending throughout the first few weeks after the explosion, the time-decay of fallout radioactivity can be approximated by the following equation.⁶

$$R_t = R_{H1} t^{-1.2} \quad (5-8)$$

where

R_t = exposure dose rate for fallout gamma radiation at time t hours after the explosion, R per hr

R_{H1} = exposure dose rate for fallout gamma radiation at 1 hr after the explosion, R per hr

t = elapsed time after the explosion, hr

Spatial redistribution of early fallout is essentially complete when all particles have reached the ground, disregarding such secondary transport mechanisms as flowing water and blowing dust. During the fallout deposition period of approximately 24 hours, wind shear at various elevations can exert a translating force on the falling particles. This also induces a sorting process, whereby the smaller particles reach the ground at the greatest distances from the explosion. The intensity of fallout activity on a unit surface area in the fallout zone, assuming a constant elapsed time since the explosion, is related to the concentration and particle size of the fallout material. Observed patterns of fallout activity are highly variable, being sensitive to localized variations in wind and in topography, but frequently form a roughly-ellipsoidal pattern which is aligned and displaced in the downwind direction.

Scaling laws (fallout intensity versus weapon yield) are not considered to be directly applicable in the near vicinity of ground zero. Reference 6 thus proposed a dose rate of 10,000 roentgens per hour, referenced to one hour after the burst, as a practical upper limit for fallout radiation levels in this region. This upper limit would become a restriction for all magnitudes of burst. An idealized fallout pattern supplied in this same publication (Fig. 9.73) indicates one-hour dose rate contours in relation to ground zero for a 1 MT fission weapon, assuming an effective wind speed of 15 mph. Appropriate adjustments can be made to the idealized fallout pattern, if so desired, for wind speeds other than 15 mph. Reference dose rates for any other yield, up to the empirical limit of 10,000 R per hr at one hour, can be estimated by multiplying these idealized dose rates by the ratio of the actual fission yield to 1 MT. It is recognized that the distribution of fallout from an actual nuclear explosion can be expected to show major variations from the idealized dose rate pattern.⁶

The design requirement for fallout radiation protection, insofar as the shelter studies^{1,2} were concerned, was based upon a worst case assumption. Such an approach was consistent with that used in establishing the shelter design environment for the initial radiation. In order to extend this concept to the entranceway study, it is first postulated that the attack occurs in the form of a burst which results in a peak residual exposure dose of 10,000 R per hr at one hour after the explosion. Next, for the limited ground ranges which are associated with the 10-200 overpressures considered herein, it is assumed that the localized variations in fallout distribution due to hydrodynamic thrusts and wind shear will be of minor significance in shielding analyses. The entire area of interest is thus assumed to experience a uniform deposition of fallout material, considered to be independent of both weapon yield and range, whose radioactivity can be represented as a one-hour dose rate of 10,000 R per hr at one hour. Admittedly, the assumptions used in developing this design concept may be somewhat conservative when only one weapon is considered. However, conceding the probability that overlapping of fallout patterns can result from a general nuclear attack, the design procedure seems fully justifiable.

5.5 BARRIER SHIELDING

Optimum compositions of barrier shielding for radiation protection are, to a considerable degree, dependent upon the predominant type of ionizing radiation and upon its energy spectrum as it reaches the barrier. The effectiveness of such shielding in decreasing the intensity of gamma radiation is roughly proportional to the mass which it interposes between the shielded area and the radiation source.⁶ For this reason, shields composed of heavy atomic nuclei (i. e., lead, iron) are particularly desirable for attenuating gamma radiation. These materials are less satisfactory when large neutron fluxes are present.

The attenuation of neutrons through their interaction with matter involves a sequential process of deceleration. Unfortunately, the material properties for optimum neutron deceleration will vary according to the neutron energy under specific consideration. The heavy elements contained within a barrier shield, which have been identified as particularly suitable for gamma ray attenuation, are also effective in slowing the high-energy neutrons. Fast neutrons interact with these heavy shielding nuclei through a process known as inelastic scattering,⁶ which is also evidenced by the emission of secondary gamma rays within the shielding. Energy degradation for the slow or thermal neutrons is largely accomplished by radiative capture and by elastic scattering. These processes are most effectively accomplished when shielding elements of medium to low densities are present.⁶

In general, it can be concluded that the energy degradation of gamma radiations and of fast neutrons is largely proportional to barrier mass thickness, hence heavy material elements are advantageous. The attenuation of thermal neutrons is aided by the presence of light elements (i. e., hydrogen in water) within the shielding material. Concrete represents a suitable choice for many shielding applications, since it contains water in addition to providing structural strength and a reasonably high density. For applications where such structural strength is not required, moist earth is also suitable. Steel plate, while furnishing excellent structural strength and providing effective shielding from gamma radiation, would appear to be unsuitable when large quantities of thermal neutrons are present.

The required thickness of a given shielding material is related to the desired degree of attenuation and to the energies of the impinging radiation. The radiation energies from a nuclear explosion will span a large range, with their absolute values dependent on such factors as weapon composition and the detailed yield-range relationships. The complexities of the generalized problem have been reduced to workable levels by preparing averaged plots which show the attenuation of radiation energy as a function of mass thickness for selected materials.⁶ This simplified analysis assumes that the actual energy spectrum of each primary form of nuclear radiation (initial gamma, fallout gamma, and neutrons) can be replaced, for purposes of analyzing shielding requirements, by a single mono-energetic source. Since range scaling laws are applied directly to these mono-energetic representations, the relative energy distribution within each energy spectrum is also considered to be independent of ground range. By utilizing this greatly-simplified approach, the mass thickness required to attenuate 100,000 roentgen of initial gamma radiation by a factor of 1000 can be stated as a single number, without any consideration as to whether this radiation field has resulted from a 1 MT or a 100 MT explosion.⁶ An additional degree of analytical refinement can be introduced, at considerable additional effort, by separately investigating the yield-range-energy relationships for more specific radiation components such as fission-product gammas, nitrogen-capture gammas, fast neutrons, and thermal neutrons.

Even excluding those considerations arising from the multiple-energy nature of the nuclear radiation forms, a precise correlation still cannot be established between the mass thickness of shielding and its effectiveness in attenuating nuclear radiation. First, as a result of multiple scattering which occurs in any finite material thickness, an energy build-up factor is evidenced.⁶ Wholly or in part, depending on the form of presentation, this factor can be incorporated into simplified plots of shielding effectiveness versus mass thickness.⁶ In addition, since actual nuclear radiations are not collimated as they impinge on a barrier, the geometry and surface area of the shielding will influence the radiation dose which is experienced within the shielded area.

The effectiveness of the attenuation of radiation by a barrier shield is strongly related to the angle of incidence between the shielding plane and the travel direction of the impinging radiation. The smaller this angle becomes, the greater is the effective mass thickness which must be penetrated by the nuclear radiation. The resulting decrease in radiation energy is usually considered to be inversely proportional to the increase in travel distance. Experimental studies²⁷ with gamma radiation indicate that the actual attenuation is somewhat greater than this proportionality would indicate. Presumably, this increased attenuation is due to greater scattering of the radiation as the incident angle becomes more acute.

While many modifying factors certainly exist, their influences on requirements for shielding thickness are not large once appropriate adjustments have been made for shielding geometry and for the angle of incidence between the mean radiation and the barrier.^{6, 23} When it is recognized that the description of the external radiation field is itself highly uncertain, the use of highly-simplified shielding theory may well be consistent with the other facets of the problem. For this reason, the earlier structural studies for the buried shelter^{1, 2} considered that the shelter roof and its cover soil would attenuate nuclear radiations by acting as a thick barrier shield of infinite lateral extent. A somewhat similar assumption will be used in the barrier shielding analyses for the shelter entranceways, although here the geometry of the entranceway will be recognized.

Figure 5-4 relates barrier reduction factors to barrier mass thickness for nitrogen-capture gamma radiation (≈ 6.5 Mev) and shows the effect of incident angle β_S on these parameters. (Note that for horizontal shielding, such as a shelter roof, $\beta_S = 90^\circ - \psi_B$.) The selection of nitrogen-capture gammas as the index component for shielding analyses appears reasonable, since this is the major form of gamma radiation at the ranges of interest in this study. The assumption thus introduced is conservative from the protective viewpoint, since the integrated energy of the remaining initial radiation components is considerably less (≈ 3.2 Mev for the fission product gammas). A degree of conservatism in establishing gamma shielding requirements may be warranted, since the production of secondary gamma rays within the shielding may add significantly to the total gamma flux.

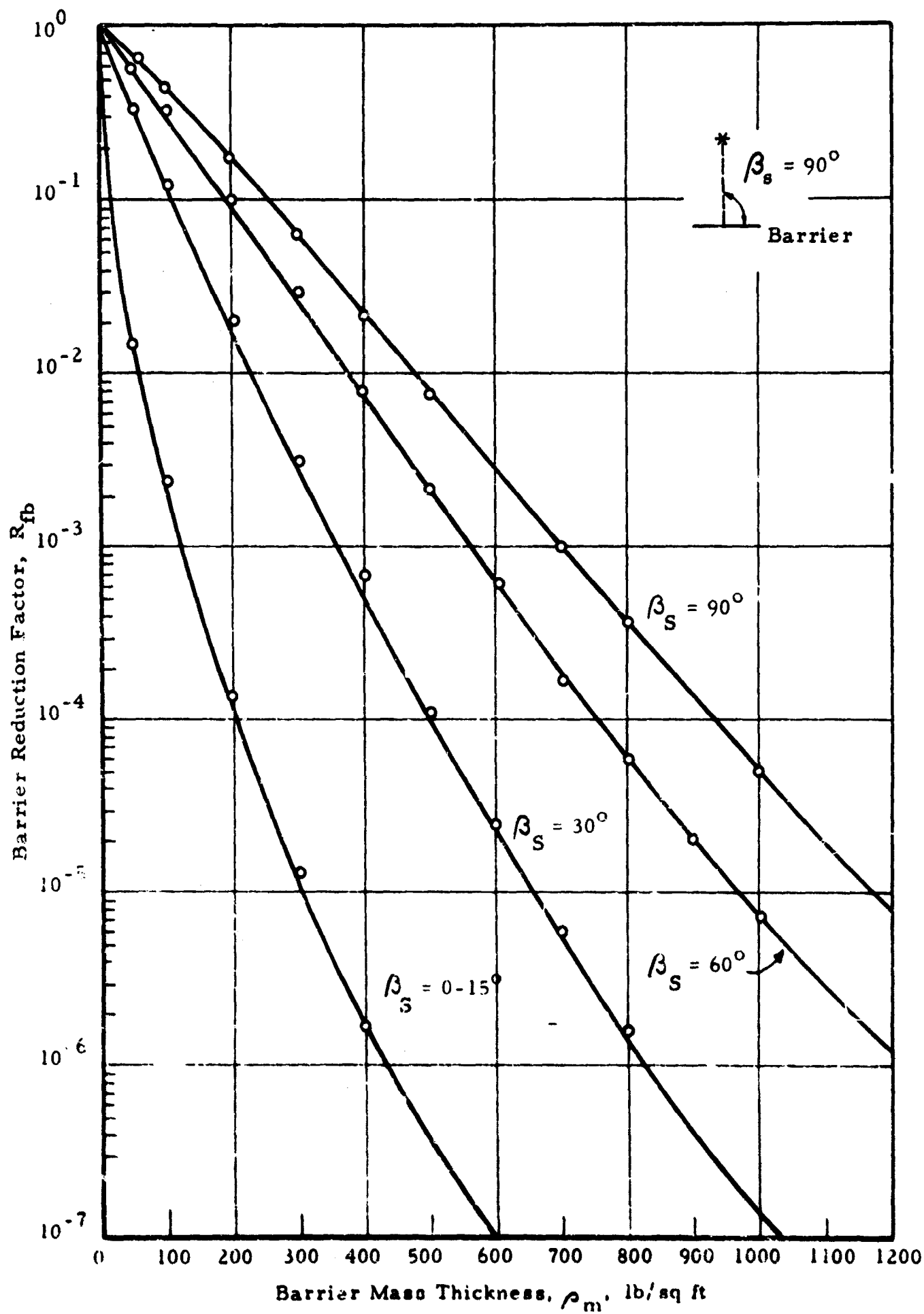


Fig. 5-4 BARRIER REDUCTION FACTORS FOR INITIAL GAMMA RADIATION (≈ 6.5 Mev) AS FUNCTIONS OF BARRIER MASS THICKNESS AND INCIDENT ANGLE, β_s

Figure 5-5 illustrates the barrier mass thicknesses which are required to attenuate gamma radiation from fallout. The angle of radiation incidence β_S no longer requires specific consideration since the fallout is deposited on all horizontal surfaces. Three representative cases are illustrated. Case 1 indicates the effect of fallout on a horizontal barrier, such as the ground above a buried structure. It is applicable when evaluating the overhead contribution of fallout by barrier penetration of the cover soil and entranceway roof. Case 2 indicates the effect of fallout adjacent to a vertical barrier, and is applicable when evaluating fallout streaming into an entranceway mouth. It is of interest to note, for both of these cases, that the shielding supplied by a given mass thickness is much more pronounced for fallout gamma radiation than for initial gamma radiation. This reflects the difference in their average energies. Case three is not pertinent.

Finally, Fig. 5-6 and 5-7 indicate the required barrier thicknesses for neutron shielding. As with Fig. 5-4, these requirements are expressed in terms of mass thickness and incident angle. Figure 5-6 is applicable to moderate-energy neutrons from nuclear fission (≈ 2.5 Mev), while Fig. 5-7 is applicable to fast (≈ 14 Mev) neutrons such as those produced by a fusion process.^{4, 6, 28, 29}

5.5.1 Entranceway Wall Attenuation of Neutron Flux

The same mechanisms which act to reduce the neutron flux in barrier shielding are also operative in reducing the neutron flux which streams down entranceways. Experimental data,³¹ while decidedly limited in extent, provide some basis for estimating the length of corridor which, through these processes, will reduce the neutron dose rate by one-half. In these referenced experiments, a thermal neutron source was placed in a corridor with a 6 ft-0 in. x 6 ft-0 in. cross section. A corridor length of 4.4 ft served to reduce the neutron dose rate by one-half. However, when a 4.5 Mev neutron source was substituted for the thermal neutron source, the corresponding corridor half-length was increased to 6 ft. Thus, the experimental evidence indicates that the neutron half-length is a function of neutron energy.

It is assumed that the neutron half-length for an entranceway corridor can be expressed as

$$L_{1/2} = \frac{1}{2} K (H + B) \quad (5-9)$$

IIT RESEARCH INSTITUTE

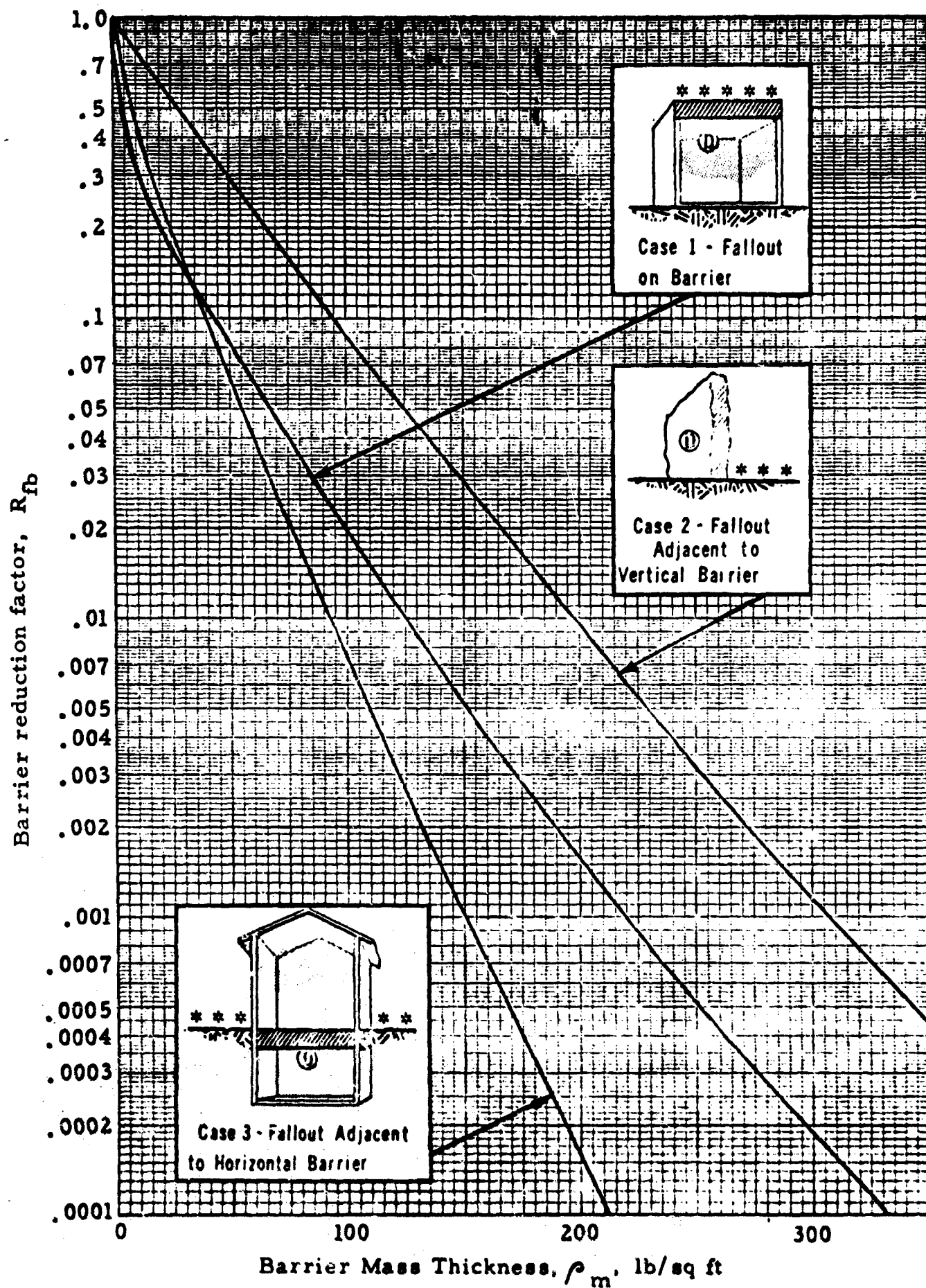


Fig. 5-5 BARRIER REDUCTION FACTORS FOR FALLOUT GAMMA RADIATION (≈ 2 Mev) AS FUNCTIONS OF BARRIER MASS THICKNESS AND SHIELDING POSITION RELATIVE TO CONTAMINATED PLANE

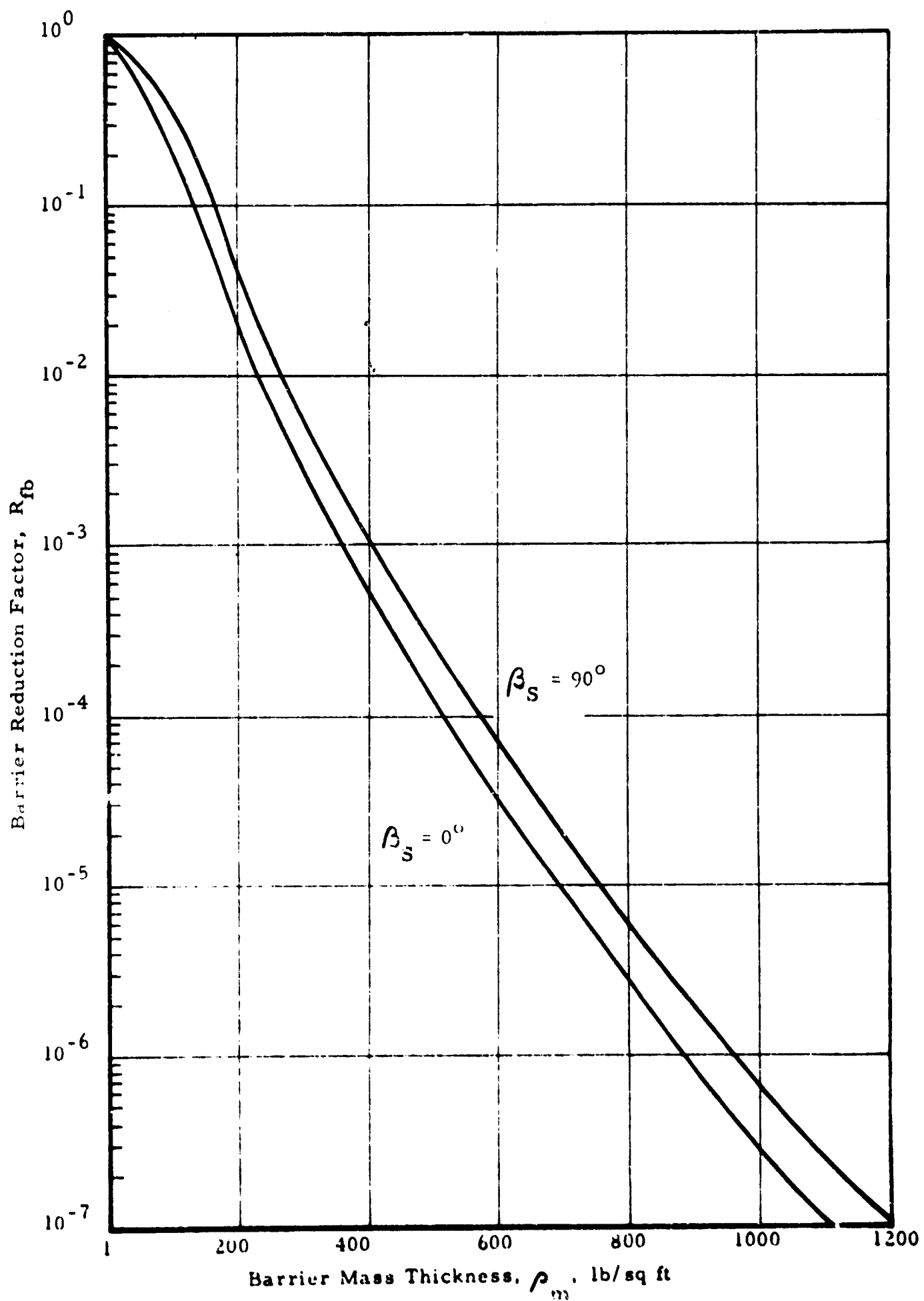


Fig. 5-6 BARRIER REDUCTION FACTORS FOR FISSION-YIELD NEUTRONS (≈ 2.5 Mev) AS FUNCTIONS OF BARRIER MASS THICKNESS AND INCIDENT ANGLE, β_s

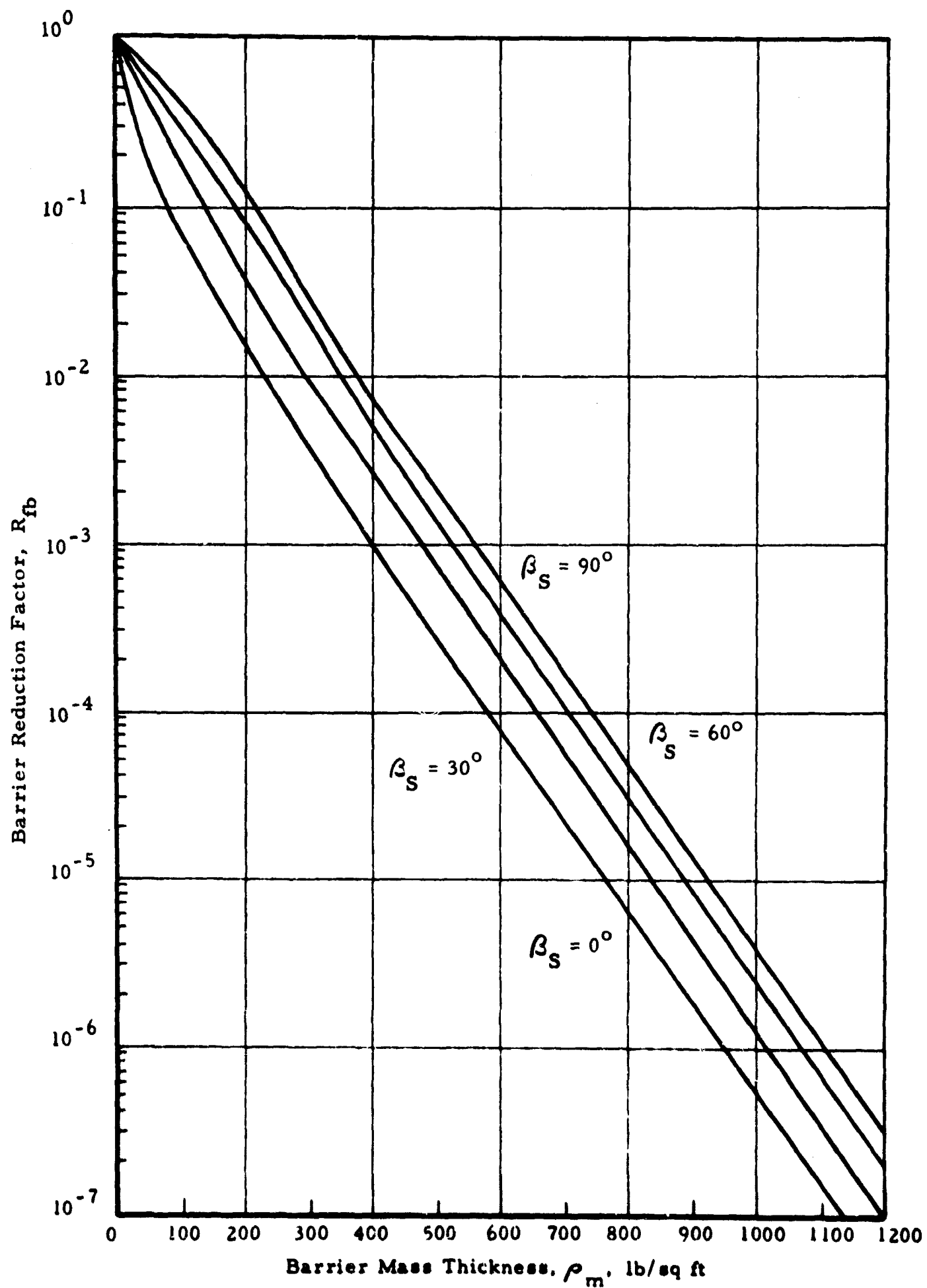


Fig. 5-7 BARRIER REDUCTION FACTORS FOR FUSION-YIELD NEUTRONS (≈ 14 Mev) AS FUNCTIONS OF BARRIER MASS THICKNESS AND INCIDENT ANGLE, β_s

where

$L_{1/2}$ = length of corridor, ft, which reduces the input neutron flux by one-half due to corridor wall attenuation

K = experimentally-determined ratio of neutron half-length to corridor width

H = clear height of corridor, ft

B = clear width of corridor, ft

For the cases of interest in this study, the neutrons which penetrate the first leg or the entranceway can conceivably contain relatively-high energy (up to 14 Mev). Since no applicable experimental data are available in this energy range, it is conservatively assumed that there is no neutron attenuation by wall interaction in the first leg of the shelter entranceway. For all subsequent legs after the first 90 deg corridor bend, it is assumed that the tendency for forward directional scatter has been sufficient to remove most of the high energy neutrons. The ratio K can then be expressed as

$$K = 4.4/6 = 0.732$$

The number of neutron half-lengths after the first bend can be expressed as

$$L_{1/2} = \frac{L}{L_{1/2}} \quad (5-10)$$

where

$L_{1/2}$ = number of neutron half-lengths

L = total length of entranceway between the first bend
the point of interest

The neutron reduction factor due to entranceway wall effects can be expressed as

$$R_{fw} = \frac{1}{(2)^{L_{1/2}}} \quad (5-11)$$

In conclusion, it should be noted that secondary gamma rays can be generated in the entranceway walls, possibly in large quantities, by inelastic scatter and neutron capture. As is the case with the secondary gamma rays resulting from neutron scatter in barrier shielding, no quantitative analysis is available to evaluate this increased gamma dosage. It has been suggested that the entranceway walls might receive a wash containing boron.⁴ This emits relatively-soft gamma radiation upon thermal neutron capture, and would tend to reduce the problem.

5.5.2 Gamma Attenuation by Corridor Bends

Experimental and theoretical studies²⁸ have been conducted to evaluate the effect of bends on gamma radiation in ducts. Subsequently, certain design criteria pertaining to this subject have been proposed,⁴ and are summarized in this section

First 90 deg Corridor Bend

$$R_{fc_1} = 0.1 \omega_1 \quad (5-12)$$

where

R_{fc_1} = gamma radiation reduction factor for first 90 deg bend beyond entrance leg

ω_1 = solid angle fraction subtended by the corridor section at the next point of interest

Subsequent 90 deg Corridor Bends

$$R_{fc_n} = 0.5 \omega_i \quad i = 2, 3, \dots \quad (5-13)$$

5.6 OVERHEAD CONTRIBUTION TO TOTAL SHELTER DOSE

Some portion of the initial radiation will penetrate the barrier shielding provided by the roof and its earth cover. This overhead contribution was considered to be the sole radiation source in the analyses of the shelter proper,^{1, 2} where it was recognized that a burst directly above the shelter would result in the maximum penetration of the barrier. For the shelter analyses, the roof and its cover were considered as a thick shield with large dimensions in plan. Thus, the radiation penetration for a given intensity of the external radiation field (initial or fallout) could be related to the total thickness of the barrier and to its material properties.

Two additional factors should be considered when analyzing the overhead contribution from the entranceway. First, since considerations of maximum entranceway streaming will require that the design weapon no longer be positioned directly overhead, the effective barrier thickness of the entranceway roof and its earth cover is now related to its slant thickness. Next, since the entranceway appears in plan view as a long narrow passage-way, it is no longer acceptable to represent its roof as a semi-infinite barrier. Consideration of the entranceway geometry, recognizing the line-of-sight to the weapon burst and the shielding afforded by the walls of the

passageway, can lead to a significant reduction in the calculated overhead dose. In order to determine this, it is necessary to determine the solid angle fraction for the entranceway, as measured in the line-of-sight plane.

Once the free-field characteristics of the initial radiation have been obtained from Table 5-1, the solid angle function for the entranceway can be read from Fig. 5-1. The corresponding entrance radiation reduction factors, expressed in terms of weapon orientation and solid angle fraction, can then be obtained from Fig. 5-2. Finally, the composite barrier reduction factor for the roof and earth cover of the entranceway is obtained from Fig. 5-4 (initial gammas) and Fig. 5-6 (fission neutrons) or Fig. 5-7 (fusion neutrons). The overhead dose contribution for the entranceway is obtained by multiplying the free-field intensities of the initial radiation components by the product of the entrance reduction factor and the appropriate barrier reduction factors.

The overhead contribution from fallout radiation is computed in a similar manner. Presumably the fallout will be deposited as a thin layer of radioactive material on the ground surfaces adjacent to shelter and its entranceway. The entranceway is thus exposed to a plane radiation source, with the entranceway roof and cover soil again providing barrier shielding. In addition, as when initial radiation was considered, the geometry of the entranceway in the (vertical) plane of radiation leads to an entrance reduction factor.

Entranceway-mouth reduction factors for a passageway exposed to a plane overhead source of fallout gamma radiation are supplied in Fig. 5-8, Case 1, as functions of the solid angle fraction obtained from Fig. 5-1 or calculated from Eq. (5-5). The barrier reduction for fallout radiation, expressed in terms of the mass thickness of the barrier shield, is obtained from Fig. 5-5, Case 1. A reference dose rate of 10,000 R per hr at one hour has been assumed for all fallout situations (Section 5.4). The overhead dose contribution from fallout radiation can be obtained by multiplying the dose rate, integrated over the time period of interest in accordance with Eq. (5-8), by the product of the entrance reduction factor and the barrier reduction factor. By way of example, the total free-field exposure dose corresponding to a reference fallout dose rate of 10,000 R per hr at one hour and a two-week period will amount to approximately 86,000 roentgen.⁶

IIT RESEARCH INSTITUTE

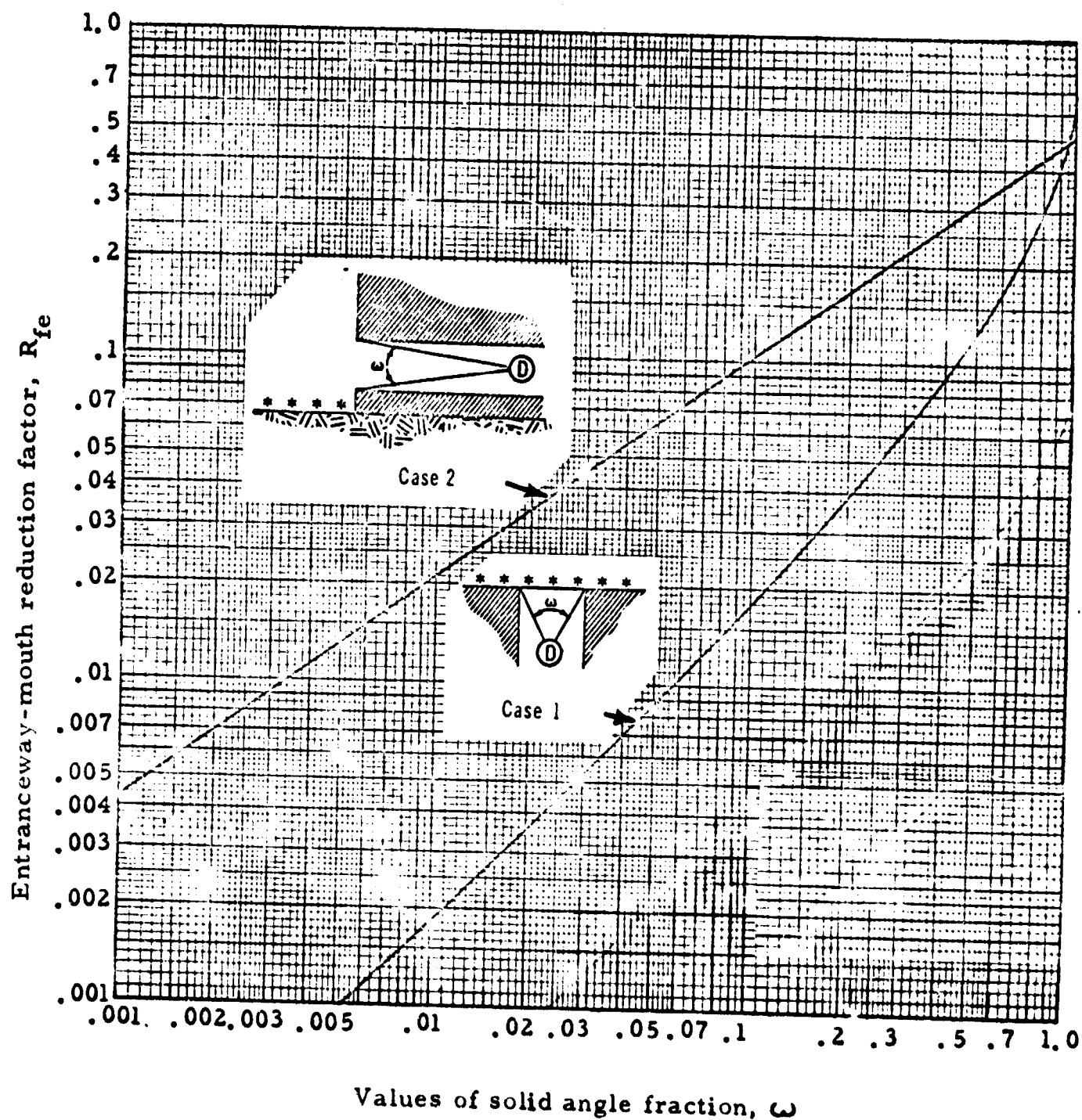


Fig. 5-8 ENTRANCEWAY-MOUTH REDUCTION FACTORS, R_{fe} , FOR FALLOUT-RADIATION STREAMING IN SHELTER ENTRANCEWAYS, AS FUNCTIONS OF ω AND POSITION OF ENTRANCEWAY MOUTH RELATIVE TO CONTAMINATED PLANE

5.7 CONTRIBUTION OF ENTRANCEWAY STREAMING TO TOTAL SHELTER DOSE

The additive shelter dose due to streaming of initial radiation along the entranceway is obtained from a sequence of calculations. Commencing with the free-field radiation at the entranceway mouth, and recognizing the weapon orientation with respect to the line-of-sight of the first entranceway leg, the entrance reduction factor for initial radiation is determined from Fig. 5-2. The reduced radiation field then streams along the first bend, with appropriate tunnel-wall attenuation of any neutron flux, and encounters the first 90 deg bend. This leads to an attenuation of gamma radiations. The net result is that the second entranceway leg is exposed to a further modification of the free-field radiation. This process can be continued as subsequent tunnel legs are encountered. The final entranceway contribution to the total shelter dose is obtained from a series of radiation streaming studies, where the results obtained for the preceding entranceway leg becomes the input parameters for the next leg. Any overhead contribution of initial radiation over the length of tunnel leg, if considered significant, can be included as an additional input parameter.

It is assumed that a streaming contribution to the shelter gamma dose can also result when fallout is deposited adjacent to the entranceway mouth or on the steps of the first entranceway leg. These situations can be analyzed with the aid of Fig. 5-4 and 5-8. First, the effect of any barrier shielding is determined from Fig. 5-4. Next, the appropriate entrance reduction factors are obtained from Case 2 of Fig. 5-8. The product of the barrier and entranceway reduction factors is then applied to the integrated free-field fallout dose over the time period of interest, and the reduced radiation field determined for the first leg of the tunnel. Since only gamma radiation is present, subsequent attenuation is attributable solely to corridor bends. The corridor bend reduction factors for initial gamma attenuation will also be extended to analyses of streaming by fallout gamma. As described for the initial radiation, it would be possible to consider the incremental streaming contributions in each tunnel leg due to barrier penetration of the tunnel roof and its cover soil. Such a contribution will undoubtedly be minor and can probably be neglected.

5.8 COMPOSITE ANALYSIS OF THE SHELTER AND ENTRANCEWAY

The design objective, at least from the standpoint of the radiation analyses, is to ensure that the total dose reaching shelter occupants will be less than some prescribed maximum. This action is predicated upon prior assumptions as to weapon yield and positioning, composition of the weapon and its casing, and direction and velocity of winds after an attack. It has been postulated that design will be based upon the worst case radiation associated with a specified level of overpressure.

Disregarding the entranceway, a maximum condition for the initial radiation dose within the shelter corresponds to a burst directly overhead. Next, considering the entranceway as well as the shelter, overhead contribution from initial radiation (hence any subsequent streaming of this radiation contribution into the shelter) will also be a maximum for the overhead burst. Penetration of the entranceway mouth by the initial radiation generally reaches a maximum when the line-of-sight for the first tunnel leg is aligned with the burst point. Any subsequent streaming of this contribution into the shelter is simultaneously maximized. For this condition, corresponding to a burst elevation of some 40 deg above the horizontal plane ($\psi_B \approx 50^\circ$) for the entranceways considered herein, the barrier penetration of the shelter and entranceway roofs will be considerably less than for the maximum condition. These factors must be evaluated as to their relative importance, and the entranceway designed accordingly. The controlling criterion, however, is that the total shelter radiation dose must not exceed the prescribed maximum for any single positioning of the weapon.

In the preceding sections, no attempt has been made to treat the question of radiation attenuation in a comprehensive or a rigorously detailed manner. The discussions presented therein have been limited, insofar as possible, to explanations of the related design tables, equations and figures. The reader desiring a more comprehensive treatment of the subject is directed to References 3, 24, 26 and the papers referenced therein.

CHAPTER

DESIGN OF STRUCTURAL ELEMENTS

6.1 INTRODUCTION

The shelter entranceway configurations of interest in this study are identified in Chapter 1 as the rectangular cubicle, full cylinder and sphere, including various combinations thereof. The structural elements discussed in this chapter are designed as integral components of these entranceway configurations. Only monolithic slab, wall and shell elements are considered, since earlier studies^{1,2} have shown that framed construction is normally not economical for the range of loadings which will be applied. The factors which govern the nature, magnitude, distribution and rate of the loading for these structural elements are discussed in Chapter 4.

The actual response of a structural element to a dynamically-applied load is influenced by material and load parameters. Many structural materials exhibit increasing yield or ultimate strengths as the rate of load application is increased. In recognition of this, appropriate values for material strengths associated with dynamic conditions of loading are introduced into the analyses of structural elements for blast-resistant structures. Also, if the dynamic loading is removed before a structural element has reached equilibrium under its action, the structural requirements may be less severe than for a longer duration of the same magnitude of load. A detailed evaluation of structural response must consider the pressure-time variation of the applied loading and the frequency response of the structural element. In order to preserve generality in the structural analyses however, the elements have been designed for an "equivalent" uniform static loading rather than for a particular dynamic loading.

The entranceway must retain its structural integrity throughout its period of projected use. This requirement may be of particular significance in the design of blast-resistant structures, due to the "negative" phase which follows the positive dynamic loading. Full or partial reversal of stresses may thus result, and should be recognized in the structural analyses. The design should provide for anticipated strain discontinuities and

concentrations of secondary stresses. If these possibilities are recognized, careful design of structural details should preclude excessive spalling of concrete surfaces or similar evidences of localized structural distress. Welded joints for steel members are considered to be desirable, and customary anchorage requirements for concrete reinforcement are supplemented by requiring that lapped steel be welded. The design detailing of structural elements should ensure that the full strength of the weakest member will be developed prior to failure of a structural connection.

In the following analyses of structural elements, many of the details which must be given recognition in the actual design of entranceways are not explicitly considered. However, minimum thicknesses are specified for major structural members, as are minimum area values for reinforcing steel in concrete elements. Cost expressions and equations which incorporate the various assumptions as to in-place costs are supplied for the several structural elements. These cost relationships may be adjusted for regional and temporal variations in cost, if so desired, by substituting revised data into the basic cost expressions. Such a procedure is recommended if detailed cost studies are required for a specific shelter. The estimated costs of structural details, where not explicitly appearing in the cost equations, are implicitly included in the unit in-place costs for the structural materials.

The generalized terms which appear in the cost equations of this and subsequent sections are expressed in several different ways. The in-place cost of a material unit is first identified. The cost for a structural element is next computed as the linear sum of its component material costs. Finally, depending on the physical form of a structural element, its composite cost may be expressed as a total cost. In order to avoid any later confusion, the cost notations and their meaning are described as follows:

(a) $X_{(n)}$

This notation, characterized by an upper case X with lower case subscripts, refers to the in-place cost of a unit of a given material. It can be expressed in dollars per unit length (ft), unit area (sq ft), unit weight (lb), or unit volume, (cu ft), of the material.

(b) $C_{(n)}$

This notation, characterized by an upper case C with a lower case subscript, refers to the unit in-place cost of a particular structural element. It is expressed in dollars per unit area of outer surface (sq ft) in the case of slabs, walls and shells, and in dollars per linear foot for rectangular frame members and for compression or tension support rings.

(c) $C_{(N)}$

This notation, characterized by an upper case C and upper case subscript, refers to the total in-place cost of a particular material in a structural element. It is expressed as a total cost, in dollars.

(d) k'_f

In specific instances where the unit cost, $X_{(n)}$, is dependent on some dimensional properties of the structural element, the $X_{(n)}$ term is replaced by a singular k term.

The material unit costs which are presented in Chapter 2 are used as the basis for determining structural element costs. The application of cost data is achieved, where possible, by formulating cost equations which contain a sufficient number of terms for an adequate representation of the cost variables. The detail with which the costs of a particular element are investigated in this study is, to a considerable degree, dependent upon the probable contribution of the element to the overall shelter cost.

6.2 RECTANGULAR CUBICLE (Monolithic Reinforced Concrete)

6.2.1 Design

The rectangular cubicle is suitable for use as an element in a shelter entranceway system. From the results of earlier studies of this configuration,^{1,2} it is anticipated that a monolithic structural system with heavily-reinforced concrete will be required for this application. One-way reinforced roof and floor slabs will then frame directly into reinforced side-walls, providing full moment continuity at the edge supports. This situation can,

for analytical studies, be represented in two-dimensional form by a column bent of unit width. In addition, of course, it will be necessary to provide end walls with adequate resistance to lateral forces. These end walls will also frame into the roof and floor slabs, initiating localized moments and corresponding localized requirements for reinforcing steel.

Two distinct loading conditions must be recognized. The first of these, which has been analyzed in the study of the shelter proper,¹ occurs when the blast wave does not reach the interior of the cubicle. As a consequence, only the exterior plane surfaces of the cubicle are loaded. The magnitudes of the blast-induced loadings on these surfaces are directly related to the surface orientation, to the soil characteristics, and to the value of the overpressure at the ground surface (Chapter 5). These dynamic loadings can be represented in their static equivalent forms as uniformly-distributed loadings of q lb per in.² for horizontal surfaces and as $k_h q$ for vertical surfaces. (Here k_h is the ratio of horizontal to vertical soil pressure,⁵ with its absolute value dependent upon the soil type.) The loadings q and $k_h q$ are inwardly-directed with respect to the cubicle and, when applied to a horizontal surface, produce compressive loading on the supporting members plus moment transfer at the beam-column (or wall-slab) connection. Similarly, loading on vertical surfaces imposes a compressive axial loading on the reacting horizontal members, again with the transfer of moment at the end connection.

A second loading condition arises when the reduced reflected pressure can actually penetrate within the cubicle interior. An outwardly-directed reflected pressure, which at any specified time is assumed to have a constant magnitude, irrespective of position or location, will then act normal to all cubicle interior surfaces. Although the exterior blast loading is also assumed operative during this same time interval, its magnitude is less than that of the interior reflected pressure. The net effect, in comparison with the first case, is to reverse the directions of loading on the cubicle surfaces.

The generalized analysis assumes a unit-width section of gross depth D inches, which is simultaneously subjected to dynamically-applied ultimate axial load of N_{du} per in. of width and to a dynamically-applied ultimate

IIT RESEARCH INSTITUTE

moment of M_{du} in. -lb per in. of width. Positive signs, in this notation, are attached to outwardly-directed axial forces (tension) and to counter-clockwise rotation due to load eccentricity e_d relative to the centerline ($M_{du} = N_{du} e_d$). A row of reinforcing steel (A_{sL} and A_{sR}) is supplied at each bending face of the section, with concrete cover d' and d'' such that $d' = d'' = 0.10 D$. From this it follows that $d = 0.90 D$, where d is the "effective depth"¹ of the bending section.

The equations of equilibrium for a reinforced-concrete section which is simultaneously subjected to axial loading and to end moment can be written in a generalized form.

$$\frac{N_{du}}{b d f'_{dc}} = -q_{dL} \left[\frac{K_{1L} + K_{2L} (c/d)}{K_{3L} + K_{4L} (c/d)} \right] - q_{dR} \left[\frac{K_{1R} + K_{2R} (c/d)}{K_{3R} + K_{4R} (c/d)} \right] + 0.85 \left[K_5 (c/d) + K_6 + \frac{K_7}{(c/d)} \right] \quad (6-1)$$

$$\frac{M_{du}}{b d^2 f'_{dc}} = 0.444 \left\{ q_{dL} \left[\frac{K_{1L} + K_{2L} (c/d)}{K_{3L} + K_{4L} (c/d)} \right] - q_{dR} \left[\frac{K_{1R} + K_{2R} (c/d)}{K_{3R} + K_{4R} (c/d)} \right] \right\} + 0.472 \left[K_5 (c/d) + K_6 + \frac{K_7}{(c/d)} \right] \left[1 - 1.80 K_8 \left(K_5 (c/d) + K_6 + \frac{K_7}{(c/d)} \right) \right] \quad (6-2)$$

where

N_{du} = dynamically-applied axial thrust, lb

M_{du} = dynamically-applied end moment, in. per lb

$$q_{dL} = \frac{A_{sL} f_{dy}}{b d f'_{dc}}$$

$$q_{dR} = \frac{A_{sR} f_{dy}}{b d f'_{dc}}$$

A_{sL} = area of reinforcing steel in row located on left side of centerline, in.² per in. of section width

A_{sR} = area of reinforcing steel in row located on right side of centerline, in.² per in. of section width

f_{dy} = dynamic yield strength of reinforcing steel, lb/in.²
(assumed equal for both tension and compression)

- f'_{dc} = dynamic ultimate strength of concrete test cylinder loaded in compression, lb/in.² (Related to compressive strength of short concrete column by applying 0.85 reduction factor, as in conventional practice. Also, the dynamic ultimate compressive strength is taken at 1.25 times the static ultimate compressive strength.)
- b = width of section, taken as 1 in. for all subsequent calculations
- d = effective depth of section (in.) taken as 0.9 times the gross depth of section
- c/d = the distance separating the extreme compressive fiber and the neutral axis of the bending section, referenced to the effective depth of the same section
- $K_{1,2}$ = constants depending upon the rotation of the bending cross section and upon the material properties. The subscripts L and R identify location relative to the centerline of the member.

By assuming that the bending cross section has a plane-strain distribution, geometrical considerations are sufficient to define limiting loading situations for combinations of N and M . Once these are obtained, specific solutions (valid within each strain-compatibility range) can be obtained for Eq. (6-1) and (6-2). Limiting conditions are realized as the load eccentricity e_d approaches zero, where the loading situation becomes that of an axially-loaded column; and similarly for decreasing N as e_d becomes very large, where the situation becomes that of bending moment in the transversely-loaded beam without end thrust.

In an actual design situation, considering the monolithic cubicle as described earlier, the situation at the wall-roof joint can be examined initially on the basis of full joint fixity. The ultimate plastic moment at the end of a roof slab of clear span L ft, supporting a uniform transverse load of q lb per in.² on its surface, is $M_{uS} = 9 q L^2$ in.-lb per in. of width. The ultimate plastic moment at the end of a wall of clear height H ft, supporting a uniform transverse load of $k_h q$ lb per in.² on its surface, is $M_{uW} = k_h q H^2$. The axial thrust on the roof slab, assuming that it furnishes reactive support to the wall, is $k_h q (6 H + D_{slab})$ lb per in. of slab width. Similarly, the axial thrust on the wall is $q (6 L + D_{wall})$ lb per in. of wall width.

In the general case, these two end moments will not be numerically equal. The joint is not fully restrained, although passive earth pressures will tend to resist any joint rotation, and there will be some tendency for moment equalization. However, since the analysis is based upon ultimate strength of the bending cross section and upon plastic redistribution of maximum bending stresses prior to collapse of a member, it is appropriate to assume that no significant moment redistribution will occur.

The designer, then, is faced with two broad choices. Either he can proportion both connecting members to resist the larger of the two fixed-end moments, recognizing that this will result in an excess moment capacity in one member, or he can proportion both connecting members to resist the smaller of the two connecting moments. In the latter situation, additional moment steel must then be added to the member with the larger fixed-end moment. In view of the many uncertainties involved, the first of these two methods appears preferable.

It is also necessary to examine the bending resistances in the central portions of the wall and the roof slab. The maximum bending moments at these locations, as a consequence of the assumption of plastic redistribution of moments, will be approximately equal to the fixed-end moments. In general, and certainly within the precision of this study, the preliminary design of the wall and roof sections can be based upon the thrusts and moments at their connection. However, it will also be necessary to ensure that the shearing mode resistances are adequate.

6.2.2 Unit Cost

The composite unit cost C_t of the eccentrically-loaded rectangular section can be expressed in terms of its component costs for concrete (C_c), for main reinforcing steel (C_s), for temperature steel (C_{st}) and for form-work (C_f). One-way reinforcement has been assumed, and diagonal-tension reinforcement has been excluded from specific consideration.

$$C_c = \frac{X_c d}{10.8} \quad (6-3)$$

$$C_s = \frac{X_s \phi_R d}{1200} \left[K_{\phi 1} + K_{\phi 2} \frac{f_{dy}}{f_{dc}} \right] \text{ positive N and M} \quad (a) \quad (6-4)$$

$$C_s = \frac{X_s \phi_L d}{1200} \left[K_{\phi 1} + K_{\phi 2} \frac{f_{dy}}{f_{dc}} \right] \quad \text{negative N and M} \quad (b) \quad (6-4)$$

$$C_{st} = \frac{X_s d \phi_{te}}{10,800} \quad (6-5)$$

$$C_f = X_f \quad (6-6)$$

$$C_t = C_c + C_s + C_{st} + C_f \quad (6-7)$$

In Eq. (6-4), $\phi_R = \frac{100 A_{sR}}{b d}$ and $\phi_L = 100 \frac{A_{sL}}{b d}$. Values of $K_{\phi 1}$ and $K_{\phi 2}$ are obtained from trial layouts of reinforcing steel and are related to the ratio of ϕ_R/ϕ_L , as indicated in Table 6-1.

Table 6-1

VALUES OF $K_{\phi 1}$ AND $K_{\phi 2}$ FOR USE IN COST EQ. (6-4)

ϕ_R/ϕ_L	$K_{\phi 1}$	$K_{\phi 2}$
1/0.50	1.531	0.0334
1/0.75	1.765	0.0389
1.00	2.000	0.0445
0.75	1.765	0.0389
0.50	1.531	0.0334

A program was prepared for the IBM 7094 computer, using the equilibrium relationships of Eq. (6-1) and (6-2). These relationships were bounded by the known compatibility constraints for the nonhomogeneous materials in the reinforced concrete, and by a requirement for plane-strain distribution across the bending cross section. Concurrently, the material cost equations were included in this program. Iterative solutions were then employed to find the minimum-cost design data corresponding to specified values of N and e_d . Typical data from this program are supplied in Table 6-2.

Table 6-2 (a)

MINIMUM IN-PLACE COST FOR ONE-WAY REINFORCED-CONCRETE
RECTILINEAR ELEMENTS WHICH ARE SUBJECTED TO TENSILE LOADING
IN THEIR AXIAL PLANE, PLUS UNIFORMLY-DISTRIBUTED TRANSVERSE
LOADING IN A SECOND PLANE

$(44,000 \leq f_{dy} \leq 75,000; 2000 \leq f'_c \leq 6000; 0.25 \leq \phi_R \leq 1.50;$
 $0.50 \leq \phi_L/\phi_R \leq 1.00)$

N_{du} (lb/in.)	M_{du} (in. -lb/in.)	f_{dy} (lb/in. ²)	f'_c (lb/in. ²)	ϕ_L/ϕ_R	ϕ_R (%)	D (in.)	C_t (\$/ft ²)
255	7,500	75,000	5,000	0.50	0.75	4.3	1.90
714	7,500	75,000	6,000	0.50	0.65	4.5	1.91
748	9,800	75,000	6,000	0.50	0.65	4.8	1.96
816	9,790	75,000	6,000	0.50	0.65	5.2	2.04
1155	33,960	75,000	5,000	0.50	0.95	7.8	2.86
1694	33,960	75,000	5,000	0.50	0.95	8.6	3.06
2880	84,670	75,000	6,000	0.50	0.95	13.5	4.26
3234	33,930	75,000	6,000	0.50	1.25	7.9	3.21
3388	44,380	75,000	5,000	0.50	0.95	10.4	3.50
3696	44,350	75,000	6,000	0.50	1.15	9.5	3.53
4224	84,690	75,000	6,000	0.50	1.05	13.4	4.40
5730	168,460	75,000	6,000	0.50	1.05	18.8	5.79
8064	84,590	75,000	6,000	0.50	1.35	13.0	4.80
8404	168,500	75,000	6,000	0.50	1.25	18.0	6.06
8448	110,670	75,000	6,000	0.50	1.35	14.5	5.27
9216	110,590	75,000	6,000	0.50	1.35	14.8	5.35
9375	275,625	75,000	6,000	0.50	1.15	23.7	7.33
10,000	30,000	75,000	6,000	0.50	1.35	9.7	3.86
16,044	168,300	75,000	6,000	0.50	1.35	20.0	6.87
16,808	220,185	75,000	6,000	0.50	1.35	22.3	7.54
18,336	220,030	75,000	6,000	0.50	1.35	22.9	7.72
26,250	275,362	75,000	6,000	0.50	1.35	27.9	9.19

Table 6-2 (b)

MINIMUM IN-PLACE COST FOR ONE-WAY REINFORCED-CONCRETE
RECTILINEAR ELEMENTS WHICH ARE SUBJECTED TO COMPRESSIVE
LOADING IN THEIR AXIAL PLANE, PLUS UNIFORMLY-DISTRIBUTED
TRANSVERSE LOADING IN A SECOND PLANE

$$(44,000 \leq f_{dy} \leq 75,000; 2000 \leq f'_c \leq 6000; 0.25 \leq \phi_R \leq 1.50;$$

$$0.50 \leq \phi_R/\phi_L \leq 1.00)$$

N_{du} (lb/in.)	M_{du} (in. -lb/in.)	f_{dy} (lb/in. ²)	f'_c (lb/in. ²)	ϕ_R/ϕ_L	ϕ_L (%)	D (in.)	C_t (\$/ft ²)
-150	-4,400	44,000	2,000	1.00	0.25	4.0	1.55
-220	-4,400	60,000	4,000	0.50	0.55	4.0	1.68
-420	-4,400	75,000	4,000	0.75	0.35	4.0	1.65
-440	-5,760	60,000	4,000	0.50	0.55	4.2	1.71
-480	-5,760	75,000	4,000	0.75	0.35	4.5	1.73
-750	-22,050	60,000	2,000	0.50	1.05	4.0	2.05
-1100	-22,050	60,000	2,000	0.50	1.05	4.0	2.05
-1500	-44,100	60,000	2,000	0.75	0.95	4.0	2.08
-2100	-22,030	60,000	2,000	0.50	0.95	4.0	1.98
-2200	-28,800	60,000	2,000	0.50	1.05	4.0	2.05
-2200	-44,100	60,000	2,000	0.50	1.05	4.0	2.05
-2400	-28,800	44,000	2,000	0.75	0.95	4.0	2.00
-3000	-88,200	60,000	2,000	0.75	0.95	4.0	2.08
-4200	-44,060	44,000	2,000	1.00	0.75	4.5	2.04
-4400	-57,600	60,000	2,000	1.00	0.75	4.8	2.21
-4400	-88,200	44,000	2,000	1.00	0.85	4.9	2.22
-4800	-57,600	60,000	3,000	0.75	1.25	4.0	2.19
-4875	-143,300	60,000	3,000	1.00	1.25	4.0	2.30
-7150	-143,400	60,000	3,000	1.00	1.25	4.9	2.60
-8400	-88,100	52,000	3,000	1.00	1.15	5.9	2.74
-8800	-115,300	60,000	3,000	1.00	1.15	6.2	2.88
-9600	-115,200	52,000	3,000	1.00	1.15	6.7	2.99
-13650	-143,200	60,000	4,000	1.00	1.25	7.4	3.31
-14300	-187,300	60,000	4,000	1.00	1.35	7.7	3.52
-15600	-187,200	60,000	4,000	1.00	1.25	8.5	3.64

6.3 THICK-WALL CYLINDER (Prestressed Concrete)

6.3.1 Design

A cylindrical structural element, with its longitudinal axis either horizontal or inclined, is suitable for use in one or more of the entranceway sections. The preliminary analysis of this element assumes that it is radially symmetric with respect to its longitudinal axis, and is loaded in these planes of radial symmetry. For this axisymmetric idealization, the weight of the member itself is neglected. Such items as nonuniform loading and structural discontinuities cannot be evaluated directly by this approach, other than by investigating their probable range of effects. Axial loading in the longitudinal plane can be evaluated, however, if symmetric with respect to the longitudinal axis.

As discussed in Chapter 4, any portion of the entranceway which is located upstream from the blast door will be subjected to two forms of blast loading. The first of these is an externally-applied loading, either applied directly to the structure or transmitted through some shallow depth of soil. The simplifying assumptions proposed in Chapter 4 for this loading situation are admittedly crude, since they eliminate any direct considerations of drag and/or reflected pressures on any above-ground projections, plus any explicit recognition of nonuniformities in the loading imposed on the structure. If these assumptions can be tolerated, however, the dynamic loading which is externally-applied in radial directions can be simply expressed as $p_m = p_{so}$. This is a long-duration loading when p_{so} is occasioned by a megaton weapon, hence p_m can be related to an equivalent uniform static load, q , by introducing the ductility ratio, μ , for the particular structure of interest.

There will also be additional loadings due to the weight of any earth cover, plus dead and live loadings on the ground surface. However, these are generally minor in relation to the overpressure loading. If they need be considered at all, they can usually be treated as an additional radial loading, externally applied. Thus, the total external loading can be approximated as $\sum q_E$, with each term in this summation representing a uniformly-distributed, equivalent static load. These loads act on the exterior of the cylindrical element and are directed radially inward.

The second form of blast loading is an outwardly-directed radial loading, which will result when the blast wave penetrates into the interior of the cylindrical element. As discussed in Chapter 4, the interior loading sequence can then be a very complicated one. The peak surface side-on overpressure is reduced in value as it enters the passageway, hence p_{so} in the Rankine-Hugoniot equations⁶ for peak reflected pressure is replaced by p_{to} , the transmitted overpressure. The resulting expression for the peak reflected interior pressure, p_{ri} , is supplied in Chapter 4 by Eq. (4-4). The front of this reflected pressure is assumed to impinge with zero degrees incidence on all interior surfaces of the passageway.

The reflected interior pressure is obviously a dynamic loading, but it too can be replaced for analytical purposes by an equivalent uniform static load. However, while we could write $p_{so} = f(\mu, q)$ for the long-duration overpressure loading from a megaton weapon, the effective duration of the peak reflected pressure may be less than that of the overpressure by one or more orders of magnitude. Therefore, as is apparent from Fig. 4-1, the functional relationship which exists between p_{ri} and q may be quite different from that existing between p_{so} and q . This could be true even if the ductility ratio of the structure remains unchanged.

The effective structural loading, as introduced into the design equations, can be appreciably less if recognition is given to the brief effective duration of the reflected interior pressure relative to the natural period of vibration of the structure. However, there is no simple method for determining the proper value for this effective duration. Detailed analyses can be made for a particular entranceway and for identified blast wave parameters, but this approach is impracticable in a generalized analysis. It is, of course, conservative from the standpoint of safety to assume that p_{ri} acts as a long-duration load. Alternatively, one might perhaps assume that $t_d/T \leq 1.0$ (Fig. 4.1) and thus obtain more realistic relationships between the ductility ratios and the equivalent static loads.

In any event, the interior loading for the cylindrical element due to the interior reflected pressure p_{ri} , can also be represented by an equivalent static loading, q_i , which is radially-directed outwards. Since the applied loadings are large, and since the traffic capacity requirements (Chapter 3)

can be satisfied with relatively-narrow entranceway elements, it follows that the ratio of cylinder interior radius to cylinder wall thickness is usually small. When this ratio falls below about ten, elastic design concepts suggest that consideration should be given to the actual distribution of stress across the cylinder wall.^{32, 33} For this thick-wall case, general equations have been derived for the radial and tangential stresses within the cylinder wall.³³ These are supplied herein in terms of the notation of References 1 and 2, on the assumption that the cylinder can be represented as a homogeneous and elastic material.

$$f_r = \left[\frac{q_I S_L^2 - \sum q_E (S_L + D/6)^2}{(S_L + D/6)^2 - S_L^2} \right] - \left[\frac{(q_I - \sum q_E) S_L^2 (S_L + D/6)^2}{4r^2 \{ (S_L + D/6)^2 - S_L^2 \}} \right] \quad (6-8)$$

$$f_t = \left[\frac{q_I S_L^2 - \sum q_E (S_L + D/6)^2}{(S_L + D/6)^2 - S_L^2} \right] + \left[\frac{(q_I - \sum q_E) S_L^2 (S_L + D/6)^2}{4r^2 \{ (S_L + D/6)^2 - S_L^2 \}} \right] \quad (6-9)$$

where

S_L = interior diameter of cylinder, ft

D = thickness of cylinder wall, in.

r = radius to interior point in cylinder wall, ft

$$\frac{S_L}{2} \leq r \leq \left(\frac{S_L}{2} + \frac{D}{12} \right)$$

q_I = static equivalent uniform load directed radially outward and acting on the inner surface of the cylinder, lb per in.²

$\sum q_E$ = summation of all static equivalent uniform loads which are directed radially inward and act on the exterior surface of the cylinder, lb per in.²

These equations can be evaluated at the boundaries of the cylinder wall.

$$f_r \bigg|_{r = \frac{S_L}{2}} = -q_I \quad (a) \quad (6-10)$$

$$f_r \bigg|_{r = \left(\frac{S_L}{2} + \frac{D}{12} \right)} = -\sum q_E \quad (b)$$

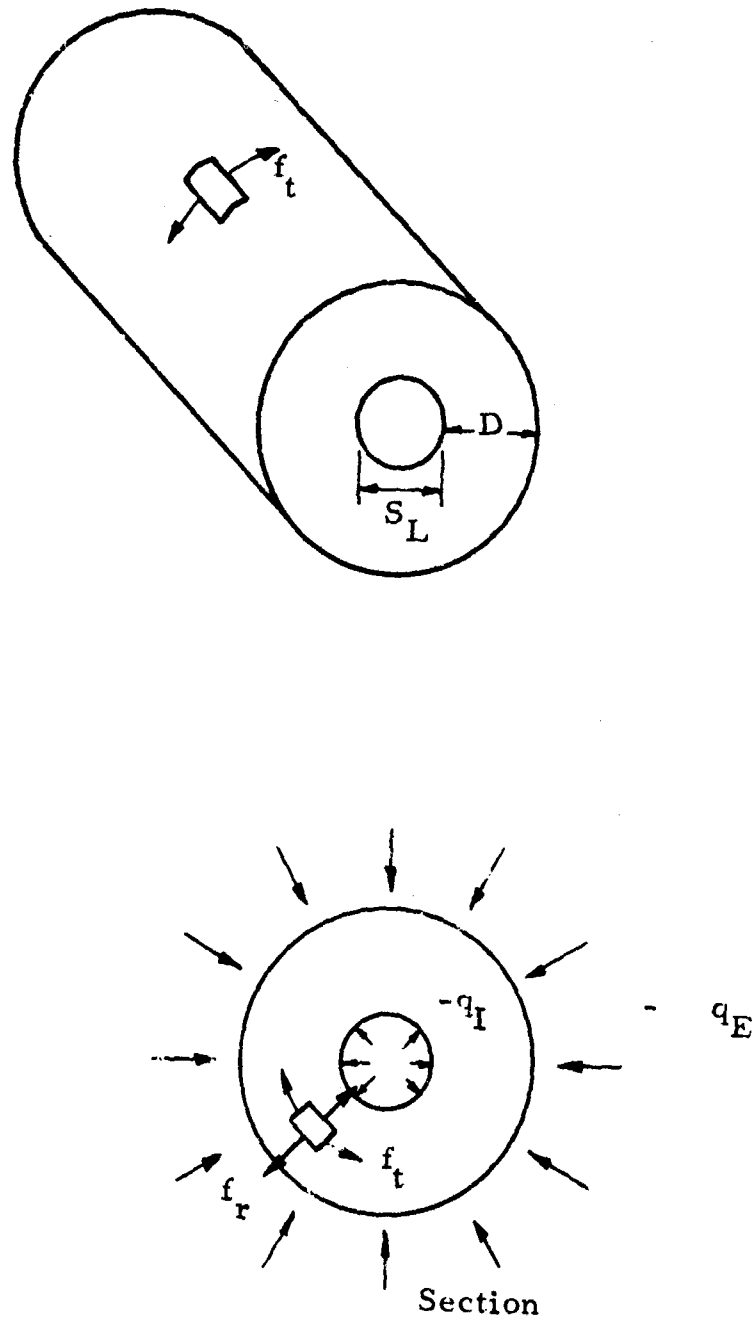


Fig. 6-1 THICK CYLINDER WALL STRESSES

$$\left. f_t \right|_{r = \frac{S_L}{2}} = \frac{q_I \left[(S_L + D/6)^2 + S_L^2 \right] - 2 \sum q_E (S_L + D/6)^2}{(S_L + D/6)^2 - S_L^2} \quad (a) \quad (6-11)$$

$$\left. f_t \right|_{r = \left(\frac{S_L}{2} + \frac{D}{6} \right)} = \frac{2 q_I S_L^2 - \sum q_E \left[(S_L + D/6)^2 + S_L^2 \right]}{(S_L + D/6)^2 - S_L^2} \quad (b)$$

It is apparent that the radial stress is always a compressive one, varying in a nonlinear fashion across a section through the cylinder wall. Equation (6-11a) also indicates that, for any loading conditions such that $\frac{\sum q_E}{q_I} < 1/2 \left[1 + \left(\frac{S_L}{S_L + D/6} \right)^2 \right]$, there will be tensile tangential stresses at the interior surface of the cylinder. A reinforced concrete section has been shown^{1, 2} to be efficient in resisting direct compressive stresses, always assuming that loading conditions are such that buckling does not occur. Hence, concrete appears as a logical choice to resist the compressive radial stress. However, the associated tensile forces due to the tangential stresses then become of concern, since tensile cracking of concrete is frequently encountered at tensile stresses approaching $0.1 f'_c$. For purposes of this study, the limiting allowable tensile stress in concrete will be set at $3\sqrt{f'_c}$.

The limiting equation for loading on the cylinder (Eq. 6-11a) can be written in terms of this maximum allowable tensile stress

$$\left. f_t \right|_{r = \frac{S_L}{2}} = q_I \frac{\left[(S_L + D/6)^2 + S_L^2 \right] - 2 \sum q_E (S_L + D/6)^2}{(S_L + D/6)^2 - S_L^2} \leq 3\sqrt{f'_c} \quad (6-12)$$

The form of this equation suggests that the tensile stresses produced by a given interior loading, q_I , could be kept within an acceptable upper bound by suitable adjustments in the magnitude of the exterior loading, $\sum q_E$. This in turn suggests the use of prestressing forces to apply an increment of radial loading, q_{Ep} , to the exterior surfaces of the cylinder. Accordingly, we will examine prestressed wall sections where an initial loading condition is introduced by post-tensioning. The steel strand for this purpose will be wrapped around the exterior of the cylinder with continuous stressing, and subsequently

grouted. The exterior loading $\sum q_E$ can then be considered as consisting of three parts; q_{Ep} , which represents the effective load component due to prestressing; q_{Es} , which represents the effect of conventional dead loads on the structure; and q_{Ed} , which represents the earth-transmitted effects of blast loading. This separation permits us to write expressions for the minimum value of the effective radial prestressing load, q_{Ep} which is sufficient to keep tensile stresses within the cylinder wall to a maximum value of $3\sqrt{f'_c}$ under the applied loadings. The parametric relationships for the desired control of tensile stresses in the cylinder wall are given by the following equation.

$$q_{Ep} \geq \frac{q_I}{2} \left[1 + \left(\frac{S_L}{S_L + D/6} \right)^2 \right] - 1.5\sqrt{f'_c} \left[1 - \left(\frac{S_L}{S_L + D/6} \right)^2 \right] - q_{Es} - q_{Ed} \quad (6-13)$$

At this stage, it is also necessary to consider the compressive stress introduced in the concrete by the prestressing forces. The prestressing forces, insofar as the cylinder is concerned, constitute a long-duration loading. For this reason, and also since any plastic flow in the concrete may reduce the effective prestressing forces, the maximum compressive design strength for concrete under prestressing forces alone has been set at $0.45 f'_c$. (Section 2.5.1) This condition corresponds to the pre-attack situation, where the blast-loading components are not operative. The maximum compressive stress in the cylinder wall, for this loading pattern, is in the tangential direction. Its peak value occurs at the interior surface of the cylinder, where $r = S_L/2$.

$$\left. \begin{array}{l} f_t \\ q_I = 0 \\ r = S_L/2 \end{array} \right| = - \left[\frac{2 \sum q_E (S_L + D/6)^2}{(S_L + D/6)^2 - S_L^2} \right] \quad (6-14)$$

Since no blast loading is operative for this situation, the externally-applied radial loading $\sum q_E$ can be considered as the sum of the radial prestressing component, q_{Ep} , and the radial loading, q_{Es} due to dead loading. Thus, we substitute in Eq. (6-14) and solve for q_{Ep} (maximum) in terms of the limiting value of $(-0.45) f'_c$ in compression

$$q_{Ep} \leq 0.225 f'_c \left[1 - \left(\frac{S_L}{S_L + D/6} \right)^2 \right] - q_{Es} \quad (6-15)$$

The effective prestressing force in the externally-wrapped strand will be designated by T_{sp} , in units of lb per lineal in. of cylindrical barrel. This force can then be identified by its inwardly-directed radial component, q_{Ep} , as follows,

$$T_{sp} = (6 S_L + D) q_{Ep} \quad (6-16)$$

The effective prestressing force, T_{sp} , should be associated with a value of q_{Ep} which satisfies the limits established by Eq. (6-13) and (6-15). These limits are not mutually exclusive for all situations of practical interest within the scope of this study, and thus must be separately investigated. If these equations are both satisfied, however, the tensile stresses in the cylinder shell will be restricted to values not exceeding $3\sqrt{f'_c}$ under the postulated magnitudes of both long-duration (prestressing) and short-duration (blast) loading. At the same time, compressive stresses in the shell will not exceed $0.45 f'_c$ under long-duration loading.

A final step involves checking the shell compressive stresses under short-duration loading. It is readily apparent from Eq. (6-9) that the effect of q_I is to reduce compressive stresses in the cylinder wall, hence it might be concluded that the critical condition for compressive stress is always associated with the long-duration loading imposed by the prestressing forces. However, the time sequence of loading could be such that the inwardly-directed blast loading component q_{Ed} continues to act after q_I has been removed. This situation can readily be investigated, recognizing that the loading component q_{Ed} will still be of short duration insofar as the response of the structure is concerned. For this situation, it should be possible to develop an ultimate compressive strength in the range from $0.85 f'_c$ to $0.85 f'_{dc}$. (Section 2.5.1) Using the lower limit of this range, and applying Eq. (6-11b), we obtain the following expression

$$q_{Ep} \leq 0.85 f'_c \left[\frac{(S_L + D/6)^2 - S_L^2}{(S_L + D/6)^2 + S_L^2} \right] - q_{Es} - q_{Ed} \quad (6-17)$$

It will generally be found that Eq. (6-17) does not control the compressive design, at least within the range of interest of this study. However, it should be checked. The most efficient design procedure will then include the following steps.

(a) Apply Eq. (6-15) to find the maximum permissible value of the prestressing radial component, assuming blast loadings are not operative. For this loading condition, the analysis assumes that tangential compressive stresses at the inner surface of the cylinder will reach their maximum working value of $0.45 f'_c$ under prestressing loads. Note that the portion of the prestressing component which remains effective after creep and relaxation, (including any compressive strain in the concrete) must be at least sufficient to satisfy (b).

(b) Apply Eq. (6-13) to find the minimum effective value of the prestressing radial component which will limit tensile stresses at the inner surface of the cylinder, under fully-loaded conditions, to a maximum of $3\sqrt{f'_c}$.

(c) Use Eq. (6-17) to find the value of the prestressing radial component which, under partially-loaded conditions, will produce compressive stresses of $0.85 f'_c$ at the interior cylindrical surface. This value of the prestressing component, which will usually not be critical, can be checked against that identified in (a). Since there will be some loss in the initial prestressing forces prior to the application of any blast-induced loading, the value of q_{Ep} from calculation (c) can be moderately in excess of that determined in calculation (a).

(d) Once a working value of q_{Ep} has been established, with any appropriate allowance for anticipated prestress losses, calculate the required prestressing force from Eq. (6-16).

6.3.2 Unit Cost

The unit costs of prestressed shell elements can be related to the cost factors C_c , C_s , C_{sp} , C_f , and C_g . The C_c cost factor refers to the cost of concrete per unit area of shell outer surface. Cost factors C_s and C_{sp} refer to costs of reinforcing and prestress steel, respectively. Here C_s is a function of shell thickness, while C_{sp} is related to the cost of the required length of prestressing strand per unit of shell area. The factors

C_f and C_g express the cost of form work and of the protective gunite covering for the prestress strand, again as a function of unit area.

It is advantageous for cost study purposes to express the effective prestressing force, T_{sp} , in terms of the total required length of prestressing strand per unit area of shell outer surface.

$$L_{sp} = \frac{12 T_{sp}}{F_{sp}} \quad (6-18)$$

where

L_{sp} = required length of prestressing strand, ft per sq ft of exterior shell surface

F_{sp} = manufacturer's recommended design load per prestressing strand, lb, (Table 2-7)

These cost factors can be expressed as follows:

$$C_c = \frac{D}{12} X_c \quad (6-19)$$

$$C_s = \frac{D \phi_t}{1200} X_s \quad (6-20)$$

$$C_{sp} = L_{sp} X_p \quad (6-21)$$

$$C_f = X_f \quad (6-22)$$

$$C_g = X_g \quad (6-23)$$

where

X_c = unit cost of concrete, lb per ft³ (Table 2-9)

X_s = unit cost of steel reinforcing rod, lb per ft³ (Table 2-6)

X_{sp} = unit cost of prestress steel, expressed as lb per ft for strand (Table 2-8)

X_f = unit cost of form work, lb per ft² (Table 2-10)

X_g = unit cost of gunite protective coating, lb per ft² (Section 2.4.2)

ϕ_t = percentage of reinforcing steel in the longitudinal direction, expressed in terms of the gross concrete area normal to the direction of reinforcement. A constant value of $\phi_t = 0.5$ percent will be used for the thick-wall cylindrical shells of this study. This steel will also satisfy any requirements for temperature reinforcement.

IIT RESEARCH INSTITUTE

The composite cost factor for a prestressed concrete cylinder, per sq ft of surface area, can be expressed as

$$C_t = C_c + C_s + C_{sp} + C_f + C_g \quad (6-24)$$

6.4 THIN-WALL CYLINDER

The discussion in Section 6.3 identified the thick-wall cylinder as one in which the ratio of interior radius to wall thickness, expressed in consistent units, is less than ten. For larger values of this ratio, it is usually satisfactory to assume that the stress distribution across the wall cross section is no longer a function of the radius. This assumption results in the thin-wall analysis, which will be described in this section. In general, this thin-wall analysis is applicable to all structural steel shells, whether designed for interior or for exterior pressure loadings. It is also applicable to shells of reinforced concrete where the requirements for structural resistance can be satisfied by a thin-wall section. This situation will frequently exist in an entranceway passage which is sealed from blast penetration. In this latter case, the only significant design loading is the earth-transmitted pressure, which is assumed to act radially on the exterior surfaces of the cylinder.^{1, 2}

6.4.1 Reinforced Concrete (Compression Loading)

1. Design

It is assumed that ground-transmitted loading of buried entranceway structures due to air blast at the ground surface will be in the form of externally-applied radial pressure loads. It is further assumed,^{14, 15} although with somewhat less confidence, that the lateral restraint provided by the surrounding earth will be adequate to preclude elastic buckling of the compressed shell elements. From these assumptions, it follows that the simple compressive failure mode will govern the structural design of cylindrical entranceway elements.

The equivalent uniformly-distributed static load which corresponds to the ultimate compressive-mode strength of a reinforced concrete cylinder can be expressed in the following form¹

$$q_c = \left[\frac{D}{6 S_L + D} \right] \left[0.85 f'_{dc} + 0.01 \phi_t f_{dy} \right] \quad (6-25)$$

where

q_c = equivalent static load which develops the ultimate strength of the section in the compressive mode, lb/in.² In this application, $q_c = q$ where q is the static representation of the overpressure loading at the ground surface.

D = thickness of wall of concrete cylinder, in.

S_L = interior diameter of concrete cylinder, ft

f'_{dc} = unit compressive ultimate strength of concrete under dynamic loading, lb/in.²

f_{dy} = unit compressive yield strength of reinforcing steel under dynamic loading, lb/in.²

ϕ_t = reinforcing steel in circumferential direction, expressed as a percentage of the gross concrete area of the cylinder wall cross section.

$(\phi_t = \frac{100 A_s}{D}, \text{ where } A_s = \text{cross sectional area of reinforcement per unit length of cylinder perimeter}).$ For the shells investigated herein, ϕ_t will be taken as 0.5 percent.¹

All values except D can be specified as input data, if subsequent recognition is given to any applicable dimensional limitations. Equation (6-25) can then be rewritten as

$$D = \left[\frac{q (6 S_L + D)}{0.85 f'_{dc} + 0.01 \phi_t f_{dy}} \right] \quad (6-26)$$

In cases where the limiting shell dimension of $D = 3$ inches governs, the preferred design variable then becomes f'_{dc} . Equation (6-25) is then written as

$$f'_{dc} = 1.18 \left[q \left(\frac{6 S_L + D}{D} \right) - 0.01 \phi_t f_{dy} \right] \quad (6-27)$$

2. Unit Cost

The unit cost per sq ft of surface area of a reinforced-concrete cylindrical shell element is a function of the cost factors C_c , C_s , and C_f . These cost factors are similar to those supplied in Section 6.3.2 for the prestressed concrete cylindrical shell.

$$C_c = \frac{D}{12} X_c \quad (6-28)$$

$$C_s = \frac{D \phi_t}{1200} X_s \quad (6-29)$$

$$C_f = X_f \quad (6-30)$$

The composite cost factor for the thin-wall reinforced-concrete cylinder is the linear sum of the material costs.

$$C_t = C_c + C_s + C_f \quad (6-31)$$

6.4.2 Reinforced Concrete (Tension Loading)

1. Design

The design of the thin-wall reinforced concrete cylinder for tension loading is very similar to the design of the thick-wall tension cylinder (Section 6.3.1). As before, it is reasonable to consider prestressed designs which utilize wrapped high-strength strands to resist the induced tensile stresses. However, due to the thinness of the cylinder wall in relation to its radius, it is now acceptable to assume that direct stresses are distributed uniformly over a cross section of the cylinder wall.

With this assumption of uniform stress distribution Eq. (6-15) of Section 6.3.1 can be rewritten to indicate the maximum permissible value of the radial prestressing component in an externally-wrapped prestressed thin-wall cylinder. This limitation, as before, (Section 6.3.1) results from the stipulation that concrete compressive stresses under the effective long-duration prestressing loads should not exceed $0.45 f'_c$.

$$q_{Ep}(\max) = 0.45 f'_c \left(\frac{D}{65 L + D} \right) - q_{Es} \quad (6-32)$$

where

$q_{Ep(max)}$ = maximum value of radial component of prestressing force, T_{sp} , corresponding to a limiting concrete compressive stress of $0.45 f'_c$ under prestressing loads plus dead loads. Units are $lb/in.^2$ of cylinder exterior surface.

f'_c = ultimate compressive strength of statically-loaded concrete, based on results of standard 28-day test on cylindrical specimens, $lb/in.^2$

D = total wall thickness of cylinder, in.

S_L = interior principal diameter of cylinder, ft

q_{Es} = radial component of dead-load forces, expressed in units of $lb/in.^2$ of cylinder exterior surface.

It is also required that the tensile stresses in the concrete be kept to a maximum value of $3\sqrt{f'_c}$. The controlling design situation will occur when the full loading is applied, since tensile stresses in the cylinder wall then reach their maximum. Since the effect of the prestressing forces is to oppose these tensile stresses, it becomes possible to specify the minimum acceptable value for the radial prestressing component. By modifying Eq. (6-13) of Section 6.3.1 to recognize thin-wall action, we obtain the following.

$$q_{Ep(min)} = \frac{q_I S_L - 0.5 D \sqrt{f'_c}}{S_L + D/6} - q_{Es} - q_{Ed} \quad (6-33)$$

where

$q_{Ep(min)}$ = minimum value of radial component of prestressing force, T_{sp} , corresponding to a limiting concrete tensile stress of $3\sqrt{f'_c}$ under blast loading. Units are $lb/in.^2$ of cylinder exterior surface.

q_I = static equivalent loading due to radial component of reduced reflected pressure within the cylinder. Units are $lb/in.^2$ of cylinder interior surface.

q_{Es} = radial component of dead-load forces, expressed in units of $lb/in.^2$ of cylinder exterior surface.

q_{Ed} = static equivalent loading due to radial earth-transmitted component of overpressure loading at the ground surface. Units are $lb/in.^2$ of cylinder exterior surface.

D = total wall thickness of cylinder, in.

S_L = interior principal diameter of cylinder, ft

f'_c = ultimate compressive strength of statically-loaded concrete, based on results of standard 28-day tests on cylindrical specimens. Units are lb/in.²

Finally, in order to check the compressive stress in the concrete under the assumption that the reduced reflected pressure is no longer acting within the cylinder, Eq. (6-17) of Section 6.3.1 can be modified as follows.

$$q_{Ep(max)} = 0.85 f'_c \left(\frac{D}{6 S_L + D} \right) - q_{Es} - q_{Ed} \quad (6-34)$$

where

$q_{Ep(max)}$ = maximum value of radial component of prestressing force, T_{sp} , corresponding to a limiting concrete compressive stress of $0.85 f'_c$ under prestressing loads, dead loads, and earth-transmitted overpressure loading. Units are lb/in.² of cylinder exterior surface.

q_{Es} = radial component of dead-load forces, expressed in units of lb/in.² of cylinder exterior surface.

q_{Ed} = static equivalent loading due to radial earth-transmitted component of overpressure loading at the ground surface. Units are lb/in.² of cylinder exterior surface.

D = total wall thickness of cylinder, in.

S_L = interior principal diameter of cylinder, ft

f'_c = ultimate compressive strength of statically-loaded concrete, based on results of standard 28-day tests on cylindrical specimens. Units are lb/in.²

Protective gunite coating (unit cost factor of X_g \$/sq ft) will be placed over the exterior-wound prestressing strand. Again, the required length of prestressing strand per sq ft of surface (L_{sp}) is expressed in terms of the total effective prestressing force per in. of cylindrical barrel length (T_{sp}) and the recommended design load per prestressing strand (F_{sp}).

IIT RESEARCH INSTITUTE

$$L_{sp} = 12 \frac{T_{sp}}{F_{sp}} \quad (6-18)$$

Longitudinal steel, which satisfies temperature steel requirements and may also contribute some nominal measure of longitudinal bending resistance, will be provided. The minimum longitudinal steel (whose area is expressed as a percentage of the gross section area normal to the direction of reinforcement) will be specified as $\phi_t = 0.50$.

2. Unit Cost

The unit costs per sq ft of cylindrical surface area are identical with those developed in Section 6.3.2 for the thick-wall prestressed cylinder.

$$C_c = \frac{D}{12} X_c \quad (6-19)$$

$$C_s = \frac{D \phi_t}{1200} X_s \quad (6-20)$$

$$C_{sp} = L_{sp} X_p \quad (6-21)$$

$$C_f = X_f \quad (6-22)$$

$$C_g = X_g \quad (6-23)$$

$$C_t = C_c + C_s + C_{sp} + C_f + C_g \quad (6-24)$$

6.4.3 Structural Steel (Tension or Compression Loading)

1. Design

Thin-wall cylinders of structural steel are suitable for either tensile or compressive loading. As with the thin-wall concrete cylinder, although with decreasing assurance, it will be assumed that the restraint afforded by the surrounding earth will be adequate to prevent elastic buckling until such time as yield occurs in a compressive or tensile mode. It will also be assumed that the loading on the cylinder, immediately prior to failure, is uniform and radial. This last assumption has been introduced into the analyses of all types of buried shells and, perhaps, is most acceptable for the thin-wall steel cylinder because of its capacity for localized deflection and consequent equalization of earth-transmitted loading.

Based on these assumptions, the design of the structural steel thin-wall cylinder can be related to its yield strength under uniaxial tensile or compressive loading. Since the yield strength of structural steel is considered to be the same for these two loading conditions, the dynamic load capacity of a cylindrical steel shell in either tension or compression can be expressed in terms of the same equivalent static load. The yield resistance of a structural steel cylinder under any radially-applied uniform loading can thus be expressed as,

$$q_t = q_I - q_{Es} - q_{Ed} = \frac{t f_{dy}}{6 S_L} \quad \text{(interior loading) (a)}$$

$$q_c = q_{Es} + q_{Ed} = \frac{t f_{dy}}{6 S_L + t} \quad \text{(exterior loading) (b)}$$

(6-35)

where

- q_t = net equivalent static load which develops the ultimate strength of the section in the tensile mode, lb/in.²
- q_c = net equivalent static load which develops the ultimate strength of the section in a compressive mode, lb/in.²
- f_{dy} = dynamic yield strength in tension or compression of structural steel, lb/in.²
- t = thickness of steel shell, in.
- S_L = interior diameter of steel cylinder, ft

Since the thickness of shell is small in comparison with the radius of the shell, we can combine these two expressions and express the parameters of the shell in terms of other tensile or compressive loading.

$$q_c = q_t = \frac{t f_{dy}}{6 S_L} \quad (6-36)$$

2. Unit Cost

Structural steel plate is generally available only in specific plate thicknesses and for a limited number of yield strengths. By rearranging the terms in Eq. (6-35) and by referring to the cost data supplied in Table 2-3, the designer can pick the combination of f_{dy} and t which satisfy the strength requirement at least cost. This least-cost, for a cylindrical shell fabricated from structural steel, is a function of the cost factor C_s for single curvature steel plate (Table 2-6). The costs listed in this table

include provision for protective coating and for fabrication.

$$C_s = X_s \quad (6-37)$$

$$C_t = C_s \quad (6-38)$$

6.5 THIN-WALL SPHERE

The design considerations for thin-wall sphere elements are analogous to those described for the thin-wall cylinder, assuming comparable loading conditions. The one-way shell action of the cylinder is now replaced by the two-way action of a doubly-curved surface. This leads to an increased load resistance for a given shell thickness, although this is obtained at the expense of an increase in fabrication costs.

6.5.1 Reinforced Concrete (Compression Loading)

1. Design

When it can be assumed that a simple compressive failure mode will govern the design of a thin-wall sphere, as when a compressive loading is radially-directed and uniform over the entire outer surface of the shell, the limiting value of the resistance of the sphere can readily be expressed in terms of a static equivalent load.

$$q_c = \left[\frac{D}{6 S_L + D} \right] \left[1.70 f'_{dc} + 0.02 \phi_t f_{dy} \right] \quad (6-39)$$

An assumption of simple radial loading is no longer valid when the sphere is used as a section of a shelter entranceway. The sphere, for this usage, will require two large openings. One of these will permit personnel to enter the sphere, while the second will function as an exit to downstream portions of the entranceway system. These openings constitute major discontinuities in the shell surface, particularly so for the relative sizes considered in this study, and appreciable departures from the assumptions of simplified shell theory are thus introduced.

The entrance and exit openings will be framed by supporting rings. These rings will provide equilibrium supports for the shell surfaces in the vicinity of the openings. In addition, the supporting rings may

themselves receive direct loading from adjacent structural elements of the entranceway system. One of these rings, for example, will customarily provide support for a blast-resistant door. The second ring, in the event that a double-locking system is required, (Section 1.3.2) will similarly be designed to support a blast-resistant door. Unless there is some deliberate provision for physical discontinuity in the entranceway system, the entrance and exit rings must also resist any longitudinal thrusts transmitted by the adjacent structural elements.

A precise analysis of shell stresses is difficult for these geometric and loading conditions, and becomes a formidable undertaking if a generalized solution is required. For purposes of this study, we will modify the actual conditions by introducing certain assumptions of axial symmetry, membrane action, and linear superposition of shell stresses. Although the existence of secondary stresses is largely ignored, their influence on shell costs should be minor. It can be expected that such stresses would be localized in the vicinity of the supporting rings.

The actual external loadings on the buried entranceway sphere will include the following.

- (a) Dead load of the shell itself
- (b) Load due to weight of soil above each element of the shell surface
- (c) Earth-transmitted dynamic loading due to the overpressure, p_{so} , at the ground surface. This loading, by previous assumptions,^{1, 5} is assumed to act radially and uniformly over the exterior surface of the shell. However, it obviously would not be acting over these shell areas which have been replaced by the exit and entrance openings.
- (d) Loads on the exit and entrance support rings, which will consist of blast-door reactions plus any thrusts transmitted from adjacent structural sections.

- (e) A reactive force, which is distributed in some unknown manner over some effective area of the shell surface. The net result of this reactive force must be such that equilibrium of the sphere is maintained. The reactive force need not be uniformly-distributed over the effective area, nor need it be radially-directed in relation to the shell surface.

The simplified analysis initially replaces this sphere by one with a single (first) circular opening. This sphere is then considered to have axial symmetry, both of form and of loading, about the radial centerline of the opening. (As a first approximation, this neglects all global effects due to the presence of the second opening.) The shell is then analyzed on the basis of an assumed pattern of loading, and the controlling stresses in the shell are determined. The next step is again to consider a sphere with a single (second) circular opening, and again to assume that the sphere has axial symmetric properties about this second opening. Controlling stresses are again determined, based upon a second assumption as to the loading pattern. The composite positive (tensile) and negative (compression) stresses at any point on the surface of the actual shell are then assumed to be the linear sum of those stresses which are separately computed for the two single-opening representations. Finally, as part of the supporting ring design, localized stresses are analyzed in the vicinity of the entrance and exit openings.

While this analytical approach involves several major simplifications, it is believed that the controlling stresses which are thus determined will constitute reasonable estimates of actual stresses. The representation becomes more valid when the supporting ring loading becomes much larger at one opening, as will be the case when only a single blast door is provided. The assumptions become more questionable when the diameter of one or both openings become large in relation to a principal diameter of the sphere. This, unfortunately, will frequently be the case in the investigations of this study. In passing, it should also be noted that the assumption of axial symmetry of the sphere about each opening is not exact, since the radial

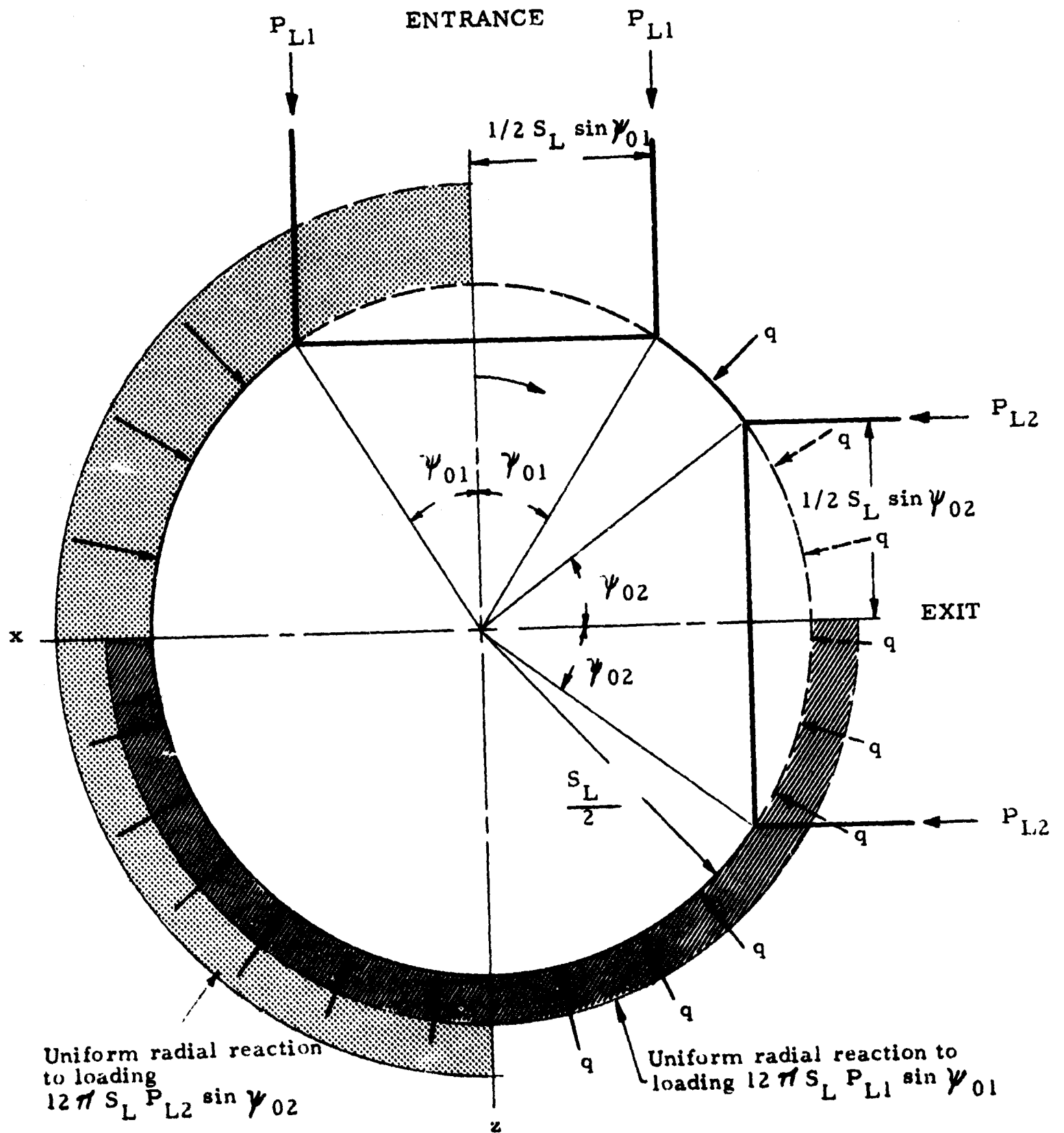


Fig. 6-2 THIN-WALL SPHERE, MERIDIAN SECTION, SINGLE-OPENING ANALYSIS (Loading Assumptions as Illustrated)

centerline of one or both openings may not pass through the center of the sphere. Finally, any assumption as to the distribution of earth resistance against the exterior surface of the blast-loaded sphere require further study and experimental verification.

The assumed pattern of loading, for purposes of this study, will be taken as follows:

- (a) Dead load of the sphere itself is neglected as inconsequential. The dead load attributable to the weight of earth above each element of shell surface is not specifically considered. As an approximation, this latter effect can be treated as an additional contribution to the blast-induced loading.^{1, 2}
- (b) The earth-transmitted blast loading is assumed to act as a uniform radial load directed inwardly over all portions of the sphere exterior surface, excluding only the area of the single opening which is considered in each step of the analysis. This dynamic loading, following the reasoning developed earlier, can be analyzed as an equivalent static load.
- (c) Thrust is transmitted to the supporting ring of the single opening considered in each phase of the analysis. This thrust is represented as an inwardly-directed line load which is uniformly distributed around the periphery of the opening. Again, this dynamic loading can be replaced by an equivalent static load. In establishing this equivalence, it should be recognized that the major portion of the loading on any ring supporting a blast door is attributable to reflected pressure on the door. Such loading is of short duration in comparison with the over-pressure-induced loadings which are transmitted through the soil.
- (d) The net soil resistance which is required to maintain equilibrium is assumed to act radially-inward against the exterior surface of the sphere and to be distributed uniformly

over the hemisphere furthest from the opening. Again, since this loading is directly related to items (b) and (c), it can be replaced by a static equivalent load.

The meridional (N_ψ) and latitudinal (N_θ) equilibrium forces at any point ψ , θ in the shell wall, assuming a single opening with central angle $2\psi_{01}$ and the pattern of loading as just described, can be computed from the following equations.^{34, 35, 36}

$$N_\psi = - \sum q_E (3S_L + \frac{D}{2}) (1 - \frac{\sin^2 \psi_{01}}{\sin^2 \psi}) - P_{L1} (\frac{\sin \psi_{01}}{\sin^2 \psi}) \quad (a)$$

$$\text{valid for } \psi_{01} \leq \psi \leq \pi/2$$

(6-40)

$$N_\psi = - \sum q_E (3S_L + \frac{D}{2}) (1 - \sin^2 \psi_{01}) - P_{L1} \sin \psi_{01} \quad (b)$$

$$\text{valid for } \pi/2 \leq \psi \leq \pi$$

$$N_\theta = - \sum q_E (3S_L + D/2) (1 + \frac{\sin^2 \psi_{01}}{\sin^2 \psi}) + P_{L1} (\frac{\sin \psi_{01}}{\sin^2 \psi}) \quad (a)$$

$$\text{valid for } \psi_{01} \leq \psi < \pi/2$$

(6-41)

$$N_\theta = - \sum q_E (3S_L + D/2) (1 - \sin^2 \psi_{01}) - P_{L1} \sin \psi_{01} \quad (b)$$

$$\text{valid for } \pi/2 < \psi \leq \pi$$

where

N_ψ = unit meridional equilibrium force in the shell, assumed uniform across the wall thickness D and expressed in lb/in.

N_θ = unit latitudinal equilibrium force in the shell, assumed uniform across the wall thickness D and expressed in lb/in.

P_{L1} = unit loading due to external thrust on the supporting ring, assumed to be distributed as a uniform inwardly-directed line load over the periphery $12\pi S_L \sin \psi_{01}$ of the shell opening, and expressed in units of lb/in.

$\sum q_E = q_{Ep} + q_{Es} + q_{Ed}$ (section 6.3.1). Since the prestressing load $q_{Ep} = 0$ for this application, $\sum q_E = q_{Es} + q_{Ed}$.

For high values of q_{Es} , it is sufficient to use
 $\sum q_E \approx q_{Es}$

q_{Es} = static equivalent load (acting radially inward on the exterior surface of the shell, excluding only the area of the single opening) due to earth-transmitted over-pressure loading at the ground surface. Units are lb/in.²

q_{Ed} = conventional dead and live loadings acting on a buried shell structure, approximated as a radial inwardly-directed loading, lb/in.

S_L = interior principal diameter of the sphere, ft

D = wall thickness of sphere, in.

ψ_{01} = one-half of the central angle for the circular shell opening of interest, deg

ψ = vertical angle, referenced to the radius which bisects the central angle of the opening, as measured to any parallel of latitude for the shell, deg.

θ = horizontal angle between principal meridians of the sphere, deg.

The tensile and compressive equilibrium forces along any meridian of the shell can be computed for the first assumption of loading (first opening) by applying Eq. (6-40) and (6-41) to values of ψ lying between $\psi = \psi_0$ and $\psi = \pi$. Due to the assumption of axial symmetry, the distribution of equilibrium forces will be the same along any other meridian. A second set of equilibrium forces, corresponding to the second loading assumption, can also be obtained from Eq. (6-40) and (6-41) by substituting $\psi' = \psi$, $\psi_{02} = \psi_{01}$ and $P_{L2} = P_{L1}$. This set of equations can be made compatible with the first by introducing the coordinate transformation

$$\psi = \psi' + \psi_R \quad (6-42)$$

where

ψ = vertical angle, referenced to the radius which bisects the central angle of the first opening and measured in a clockwise direction to any point on a meridian of the shell, deg

ψ' = vertical angle to this same meridian point, measured in a clockwise direction from the radius which bisects the central angle of the second circular opening.

MIT RESEARCH INSTITUTE

ψ_R = vertical angle, measured along a meridian and in a clockwise direction, between the bisectors of the central angles of the first and the second opening, deg. Note that ψ_R is not a constant if the radial bisectors of one or both openings do not pass through the centroid of the sphere. However, our preliminary analysis will assume that ψ_R remains constant.

Equations can also be formulated for the summations of meridional and latitudinal equilibrium forces, $\sum N_\psi$ and $\sum N_\theta$, referenced to any point on the shell surface defined by $\psi = \psi_0$, which will result from a linear combination of those equilibrium forces required by each of the two loading assumptions. Equations in terms of $\sum N_\psi$ and $\sum N_\theta$ are awkward to apply, primarily because of the loading discontinuities between $\pm \psi_{01}$ and $\pm \psi_{02}$. For this reason, particularly when $P_{L1} \gg P_{L2}$, it is probably simpler to establish those structural requirements for the shell which result by taking the first loading assumption as the more severe of the two assumptions. The shell is then reexamined for the second loading assumption and, if required, appropriate structural changes are then made.

The equations for N_ψ and N_θ , which are separately expressed for each of the two loading assumptions, become identical in form when we set $\psi_{01} = \psi_{02}$ and $P_{L1} = P_{L2}$. Thus, while the subsequent discussions are related by subscript identification to the equilibrium force equations for the first loading assumption, they are equally applicable to the second loading assumption by substitution of the appropriate subscripts.

A convenient first step is to establish the required thickness of the shell. A minimum value of $D = 3.0$ in. is specified as an initial constraint. It is assumed that any compressive equilibrium forces in the shell will be resisted by the reinforced concrete and by any compressive reinforcement, and that all tensile forces will be resisted by tensile reinforcement. Since it is also assumed that the shell will have a uniform thickness, any requirement for a shell thickness in excess of 3.0 in. can be determined by evaluating the maximum compressive forces in the shell.

$$D_{(max)} = D = \frac{-N_{t(max)}}{0.85 f'_{dc} + 0.01 \phi_{t(max)} f_{dy}} \quad (6-43)$$

where

D = total shell thickness, in.

$-N_{(\max)}$ = maximum absolute value of negative-sign equilibrium membrane forces in the shell, lb/in.

f'_{dc} = ultimate dynamic compressive strength of concrete, related by $f'_{dc} = 1.25 f'_c$ to the results of standard 28-day static test on cylindrical specimens, lb/in.²

$\phi'_{t(\max)}$ = maximum value of the required compressive reinforcing steel in the direction of maximum compressive forces, expressed as a percentage of the gross area of the shell cross section

f_{dy} = dynamic yield strength of reinforcing steel in tension or compression, lb/in.²

If the inequality $P_{L1} / \sum q_E > (3S_L + D/2) \sin \psi_{01}$ is satisfied, then the maximum compressive membrane force occurs in the meridional direction. Its maximum value is then obtained at $\psi = \psi_0$ which leads to the following expression for shell thickness

$$D_{\max} \equiv D = \frac{P_{L1}}{(0.85 f'_{dc} + 0.01 \phi'_{tM(\max)} f_{dy}) \sin \psi_{01}} \quad (6-44)$$

valid at $\psi = \psi_{01}$ for $\frac{P_{L1}}{\sum q_E} > (3S_L + D/2) \sin \psi_{01}$

where

$\phi'_{tM(\max)}$ = maximum required value of the compressive reinforcing steel in the meridional direction, expressed as a percentage of the gross area of the shell cross section.

If the inequality $P_{L1} / \sum q_E > (3S_L + D/2) \sin \psi_{01}$ is not satisfied, the maximum value of the compressive membrane force occurs in the region defined by $\pi/2 \leq \psi \leq \pi$. It is constant throughout this entire region, and is equal in the meridional and latitudinal directions. For this situation,

$\phi'_{tM(\max)} = \phi'_{tL(\max)} = \phi'_{t(\max)}$ and

$$D_{\max} \equiv D = \left[\frac{\sum q_E (3S_L + D/2) (1 - \sin^2 \psi_{01}) + P_{L1} \sin \psi_{01}}{0.85 f'_{dc} + 0.01 \phi'_{t(\max)} f_{dy}} \right] \quad (6-45)$$

valid for $P_{L1} / \sum q_E < (3S_L + D/2) \sin \psi_{01}$ in the region $\pi/2 \leq \psi \leq \pi$

Although D is required to remain constant, this need not be the case with ϕ'_t , the percentage of tensile reinforcement. It is obvious from

Eq. (6-40) and (6-41) that the compressive equilibrium forces will vary from point to point along a meridian of the shell. Thus, if some value of $\phi'_t = \phi'_{t(\max)}$ is assumed at the location of maximum compressive forces, there is also some location (defined by an appropriate value of the vertical angle, ψ) beyond which compressive equilibrium in the shell is satisfied with $\phi'_t = 0$.

The requirement for tensile reinforcement is established in comparable fashion. From Eq. (6-40) and (6-41) tensile equilibrium forces in the shell will only be present if the inequality

$$\frac{P_{L1}}{\sum q_E} > \frac{(3 S_L + D/2) (\sin^2 \psi + \sin^2 \psi_{01})}{\sin \psi_{01}}$$

is satisfied in the region defined by $\psi_{01} \leq \psi \leq \pi/2$. These tensile forces, if they exist, are only operative in the latitudinal direction and reach their maximum value of $\psi = \psi_{01}$. The required percentage of tension steel which corresponds to this peak tensile force is

$$\phi_{tL}(\max) = \frac{+N_{\theta}(\max)}{0.01 f_{dy} D} = \left[\frac{P_{L1}/\sin \psi_{01} - \sum q_E (6 S_L + D)}{0.01 f_{dy}} \right] \quad (6-46)$$

where

$\phi_{tL}(\max)$ = maximum value of the required tensile reinforcing steel in the (latitudinal) direction of maximum tensile forces, expressed as a percentage of the gross area of the shell cross section.

$+N_{\theta}(\max)$ = maximum value of positive-sign equilibrium membrane forces in the shell, latitudinal direction, lb/in.

As with ϕ'_t , values of ϕ_{tL} can vary as the tensile equilibrium forces in the shell vary. Any requirement for tensile reinforcement in the latitudinal direction will end if there exists a value of ϕ in the region $\psi_{01} < \psi \leq \pi/2$, which satisfies the relationship $P_{L1} \sin \psi_{01} - \sum q_E (3 S_L + D/2) \times (\sin^2 \psi + \sin^2 \psi_{01}) = 0$.

In general, for the single-opening assumption, the maximum negative and positive values of the equilibrium forces will occur at

$\psi = \psi_{01}$ or $\psi = \pi/2$. It is a simple process to substitute directly in Eq. (6-40) and (6-41) and thus find controlling values of (+N) and (-N). For practical applications, a minimum value of 0.50 percent reinforcement has been postulated for each principal direction. We can thus write

$\phi_{tM}(\min) \equiv \phi_{tL}(\min) \equiv \phi'_{tM}(\min) \equiv \phi'_{tL}(\min)$. As a further assumption, based upon the evaluations developed in earlier studies,^{1,2} it will be postulated that it will be uneconomic to provide compression steel in excess of the 0.50 percent minimum. These assumptions can now be introduced into Eq. (6-44) and (6-45), leading to direct solutions for D_{\max} in terms of known quantities.

$$D_{\max} \equiv D = \left[\frac{P_{L1}}{(0.85 f'_{dc} + 0.005 f_{dy}) \sin \psi_{01}} \right] \quad (6-47)$$

evaluated at $\psi = \psi_{01}$ where 0.5 percent compressive reinforcement is provided and where the inequality $P_{L1} / \sum q_E \geq (3 S_L + D/2) \sin \psi_{01}$ is satisfied.

$$D_{\max} \equiv D = \left[\sum q_E \frac{(3 S_L + D/2)(1 - \sin^2 \psi_{01}) + P_{L1} \sin \psi_{01}}{0.85 f'_{dc} + 0.005 f_{dy}} \right] \quad (6-48)$$

evaluated in the region $\pi/2 < \psi \leq \pi$, where 0.5 percent compressive reinforcement is provided and where the inequality $P_{L1} / \sum q_E \leq (3 S_L + D/2) \sin \psi_{01}$ is satisfied.

We thus can consider a sphere of uniform wall thickness, D . The maximum compressive requirements in this shell are satisfied by the resistance of the concrete, plus the contributions of 0.50 percent of reinforcing steel in each of the two principal directions. The only remaining question is whether or not the 0.50 percent minimum latitudinal steel between $\psi = \psi_{01}$ and $\psi = \pi/2$ will also satisfy any requirements for tension steel (Eq. 6-45). If it does not, additional latitudinal tensile steel must be provided between those parallels of latitude bounded by $\psi = \psi_{01}$ and by some value of the meridional angle, ψ_T , where

$$\phi_{tL} = 0.5 = \sin^{-1} \sqrt{\frac{P_{L1} - \sum q_E \sin \psi_{01} (3 S_L + D/2)}{0.05 D + q (3 S_L + D/2)}} \quad (6-49)$$

valid for $\psi_{01} \leq \psi_T \leq \pi/2$

III RESEARCH INSTITUTE

2. Unit Cost

The unit cost of a reinforced-concrete spherical shell element, as with other types of reinforced-concrete elements, can be expressed as the linear sum of the cost factors C_c , C_s , and C_f . Due to the lack of axial symmetry in a sphere with openings at $\psi = \psi$ and $\psi' = \psi + \psi_R$, much of the advantage of such a presentation is lost. The thickness of the concrete shell, by definition, will remain constant at all points on the shell surface. The steel requirement, at least in theory, can vary in both the meridional and latitudinal directions. In the general case, as explained earlier, it will be necessary to evaluate the equilibrium force in the shell due to each of the two single-opening assumptions, and combine these to obtain the controlling tensile and compressive forces. This process, in turn, would lead to composite solutions for the required shell thickness, (Eq. (6-44) or (6-45)), the maximum required percentage of tensile reinforcement (Eq. (6-45)), and the meridional angle at which any requirement for tensile steel in excess of 0.50 percent will end (Eq. (6-49)). Where $P_{L1} \gg P_{L2}$, as will be true when there is a single blast door which spans between $\pm \psi_{01}$, a reasonable estimate of unit costs can be obtained by utilizing the values of D_{max} , $\phi_{tL} (max)$ and ψ_T as determined for the single-opening case.

In any event, the unit costs of the materials in a unit element of the reinforced concrete sphere are expressed as follows:

$$C_c = \left(\frac{D}{12} \right) X_c \quad (6-50)$$

$$C_s = \frac{D}{1200} \left[1.00 + \phi_{tL} \left(\frac{\psi_T - \psi_{01}}{180 - \psi_{01}} \right) \right] X_s \quad (a)$$

valid for $\psi_T \geq \psi_{01}$

Where tension steel is not required ($\psi_T \leq 0$ in Eq. 6.46) use a minimum percentage of steel ($\phi_t = 0.50$) in both the latitudinal and meridional directions. Then

$$C_s = \frac{D \sum \phi_t}{1200} X_s \quad (b)$$

$$C_f = X_f \quad (6-52)$$

The total cost of the reinforced-concrete compression sphere, exclusive of reinforcing rings at the two circular openings defined by $2\psi_{01}$ and $2\psi_{02}$, can then be expressed as

$$C_T = \pi S_L^2 \cos\left(\frac{\psi_{01} + \psi_{02}}{2}\right) C_t \quad (6-53)$$

where

$$C_t = C_c + C_s + C_f$$

and it is implicitly assumed that the radial bisectors of each opening will pass through the centroid of the sphere.

6.5.2 Structural Steel (Compression Loading)

1. Design

The design of the thin-wall compression sphere of structural steel is very similar to the reinforced-concrete design which was developed in Section 6.5.1. The same expressions (Eq. (6-40) and (6-41)) are valid for the meridional and latitudinal equilibrium forces in the shell, under the stated assumptions. Since the yield strength of structural steel is considered to be equal in the tensile and compressive modes, the detailed design of the structural steel sphere is considerably simplified.

As with the reinforced-concrete sphere, the thickness of the sphere wall is assumed to remain constant. Following the notation developed in the earlier studies,^{1,2} the thickness of a steel plate is represented by t , in units of inches. Substituting t for D in Eq. (6-40) and (6-41), the design requirement is established by the absolute maximum value of N_ψ and N_θ over the range $\psi_{01} \leq \psi \leq \pi$. This yields the following equations, assuming that t is small in comparison with S_L .

$$t_{\max} \equiv t = \frac{P_{L1}}{f_{dy} \sin \psi_{01}} \quad (6-54)$$

evaluated at $\psi = \psi_{01}$ and valid when the inequality

$\frac{P_{L1}}{\sum q_E} \leq 3 S_L \sin \psi_{01}$ is satisfied. For this case, the maximum equilibrium force in the shell is compressive and acts in the meridional direction.

$$t_{\max} \equiv t = \left[\frac{(3 \sum q_E S_L)(1 - \sin^2 \psi_{01}) - P_{L1} \sin \psi_{01}}{f_{dy}} \right] \quad (6-55)$$

evaluated in the region $\pi/2 \leq \psi \leq \pi$, and valid when the inequality

$$\frac{P_{L1}}{\sum q_E} \geq 3 S_L \sin \psi_{01}$$

is satisfied. For this case, the maximum equilibrium force in the shell is compressive. It is uniform throughout the region and is equal in both the meridional and latitudinal directions.

2. Unit Costs

Unit costs for doubly-curved steel plate, as presented in Table 2-3, include the costs of fabrication and protective coating.

$$C_s = X_s \quad (6-56)$$

The total cost of the structural steel compression sphere, exclusive of reinforcing rings at the two circular openings which are defined by $2\psi_{01}$ and $2\psi_{02}$, can be expressed in the same form as for the reinforced-concrete sphere.

$$C_T = \pi S_L^2 \cos \left(\frac{\psi_{01} + \psi_{02}}{2} \right) C_t \quad (6-57)$$

where

$$C_t = C_s$$

6.5.3 Structural Steel (Tension Loading)

1. Design

If a single blast-resistant door is placed at the downstream opening in the sphere, the interior of the sphere will be subjected to reduced reflected pressures as the blast wave advances into the entranceway system. For this situation, since the peak value of the reduced pressure is normally much larger than that of the earth-transmitted blast loading acting on the exterior of the sphere, the net loading will introduce tensile stresses in the shell walls. In addition, the reflected pressures on the blast-resistant door will result in a line loading along the periphery of the supporting ring

which frames the downstream opening of the shell.

To facilitate the analysis of this situation, it is necessary to introduce certain simplifying assumptions. These assumptions, it will be seen, are analogous to those discussed (Section 6.5.1 - Design) for the reinforced-concrete compression sphere. The direct loadings on the tension sphere are those described in this earlier section, plus a radial outwardly-directed loading due to internal reflected pressures. The simplified analysis replaces the sphere by one with a single (downstream) circular opening, and considers the shell to have symmetry of form and of loading about an axis which bisects this opening. A second loading assumption, in which the shell is considered as axisymmetric about a single (upstream) circular opening, will be necessary to investigate the localized stresses in the vicinity of the framing ring for the upstream opening. The assumed pattern of loading on the sphere with the single (downstream) opening is described as follows.

- (a) Dead load of the sphere itself is neglected as inconsequential. The dead load attributable to the weight of earth above each element of shell surface is not specifically considered. As an approximation, this latter effect can be treated as an additional contribution to the blast-induced loading.^{1, 2}
- (b) The earth-transmitted blast loading is assumed to act as a uniform radial load directed inwardly over all portions of the sphere exterior surface, excluding only the area of the single opening. This dynamic loading, following the reasoning developed earlier, can be analyzed as an equivalent static load.
- (c) The peak reflected pressure is assumed to act as a uniform outwardly-directed load over all interior surfaces of the sphere, excluding only the area of that single opening which contains the blast-resistant door. This dynamic loading can also be replaced by a static equivalent load. In developing this equivalence, it is appropriate to recognize that the duration of the peak

reflected pressure is brief in comparison with the duration of the earth-transmitted blast loading.

The meridional (N_ψ) and latitudinal (N_θ) equilibrium forces at any point ψ , θ in the shell wall, assuming a single opening with central angle $2\psi_{01}$ and the pattern of loading just described, can be computed from the following equations. ($t/6 S_L$ assumed very small)

$$N_\psi = 3 S_L q_I - 3 S_L \sum q_E \left(1 - \frac{\sin^2 \psi_{01}}{\sin^2 \psi} \right) \quad (a)$$

(6-58)

valid for $\psi_{01} \leq \psi \leq \pi - \psi_{01}$

$$N_\psi = 3 S_L (q_I - \sum q_E) \quad (b)$$

valid for $\pi - \psi_{01} \leq \psi \leq \pi$

$$N_\theta = 3 S_L q_I - 3 S_L \sum q_E \left(1 + \frac{\sin^2 \psi_{01}}{\sin^2 \psi} \right) \quad (a)$$

(6-59)

valid for $\psi_{01} \leq \psi \leq \pi - \psi_{01}$

$$N_\theta = 3 S_L (q_I - \sum q_E) \quad (b)$$

valid for $\pi - \psi_{01} \leq \psi \leq \pi$

where

N_ψ = unit meridional equilibrium force in the shell, assumed uniform across the wall thickness t and expressed in lb/in.^2

N_θ = unit latitudinal equilibrium force in the shell, assumed uniform across the wall thickness t and expressed in lb/in.^2

$\sum q_E = q_{Ep} + q_{Es} + q_{Ed}$, or, since $q_{Ep} = 0$ for no prestressing,
 $\sum q_E = q_{Es} + q_{Ed}$ (Section 6.3.1 and 6.5.1)

q_{Ed} = static equivalent load acting radially inward on the exterior surface of the shell (excluding only the area of the exit opening) due to earth-transmitted over-pressure loading at the ground surface. Units are lb/in.^2

III RESEARCH INSTITUTE

- q_{Es} = conventional dead and live loadings acting on a buried shell structure, approximated as a radial inwardly-directed loading, lb/in.²
- q_I = static equivalent load acting radially outward on the interior surface of the shell (excluding only the area of the exit opening) due to the reduced reflected pressure within the shell. This loading is of short duration, and is expressed in lb/in.²
- S_L = interior principal diameter of the sphere. Also, since the shell thickness t is assumed small, S_L is approximately equal to the exterior principal diameter
- ψ_{01} = one-half of the central angle for the exit opening, deg
- ψ = vertical angle, references to the radius which bisects the central angle of the opening, and measured to any parallel to latitude for the shell, deg
- θ = horizontal angle between principal meridians of the sphere, deg

The structural parameters of the spherical steel shell, again assuming a constant wall thickness $t_{\max} = t$, are established by the absolute maximum value of N_ψ , N_θ in the region $\psi_{01} \leq \psi \leq \pi$. By inspection, since $q_I > q_E$, this will occur at $\psi = \psi_{01}$ where $N_{\psi(\max)} = 3 S_L q_I$. From this, we obtain the required wall thickness, t .

$$t_{\max} \equiv t = \frac{3 S_L q_I}{f_{dy}} \quad (6-60)$$

2. Unit Cost

Unit costs for the doubly-curved plate, as with the compression sphere, are obtained from Table 2-3. The same expressions remain valid for C_s and C_T , as previously defined for the structural steel compression sphere (Section 6.5.2).

$$C_s = X_s \quad (6-56)$$

$$C_T = \pi S_L^2 \cos\left(\frac{\psi_{01} + \psi_{02}}{2}\right) C_t \quad (6-57)$$

where

$C_s = C_t$ and the two openings (assumed circular) are defined by their central angles, ψ_{01} and ψ_{02} .

IIT RESEARCH INSTITUTE

6.6 SUPPORT RINGS FOR OPENINGS IN SPHERES

6.6.1 Analysis

The thin-wall sphere, as discussed in Section 6.5, has exit and entrance openings (assumed circular in plan) in the shell surface. These openings must be framed by reinforcing rings, which will act in conjunction with the spherical shell to maintain equilibrium under composite conditions of loading.

The simplified analysis of the sphere (Section 6.5) considered two orientations and loading patterns for an axisymmetrical single-opening sphere. The first of these two cases considered only the entrance opening, neglecting any global effects due to the presence of the second opening, and computed the membrane equilibrium forces in the shell. The second case was a repetition of the first, except that now only the exit opening was considered. Finally, it was proposed that the limiting structural requirements for the shell (except for localized requirements in the vicinity of each opening) could be obtained by linear superposition of these two cases. The problems remain, however, of evaluating the localized requirements for stability at the two openings.

The primary loadings on the supporting rings, continuing the earlier assumption of two orientations and loading patterns (Section 6.5), can be described as follows:

(a) For the first loading case, Ring No. 1 (entrance for the compression sphere or exit for the tension sphere) must satisfy shell equilibrium forces N_ψ and N_θ at the boundary described by $\psi = \pm \psi_{01}$. In addition, for the compression sphere, the ring must support a line loading P_{L1} along its circumference. The ring is axisymmetric with respect to both loadings.

(b) For the first loading case, Ring No. 2 (exit for the compression sphere or entrance for the tension sphere) must satisfy shell equilibrium forces N_ψ and N_θ at the boundary described by $\psi' = \pm \psi_{02}$. Equation (6-42) can be used to relate ψ and ψ' for a given sphere through the relationship $\psi = \psi' + \psi_R$. For the usual case of one right-angle turn within the sphere, $\psi_R = \pi/2$. In addition, since the analysis for the first loading case assumes that external reactive forces (compression sphere only) or internal radial

forces (tension sphere only) act on a spherical surface which includes the area of the second opening, a compensating radial thrust should be supplied by the supporting ring. In the general case, neither of these two types of loading is axisymmetric with respect to the supporting ring.

(c) For the second loading case, Ring No. 1 must satisfy a new set of shell equilibrium forces N_ψ and N_θ at the boundary (still described by $\psi = \pm \psi_{01}$, after applying the coordinate transformation of Eq. (6-42)). These forces, since they result from loading which is axisymmetric with respect to $\psi = \psi_R$, are not symmetric with respect to Ring No. 1. A compensating radial thrust, similar to that described for Ring No. 2 in (b) above, should also be included in the loading for Ring No. 1.

(d) For the second loading case, Ring No. 2 must satisfy a new set of shell equilibrium forces N_ψ and N_θ at the boundary described by $\psi = \psi_R \pm \psi_{02}$. In addition, if axial thrust is transferred from an adjacent structural section to a compression sphere, it will be necessary to consider a second line loading, P_{L2} , which is directed along the circumference of the ring. Both of these loadings are axisymmetric with respect to the supporting ring.

Obviously, it will be difficult for any practicable ring to satisfy these theoretical requirements. In addition, two types of secondary loadings must be recognized. First, to the extent that strain compatibility between a ring and the adjacent shell surface are not satisfied simultaneously with stress compatibility, there will be secondary stresses developed in the ring (and in the adjacent shell). Secondly, due to the requirement that local equilibrium must be satisfied at each ring-shell boundary, there can be torsional and moment forces developed both in the shell and in the ring.

The analytical process for a solution to this composite loading is relatively straightforward for a given set of input parameters, and would constitute a necessary step in any actual design of this type of structural element. While it is highly desirable to generalize such load-resistance relationships, our initial attempts have led to serious complexities. Lacking the time to pursue this effort, we have concluded that further simplifying assumptions must be introduced into the analysis. These assumptions should provide a reasonable basis for estimating the costs of a supporting

ring, but must not be considered as an adequate basis for its design.

For the common situation, the predominant loading on Ring No. 1 is either axial compression (compression sphere) or axial tension (tension sphere). As a first approximation, Ring No. 1 will be designed to resist this loading plus a second loading, arbitrarily specified, which is reversed in direction and whose magnitude is 25 percent of the first loading. These requirements, in conjunction with the optimum location of reinforcing steel within the supporting ring, should normally provide adequate resistance to primary loading and to most secondary stresses, with the possible exclusion of torsion.

For these same assumptions, the loading on Ring No. 2 can be considerably more complex. However, its peak loading is frequently (although not invariably) of lesser magnitude than the loading on Ring No. 1. Bending in one or more planes can be expected, hence significant moment resistance may be required. Lacking any ready means of evaluating the actual design requirement, this second ring (for costing purposes) will be designed to resist, simultaneously, the maximum compressive and maximum tensile equilibrium forces which are present anywhere in the shell adjacent to the periphery of the ring. Finally, although secondary stresses adjacent to the supporting rings will undoubtedly influence the localized structural requirements for the shell surface, it will be assumed that there will be no significant effect on total shell costs. (Section 6.5.1)

6.6.2 Ring No. 1 (Reinforced Concrete, Compression Sphere)

1. Design

Since the reinforced concrete sphere of Section 6.4.1 was designed only for compression loading, it follows from Eq. (6-40a) that the equilibrium load on Ring No. 1 (framing the circular opening defined by $\pm \psi_{01}$) will be compressive. The design of a typical reinforced-concrete supporting ring, for this condition of uniform and inwardly-directed radial loading, is analogous to the design of the thick-wall cylinder (Section 6.3.1). The compressive loading of interest is the horizontal component of N_ψ , evaluated at $\psi = \psi_{01}$ and acting on the exterior circumference of the ring. Eq. (6-8) and (6-9) can thus be rewritten as:

$$f_r = \left[\frac{\left(\frac{-P_{L1}}{b \tan \psi_{01}} \right) (S_L + D/6)^2}{(S_L + D/6)^2 - S_L^2} \right] \left[1 - \frac{S_L^2}{4r^2} \right] \quad (6-61)$$

$$f_t = \left[\frac{\left(\frac{-P_{L1}}{b \tan \psi_{01}} \right) (S_L + D/6)^2}{(S_L + D/6)^2 - S_L^2} \right] \left[1 + \frac{S_L^2}{4r^2} \right] \quad (6-62)$$

where

f_r = radial stress in supporting ring (tension assumed positive) due to the maximum (tensile) value of the equilibrium membrane force, N_{max} , in the shell adjacent to the ring, lb/in.²

f_t = tangential stress in supporting ring (tension assumed positive) due to the same equilibrium force, N_{max} , lb/in.²

S_L = interior diameter of supporting ring, ft

D = gross depth of ring wall in the plane of the ring, in.

b = gross thickness of ring wall in a plane normal to the plane of the ring, in.

r = radius to an interior point within the ring wall, ft, subject to the constraint

$$\frac{S_L}{2} \leq r \leq \left(\frac{S_L}{2} + \frac{D}{12} \right)$$

The maximum negative value of f_r occurs at $r = \left(\frac{S_L}{2} + \frac{D}{12} \right)$, while the maximum negative value of f_t occurs at $r = \frac{S_L}{2}$. This latter stress will control the design of the reinforced-concrete supporting ring (compression case).

$$f_t \bigg|_{r = \frac{S_L}{2}} = \left[\frac{\left(\frac{-2 P_{L1}}{b \tan \psi_{01}} \right) (S_L + D/6)^2}{(S_L + D/6)^2 - S_L^2} \right] \quad (6-63)$$

The ultimate compressive resistance of a dynamically-loaded member of reinforced concrete, neglecting the resistance afforded by any compression steel, is

$$-f_{t(max)} = 0.85 f'_{dc} \quad (6-64)$$

III RESEARCH INSTITUTE

Equations (6-63) and (6-64) can be combined, and a quadratic solution for ring depth, D , can then be formulated in terms of known parameters and a postulated ring thickness, b . However, it is probably simpler to effect the solution through repeated substitution, using trial values for both D and b . It will be recalled from Section 6.5.1 that P_{L1} is the line-load representation of such dynamic forces as may act against a blast-resistant door, which in turn will react against the supporting ring. The loading P_{L1} may thus be replaced by an equivalent static loading, whose magnitude is related to the blast-door loading duration and to the ductility of the structural section which forms the supporting ring.

The requirement for tensile reinforcement in Ring No. 1 is obtained from the arbitrary stipulation (Section 6.6.1) that the ring shall be designed for a reversed loading whose magnitude is 25 percent of the primary loading.

$$\text{Tension loading} = 0.25 (\text{compression loading}) = \frac{N \psi_{01}}{4} (6 S_L + D).$$

From this, direct substitution yields an expression for the required percentage of tension reinforcement.

$$\phi_t = \frac{25 P_{L1} (6 S_L + D)}{b D f_{dy} \tan \psi_{01}} \quad (6-65)$$

where

ϕ_t = axial tension reinforcement in compression ring, expressed as a percentage of the gross area of the ring wall cross section. ($\phi_t = 100 A_s / b D$, where A_s = cross sectional area of reinforcement)

$P_{L1} / \tan \psi_{01}$ = horizontal component of meridional equilibrium force in the shell, evaluated at $\psi = \psi_{01}$. This force component acts on the supporting ring as a radial inwardly-directed dynamic loading, lb/in.

S_L = interior principal diameter of supporting ring, ft

D = gross depth of ring wall in the plane of the ring, in.

b = gross thickness of ring wall in a plane normal to the plane of the ring, in.

f_{dy} = dynamic yield stress of reinforcing steel, lb/in.

Since there is a probability that the ring will also be subjected to localized moments, as discussed earlier in this section, it seems wise to include some empirical provisions for moment resistance. The required percentage of tension steel, for example, could be placed with minimum concrete cover and distributed uniformly around the periphery of the ring cross section. The ring dimension, b , assuming equal probabilities of applied moment for the two planes, should then be approximately equal to D .

Although the main steel in the compression ring is specified only to afford resistance to secondary tensile stresses (Eq. 6-65), it will normally be subjected to compressive loading. Tie steel should therefore be provided, with appropriate spacing between ties.

It was also noted that torsional stresses would be imposed on the supporting ring for those cases where the resultant forces do not pass through the center of torsion for the member. For these cases, which will represent the usual design condition, shear steel in the form of vertical closed stirrups can be used to resist torsional shearing stresses. A preliminary estimate of the required percentage of torsional reinforcement can be obtained as follows.³⁷

$$\phi_{vt} \approx \frac{200 M_t - 50 b^2 D (f'_{dc})^{2/3}}{b^2 D f_{dy}} \quad (6-66)$$

where

ϕ_{vt} = total required percentage of torsional stirrup steel, expressed as a percentage of the gross area of exterior ring surface.

$$(\phi_{vt} = \frac{100 A_s}{2 \pi (6 S_L + D) b} -$$

where A_s = total cross sectional area of torsional reinforcement in length $2 \pi (6 S_L + D)$ and width b ,

measured normal to plane surface of supporting ring).

M_t = applied torsional moment per unit length of supporting ring, in.-lb per in.

An equal cross sectional area of longitudinal steel is required in order to resist the horizontal component of the torsional induced tension. This steel can be considered as additive to the main reinforcing steel specified by Eq. (6-65) and will be similarly distributed over the ring cross section.

2. Unit Cost

The unit cost of the reinforced concrete compression ring is a function of the cost factors for concrete (C_c), main reinforcing steel (C_s), tie steel (C_{st}), torsional steel (C_{vt}) and formwork (C_f). If torsion is also a consideration, requiring the inclusion of torsional steel, there is then an additional cost factor, C_v .

$$C_c = \frac{bD}{144} X_c \quad (6-67)$$

$$C_s = \frac{\phi_t bD}{14,400} X_s \quad (6-68)$$

$$C_{st} = \frac{\phi_{te} bD}{14,400} X_s \quad (6-69)$$

$$C_{vt} = \frac{\phi_{vt} b}{14,400} (1 + 0.80 (b + D)) X_v \quad (6-70)$$

(includes longitudinal
torsional steel)

$$C_f = \frac{b + D}{6} X_f \quad (6-71)$$

The composite cost per lineal foot of reinforced concrete compression ring can then be expressed as

$$C_t = C_c + C_s + C_{st} + C_{vt} + C_f \quad (6-72)$$

6.6.3 Ring No. 1 (Structural Steel, Compression Sphere)

1. Design

The structural steel compression sphere is described in Section 6.5.2. The supporting ring which frames the principal opening must withstand the horizontal component of the compressive meridional equilibrium

force at $\psi = \psi_{01}$. It can be postulated that the probable form of the structural steel supporting ring, for this application, would be either a steel beam or built-up member. In any event, for the assumption of axial compressive loading, the maximum loading condition is realized when the entire cross section of the ring is yielding in compression.

The hoop compression which results from the horizontal component of the meridional equilibrium force can be related to the required cross sectional area of the supporting ring.

$$A = \frac{P_{L1}}{f_{dy} \tan \psi_{01}} (6 S_L + D) \quad (6-73)$$

where

A = gross cross sectional area of the ring, in.² (If a beam section is used, it is understood that web and flange stiffeners will be included, as required, to preclude localized buckling prior to full yielding of the section.)

$\frac{P_{L1}}{\tan \psi_{01}}$ = horizontal component of meridional equilibrium force in the shell, evaluated at $\psi = \psi_{01}$. This force component acts on the supporting ring as a radial inwardly-directed dynamic loading, lb/in.

f_{dy} = dynamic compressive yield strength of structural steel, lb/in.²

S_L = interior principal diameter of supporting ring, ft

D = gross depth of supporting ring section in the plane of the ring, in.

2. Unit Cost

The unit cost of the structural steel compression ring is expressed as follows

$$C_s = w X_s \quad (6-74)$$

where

w = weight of supporting ring, lb/ft

$$C_t = C_s \quad (6-75)$$

6.6.4 Ring No. 1 (Structural Steel, Tension Sphere)

1. Design

The structural steel tension sphere is described in Section 6.5.3. The supporting ring which frames the principal opening must be designed to withstand the horizontal component of the tensile meridional equilibrium force, evaluated at $\psi = \psi_{01}$. As with the structural steel compression ring, it is probable that the steel tension ring will consist of a beam section or of a built-up member. Maximum load-carrying capacity is realized when the entire cross section is yielding in tension. The required section area, based on the loading obtained from Eq. (6-58a), is as follows

$$A = 3 q_I S_L (\text{sphere}) \cos \psi_{01} \left[\frac{6 S_L (\text{ring}) + D \text{ ring}}{f_{dy}} \right] \quad (6-76a)$$

Or, since $S_L (\text{ring}) = S_L (\text{sphere}) \sin \psi_{01}$

$$A = 3 q_I \frac{S_L (\text{ring})}{\tan \psi_{01}} \left[\frac{6 S_L (\text{ring}) + D \text{ ring}}{f_{dy}} \right] \quad (6-76b)$$

where

A = gross cross sectional area of the ring, in.²

q_I = static equivalent uniform load, acting radially outward on the interior surface of the tension sphere, which results from the reduced reflected pressure within the sphere. This loading, which is of brief duration, has units of lb/in.²

$S_L (\text{sphere})$ = interior principal diameter of sphere, ft

$S_L (\text{ring})$ = interior principal diameter of supporting ring, ft

ψ_{01} = one-half of the central angle of the principal opening in the shell, deg

2. Unit Cost

The unit cost of the structural steel tension ring can be expressed in the same form as for the steel compression ring.

$$C_s = w X_s \quad (6-74)$$

where w = weight of supporting ring, lb/ft

$$C_t = C_s \quad (6-75)$$

IIT RESEARCH INSTITUTE

D = gross depth of supporting ring section in the plane of the ring, in.

f_{dy} = dynamic tensile yield strength of structural steel, lb/in.

6.6.5 Ring No. 2 (Reinforced Concrete, Compression Sphere)

1. Design

As discussed in Section 6.5.1, the supporting ring which frames the second opening in the sphere will be designed to resist both the maximum tension and the maximum compression equilibrium forces along its periphery. We can proceed to estimate these controlling equilibrium forces.

The second opening in the shell surface is defined by the region $\psi' = \pm \psi_{02}$. By analyzing Eq. (6-42) this same region can be expressed as $(\psi_R - \psi_{02}) \leq \psi \leq (\psi_R + \psi_{02})$, with $\psi_R = \pi/2$ and $\psi_{02} = \psi_{01}$ in the usual case. First let us consider the membrane forces in this region due solely to the assumed loading pattern which has been associated with Ring No. 1. Applying Eq. (6-40) and (6-41), it can be shown that the maximum value of the compressive membrane force, $(-N_{\max})$ in the defined region is given by the following

$$(-N)_{\max} = - \sum q_E (3 S_L + D/2) \left[1 - \frac{\sin^2 \psi_{01}}{\sin^2 (\psi_R - \psi_{02})} - P_{L1} \frac{\sin \psi_{01}}{\sin^2 (\psi_R - \psi_{02})} \right] \quad (6-77)$$

$$\text{valid for } P_{L1} / \sum q_E > (3 S_L + D/2) \sin \psi_{01}$$

Also, $\psi_R = \pi/2$ and $\psi_{01} = \psi_{02}$

$$(-N)_{\max} = - \sum q_E (3 S_L + D/2) (1 - \tan^2 \psi_{01}) - P_{L1} \left(\frac{\tan \psi_{01}}{\cos \psi_{01}} \right)$$

$$\text{valid for } P_{L1} / \sum q_E > (3 S_L + D/2) \sin \psi_{01}$$

$$(-N)_{\max} = - \sum q_E (3 S_L + D/2) (1 - \sin^2 \psi_{01}) - P_{L1} \sin \psi_{01}$$

$$\text{valid for } P_{L1} / \sum q_E < (3 S_L + D/2) \sin \psi_{01}$$

The following notation applies for Eq. (6-77) to (6-79).

$(-N)_{\max}$ = maximum value of compressive equilibrium membrane force in the shell within the region of interest. This force acts in the meridional direction where Eq. (6-77) and (6-78) are applicable, and is equal in the latitudinal and meridional directions where Eq. (6-79) is applicable. Units are lb/in.

$\sum q_E = q_{Ep} + q_{Es} + q_{Ed}$, or since $q_{Ep} = 0$ for no prestressing, $\sum q_E = q_{Es} + q_{Ed}$
(Section 6.3.1 and 6.5.1)

q_{Ed} = static equivalent load (acting radially inward on the exterior surface of the shell, excluding only the area of the single opening defined by $\psi = \pm \psi_{01}$) due to earth-transmitted overpressure loading acting at the ground surface. Units are lb/in.²

q_{Es} = conventional dead and live loadings acting on a buried shell structure, approximated as a radial inwardly-directed loading, lb/in.²

S_L = principal interior diameter of the sphere, ft

D = wall thickness of the sphere, in.

ψ_{01} = one-half the central angle of the principal opening defined by Ring No. 1, deg

ψ_{02} = one-half the central angle of the second opening defined by Ring No. 2, deg

Equations (6-77) to (6-79), inclusive, describe the maximum (compressive) equilibrium membrane force in the region $\psi' = \pm \psi_{02}$ due to loading on Ring No. 1 in the region $\psi = \pm \psi_{01}$. It is also necessary to examine the effects of the second loading case on compressive equilibrium forces in the region $\psi' = \pm \psi_{02}$. Here the line loading P_{L2} along the periphery of the second opening includes at least two components. The first of these is outwardly directed and simply serves to maintain whole-body equilibrium for the sphere, recognizing that q (and the assumed radial resistance to P_{L1}) actually do not act over the shell area removed by the second opening. This equilibrium force is evidenced as a uniform outwardly-directed line loading component $P'_{L2} = 3 \sum q_E S_L \sin \psi_{02}$ acting over the entire periphery of the opening, and by a second outwardly-directed line loading component $P''_{L2} = P_{L1} \sin \psi_{01} \sin \psi_{02} - 3 \sum q_E \sin^2 \psi_{01} \sin \psi_{02}$ which acts over the

IIT RESEARCH INSTITUTE

region $\pi/2 \leq \psi \leq (\psi_R' + \psi_{02})$. In addition, due to the transfer of thrust from adjacent structural elements, there may be an additional line loading component P_{L2}''' , which could be either inwardly-directed or outwardly-directed.

The membrane forces at any point in the region $\psi' = \pm \psi_{02}$ due to loadings P_{L2}' , P_{L2}'' , P_{L2}''' , are linearly and algebraically additive to the membrane forces due to the first loading. Since we are presently interested in establishing a maximum value for the compressive equilibrium force, and since the effects of loadings P_{L2}' and P_{L2}'' will be to initiate tensile equilibrium forces in the region of interest, it is probably adequate for our purposes to use only Eq. (6-77) to (6-79) in a preliminary evaluation of the requirements for ring compressive resistance. For consistency in degree of precision, any compressive resistance due to the presence of circumferential reinforcing steel will be neglected. The following expressions are then obtained for the required cross sectional area of the supporting ring

$$A_{\text{ring}} = \frac{\cos \psi_{02}}{0.85 f_{dc}} \left\{ \sum q_E \left[3 S_{L(\text{shell})} + \frac{D_{\text{shell}}}{2} \right] \left[1 - \tan^2 \psi_{01} \right] + P_{L1} \left(\frac{\tan \psi_{01}}{\cos \psi_{01}} \right) \right\} \quad (6-80)$$

valid for $P_{L1} / \sum q_E > (3 S_L + \frac{D_{\text{shell}}}{2}) \sin \psi_{01}$, assuming $\psi_R = \pi/2$ and $\psi_{01} = \psi_{02}$.

$$A_{\text{ring}} = \frac{\cos \psi_{02}}{0.85 f_{dc}} \left\{ \sum q_E \left[3 S_{L(\text{shell})} + \frac{D_{\text{shell}}}{2} \right] \left[1 - \sin^2 \psi_{01} \right] + P_{L1} \sin \psi_{01} \right\} \quad (6-81)$$

valid for $P_{L1} / \sum q_E < (3 S_L + \frac{D_{\text{shell}}}{2}) \sin \psi_{01}$

The maximum tensile stress in the region $\psi' = \pm \psi$ could, conceivably, also result from the first case of loading. In this event, as is indicated by Eq. (6-41a), the maximum tensile stress would occur in the latitudinal direction and would reach a maximum at $\psi' = -\psi_{02}$ (assuming $\psi_R - \psi_{02} \leq \pi/2$). Tension occurs in the region

$$\psi_{01} \leq \psi \leq \pi/2 \text{ if } P_{L1} / \sum q_E > (3 S_L + D/2) (\sin \psi_{01} + \sin^2 \psi / \sin \psi_{01}).$$

It seems probable that the maximum tension in the region $\psi' = \pm \psi_{02}$ would be attributable to the second loading case, since tension is initiated by loadings P'_{L2} and P''_{L2} . Neglecting any effect of a possible loading component P'''_{L2} , and assuming $\psi'_{01} = \psi_{02}$, we can express the horizontal component of this combined tensile force as $P_{L2}/\tan \psi_{01}$. Substituting $P'_{L2} = 3 \sum q_E S_{L(\text{ring})}$ and $P''_{L2} = P_{L1} \sin^2 \psi_{01} - 3 \sum q_E S_{L(\text{ring})} \sin^2 \psi_{01}$, the tensile steel requirement is

$$\phi_t = \frac{100}{b D f_{dy} \tan \psi_{01}} \left[3 \sum q_E S_L (1 - \sin^2 \psi_{01}) + P_L \sin^2 \psi_{01} \right] \quad (6-82)$$

where

ϕ_t = required tensile steel, expressed as a percentage of the gross cross sectional area of the supporting ring

P_{L1} = line load acting on periphery of first opening, lb/in.

b = gross thickness of ring wall in a plane normal to the plane of the ring, in.

D = gross depth of supporting ring section in the plane of the ring, in.

S_L = interior principal diameter of supporting ring, ft

f_{dy} = dynamic tensile yield strength of reinforcing steel, lb/in.²

ψ_{01} = one-half of the central angle of the first opening in the sphere, deg

$\sum q_E$ = composite static equivalent load on shell surface due to blast-induced loading at the ground surface, plus conventional dead and live loading ($\sum q_E = q_{Ep} + q_{Es} + q_{Ed}$, with $q_{Ep} = 0$ for no prestressing). Units are lb/in.²

2. Unit Cost

The unit cost of the reinforced concrete ring is a function of the cost factors for concrete (C_c), main reinforcing steel (C_s), any required tie steel in compression areas (C_{st}) and the formwork (C_f). If torsion is also a consideration, its requirements can be evaluated by Eq. (6-62). The cost equations of Section 6.6.2 remain applicable.

$$C_c = \frac{bD}{144} X_c \quad (6-67)$$

$$C_s = \frac{\phi_t b D}{14,400} X_s \quad (6-68)$$

$$C_{st} = \frac{\phi_{te} b D}{14,400} X_s \quad (6-69)$$

$$C_{vt} = \frac{\phi_{vt} b}{14,400} \left[1 + 0.80 (b + D) \right] X_v \quad (6-70)$$

(includes longitudinal torsional steel)

$$C_f = \frac{b + D}{6} X_f \quad (6-71)$$

The composite cost per lineal foot for Ring No. 2 (reinforced concrete) can then be expressed as

$$C_t = C_c + C_s + C_{st} + C_v + C_f \quad (6-72)$$

6.6.6 Ring No. 2 (Structural Steel, Compression Sphere)

1. Design

From Eq. (6-40) and (6-41), substituting t for D (sphere) and assuming that t/S_L is small, we can find the maximum (compressive) values of the equilibrium forces which act on the periphery of Ring No. 2 due to the first loading case. Assuming $\psi_R = \pi/2$ and $\psi_{01} = \psi_{02}$, the following expressions can be obtained for the required section area (compression).

$$A_{(compression)} = \frac{6 S_{L(ring)} + D_{ring}}{f_{dy} \tan \psi_{01}} \left[3 \sum q_E S_{L(ring)} (1 - \tan^2 \psi_{01}) + P_{L1} \tan^2 \psi_{01} \right] \quad (6-83)$$

valid for $P_{L1} / \sum q_E \geq \frac{3 S_L}{\sin \psi_{01}}$, assuming $\psi_R = \pi/2$ and $\psi_{01} = \psi_{02}$.

$$A_{(compression)} = \frac{6 S_{L(ring)} + D_{ring}}{f_{dy} \tan \psi_{01}} \left[3 \sum q_E S_{L(ring)} (1 - \sin^2 \psi_{01}) + P_{L1} \sin^2 \psi_{01} \right]$$

valid for $P_{L1} / \sum q_E \leq \frac{3 S_L}{\sin \psi_{01}}$, assuming $\psi_R = \pi/2$ and $\psi_{01} = \psi_{02}$.

The tensile forces acting on the periphery of Ring No. 2 due to the first loading case, if they exist at all, will be of a lesser magnitude than the maximum compressive forces (Eq. (6-40) and (6-41)). Since $f_{dy}(\text{compression}) = f_{dy}(\text{tension})$, it may perhaps be sufficient to design the ring only for the compressive forces. There is a definite possibility that moment will also occur at this section. Because of this, and also to make provision for any additive stresses resulting from the second loading case, the cost estimates will assume that the total required section area is 1.5 times the compression area requirements indicated by Eq. (6-83) and (6-84).

2. Unit Cost

The unit cost of the structural steel ring for the second opening in a steel compression sphere is analogous to that derived in Section 6.6.3 for Ring No. 1.

$$C_s = w X_s \quad (6-74)$$

where

w = weight of supporting ring, lb/ft

$$C_t = C_s \quad (6-75)$$

6.6.7 Ring No. 2 (Structural Steel, Tension Sphere)

1. Design

The design of the structural steel tension sphere is presented in Section 6.5.3. From Eq. (6-58) and (6-59) of this section, it is apparent that the maximum tensile equilibrium forces which exist on the periphery of Ring No. 2 will occur at $\psi' = -\psi_{02}$. Assuming $\psi_R = \pi/2$ and $\psi_{01} = \psi_{02}$, we thus obtain the following (tensile) requirement for section area in the supporting ring

$$A_{(\text{tension})} = \left[\frac{6 S_{L(\text{ring})} + D_{\text{ring}}}{f_{dy} \tan \psi_{01}} \right] \left[3 q_I S_{L(\text{ring})} - 3 \sum q_E S_{L(\text{ring})} (1 - \tan^2 \psi_{01}) \right] \quad (6-85)$$

Following the argument of Section 6.6.6 (Design), it is suggested that the cost estimates assume a total section-area requirement which is 1.5 times that indicated as adequate for direct tension resistance.

2. Unit Cost

The unit cost of this structural steel ring, which frames the second opening in the steel tension sphere, is analogous to that derived in Section 6.6.3 (Unit Cost) for Ring No. 1.

$$C_s = w X_s \quad (6-74)$$

where

w = weight of supporting ring, lb/ft

$$C_t = C_s \quad (6-75)$$

6.7 BLAST-RESISTANT DOOR

6.7.1 Discussion

The most critical structural element in the blast-resistant shelter system is the blast door. If the blast door either collapses under load or fails to seal the entrance structure effectively, all other design considerations become meaningless. Deformation of the door in the elasto-plastic range, for example, may cause excessive pressure leaks past its sealing mechanism. For this reason, blast door design is frequently predicated on a requirement that the material remain within its elastic range under the assumed conditions of loading.

Despite the importance of the blast door in the entranceway system, it is not acceptable to resort to a design which includes an unduly-large strength reserve. The blast door must be a movable element, thus requiring a support and mobility system whose total cost is quite sensitive to the weight and dimensions of the door. As a result, in order to obtain an adequate margin of safety while avoiding extravagant provisions for excess strength, it is appropriate to examine the design of the blast door in a more rigorous fashion than has been employed in certain other portions of this study.

It will subsequently be shown that the cubicle entranceway structures are desirable at low levels of design overpressure, but that cylindrical and spherical shell entranceway structures are more economical in regions where relatively-high levels of pressure must be considered. When these

latter structural configurations are employed, the blast door should have a curved shape which is compatible with that of its supporting structure.

6.7.2 Flat Plate

1. Analysis

Cubicle structures, as a consequence of their form, will normally employ a blast door which is a flat plate. The door will be held with restraining clamps, thus ensuring that the closure remains effective despite shock buffeting or any period of negative pressures. Initially, it will be assumed that the edge restraint thus afforded the plate is negligible. The door will be analyzed as a simply-supported rectangular plate with long dimension L_L ft, and short dimension L_S ft.

The maximum values of the plate moments due to a uniformly-distributed load of q_I lb per in.² will occur in the centers of the spans

$$M_{10} = 144 q_I K_{10} L_S^2 \quad (a) \quad (6-86)$$

$$M_{20} = 144 q_I K_{20} L_S^2 \quad (b)$$

where

M_{10} = resultant moment in the plate, evaluated in the center of the L_S (short) span and acting in a direction paralleling the short edges of the plate. Units are in. -lb per in. of length in the L_L (long) direction of the plate.

M_{20} = resultant moment in the plate, evaluated in the center of the L_L (long) span and acting in a direction paralleling the long edges of the plate. Units are in. -lb per in. of length in the L_S (short) direction of the plate.

K_{10} = influence coefficient for maximum simply-supported moment in the L_S direction of a flat plate, evaluated from Eq. (6-87a)

K_{20} = influence coefficient for maximum simply-supported moment in the L_L direction of a flat plate, evaluated from Eq. (6-87b)

L_L = length of plate in long direction, ft

L_S = length of plate in short direction, ft

q_I = static equivalent representation of short-duration reflected pressure loading which acts on the blast-resistant door, lb per in.

A rapidly-converging double-series solution is used to evaluate K_{10} and K_{20} .³⁵

$$K_{10} = \frac{16}{\pi^4} \sum_{i=1,3,\dots}^{\infty} \sum_{j=1,3,\dots}^{\infty} \frac{i^2 + \nu \alpha^2 j^2}{ij(i^2 + \alpha^2 j^2)^2} \quad (a) \quad (6-87)$$

$$K_{20} = \frac{16}{\pi^4} \sum_{i=1,3,\dots}^{\infty} \sum_{j=1,3,\dots}^{\infty} \frac{\alpha^2 j^2 + \nu i^2}{ij(i^2 + \alpha^2 j^2)^2} \quad (b)$$

where

i, j = summation indices, odd natural numbers only

ν = Poisson's ratio for the material used in the plate.

Typically, $\nu = 0.16$ for concrete and 0.30 for steel

$\alpha = L_S / L_L$ (refer to two-way reinforced slabs)¹

The series is a rapidly-convergent one. A fair approximation of M_{10} and M_{20} can be obtained by considering only the first terms in Eq. (6-87a) and (6-87b)

$$M_{10} \approx 2304 \frac{q_I L_S^2}{\pi^4} \left[\frac{1 + \nu \alpha^2}{(1 + \alpha^2)^2} \right] \quad (6-88)$$

$$M_{20} \approx 2304 \frac{q_I L_S^2}{\pi^4} \left[\frac{\nu + \alpha^2}{(1 + \alpha^2)^2} \right] \quad (6-89)$$

For the situation of interest in this study, L_L represents the height of a blast door while L_S represents its width. Therefore $\alpha < 1$. Manipulation of Eq. (6-88) and (6-89) indicates that, for $\alpha < 1$, $M_{10} > M_{20}$. Thus, as shown elsewhere,¹ the maximum moment in a simply-supported rectangular flat plate occurs at the center of the short span. Tables 6-3 and 6-4 list accurate values of K_{10} and K_{20} for use in determining M_{10} and M_{20} from Eq. (6-86), obtained with an IBM 7090/94 computer and expressed in terms of the reciprocal of α .

Table 6-3

COEFFICIENTS FOR CENTRAL FLAT-PLATE BENDING MOMENTS
IN SIMPLY-SUPPORTED, RECTILINEAR, REINFORCED-CONCRETE
SLABS ($\nu = 0.16$) WHICH ARE SUBJECTED TO UNIFORMLY-
DISTRIBUTED TRANSVERSE LOADING

$1/\alpha$	K_{10}	K_{20}
1.00	0.04273	0.04273
1.10	0.05046	0.04391
1.20	0.05787	0.04429
1.30	0.06485	0.04407
1.40	0.07131	0.04341
1.50	0.07724	0.04242
1.60	0.08263	0.04121
1.70	0.08749	0.03984
1.80	0.09186	0.03837
1.90	0.09577	0.03684
2.00	0.09925	0.03527
2.50	0.11155	0.02759
3.00	0.11811	0.02096
3.50	0.12152	0.01571
4.00	0.12326	0.01180
4.50	0.12415	0.00903
5.00	0.12460	0.00714

Table 6-4

COEFFICIENTS FOR CENTRAL FLAT-PLATE BENDING MOMENTS
IN SIMPLY-SUPPORTED, RECTILINEAR STEEL PLATES ($\nu = 0.30$)
WHICH ARE SUBJECTED TO UNIFORMLY-DISTRIBUTED
TRANSVERSE LOADING

$1/\alpha$	K_{10}	K_{20}
1.00	0.04789	0.04789
1.10	0.05549	0.04999
1.20	0.06269	0.05122
1.30	0.06939	0.05175
1.40	0.07555	0.05172
1.50	0.08117	0.05125
1.60	0.08623	0.05044
1.70	0.09079	0.04936
1.80	0.09485	0.04806
1.90	0.09848	0.04661
2.00	0.10169	0.04504
2.50	0.11295	0.03635
3.00	0.11888	0.02791
3.50	0.12193	0.02082
4.00	0.12349	0.01541
4.50	0.12428	0.01157
5.00	0.12467	0.00904

2. Prestressed Concrete

(a) Design

The importance of the blast-resistant door as a structural element in the entranceway system has already been emphasized. This importance has led to the recommendation that the door and its immediate support structure be designed on the assumption of elastic behavior. Prestressed concrete appears to be a suitable material for this application.

A rectangular cubicle slab, of uniform thickness, is considered to be subjected to initial prestressing forces of effective magnitude and distribution. The extreme fibers of the loaded slab, both upper and lower, will simultaneously reach some specified maximum stress at the section of greatest moment. This maximum moment will be taken as the yield-moment-capacity of the section. By simple geometric relationships, the maximum moment can be expressed in terms of the magnitude of the distributed loading on the slab. The assumption will be that the stress distribution on the critical cross section, under the full design loading, will vary linearly between maxima of opposite sign.

The prestressing forces apply a long-duration load to the concrete of the prestressed slab. For this reason, since any undue creep or stress relaxation would be highly undesirable, the compressive stress on the concrete under the effective prestressing forces will be held to the conventional limit of $0.45 f'_c$. The maximum allowable tension in the concrete will be limited to $3\sqrt{f'_c}$ (Section 6.3.1). The yield-moment capacity of the prestressed rectangular section, under the postulated conditions, can then be written as

$$M_{(yield)} = \left[0.45 f'_c + 3\sqrt{f'_c} \right] \frac{D^2}{6} \quad (6-90)$$

where

$M_{(yield)}$ = resisting yield moment capacity of the rectangular section, assuming initial prestressing according to the preceding description, and postulating a linear distribution of stress between the top and bottom edges of the slab. Units are in. -lb per in. of slab length, measured along an axis normal to the plane in which the moment is acting.

f'_c = ultimate compressive strength of concrete in a standard 28-day cylinder test, lb per in.²

D = total depth of slab, in.

Equation (6-90), to some extent, may understate the moment resistance of the slab under a condition of dynamic loading. For this condition, the compressive stress at the extreme compressive fiber might be allowed to reach $0.85 f'_{dc}$ rather than $0.45 f'_c$. The resulting increase in moment resistance would not be large, since the slab is deliberately under-reinforced. Disregarding this factor, Eq. (6-86a) and (6-90) can be combined to obtain an expression for the required thickness of slab.

$$D = L_S \left[\frac{864 q_I K_{10}}{0.45 f'_c + 3\sqrt{f'_c}} \right]^{1/2} \quad (6-91)$$

Since the door has a short span in the L_S direction, it is realistic to estimate the requirements for prestress steel on the assumption that full resistance to the maximum bending moment must be provided at any section along the L_S span. This permits a crude estimate of the required length of prestress cable per sq ft of slab surface, by assuming that the section at depth D is initially prestressed from zero at the top face to $0.45 f'_c$ at the bottom face.

$$L_{sp} = \frac{2.70 f'_c D}{F_{sp}} \quad (6-92)$$

where

L_{sp} = required length of prestressing strand, ft per sq ft of door surface

F_{sp} = manufacturer's recommended design load per prestressing strand, lb (Table 2-7)

Since moment M_{20} is acting in the L_L direction, it may be necessary to place a band of conventional reinforcement at right angles to the prestressing strands. It would be customary in blast-resistant design to require a minimum of $\phi_t = 0.50$ distributed equally between the upper and lower faces and extending in the L_L direction. This would be adequate for temperature steel, and might also be adequate to resist M_{20} . If such is not the case, additional steel must be added. The steel requirement in

the L_L direction, based on moment, can be obtained from Eq. (6-86b) by considering the ultimate moment resistance of a reinforced-concrete cross section.¹

$$\phi_{cL} (L_L \text{ direction}) = 17,800 q_I K_{20} \left(\frac{L_S}{D} \right)^2 \quad (6-93)$$

where $\phi_{cL} = \frac{100 A_s}{D} =$ required bottom steel in L_L direction at the center of the span, expressed as a percentage of the gross cross section area

Assuming $d = 0.9 D$ and with equal distribution of the specified minimum steel ($\phi_t = 0.50$) at top and bottom faces, moment steel in excess of $\phi_t = 0.50$ will be required only when values of ϕ_{cL} from Eq. (6-93) exceed $\left(\frac{0.9 \times 0.50}{2} \right) = 0.225$.

Some recognition should be given to the existence of induced edge moments due to the presence of the support clamps. The absolute maximum value of these will be the fixed-end (elastic) moments, and the probable maximum values will be somewhat less. Adequate moment resistance should be possible through the efficient layout of the reinforcing steel which has already been specified for other purposes.

Shear stresses in the flat slab should also be examined. Due to the short span and heavy loading, diagonal tension or shear compression stresses would present a major problem in conventional reinforced-concrete design. It will be assumed that the axial load imposed on the slab by the initial prestressing forces will be adequate to prevent this mode of failure. However, the subject is imperfectly understood and further investigation would be highly desirable.

Excluding the diagonal tension and/or shear compression modes, it is still necessary to investigate the possibility of a pure shearing failure.¹ The ultimate shear capacity of the section will be taken as¹⁵

$$V_u = 0.20 f'_c D \quad (6-94)$$

where

V_u = ultimate shearing capacity of section, lb per in. of slab along a section of maximum shear

An upper bound to the effective shearing load, expressed in lb per in. of slab, is obtained by evaluating the reaction at the slab support.

$$V_{\max} = 6 q_I L_S \quad (6-95)$$

Combining Eq. (6-94) and (6-95) yields the required slab thickness, based on considerations of pure shear on a vertical section at the slab supports.

$$D_{(\text{shear})} = \frac{30 q L_S}{f'_c} \quad (6-96)$$

(b) Unit Cost

The unit cost per sq ft of prestressed concrete flat slab is a function of the component costs of concrete (C_c), reinforcing steel (C_s), prestressing strand (C_{sp}) and formwork (C_f).

$$C_c = \frac{D}{12} X_c \quad (6-97)$$

$$C_s = \frac{\phi_t D}{1200} X_s \quad (6-98)$$

(use $\phi_t = 0.50$ minimum in the L_L direction, plus any additional steel necessary to satisfy Eq. (6-93))

$$C_{sp} = L_{sp} X_p \quad (6-99)$$

$$C_f = X_f \quad (6-100)$$

The composite cost factor, per sq ft of slab surface, can be expressed as

$$C_t = C_c + C_s + C_{sp} + C_f \quad (6-101)$$

3. Structural Steel

(a) Design

Based on a requirement for elastic design, the yield moment capacity of a dynamically-loaded rectangular steel plate is

$$M_{(yield)} = \frac{f_{dy} t^2}{6} \quad (6-102)$$

where

$M_{(yield)}$ = resisting yield moment capacity of the rectangular section, in.-lb per in. of slab along an axis normal to the plane of the resisting moment.

f_{dy} = dynamic yield strength of structural steel, lb/in.²

t = thickness of steel plate, in.

The maximum moment in the simply-supported plate occurs at the center of the L_S span. As described in the preceding section, the value of this is obtained from Eq. (6-86a). Equations (6-82a) and (6-98) can be combined to obtain an expression for the required thickness of plate, based on bending stresses.

$$t = L_S \left[\frac{864 K_{10} q_I}{f_{dy}} \right]^{1/2} \quad (6-103)$$

Shear stresses in the structural steel plate, as in the pre-stressed concrete slab, should also be examined. The yield shearing capacity of the section will be taken as¹

$$V_p = 0.60 f_{dy} t \quad (6-104)$$

The upper-bound value of the shearing load, as expressed by Eq. (6-95), remains unchanged.

$$t_{(shear)} = \frac{10 q_I L_S}{f_{dy}} \quad (6-105)$$

(b) Unit Cost

The cost factors per sq ft of structural steel plate are as follows

$$C_s = X_s \quad (6-106)$$

$$C_t = C_s$$

6.7.3 Single-Curvature Surface

1. Analysis

When a blast-closure in a cylindrical entranceway structure must be considered, the door is developed as a portion of the same cylindrical

shell rather than as a flat-plate element. This is generally advantageous, since when bending stresses control the door design the cylindrical shell is markedly more efficient than the flat plate in carrying uniform transverse load. By taking advantage of the curved shape, it is frequently possible to reduce the weight and thickness of this structural element.

The resisting moments induced in the cylindrical shell element by surface loading can be attributed to two distinct processes. First, there exist the simply-supported flat-plate moments whose values are restricted to the length-to-width ratio of the shell element and to the physical properties of the shell material. Next, these flat-plate moments are modified by the effects of the rise-to-span and rise-to-thickness relationships for the shell. A double-series solution, with rapid convergence characteristics, can be employed to evaluate the controlling moment.³⁵

$$K_{10} = \frac{16}{\pi^4} \sum_{i=1,3}^{\infty} \sum_{j=1,3}^{\infty} \frac{i^2 + \nu \lambda^2 j^2}{i j (i^2 + \lambda^2 j^2)^2} \quad (a) \quad (6-108)$$

$$K_{20} = \frac{16}{\pi^4} \sum_{i=1,3}^{\infty} \sum_{j=1,3}^{\infty} \frac{\lambda^2 j^2 + \nu i^2}{i j (i^2 + \lambda^2 j^2)^2} \quad (b)$$

$$K_{1k} = \frac{16\mu}{\pi^4} \sum_{i=1,3}^{\infty} \sum_{j=1,3}^{\infty} \frac{i^3 (i^2 + \nu \lambda^2 j^2)}{j (i^2 + \lambda^2 j^2)^2 [(i^2 + \lambda^2 j^2)^4 + \mu i^4]} \quad (a) \quad (6-109)$$

$$K_{2k} = \frac{16\mu}{\pi^4} \sum_{i=1,3}^{\infty} \sum_{j=1,3}^{\infty} \frac{i^3 (\lambda^2 j^2 + \nu i^2)}{j (i^2 + \lambda^2 j^2)^2 [(i^2 + \lambda^2 j^2)^4 + \mu i^4]} \quad (b)$$

$$M_{10} = 144 q_1 L_S^2 (K_{10} - K_{1k}) \quad (6-110)$$

$$M_{20} = 144 q_1 L_S^2 (K_{20} - K_{2k}) \quad (6-111)$$

where

K_{10} = influence coefficient for simply-supported, flat plate moment in shell, evaluated at a transverse section through the midpoint of the shell barrel.

IIT RESEARCH INSTITUTE

K_{20} = influence coefficient for simply-supported, flat-plate moment in shell, evaluated at a longitudinal section through the midpoint of the shell span.

K_{1k} = influence coefficient for moment reduction in shell due to shell curvature, evaluated at a transverse section through the midpoint of the shell barrel.

K_{2k} = influence coefficient for moment reduction in shell due to shell curvature, evaluated at a longitudinal section through the midpoint of the shell span.

M_{10} = resultant moment in shell, evaluated at the midpoint of the shell barrel and acting in a direction paralleling the straight edges of the shell. Units are in. -lb per in. of curved-edge length.

M_{20} = resultant moment in shell, evaluated at the midpoint of the shell span and acting in a direction paralleling the curved edges of the shell. Units are in. -lb per in. of straight-edge length.

i, j = summation indices, odd natural numbers only

ν = Poisson's ratio for the material used in the shell. Typically, $\nu = 0.16$ for concrete and 0.30 for steel.

λ = ratio of straight-edge length to curved-edge length for the shell, $\frac{L_S}{\widehat{L}_L}$

$$\mu = \frac{6912 (1 - \nu^2) L_S^4}{\pi^4 S_L^2 D^2}$$

q = static equivalent uniformly-distributed load, representing the effect of reflected pressure loading and acting radially-inward on the shell surface, lb/in.²

L_S = barrel length of shell, ft (For the application considered herein, this will be the shorter edge of the cylindrical shell element. This length is related to the width of the door.)

\widehat{L}_L = arc length of curved edge of shell, ft (This length is related to the height of the door.)

$S_L/2$ = radius of curvature of cylindrical shell element, ft

D = thickness of shell, in.

The series indicated in Eq. (6-108) and (6-109) converge quite rapidly with increasing values of i and j . Some insight into the relative contributions to the central bending moment in each principal direction can,

IIT RESEARCH INSTITUTE

as a consequence, be gained by considering only the first term in each series. By factoring common terms in Eq. (6-108) and (6-109), Eq. (6-110) and (6-111) can be written as follows

$$M_{10} = 144 K_{10} q_I L_S^2 \left[1 - \mu \sum_{i=1,3}^{\infty} \sum_{j=1,3}^{\infty} \frac{i^4}{(i^2 + \lambda^2 j^2)^4 + \mu i^4} \right] \quad (6-112)$$

$$M_{20} = 144 K_{20} q_I L_S^4 \left[1 - \mu \sum_{i=1,3}^{\infty} \sum_{j=1,3}^{\infty} \frac{i^4}{(i^2 + \lambda^2 j^2)^4 + \mu i^4} \right] \quad (6-113)$$

The separate influences of plate bending and of plate curvature are readily apparent in Eq. (6-112) and (6-113). The summation term in each of these equations results from plate curvature, and acts to reduce the effective maximum moment in the cylindrical element. As S_L becomes large in relation to L_S^2/D , the value of μ becomes less and the effect of plate curvature is correspondingly reduced. The limiting case is reached when $S_L \rightarrow \infty$ (flat plate), for here $\mu \rightarrow 0$

Similarly, the effect of λ on flat-plate moments can be evaluated. This term, as defined, represents the ratio of the side lengths for the element ($\lambda = L_S/\widehat{L}_L$). For the flat plate ($\mu \rightarrow 0$), the arc length \widehat{L}_L of the curved side is identical with its principal chord length L_L . The case of interest then becomes identical with the two-way flat slab. There it was suggested that, when values of λ (notation of Ref 1) were 0.5 or less (or in the more general case, exceeded 2.0), the two-way slab could be treated as a one-way slab with significant moments only in its short direction. For the blast-door dimensions contemplated in this study (Table 3-1) the ratios of door-width to door-height are usually such that two-way action will not have a major effect in reducing the maximum moments in the door slab.

The relative magnitudes of M_{10} and M_{20} can be examined by considering only the first terms of Eq. (6-110) and (6-111). It is then found that, if the larger of these two moments is that acting in the L_S direction (parallel to the straight edges of the cylindrical element), then the inequality $M_{10}/M_{20} \geq 1$ must hold. By substitution, it can be demonstrated

that a necessary condition for this inequality is ($\lambda^2 \leq 1$). Since $L_S < L_L$ for the doorway under consideration, $\lambda < 1$ and $\lambda^2 < 1$. Hence, M_{10} represents the maximum moment in the shell, for the stated relationships and within the precision limits obtainable by evaluating only the first term of each moment series.

In addition to the principal bending moments M_{10} and M_{20} axial thrusts and transverse shearing forces will act on the cross section of the cylindrical element. It will be assumed that the shell section, proportioned to resist direct and bending stresses, will be adequate in its shearing resistance. However, since the stresses due to axial thrust can be directly additive to those produced by bending moments, it is of interest to evaluate the principal thrusts N_1 and N_2 at the sections of maximum bending moment.

As with the bending moment components,³⁵ double series solutions can be employed to evaluate the principal thrusts at any point on the cylindrical element. These series will be evaluated at the centers of the two spans, where M_1 and M_2 were seen to reach their maxima, M_{10} and M_{20} .

$$N_{10} = \frac{2304 q_I L_S^2 \lambda^2 \mu}{D \pi^4} \sum_{i=1,3}^{\infty} \sum_{j=1,3}^{\infty} \frac{i j}{(i^2 + \lambda^2 j^2)^4 + \mu i^4} \quad (6-114)$$

$$N_{20} = \frac{2304 q_I L_S^2 \mu}{D \pi^4} \sum_{i=1,3}^{\infty} \sum_{j=1,3}^{\infty} \frac{i^3}{j [(i^2 + \lambda^2 j^2)^4 + \mu i^4]} \quad (6-115)$$

where

N_{10} = axial thrust in shell, evaluated at the midpoint of the shell barrel and acting in a direction paralleling the straight edges of the shell. Units are lb-in. of curved-edge length.

N_{20} = axial thrust in shell, evaluated at the midpoint of the curved span and acting in a direction paralleling the the curved edges of the shell. Units are lb-in. of straight-edge length.

For homogeneous rectangular sections, with isotropic strength properties satisfying Hooke's law, the combined effects of axial thrust and of bending in the elastic range can be approximated as

IIT RESEARCH INSTITUTE

$$f = \frac{N}{D} \pm \frac{6M}{D^2} \quad (a) \quad (6-116)$$

where

f = maximum stress on rectangular cross section, assuming linear stress distribution between maxima of equal magnitudes and opposite sign.

Or, rearranging terms, the required gross depth of section is as follows.

$$D_{(min)} = \left[\frac{6}{f_{(max)}} \left(M + \frac{DN}{6} \right) \right]^{1/2} \quad (b) \quad (6-116)$$

Equations (6-112) and (6-114) can be substituted for M and N in Eq. (6-116b), leading to an expression for D which is valid for the stated conditions of isotropy and elastic behavior.

$$D_{(min)}^2 = \frac{864 K_{10} q_I L_S^2}{f_{(max)}} \left\{ 1 - \mu \sum_{i=1,3}^{\infty} \sum_{j=1,3}^{\infty} \frac{i}{3 K_{10} \pi^4} \left[\frac{3i K_{10} \pi^4 - 8\lambda^2 j}{(i^2 + \lambda^2 j)^4 + \mu i^4} \right] \right\} \quad (6-117a)$$

As a reasonable approximation, since the series converges rapidly and since the relative effects of plate curvature and of axial load are small in comparison with that of plate bending, the following equation can be substituted for Eq. (6-117a)

$$D^2 \approx \frac{864 K_{10} q_I L_S^2}{f_{(max)}} \left[\frac{(1 + \lambda^2)^2}{1 + \nu \lambda^2} \right] \left[\frac{(1 + \lambda^2)^2 (1 + \nu \lambda^2) + \mu \lambda^2 / 6}{(1 + \lambda^2)^4 + \mu} \right] \quad (6-117b)$$

As indicated by Eq. (6-108a), values of K_{10} can be obtained as functions of λ , assuming a fixed value of ν . Computer solutions of this equation are supplied in Section 6.7.2 as Table 6-3 ($\nu = 0.16$) and Table 6-4 ($\nu = 0.30$). Values of K_{10} from these tables can be substituted directly in Eq. (6-117a) or (6-117b) and used to determine the required cylindrical-element thicknesses of reinforced concrete slab ($\nu = 0.16$) or of steel plate ($\nu = 0.30$, $t = D$).

The actual boundary conditions at the supports for the door element will differ somewhat from those assumed in the derivation of

Eq. (6-103) to (6-110) where it was postulated that all element edges would be simply-supported, permitting free rotation but with no linear displacements. For the door element under consideration, rotation of the curved edges will be constrained to some degree by the presence of support clamps. These clamps are necessary in order to keep the door in a tightly-sealed condition during the later states of blast loading, when shock buffeting and a negative pressure phase can be anticipated. The influence of these clamps will decrease in relative importance as the door thickness is increased. In general, any restraint thus afforded will reduce the maximum central moments in the shell element near the curved supporting edges. It should also be recognized that the supports for the door edges are not rigid, as assumed in the derivation, but actually can deflect under load. The effect of such yielding will be to redistribute any edge moments in the door element. An upper limit for these moments can be obtained by assuming the edge to be completely constrained at a rigid boundary. For this condition,

$$M_{le} = \frac{q_I D S_L}{K_m} \left[6 - \frac{0.93 (S_L D)^{1/2}}{L_S} \right] \quad (6-118)$$

where

M_{le} = value of moment at curved edge of cylindrical door element, assuming full restraint at a rigid boundary. Units are in-lb per in. of curved-edge length.

q_I = static equivalent uniformly-distributed load, representing the effect of reflected pressure loading and considered as acting radially-inward on the surface of the door element, lb/in.²

D = thickness of door element, in.

$S_L/2$ = radius of curvature of door element, ft

K_m = constant, related to Poisson's ratio for the material. Typical values range from 3.30 for steel to 3.46 for concrete.

L_S = length of straight edge of the curved door element (barrel length), ft

2. Prestressed Concrete

(a) Design

Initially it is assumed that the curved door slab is of uniform thickness. This slab is subjected to prestressing forces whose effective

magnitude and distribution are such that the extreme fibers of the slab, both upper and lower, will simultaneously reach some specified maximum stress under load at the section of maximum moment. This maximum moment will then be considered to be the yield moment capacity of the section, and can be related to the magnitude of the associated uniformly-distributed load. The stress distribution on the critical cross section varies linearly between maxima of opposite sign.

The prestressing forces apply a long-duration load to the concrete of the slab cross section. As discussed (Section 6.3.1), the concrete compressive stress under the effective prestressing forces will be restricted to the conventional limit of $0.45 f'_c$. The maximum allowable tensile stress in the concrete will be limited to $3\sqrt{f'_c}$. Considering the stress reversal afforded by initial prestressing, the maximum stress which can be applied to the slab cross section will be taken as $0.45 f'_c + 3\sqrt{f'_c}$. This can then be substituted for $f_{(\max)}$ in Eq. (6-117b) to yield Eq. (6-119). An iterative process must then be employed (since D also enters into the calculation of μ) in order to establish the approximate section depth, D , which is required to resist axial thrust and bending. Finally, if so desired, the value of D from Eq. (6-119) can be substituted into Eq. (6-117a), and the iterative process continued to obtain an exact value of D . This latter step, however, is frequently unnecessary.

$$D \approx \left\{ \left[\frac{864 K_{10} q_I L_S^2}{0.45 f'_c + 3\sqrt{f'_c}} \right] \left[\frac{(1 + \lambda^2)^2}{1 + \nu \lambda^2} \right] \left[\frac{(1 + \lambda^2)^2 (1 + \nu \lambda^2) + \mu \lambda^2 / 6}{(1 + \lambda^2) + \mu} \right] \right\}^{1/2} \quad (6-119)$$

Since the door elements considered have short barrel lengths, it is realistic to estimate the requirements for prestress steel by considering the maximum stress, rather than the average. The required length of prestress cable per sq ft of slab can be approximately expressed in the same form as for the flat prestressed door slab of Section 6.7.2.

$$L_{sp} = \frac{2.70 f'_c D}{F_{sp}}$$

where

L_{sp} = required length of prestressing strand, ft per sq ft of door surface

IIT RESEARCH INSTITUTE

F_{sp} = manufacturer's recommended design load per prestressing strand, lb (Table 2-7)

It is also necessary to determine the quantity of reinforcing steel; conventional, prestress or both; which will be required in the slab. Since the maximum moment in the slab (for $\lambda^2 < 1$, as is true for this application) occurs either as M_{10} or M_{1e} , it follows that prestressing steel will parallel the barrel length of the element. There is also a moment of lesser magnitude in the circumferential direction (M_{20} of Eq. (6-113)) which must be accommodated. Conceivably, reinforcement in this direction could be either conventional reinforcement or prestress steel. While recognizing that major difficulties in steel placement could be present, the former type of reinforcement will be postulated. This will lead to a requirement for reinforcing steel in the \widehat{L}_L (circumferential) direction.

The steel requirement in the circumferential direction can be estimated by equating the maximum moment in this direction (M_{20} of Eq. (6-113)) to the ultimate moment capacity of a rectangular section.¹ the prestress strand, it will be assumed that the steel percentage remains constant throughout the element length. It will also be assumed that the effective depth of the slab, for bending resistance, is 0.9 times its total depth. Substitution of the relationship¹ $M = 0.0081 \phi_{cL} D^2 f_{dy}$ into Eq. (6-113), evaluating this on an approximate basis for the first term of the series, yields an expression which is similar in form to Eq. (6-93) for the flat prestressed slab. However, recognition is given to the effects of plate curvature

$$\phi_{cL} \approx 17,800 K_{20} \frac{q_1}{f_{dy}} \left(\frac{L_s}{D} \right)^2 \left[1 - \frac{\mu}{(1 + \lambda^2)^4 + \mu} \right] \quad (6-120)$$

where $\phi_{cL} = \frac{100 A_s}{D} =$ required bottom steel in \widehat{L}_L direction
at the center of the span, expressed as
a percentage of the gross cross section
area

Assuming $d = 0.9 D$ and with equal distribution of the specified minimum steel ($\phi_t = 0.5$) at the top and bottom faces, additional moment steel must be supplied when values of ϕ_{cL} from Eq. (6-120) exceed

$$\frac{0.50 \times 0.90}{2} = 0.225.$$

As with the flat slab, it will be assumed that proper placing of the conventional and prestressed reinforcement will be adequate to resist any edge moments due to the restraining door clamps. As indicated earlier, an upper bound for these moments can be obtained by applying Eq. (6-118).

As a result of the initial prestressing, the entire door slab cross section in the high shear region near the supports is in a state of axial compression. For the range of compressive stresses considered within the prestressing allowable, an increase in the ultimate shear capacity of the beam is expected.³⁸ For design purposes, this increased pure shear capacity, plus a liberal estimate of the total applied shear at the supports, is presumed sufficient to preclude the possibility of a diagonal tension or shear compression failure. In terms of ultimate shear capacity¹³

$$V_u = 0.20 D f'_c \quad (6-121)$$

where an upper bound to the applied shear load is

$$V = 6 q_I L_S \quad (6-122)$$

therefore

$$D = 30 \frac{q_I L_S}{f'_c} \quad (6-123)$$

where

V_u = ultimate shear capacity of the door slab, lb/ in.

V = maximum applied shear on the door slab, lb/in.

(b) Unit Cost

The unit cost per sq ft of cylindrical-element blast door surface can be expressed as follows.

$$C_c = \frac{D}{12} X_c \quad (6-124)$$

$$C_s = \frac{D \phi_{tL}}{1200} X_s \quad (6-125)$$

$$C_{sp} = L_{sp} X_p \quad (6-126)$$

$$C_f = X_f \quad (6-127)$$

The composite cost factor per sq ft of surface can be expressed as

$$C_t = C_c + C_s + C_{sp} + C_f \quad (6-128)$$

3. Structural Steel

(a) Design

The design of the cylindrical element blast door in structural steel is very similar to that just described for prestressed concrete. The thickness of the steel shell, continuing the notation developed earlier, is now designated as t . The required t for a steel plate, based on a given set of initial requirements, is considerably less than the required Γ for a comparable prestressed concrete slab. For this reason, the effects of slab curvature in modifying the flat plate moments (Eq. (6-112) and (6-113)) are more pronounced for the curved steel plate.

As with the prestressed concrete slab, the design of the steel door will be predicated on elastic action throughout the contemplated loading range. Since the applied load is of short duration, it is reasonable to anticipate that the dynamic yield strength of the material can be developed. On this basis, an approximate expression for the thickness of steel plate required to resist axial stresses and bending moments can be obtained from Eq. (6-117b). As with the prestressed concrete element, (Section 6.7.3), an iterative process is necessary since the plate thickness, t , also enters into the expression for

$$t \approx \left\{ \frac{864 K_{10} q_I L_S^2}{f_{dy}} \left[\frac{1 + \lambda^2}{1 + \nu \lambda^2} \right] \left[\frac{(1 + \lambda^2)^2 (1 + \nu \lambda^2) + \mu \lambda^2 / 6}{(1 + \lambda^2) + \mu} \right] \right\} \quad (6-129)$$

If so desired, the value of t satisfying Eq. (6-129) can be substituted into an analogous expression utilizing Eq. (6-117a). This leads to a more exact solution, since the effects of plate curvature are summed for the entire i, j series. However, little if any change in t will result.

Since the plate is isotropic with respect to its strength properties, and since $\left(M_{10} + \frac{t N_{10}}{6} \right) > \left(M_{20} + \frac{t N_{20}}{6} \right)$ at their maximum values, the plate thickness satisfying Eq. (6-129) will automatically satisfy the strength requirements in the \hat{L}_L direction. There is a possibility that edge-restraint moments may govern the design, and this should be checked by substituting into Eq. (6-118). Shearing stresses at the edges of the single-curvature plate can be checked by Eq. (6-104), as with the flat plate.

b. Unit Cost

The unit cost of a structural steel door, per sq ft of surface area, is expressed in the same form as for the flat plate of Section 6.7.2.

$$C_s = X_s \quad (6-106)$$

(values of X_s are supplied in
Table 2-3)

$$C_t = C_s \quad (6-107)$$

6.7.4 Double-Curvature Surface

Blast closures are required for exposed openings in the spherical entranceway structures (Section 6.5). From the standpoint of structural efficiency, the preferred shape for the blast closure would be that of a right spherical cap. The trace of the intersection of this cap with the sphere proper would then be in the form of a circle, whose diameter would be related to the central angle $2\psi_0$ of the opening, as follows

$$S_{L(\text{cap})} = S_{L(\text{sphere})} \sin \psi_0 \quad (6-130)$$

Solutions for the axial thrusts and stresses in a shallow spherical cap of this type, under conditions of radial uniformly-distributed loading, are readily available.³⁵ These solutions are similar to those furnished for the cylindrical element, with the effect of double curvature serving to reduce still further the flat-plate moments. Normal and shearing forces are set up in the shell, in addition to moments and transverse forces, as a consequence of the double curvature.

The spherical cap, as just described, would intersect with the sphere proper and would transfer its loading to a supporting circle. This circular support would then correspond to Ring No. 1 of Section 6.6, where the blast-door reaction was analyzed as an axially-directed line load. This load is axially applied to the ring which frames a circular opening in a symmetrically-loaded spherical shell. Any horizontal component for this loading, such as would result if the spherical cap has a hinged connection at its base,³⁵ would not present problems. Some moment transfer to the support ring could be anticipated, due both to minor load eccentricities and to the presence of door clamps, but this could be accommodated by providing adequate torsional resistance for the support ring (Eq. 6-66).

Since this analytical approach is a straightforward one, it is unfortunate that this form of spherical cap is not entirely suitable for the contemplated application. Its intersection with the sphere proper is not in the form of a circle and the characteristic shape of aperture for the rapid movement of people is rectangular (Section 3.3). In order to circumscribe a rectangle of the required dimensions, the spherical cap must either have a circular intersection with a large base radius or it must have an intersection which approximates the required rectangle.

If the first of these two concepts is adopted, the analysis of the blast door and its supporting ring can be readily accomplished. However, two practical difficulties are encountered. First, since the span length of the blast door is relatively large, the door can become a rather costly item. Next, recognizing that the door must be a movable one, the size and bulk of a circular door impose major problems in the design of the support and closure systems. These difficulties are considerably enhanced if it is specified that the entranceway system must remain serviceable after the design level of attack.

Alternatively, the second concept could be utilized. The intersection of the cap with the sphere proper would then be rectangular in form, with dimensions approximating those specified for a door opening (Table 3-1). The controlling span length of the door element would be significantly less than for the first case, and it can be anticipated that any bending moments in its central portion would be correspondingly reduced. The size and mass

of the door element would be considerably less, leading to probable savings in its support and closure systems. The door element and its loading are no longer symmetric about an axis of rotation. Generalized solutions to this category of problem, as noted in Section 6.5.1 (Design), are not practicable within the scope of this study. A superficial examination of the problem suggests that the major design complexities would be encountered at the base support of the door element, where significant bending stresses can be expected at the re-entrant corners. In addition, if this blast door is to rest directly on a support ring, the design of this supporting ring (and of the sphere proper) will be complicated by the nonsymmetrical pattern of loading.

While it did not appear feasible to pursue these investigations, it was necessary to develop some representative cost data for a spherical-shell closure. In order to accomplish this, certain simplifying assumptions will now be introduced. First, the form for the blast door will be taken to be a surface element of the sphere to which it is attached. Next, its intersection with this sphere will be assumed to have the form of the optimum rectangular doorways of Table 3-1. Rather than actually design the door element, it will be assumed that its resistance (due to double curvature) would be at least equal to that of a corresponding cylindrical-element door. Design and cost data for this latter type of doorway will then be utilized as an approximation to equivalent data for the spherical-element door.

The circular supporting ring of Section 6.6 will be retained, despite the rectangular shape of the blast door. This will be accomplished by providing a thick, rigid disk, which is contained within the circular ring and which has a rectangular opening to accommodate the blast door. Edge reactions from the blast door are thus transferred to the disk as shearing forces. And, with the disk partially-restrained at the supporting ring (Ring No. 1), will act as a moment and a line loading along this boundary.

6.8 CHANNEL GUIDES FOR BLAST-RESISTANT DOOR

The blast doors considered in this study are designed to open or close by horizontal movement in the plane of the door opening. As a consequence, the door will rest on horizontal rollers to facilitate such movement. These

rollers are positioned between the flanges of a structural steel guide-channel, which may either be a rolled shape or one built-up from component elements. The web thickness of the guide channel is largely determined by the weight of the blast door, while the channel depth is governed by the thickness of the blast door. The channel minimum length is approximately twice the width of the blast door which it supports. Finally, the longitudinal axis of the channel guide must conform in shape to that of the supported edge of the blast door.

Channel guides are provided both at the top and at the bottom of the blast door. These will facilitate tracking during opening and closing, and will also help to keep the door sealed during shock buffeting and negative-phase loading. A similar guide is provided along one side of the door, so that, in its closed position, the door is restrained on three of its four sides by the channel flange. Retractable clamps or "dogs" will be used to provide positive closure on the remaining side.

The channel will be attached by one leg to its support structure. Hence, the required web thickness for the bottom guide may be established by either the cantilever bending moment or the shear at the web-flange junction of the channel. Assuming that the blast door dead-weight of w lb per lineal ft is applied as a uniformly-distributed load over the depth of the channel web (web depth d_w in. and web thickness t_w in.), the required web thickness for conventional loading is obtained as the larger value of the following.

$$t_{w(\text{bending})} = \frac{w}{f_y} \left(\frac{d_w}{2} \right)^2 \quad (6-131)$$

$$t_{w(\text{shear})} = \frac{w}{7.2 f_y} \quad (6-132)$$

The static-loading value, f_y , is used for the yield point of structural steel in Eq. (6-131) and (6-132). The reason for this is that the blast door constitutes a long-duration loading on the channel guide. Also, if the configuration of the door and the anticipated orientation of the reduced pressure front are such that lateral blast forces can be applied to the guides, an additional strength capacity should be furnished. It is almost impossible to

place quantitative measures on these additional requirements, largely because of the complex wave form of the pressure front. Considering the importance of maintaining effective blast sealing, a factor of safety of at least two (with respect to static loading) would appear justifiable in the design of the support guides.

6.9 SUPPORTS FOR BLAST-RESISTANT DOOR

6.9.1 Discussion

For the entranceway layouts contemplated in this study, a surface transition section (Section 1.3.3) and depth transition section will lead from the ground surface to a blast-exclusion section. This latter section, which contains the blast door and may also contain its supporting structure, can take the configuration of a cubicle (Section 6.2), a horizontal cylinder (Section 6.3 and 6.4) or a sphere (Section 6.5). The primary loading on this blast-exclusion section can be either tensile or compressive, depending upon whether the blast-resistant door is located at its upstream or its downstream face.

The dead load of the blast door, plus any allowance for anticipated lateral reactions at the door edges during blast loading, is carried by the channel guides described in Section 6.8. In addition, an adequate normal reaction must be supplied to resist the primary loading on the blast-exclusion door. While this door loading could conceivably be transferred directly to the structural surfaces adjacent to the door opening, it is generally advantageous to provide supplementary supporting members to receive the edge reactions of the blast-loaded door.

The layout of the door supports is to some extent, dependent upon the configuration of the blast-exclusion section. For example, in the case of a door opening in a cubicle, transverse rectangular frames of beam and column sections are placed along the vertical edges of the opening. The door reaction then subjects these framing members to a bending moment and to an axial loading which, depending on the location of the door relative to the blast-stream, can be either tensile or compressive. A similar layout is used for door openings in cylinders except that the support members, again placed normal to the loaded surface, are now circular rings rather

than rectangular frames. An exception is made in the case of the doorway for the sphere. Here the door reaction is transferred to a support ring, normal to the plane of ring curvature, (Ring No. 1 of Sections 6.5 and 6.6) and thus is transferred to the doubly-curved surface of the shell itself.

6.9.2 Door Supports, Cubicle Structure

1. Design

Here the blast-resistant door, (Section 6.7.2), is rectangular in form and will consist of either a flat slab of prestressed concrete or a flat steel plate. This door can be moved laterally on its channel guides (Section 6.8), and in its closed position, under conditions of blast loading, will bear against two rectangular support frames whose vertical members parallel the long (vertical) edges of the door. Bending moments are thus introduced into the vertical members of the support frames, and their end reactions are transferred to horizontal framing members which are integral with the external surfaces of the roof and floor slabs. Axial forces in these horizontal members can be either tensile or compressive, depending upon the positioning of the blast door relative to the pressure front. While there could be some moment transfer between the vertical and the horizontal members, the structural stiffness resulting from the integral action of the cross beams and the roof (or floor) slab suggests that significant rotation of the beam-column joint is unlikely. Finally, the whole-body equilibrium forces for the blast door loading will be assumed to act on that portion of the rear entranceway wall which is bounded by the roof slab, the floor slab, and the rear vertical members of the two rectangular frames. This equilibrium force would result from the internal pressure load for a downstream location of the blast door, or from the passive earth pressures in the event of an upstream location for the blast door.

Let us consider the case of a transition section, rectangular in cross section, whose upper end is open to the blast wave. At some interior point, whose exact location is dependent upon the details of the entranceway layout, its side wall will merge with the end wall of a blast-exclusion cubicle. A blast-exclusion door is located in the side of the transition passage (coincidental with the end wall of the blast-exclusion cubicle) and some distance

from its terminal end. This door is also rectangular, with dimension L_S and L_L (ft). The blast-exclusion cubicle, as viewed from the blast door, has a height H ft and a width of B_T ft. There will only be minor differences between the magnitudes of L_L and H since minimum head-room requirements normally control this dimension for both elements. In addition, since the entranceway width requirements are established by the expedient movement of people (Chapter 3), the cubicle width B_T will not greatly exceed the door width L_S . To permit it to slide from an open to a closed position, the blast door will probably not be centrally located within the width B_T .

The reduced pressure wave, probably with multiple intermediate reflections (Chapter 4), will proceed along the rectangular transition passage and will be reflected from its interior surfaces. Concurrently, all exterior surfaces in contact with the ground will receive earth-transmitted overpressure loading. However, over the width B_T (end wall of blast-exclusion cubicle, also containing the blast door), only the reduced reflected pressure is acting. The reflected pressure produces a dynamic loading of very brief duration on the interior surfaces of the passageway. This (Chapter 4 and Section 6.3), can be represented for analytical purposes as an equivalent uniformly-distributed static load, q_I lb/in.² The overpressure loading and conventional loading on ground-contacting exterior surfaces of the passageway, can be represented as $q_{Ed} + q_E$ for horizontal surfaces and $k_h (q_{Ed} + q_{Es})$ for vertical surfaces. Since q_I is appreciably larger than $\sum q_E$ in the general case, the net loading within the passageway is outwardly-directed.

The blast-resistant door, for all design situations considered in this study, will bear in compression on its support structures under blast-loading conditions. It will be assumed that sufficient longitudinal steel will be incorporated in the end wall of the blast-exclusion cubicle to ensure its two-way action throughout that region which is coincidental with the side wall of the transition passageway. In the case of the cubicle blast door, the near vertical legs of each rectangular frames will receive a total loading of $72 q_I L_L L_S$ lb from the blast door. Assuming that the vertical support is much stiffer than the door slab, and recognizing that the cubicle height H is approximately equal to the door height L_L , we will assume that each vertical member of height H (ft) and width b (in.) supports a uniformly

distributed loading of $6 q_I L_S$ lb per in. and a torsional moment of $3 q_I b L_S$ in. lb per in.

The vertical members will be analyzed as fully-fixed at their ends, in recognition of the stiffening influence of the roof and floor slab. Based on the justifications for elastic response of the blast door system (Section 6.7.1), the assumption of yield redistribution of moments, as used elsewhere in these studies,^{1,2} will not be extended to the columns. In addition to providing adequate resistance to bending and torsional moments, it will be necessary to check the strength of the section in the diagonal tension and/or shear compression modes. The same analysis will also be applied, with some implicit degree of conservatism, to the rear vertical members of the frame.

The ultimate load capacity of a uniformly-loaded reinforced-concrete member as it approaches failure in its bending mode, prior to any inelastic redistribution of bending moments along its length, can be expressed as follows.¹

$$q_f = 0.00075 \phi_e \left(\frac{d}{H} \right)^2 f_{dy} \quad (6-133)$$

where

q_f = static equivalent uniformly-distributed load, lb/in.²
corresponding to the ultimate bending moment capacity
at the end sections of a fixed end reinforced-concrete
flexural member

ϕ_e = area of tension steel reinforcement at the fixed ends of
the flexural member, expressed as a percentage of the
net cross section area, bd

d = effective depth of flexural member (depth from com-
pression face to centroid of tension steel), in.

H = clear-span length of flexural member, ft

f_{dy} = dynamic yield strength of reinforcing steel, lb/in.²

The shearing mode resistance can be approximated as follows.⁵

$$q_{sc} = \frac{1.765}{(2 + \phi_v)} \left(\frac{d}{H} \right)^2 \sqrt{f'_c \phi_e} \left[1 + 0.0002 \phi_v f_{dy} \right] \quad (6-134)$$

where

q_{sc} = static equivalent uniformly-distributed load, lb/in.²
corresponding to the ultimate strength of the section
in diagonal tension and/or shear compression,
assuming fixed-end support

MIT RESEARCH INSTITUTE

θ' = ratio of percentages of compression reinforcement and tension reinforcement. ($\theta' = 0.25$ is assumed in this study)

f'_c = ultimate static compressive strength of concrete, based on standard 28-day tests on cylindrical specimens, lb/in.²

ϕ_v = area of shear reinforcing steel (vertical stirrups) expressed as a percentage of the section area of the flexural member

For equal strengths in both flexural and shearing modes, $q_f = q_{sc}$ and

$$\phi_e \left| \begin{array}{l} q_f = q_{sc} \\ \theta' = 0.25 \end{array} \right. = \left[\frac{1045 + 0.0209 \phi_v f_{dy}}{f_{dy}} \right]^2 f'_c \quad (6-135)$$

Substituting $q_f = q_{sc} = \frac{q_I (6L_S + b)}{b}$ where b is the width in inches of the flexural member, the following equation is obtained for the design of the vertical frame member

$$d = \left[\frac{36.5 H}{1045 + 0.0209 \phi_v f_{dy}} \right] \frac{q_I (6L_S + b) f_{dy}}{b f'_c}^{1/2} \quad (6-136)$$

The required area of torsional steel (vertical stirrups) can be determined from Eq. (6-66), substituting $M_t = 3 q_I b L_S$. An equal area of longitudinal steel is also required. This will be spaced around the periphery of the cross section.

$$\phi_{vt} = \frac{600 q_I b L_S - 70 b^2 D (f'_c)^{2/3}}{b^2 D f_{dy}} \quad (6-137)$$

where

ϕ_{vt} = total required cross sectional area of torsional stirrup steel, expressed as a percentage of the gross plan area of the beam.

($\phi_{vt} = \frac{100 A_s}{12 b H}$, where A_s = total cross

sectional area of reinforcement measured normal to $b H$ plane)

q_I = static equivalent uniformly-distributed representation of reduced reflected pressure loading on blast door, lb/in.²

b = width of rectangular support column, measured in plane of blast door, in.

D = gross depth of rectangular support column, measured normal to plane of blast door, in. ($d = 0.9 D$)

L_S = width of blast door, ft

f'_c, f_{dy} = as previously defined.

In an actual design situation, assuming that the blast door can be centrally-located in the width B_T , it may be advantageous to set the column width at $6 (B_T - L_S)$. If this is done, the portions of the end wall of the blast-exclusion structure which are immediately adjacent to the blast door would be designed for a loading of $q_I \left(\frac{B_T}{B_T - L_S} \right)$ rather than for a loading of $(q_I - k_h q_{Ed})$.

The horizontal members for each rectangular support frame will be analyzed as axially-loaded struts, on the assumption that any moment transfer at the beam-column connection will be resisted through T-beam action by the roof and floor slabs. Two separate cases must be recognized in the analysis, since the strut loading is influenced by the layout of the blast door and its supporting frames. The first of these will occur when the end reactions of the vertical frame members impose compressive loading on the strut. With the assumption of no moment transfer, the horizontal member will then be proportioned for a dynamically-applied axial load of brief duration, whose static representation is

$$N_{du} = 36 q_I (L_S + b/6) H \quad (6-138)$$

where

N_{du} = total axial load on horizontal member due to end reaction of vertical frame members, lb

q_I = static uniformly-distributed loading which represents the effects of reflected pressure loading on the blast-resistant door, lb/in.²

L_S = width of door, ft

H = interior height of blast-exclusion cubicle, ft
(As in the analysis of the vertical member, the door loading is assumed to act over the distance H , rather than L_L .)

The required gross depth of the section is

$$D_{\text{strut}} = \frac{36 q_I (L_S + b/6) H}{0.85 f'_{dc} b_{\text{strut}}} \quad (6-139)$$

where

D_{strut} = required gross depth of horizontal member, in.

b_{strut} = width of horizontal member, in.

f'_{dc} = ultimate dynamic compressive strength of concrete,
taken as $1.25 f'_c$ and expressed in units of lb/in.²

q_I, L_S, H = as previously defined

In order to provide localized bending resistance, it is desirable that $D_{\text{strut}} \geq b_{\text{strut}}$. In addition, it will arbitrarily be specified that 0.50 percent of reinforced steel is to be placed at the top and at the bottom faces of the strut ($\sum \phi_t = 1.00$).

The second case of interest arises when the end reactions of the vertical framing members place tensile loading on the horizontal members. For this tension case, it is suggested that the entire cross section of the strut be axially prestressed so as to develop a uniform initial compressive stress of $0.45 f'_c$. The section could then support an axial tensile loading of $(0.45 f'_c + 3\sqrt{f'_c})$ prior to concrete cracking, and could support an ultimate tensile loading of $0.90 f'_c$. Since elastic behavior is desirable for the entire support frame, and since it is probable that some localized bending moments will exist, a degree of conservatism is deliberately included in the following design equations.

$$T_{sp} = 0.45 f'_c D_{\text{strut}} \quad (a)$$

$$D_{\text{strut}} = \frac{36 q_I (L_S + b/6) H}{(0.45 f'_c + 3\sqrt{f'_c}) b_{\text{strut}}} \quad (b) \quad (6-140)$$

The expression for the required length of prestress strand, per lineal ft of horizontal member, is very similar to that of Section 6.3, as expressed in Eq. (6-18). L_{sp} now represents the required length of prestressing strand per unit length of member rather than per unit area.

$$L_{sp} = \frac{b T_{sp}}{F_{sp}} \quad (6-141)$$

where

- b = width of prestressed member, in.
- L_{sp} = required length of prestressing strand, ft per lineal ft of strut
- T_{sp} = effective prestressing force on the strut, lb per in. of strut width (Eq. (6-140a))
- F_{sp} = manufacturer's recommended design load per prestressing strand, lb (Table 2-7)

Alternatively, if so desired, the strut could be designed with conventional reinforcing steel. Such a design would be comparable to the $e_d = 0$ case of the eccentrically-loaded element, as described for rectangular cubicles in Section 6.2 (Table 6-2 ; typical results). The basic postulate, in this general analysis of a member subjected to axial stress and bending, is that all tensile axial loading is resisted by the conventional steel reinforcement. This leads, for this particular application and loading condition, to the following equation.

$$\phi_t = \frac{3600 q_I (L_S + b/6) H}{f_{dy} b_{strut} D_{strut}} \quad (6-142)$$

where

- ϕ_t = total area of tensile steel, expressed as a percentage of the gross cross section area

This steel must be distributed uniformly across the strut cross section, and positive anchorage must be provided for it. In addition, some minimum specifications for section dimensions and concrete strength are obviously required. Lacking other information, it seems appropriate to apply Eq. (6-138) for this purpose. The strut is then proportioned so that the concrete will crack under the design loading. The strains in the strut will not be compatible with those anticipated for the attached slab. For these reasons, the design utilizing conventional reinforcement does not appear to be particularly suitable.

2. Unit Cost

The unit costs per lineal ft for each vertical framing member can be expressed as the sum of the cost of concrete (C_c), main reinforcement (C_s), shear steel, if required (C_v) and formwork (C_f).

$$C_c = \frac{bD}{144} X_c \quad (6-143)$$

$$C_s \approx \frac{\phi_e b D}{10,650} X_s \quad (6-144)$$

$$C_v = \frac{\phi_v b D}{900} \left[0.196 \phi_v + 0.347 \right] \quad (6-145)$$

(Eq. 3.33.27b)¹

$$C_{vt} = \frac{\phi_{vt} b}{14,400} \left[1 + 0.80 (b + D) \right] \quad (6-70)$$

$$C_f = \left(\frac{b + D}{6} \right) X_f \quad (6-146)$$

$$C_t = C_c + C_s + C_v + C_f \quad (6-147)$$

The unit costs per lineal ft of strut can be similarly expressed.

$$C_c = \left(\frac{b D}{144} \right) X_c \quad (6-148)$$

$$C_s = \frac{\sum \phi_t b D}{14,400} X_s \quad (a)$$

(compression loading) (6-149)

$$C_s = \frac{\phi_t b D}{14,400} X_s \quad (b)$$

(tension loading and conventional reinforcement, Eq. (6-142))

$$C_{sp} = L_{sp} X_p \quad (6-150)$$

(tension loading, prestressed reinforcement of Eq. (6-141))

$$C_f = \left(\frac{b + 2D}{12} \right) X_f \quad (6-151)$$

$$C_t = C_c + C_s + C_{sp} + C_f \quad (6-152)$$

6.9.3 Door Supports, Cylindrical Structure

1. Support Rings

(a) Design

Here the blast-resistant door, (Section 6.7.3), will consist of a cylindrical-surface element. As with the flat slab door, it can be fabricated either from prestressed concrete or from structural steel. It

can be moved laterally in its channel guides (Section 6.8) and, in its closed position and under conditions of blast loading, will bear against two circular support rings whose curved surfaces are parallel to the long (curved) edges of the door.

Two design situations must be recognized, depending upon the layout of the blast-exclusion cylinder and of its door support rings. If the blast door is in an upstream location relative to the cylindrical blast-exclusion structure, the cylinder is loaded in compression and the static equivalent of the reflected pressure, q_I lb per in.² will act on the blast door as a radial inwardly-directed loading of short duration. The support rings are then placed within the cylinder, and the long curved L_L edges of the door will bear against them. This will impose a radial inwardly-directed loading on each support ring, uniformly-distributed over a ring length equal to the curved length L_L (door height). It will be assumed that an equilibrating reactive force is simultaneously mobilized over the far semi-circle of each support ring.

The design situation, for this loading case, is that of a circular ring under radial inwardly-directed compression, one component of which is uniformly distributed over the curved length L_L and the other component of which is distributed uniformly over the length $1/2 \pi (S_L + 2D)$ where S_L is the interior principal diameter of the curved ring and D is the ring depth in its plane of curvature (Note that $S_{L(\text{cylinder})} = S_{L(\text{ring})} + 2 D_{(\text{ring})}$, according to this notation). As an approximation, in order to avoid the explicit consideration of ring bending moments in this analysis, it will be assumed that each cylindrical ring is subjected to a uniform radial inwardly-directed loading of magnitude $6 q_I L_S$ lb per in. where q_I is the static equivalent of the short-duration reflected pressure on the blast door (lb per in.²) and L_S (ft) is the width of the blast door. At the same time, the compression ring will be proportioned so as to furnish appreciable localized resistance to bending moments. Also, the loading which the door imposes along its L_S supports will be examined for its localized effect on the cylindrical shells. In so doing, consideration will be directed to that portion of the cylindrical shell surface which is bounded by the two circular support rings.

Assuming that the support ring is a conventionally-reinforced concrete beam of rectangular cross section, and neglecting any compressive resistance which may be afforded by hoop reinforcement, the required ring section for the compressive loading case can be expressed approximately as follows.

$$D_{(ring)} = \frac{36 q_I (L_S + b/6)}{0.85 b f'_{dc}} \left[S_{L(ring)} + \frac{D_{(ring)}}{6} \right] = \frac{36 q_I (L_S + b/6)}{0.85 f'_{dc}} S_{L(cylinder)} \quad (6-153)$$

where

D = gross depth of ring section in plane of ring curvature, in.

q_I = static equivalent loading, uniformly-distributed and directed radially-inward on the exterior surface of the ring, lb per in.². This equivalent loading represents the effect of the short-duration reflected pressure loading on the blast door.

L_S = width of blast door, ft

b = width of concrete ring, measured in plane normal to that of ring curvature, (in.). In order to supplement localized resistance to bending and torsional moments, it is recommended that $b \approx D$.

f'_{dc} = ultimate strength in compression of dynamically-loaded concrete cylinder, lb per in.², taken as $1.25 f'_c$

$S_{L(ring)}$ = interior principal diameter of ring, ft

$S_{L(cylinder)}$ = interior principal diameter of cylinder, ft

It is recommended that hoop reinforcement, $\phi_t = 0.50$, be distributed equally at each curved face. In addition, if considered appropriate, the resistance of the ring to torsional moment can be investigated by assuming that the line loading $6 q_I L_S$ acts at the ring face (ring width b in.), to produce a torsional moment $M_t = 3 q_I b L_S$ in.-lb per in. The requirements for torsional reinforcement can then be investigated by Eq. (6-66).

$$\phi_{vt} \approx \frac{200 M_t - 50 b^2 D (f'_{dc})^{2/3}}{b^2 D f_{dy}} \quad (6-66)$$

where

$$\phi_{vt} = \frac{100 A_s}{2\pi b [6 S_{L(ring)} + D_{(ring)}]}$$

A_s = total cross sectional area of torsional reinforcement in length $2\pi (6 S_L + D)$ and width b , measured normal to plane surface of supporting ring. Units are in.²
 Note that an equal cross sectional area of longitudinal steel will also be required.

It will also be assumed, for further generality, that the support ring can be a curved structural-steel section. The design relationship is then approximated by the following.

$$A = \frac{36 q_I (L_S + \frac{b}{6})}{f_{dy}} \left[S_{L(\text{ring})} + \frac{D_{(\text{ring})}}{6} \right] = \frac{36 q_I (L_S + \frac{b}{6})}{f_{dy}} S_{L(\text{cylinder})} \quad (6-154)$$

where

A = required cross sectional area of steel member, in.²
 f_{dy} = dynamic yield strength of structural steel, lb/in.²
 and all other terms are as defined in Eq. (6-153).

A second design situation will arise when the location of the blast door, relative to the blast-exclusion cylinder, is downstream from the advancing pressure front. The reflected pressure will then enter the cylinder, placing it under a loading which is predominately tensile (Sections 6.4.2 and 6.4.3) and thus imposing an outwardly-directed radial loading on the blast door. For this situation, the circular support rings will be installed on the outside of the cylinder and the curved edges of the door will bear against their inner faces. By similar assumptions to those just described for the compression-loading case, the rings will be assumed to act in tension due to a uniform radial load of $6 q_I L_S$ acting on their inner faces.

The requirements are such that a prestressed concrete ring would be suitable. It will be assumed that the rings are rectangular in cross section and are initially loaded by an effective prestressing force, T_{sp} lb per in. so that each section is uniformly stressed to $0.45 f'_c$ lb per in.² in compression. The required section area is then as follows

$$D = \frac{36 q_I [S_{L(\text{ring})} L_S + b/6]}{(0.45 f'_c + 3\sqrt{f'_c}) b} \quad (6-155)$$

where

D = gross depth of ring section in plane of ring curvature, in.

q_I = static equivalent loading, uniformly-distributed and directed radially outward on the exterior surface of the ring, lb per in.² This equivalent loading represents the effect of the short-duration reflected pressure loading on the blast door.

L_S = width of blast door, ft

b = width of concrete ring, measured in plane normal to that of ring curvature, (in.). In order to supplement localized resistance to bending and torsional moments, it is recommended that $b \approx D$.

f'_c = ultimate strength in compression of statically-loaded concrete, based on standard 28-day tests on cylindrical specimens, lb per in.²

Requirements for torsional moment resistance can be checked by the procedure described for the compression ring. The required length of prestress strand per lineal ft of ring surface is given by

$$L_{sp} = \frac{b T_{sp}}{F_{sp}} \quad (6-141)$$

where

L_{sp} = required length of prestressing strand, ft per lineal ft of mean ring circumference

$T_{sp} = 0.45 f'_c D$ = effective prestressing force per in. of width, lb per in.

F_{sp} = manufacturer's recommended design load per prestressing strand, lb (Table 2-7)

In the event that a structural steel tension ring is desired, its design is almost identical with that of the steel compression ring.

$$A = \frac{36 q_I [S_{L(\text{ring})} (L_S + b/6)]}{f_{dy}} \quad (6-156)$$

(All terms are as described for Eq. (6-154))

(b) Unit Cost

The unit cost per lineal ft of reinforced-concrete compression ring, total length $\pi (S_{L(\text{ring})} + \frac{D_{\text{ring}}}{12})$, is as follows

$$C_c = \frac{b D}{144} X_c \quad (6-157)$$

$$C_s = \frac{\phi_t b D}{14,400} X_s \quad (6-158)$$

$$C_{vt} = \frac{\phi_{vt} b}{14,400} \left[1 + 0.80 (b + D) \right] X_v \quad (6-69)$$

$$C_f = \left(\frac{b + D}{6} \right) X_f \quad (6-159)$$

$$C_t = C_c + C_s + C_{vt} + C_f \quad (6-160)$$

The unit cost per lineal ft of structural steel compression ring is

$$C_t = C_s = w X_s \quad (6-161)$$

where

w = unit weight, lb per ft

The unit cost per lineal ft of prestressed-concrete tension ring is as follows.

$$C_c = \frac{b D}{144} X_c \quad (6-157)$$

$$C_{sp} = L_{sp} X_p \quad (6-162)$$

$$C_f = \left(\frac{b + D}{6} \right) X_f \quad (6-159)$$

$$C_t = C_c + C_{sp} + C_f \quad (6-163)$$

The unit cost per lineal ft of structural steel tension ring is

$$C_t = C_s = w X_s \quad (6-161)$$

2. Beam Members Between Support Rings

(a) Design

The blast-door openings in the shell surface of a cylindrical blast-exclusion structure are, insofar as the shell equilibrium forces and strains are concerned, localized discontinuities in the shell surface. Therefore, it becomes advantageous to supply some framing arrangement which can transmit shell equilibrium forces around each opening. The type of door which is contemplated, (Section 6 7 3), is itself an element of a cylindrical surface. The door, as visualized, is rectangular in plan, with

long curved edges \widehat{L}_L (ft) and with a transverse span of L_S (ft). Let us consider the effect produced by a rectangular opening of these dimensions in a loaded cylindrical shell.

Consider a radial section of the cylinder, taken at any point within that region which is defined by the length L_S . The length \widehat{L}_L of the door opening can then be considered as subtending a central angle, $2\psi_o$, where $\psi_o = \frac{180}{\pi} \left[\frac{\widehat{L}_L}{S_L + D/6} \right]$. The primary loading on the cylindrical shell is radial, uniformly distributed, and either inwardly-directed (compressive cylinder) or outwardly-directed (tension cylinder). In addition, the loading on the blast door could result in a vertical line loading along the shell length L_S . It can be reasoned that the stiffening effect of the circular door-support rings along the \widehat{L}_L edges will be sufficient to reduce any loading on the L_S edges to a minor quantity.

In greatly-simplified form, we will postulate that the primary requirement of the opening support frame is to transfer shell equilibrium forces (and, by inference, compatible shell strains) across an opening of arc length \widehat{L}_L (ft), assuming that the shell is loaded solely by a radial loading whose magnitude is q lb per in.² The loading on the transverse frame member of length L_S , acting in the plane of the support ring, is thus

$$q_{\text{frame}} = \frac{q_{\text{shell}}}{\tan \psi_o} \quad (6-164)$$

where

q_{frame} = unit load acting on those framing members which parallel the long axis of the cylinder, lb per in.²

q_{shell} = net equivalent loading on cylindrical shell surface due to earth-transmitted pressure and/or reflected pressure, lb per in.²

$$\psi_o = \frac{180}{\pi} \left[\frac{\widehat{L}_L}{S_L + D/6} \right]$$

S_L = interior principal diameter of cylinder, ft

\widehat{L}_L = length of curved edge (long dimension) of blast-door, taken as an approximation of the length of the door opening in this analysis. ft

L_S = width of blast door (short dimension), taken as an approximation of the width of door opening in this analysis, ft

IIT RESEARCH INSTITUTE

D = gross thickness of shell cross section, in.

b = width of frame member, measured normal to the line of action of q_{shell} , in.

The framing member under consideration will be assumed to extend between the two circular door-support rings, and to be fixed at these connections. On this basis, it can be designed in the same manner as the vertical framing member for the cubicle doorway, Section 6.9.2. Equation (6-136), which expresses the reinforced-concrete rectangular section requirements for balanced strengths in both flexural and shearing modes, can thus be rewritten in a suitable form. For $q_f = q_{sc}$ and $\theta' = 0.25$, the required percentage of tensile steel at the fixed ends of the members is given by Eq. (6-135).

$$\phi_e \left| \begin{array}{l} q_f = q_{sc} \\ \theta' = 0.25 \end{array} \right. = \left[\frac{1045 + 0.0209 \phi_v f_{dy}}{f_c} \right]^2 \quad (6-135)$$

$$(a) \quad d = \left[\frac{36.4 L_S}{1045 + 0.0209 \phi_v f_{dy}} \right] \left[\frac{(q_{Es} + q_{Ed})(6S_L + D_{\text{shell}}) f_{dy}}{b f_c} \right]^{1/2} \quad (6-165)$$

(compression loading on cylinder)

$$(b) \quad d = \left[\frac{36.4 L_S}{1045 + 0.0209 \phi_v f_{dy}} \right] \left[\frac{(q_1 - q_{Es} - q_{Ed}) S_L f_{dv}}{b f_c} \right]^{1/2}$$

(tension loading on cylinder)

where

ϕ_e = required area of tension reinforcing steel at end of framing member, expressed as percentages of net area, bd , of member

d = required effective depth of reinforced concrete flexural member (depth of tension steel), in.

b = width of flexural member, in.

ϕ_v = area of shear reinforcing steel (vertical stirrups) expressed as a percentage of the section area of the flexural member

f_{dy} = dynamic yield strength of reinforcing steel, lb/in.²

f_c = ultimate compressive strength of loaded concrete, lb/in.² based on standard 28-day tests on cylindrical specimens

q_{Es} = radial inwardly-directed equivalent static loading acting on a buried cylinder due to conventional dead loads, lb per in.² (Section 6.3.1)

q_{Ed} = radial inwardly-directed equivalent static loading acting on a buried cylinder to earth-transmitted overpressure, lb per in.²

q_I = radial outwardly-directed equivalent static loading acting within a buried cylinder due to reflected pressure within the structure, lb per in.²

For purposes of this study, it will be assumed without further investigation that the equilibrating forces in the circumferential ψ direction, due to the end reactions of the framing members just analyzed, can be accommodated by the circular door-support rings to which they connect. It is recognized that the presence of these framing members and rings will produce strain discontinuities which will affect idealized shell action, undoubtedly leading to bending moments in the adjacent shell surfaces. These stresses should be localized, and, while of significance in design, they are not expected to have any large effect on structural costs.

A structural steel framing member would be required in the event that this material is used for the door-support rings. Again, consider a beam of length L_S (ft), which is fixed at the support rings, and restrict the behavior of the beam to the elastic range for structural steel under dynamically-applied loading. We obtain the following equation.

$$S = \frac{12 (q_{Es} + q_{Ed}) L_S^2}{f_{dy} \tan \psi_o} \quad (a)$$

(compression loading on cylinder)

(6-166)

$$S = \frac{12 (q_I - q_{Es} - q_{Ed}) L_S^2}{f_{dy} \tan \psi_o} \quad (b)$$

(tension loading on cylinder)

where

$S = \frac{D}{2I} =$ required elastic section modulus of steel beam, in.³

$D =$ gross depth of steel beam, in.

$I =$ moment of inertia of steel beam about transverse bending axis, normal to direction of loading, in.⁴

L_S = width of blast door, ft

(q_I , q_{Es} , q_{Ed} , f_{dy} , ψ_o as earlier defined).

(b) Unit Cost

The unit costs per lineal ft of reinforced-concrete beam are

$$C_c = \frac{bD}{144} X_c \quad (6-167)$$

$$C_s \approx \frac{\phi_e b D}{10,000} X_s \quad (6-168)$$

$$C_v = \frac{\phi_v b D}{900} \left[0.196 \phi_v + 0.347 \right] X_v \quad (6-169)$$

$$C_f = \left(\frac{b + D}{6} \right) X_f \quad (6-170)$$

$$C_t = C_c + C_s + C_v + C_f \quad (6-171)$$

The unit cost per lineal ft of steel beam is

$$C_t = C_s = w X_s \quad (6-172)$$

6.9.4 Circular Slab, Spherical Structure

1. Design

As noted in Section 6.9.1, the blast-door support structure for the spherical blast exclusion differs in concept from that considered for the cubicle and spherical configurations. In these latter cases, the edge loading imposed by the blast door was transferred as a bending load to its support structure. As clarification to this statement, it should be recognized that we were able to ignore bending moments in the analysis of the circular support ring by reasoning that the composite loading approached a uniform radial-load condition. In the analysis of the door-support system for the sphere, the support frame merely provides a boundary condition for equilibrium forces in the shell. Accordingly, blast-door loading is transferred through the support ring to the shell itself. This condition was recognized in the analysis of the sphere and its support rings (Sections 6.5 and 6.6) and there remains only the matter of transferring door loads to the support ring.

The support ring was assumed to be circular in plan (Section 6.6) and to be subjected to a vertical uniform line load, P_L , which is attributable to the blast door loading. Since we wish to avoid inclined reactive forces and/or moment transfer at the support ring, we shall consider a simply-supported slab, circular in plan, which contains an opening for the blast door. This opening is asymmetrical with respect to the slab center, and removes a large portion of the slab area.

A simplified analysis for this situation, suitable for use in this generalized investigation, does not appear to be available. We can reason that it would be desirable for the slab to approximate a rigid disk. This could be accomplished by increasing the disk depth and holding reinforcement to some reasonable value. Alternatively, and perhaps preferably, the disk could be circumferentially prestressed. Current experimental investigations suggest that such a procedure, in addition to reducing deflections, can effect a substantial increase in shearing resistance.

As a very crude approximation, we will analyze the disk requirements by considering a simply-supported concrete slab, circular in plan, with two-way isotropic reinforcement. This slab, whose maximum span is $S_{L(\text{ring})}$, is subjected to a uniform loading q lb per in.² On this basis, for $q_f = q_{sc}$ and with θ' taken as 0.25, we obtain the following.^{1, 5}

$$\phi_c = \left[\frac{289 + 0.00572 \phi_v f_{dy}}{f_{dy}} \right]^2 f'_c \quad (6-173)$$

Equal percentages of steel will be provided, top and bottom, in the L_L and L_L doorway directions. We will assume, for costing purposes, that these steel percentages remain constant. Additional corner reinforcement will also be required in the vicinity of the opening. The required effective depth of slab is as follows

$$d = \left[\frac{25.8 S_L}{289 + 0.00572 \phi_v f_{dy}} \right] \left[\frac{q_f f_{dy}}{f'_c} \right]^{1/2} \quad (6-174)$$

where

ϕ_c = maximum requirement for area of tensile reinforcement expressed as a percentage of the net section area

ϕ_v = maximum requirement for area of shear reinforcement vertical stirrups assumed, expressed as a percentage of the net section area

d = required effective depth of slab, in.

S_L = interior principal diameter of support rings of Section 6.6 (ft)

f_{dy} = dynamic yield strength of reinforcing steel, lb/in.²

f'_c = ultimate compressive strength of concrete, lb/in.²

q_I = static equivalent, uniformly-distributed, or reflected pressure loading on area enclosed within support ring, lb/in.²

2. Unit Cost

The unit costs per sq ft of slab, as expressed herein, are applicable to a total area A , where A is given by Eq. (6-175).

$$A_{\text{slab}} = \frac{\pi}{4} S_{L(\text{ring})}^2 - \left[L_{S(\text{slab})} \times L_{L(\text{slab})} \right] \quad (6-175)$$

$$C_c = \frac{b D}{144} X_c \quad (6-176)$$

$$C_s \approx \left[\frac{2 \phi_c d}{1200} \right] X_s \approx \left[\frac{\phi_c D}{660} \right] X_s \quad (6-177)$$

$$C_v = \frac{\phi_v D}{1200} X_s \quad (6-178)$$

$$C_f = X_f \quad (6-179)$$

$$C_t = C_c + C_s + C_v + C_f \quad (6-180)$$

$$C_T = C_t A_{\text{slab}} \quad (6-181)$$

CHAPTER 7

STRUCTURAL DESIGN OF ENTRANCEWAYS FOR 100-500-1000 MAN SHELTERS

7.1 INTRODUCTION

Chapter 6 supplies the general data required to design and cost entranceway structural elements. In order to evaluate structural costs for entire entrance systems, these elements must be utilized in actual shelter designs. Understandably, there are myriad ways in which structural elements of different materials can be combined to form a complete structure. Fortunately, the findings of other investigations^{1, 23, 24} supply some guidance as to the required configurations and layouts for entrance systems at selected overpressure levels.

From the results of these earlier studies, and from cost and analytical relationships developed in this report, representative entranceway configurations and material combinations can be selected for detailed study. The paramount consideration in making these selections is minimum structural cost for the total entrance, while utilizing only those construction materials and methods which lend themselves to a mass shelter construction program. The entranceways are designed as 1, 2 and 4 traffic lane models. By using the criteria presented in Chapter 3, the required number of traffic lanes can be related to the shelter capacity.

Many of the entrance costs presented in this chapter are based on theoretical requirements for material quantities, using the design relationships established in Chapter 6. In practical situations, it can be expected that limitations in size and material availability will dictate substitutions or slight revisions in the material quantities and result in minor cost increases. While the conceptual designs presented in this chapter are not the only feasible possibilities, they do use all the basic structural elements as developed in Chapter 6 in what is generally accepted as their most efficient employment. For this reason, it is felt that other arrangements of these basic structural elements would not lead to any significant reduction in the cost of blast-resistant entranceway systems. In particular, the layouts presented are typical of the various types studied in the preparation of this

IIT RESEARCH INSTITUTE

report. Optimum entranceway configurations for particular traffic lane capacities and selected overpressure levels are discussed in Chapter 8.

7.2 DESIGN CONFIGURATIONS

7.2.1 Discussion

The design configurations considered in this study fall into two broad categories, blast-resistant and nonblast-resistant structures. The blast-resistant entranceways are designed to withstand both air and ground pressure loading upstream from the blast door, as well as ground pressure loading between the blast door and the shelter. It is assumed in design that any structural damage, short of collapse, will be sufficiently restricted so that the blast door remains operable after the attack. The entrance structure is thus available for entrance before the attack and for exit following the attack. In addition, as noted in Chapter 1, a supplementary exit will be provided in all cases. By inference, the blast-resistant entranceway structure will have a multi-attack capability.

The nonblast-resistant entrance structure is designed to withstand only nominal (10 psi) earth loading upstream from the blast door. Consequently, this portion of the structure is expected to collapse as a result of blast action. Between the blast door and the shelter, however, the entranceway is designed to withstand the blast-induced ground pressure loading. This nonblast-resistant entranceway structure will be available for entrance only, and will not have a multi-attack capability. A separate exit thus becomes an essential feature for this design option.

7.2.2 Blast-Resistant Structures

A number of design concepts have been examined in this category. For comparative purposes, all designs consider the same four basic section types. The first of these is a surface transition section consisting of an open V-shaped cut whose 2:1 side slopes are stabilized by a 3 in. bituminous or concrete surface treatment. The bottom of this cut contains a concrete stairway, which provides for some change in elevation and thus permits below-grade burial of the other three structural sections.

The form of the depth transition section is dependent on the design loading and required traffic capacity. It can consist of a reinforced concrete cubicle, a prestressed concrete cylinder, or a steel cylinder. This transition section contains the second set of concrete steps, which are intended to provide the major change in elevation. The length-to-width ratio of the transition section is sufficient to develop the "tunnel effect" reduction of peak free-field overpressures, as discussed in Chapter 4.

The blast exclusion sections, which can have varying configurations, will provide the support for the blast door. They serve to separate the upstream portion of the entrance structure, which is designed to carry both interior air blast and exterior ground loading, from the downstream portion which receives only ground loading. In some instances, limited additional depth transition capability is available in this section.

The fourth type consists of two right-angle radiation attenuation sections (R_1) and (R_2). Again, depending on design loads and traffic capacity, these sections are either cubicles or cylinders of reinforced concrete. Two such sections are considered to be the minimum number for the efficient attenuation of radiation streaming. Any further requirements for radiation attenuation will then be satisfied by barrier shielding placed in either of the radiation sections or in the shelter proper.

1. Compression Sphere Blast Section

The compression sphere design is pictured in Fig. 7-1. This shows a cylindrical depth transition section which leads from the open cut (ground level opening) to a compression sphere which supports the blast door. The transition section is connected to this blast section by a flexible mild steel plate, which maintains full structural continuity. At the same time, the connection will permit relative displacements between the transition and blast sections, during blast buffeting, without inducing additional stresses in the structural elements.

In addition to the spherical shell itself, the spherical blast section will include an entrance ring, a blast door support slab, and an exit ring. The concrete support slab is designed as a simply supported two-way isotropic slab, and will supply bearing for the cylindrical-shell blast door.

MIT RESEARCH INSTITUTE

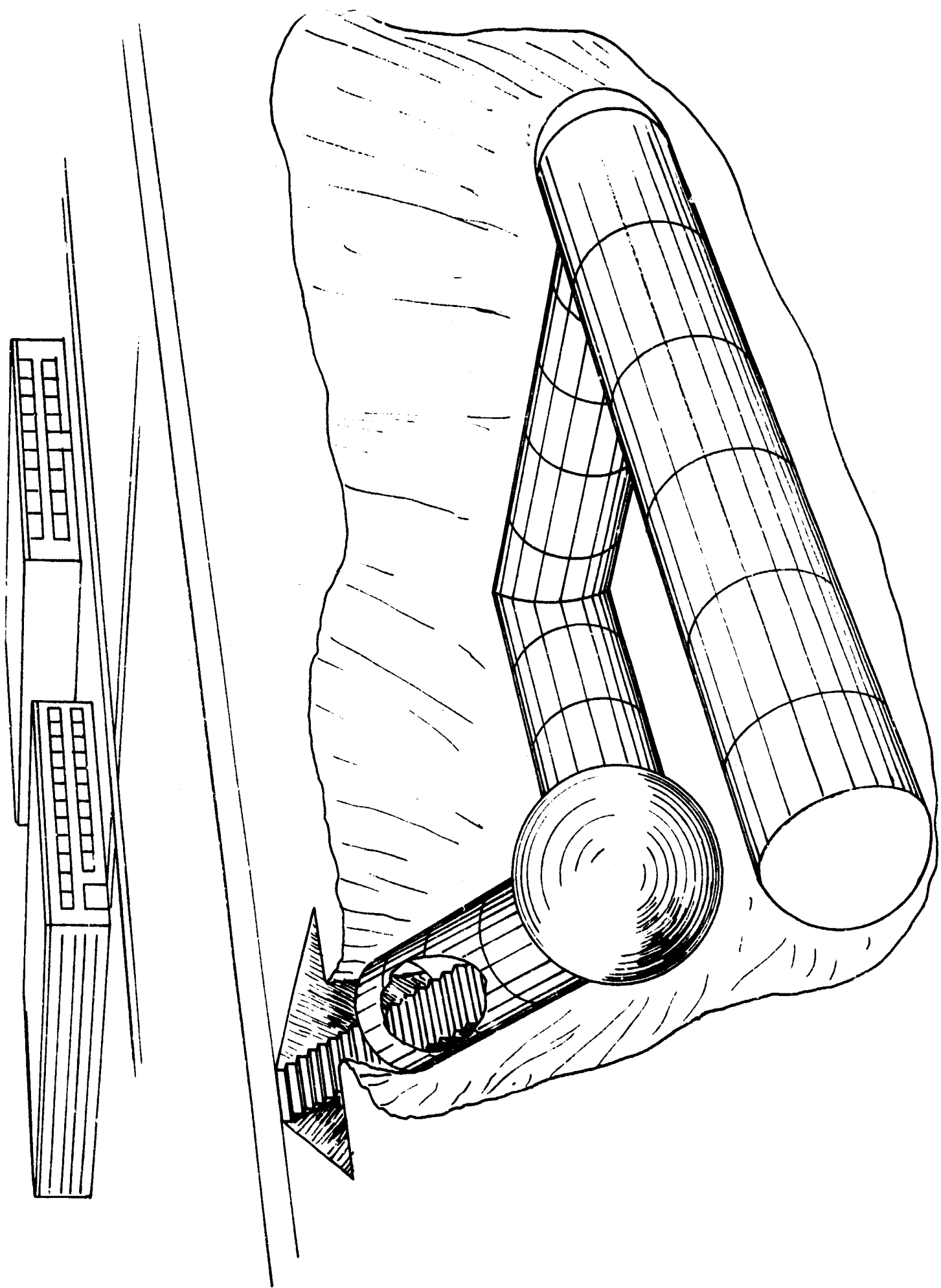


Fig. 7-1 ENTRANCEWAY CONFIGURATION WITH COMPRESSION SPHERE BLAST SECTION

The entrance ring, in turn, provides support for the blast slab and is assumed to transmit these loads to the spherical shell as axial thrusts. The exit ring is designed to carry the shell boundary stresses at the intersection of the radiation and blast sections. The compression sphere permits a 90 deg horizontal angle change and also allows considerable change in elevation.

* **Advantages** - This configuration is suited for use in high overpressure regions where the two-way membrane action of the thin spherical shell can be employed effectively. The spherical shape lends itself to the simple inclusion of an interlock system by adding a second blast door at the exit port.

* **Disadvantages** - The requirements for a relatively large cross section will restrict the feasible traffic design capacities of an entranceway using a spherical element. Costs are appreciably higher for this layout in the low and middle pressure ranges. In the multiple lane designs, a blast door sleeve or flared transition element is required to accommodate the blast door in its open position.

2. Tension Cylinder Blast Section

The layout shown in Fig 7-2 employs a steel or prestressed concrete transition element which is rigidly connected to a horizontal in-line cylindrical blast section. The blast door, which is also a segment of a cylindrical shell, is positioned in the side of the blast cylinder and is supported on its curved sides by two stiff tension rings. These rings are constructed integrally with the cylindrical shell of the blast section. Shell boundary stresses at this opening are resisted by two horizontal beam members which run parallel to the long axis of the cylinder and frame into the tension rings. The downstream portion of the cylindrical blast section consists of a flexible steel spherical cap which is supported by a rolled steel slip-ring. This cap is designed to displace under interior pressure loading without stressing the blast cylinder.

* **Advantages** - The blast door is located inside the blast section structure, thus no sleeve or flaring of the transition element is required to accommodate the door in its open position. The crushable end cap and the additional lengths of the transition and blast sections should contribute to

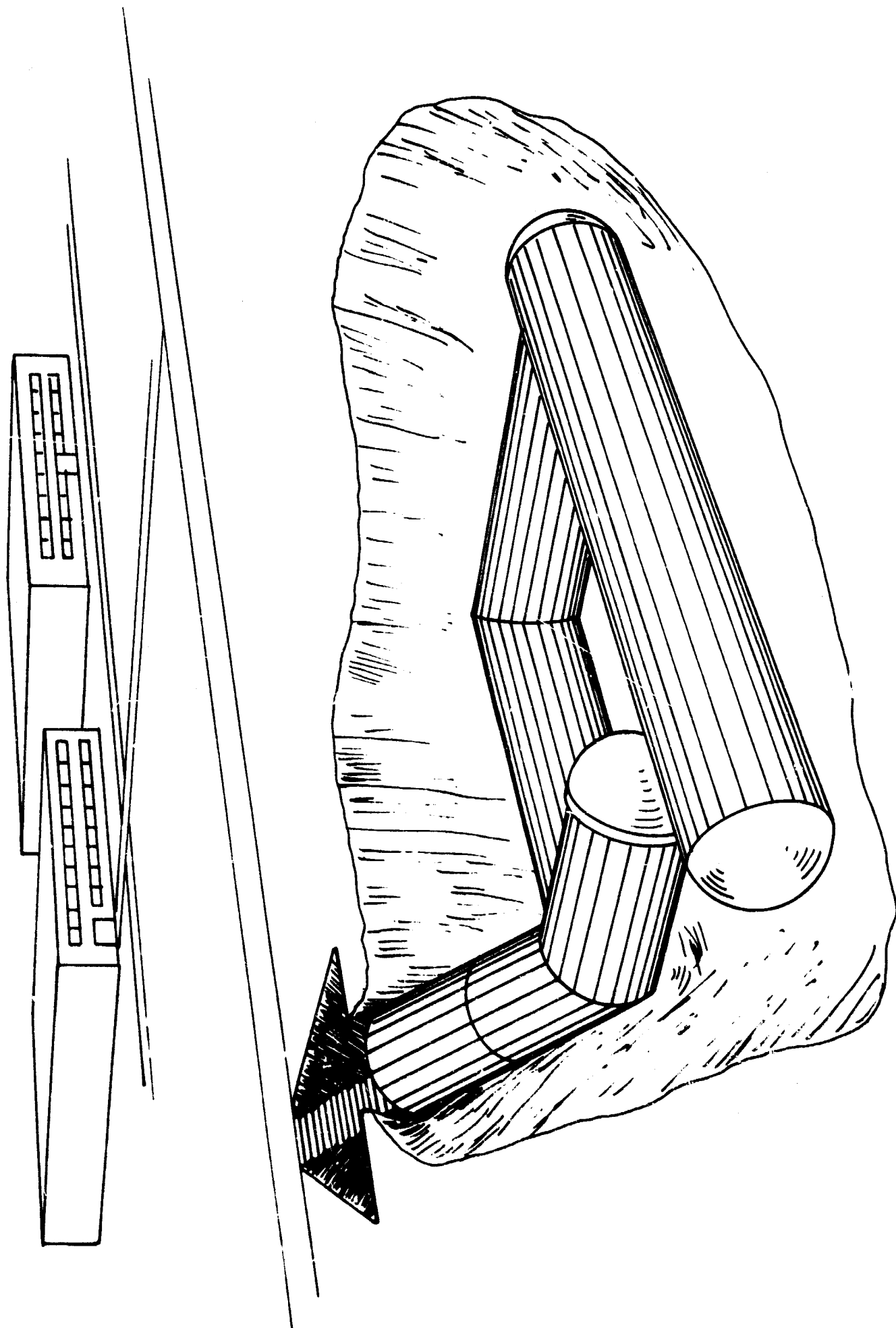


Fig. 7-2 ENTRANCEWAY CONFIGURATION WITH TENSION CYLINDER BLAST SECTION

the dissipation of the reflected blast wave, and thus reduce interior loading on the blast section.

* **Disadvantages** - Both the transition section and the blast section must be designed to resist interior pressures. This tensile loading will require that either a curved steel plate or a thick prestressed concrete cylinder element be used for both sections. As a result, high costs can be expected when the design overpressure is large. In addition, this blast section design does not possess any significant capability for a change in elevation.

3. Compression Cylinder Blast Section

This blast section has a capacity for limited changes in elevation. As shown in Fig. 7-3, the cylindrical section connects at a 90 deg horizontal angle with the transition section. As in the case of the compression sphere, structural continuity between the transition and the blast sections is maintained by a flexible mild steel expansion plate. The blast cylinder is constructed of reinforced concrete and has a monolithically-poured concrete dome enclosing its upstream end. Its downstream end will phase directly into the first radiation section. The blast door is again a cylindrical shell segment, and is supported on the outer surface of the blast cylinder by two compression rings which are poured integral with the blast cylinder shell. Two horizontal beam members carry shell boundary stress across the door opening and frame into the compression ring.

* **Advantages** - This concept utilizes concrete in compression for maximum economy in the design of the blast section. In the middle and high design pressure ranges, this design tends to be the most economical.

* **Disadvantages** - The positioning of the blast door on the outside of the blast cylinder requires a blast door sleeve or flared transition element for use with multiple lane designs.

4. Tension Cubicle Blast Section

This reinforced concrete design duplicates the basic features of the tension cylinder, but is somewhat more economical in the lower pressure range. Its basic layout is illustrated in Fig. 7-4. The wall, roof and floor elements of the cubicle blast section are designed as tension-loaded members

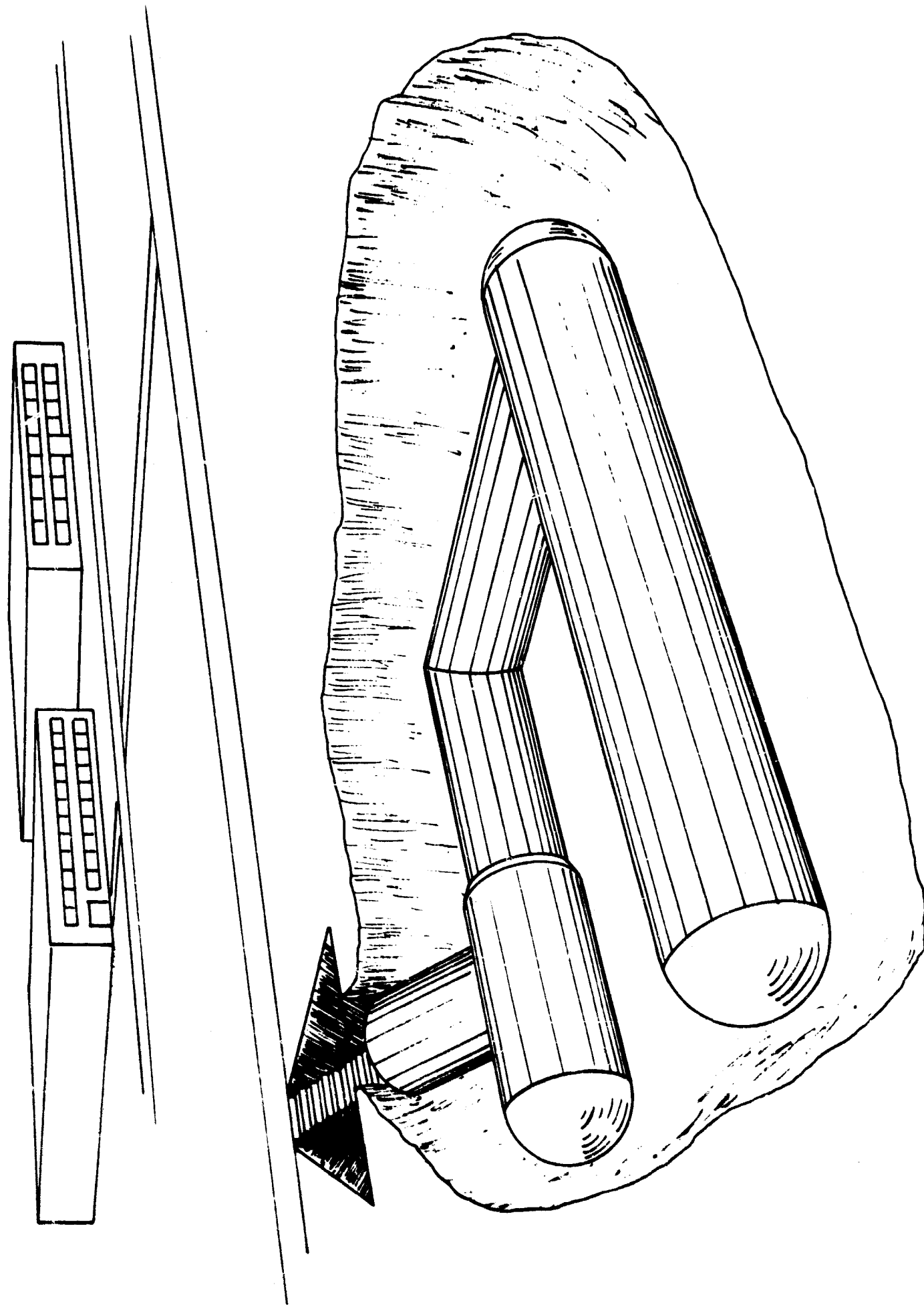


Fig. 7-3 ENTRANCEWAY CONFIGURATION WITH COMPRESSION CYLINDER BLAST SECTION

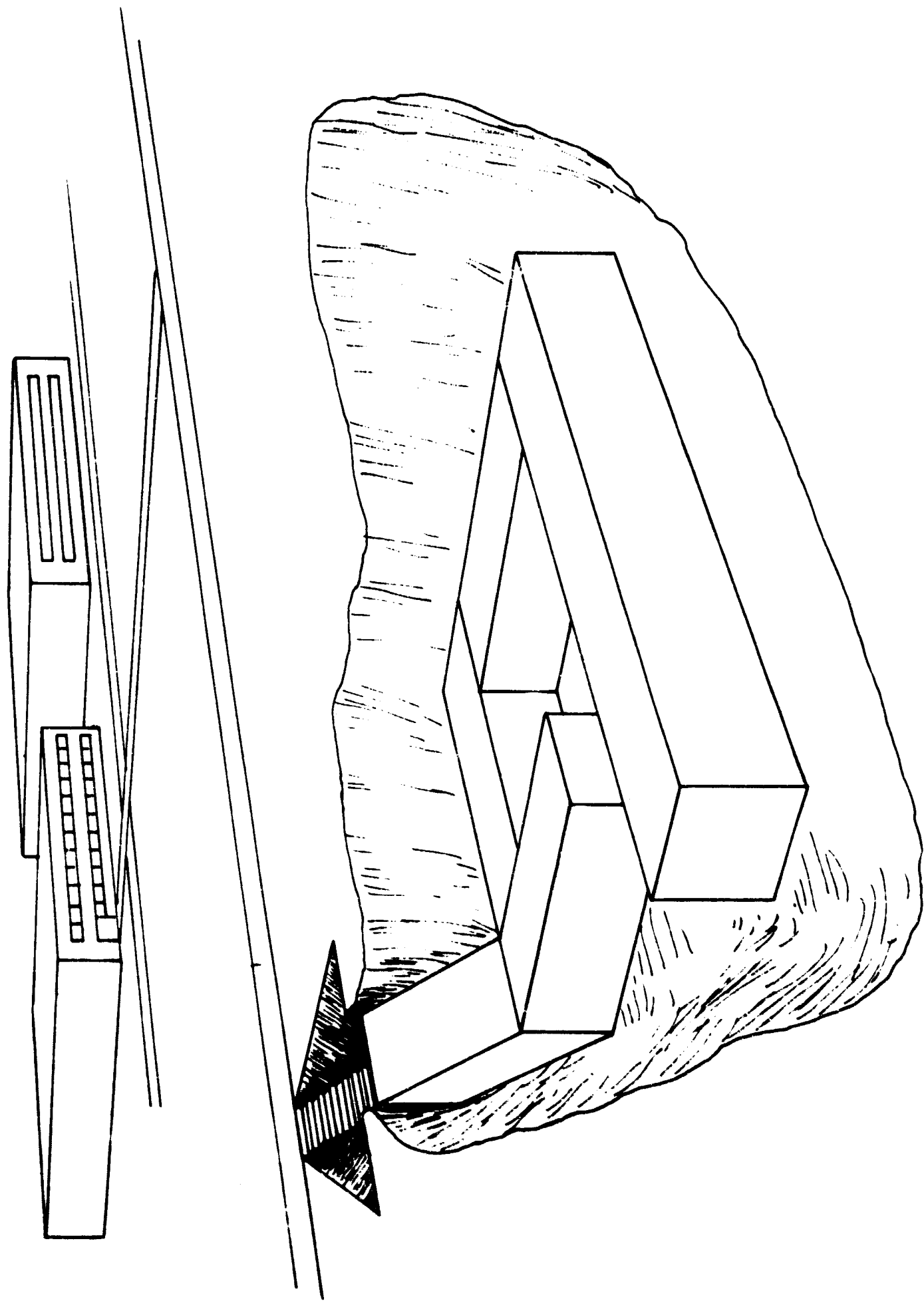


Fig. 7-4 ENTRANCEWAY CONFIGURATION WITH TENSION CUBICLE BLAST SECTION

which are also subjected to end moments. The primary loading is induced by interior pressure as the blast wave enters the section. The cubicle elements are also designed to carry the axial and bending loads, reversed in sign and significantly reduced in magnitudes, which are induced either by a negative pressure phase or by the ground-transmitted pressure load on the cubicle exterior. The blast door slab is supported by two bending members, which are either vertical or horizontal, depending on doorway height-to-width ratios as measured in the plane containing the door slab. The loads on these beams are then distributed to the cubicle walls by means of reinforced concrete tension struts. These struts are placed in the roof and floor slabs and run perpendicular to the blast door plane. The upstream end element of the blast section is designed to carry the same loading as the wall elements.

* Advantages - This design allows greatly simplified forming and conventional construction techniques. In addition, the waste interior volume which is inherent in shell designs is eliminated. The cubicle structure leads to the most economical design in the low pressure range.

* Disadvantage - The design is economically feasible in the low and middle pressure ranges only.

7. 2. 3 Nonblast-Resistant Structures

Two nonblast-resistant entranceway systems are considered in detail. While these will contain the same four basic sections which have been described for the blast-resistant systems, the transition and radiation sections are now designed for only a nominal external loading ($q_E = 10$ psi, which is equivalent to approximately 12-14 ft of soil overburden). The actual cover depths for the entranceway will vary from 3 to 13 ft. It is thus apparent that no appreciable factor of safety against static earth loads is included in the designs for the higher pressure ranges. Subsequent modifications may be required to introduce working load safety factors into the design, but these are not expected to have any significant effect on the cost factors which are presented for the 10 psi level. Any redesign which may thus be involved is left as a future task for the final design stage.

Complete collapse of any entranceway sections which are designed for this nominal 10 psi resistance is expected to occur as a result of blast loading. The cost-saving features of this design, understandably, are greater in the higher pressure ranges. In addition to this economic factor, it is felt that the collapsing upstream structure will absorb blast energy and thus reduce the air pressure loading on the blast section. The collapsed structure will effectively shield the blast section from any subsequent air pressure loading, as in the case of a multiweapon attack, and will inhibit the streaming of fallout radiation through the entranceway.

1. Compression Cylinder or Cubicle

This design concept is shown in Fig. 7-5. The sections upstream from the blast section, as illustrated, are compression cubicles which are designed for 10 psi static equivalent pressure. The use of the cylindrical versus the cubicle blast section is purely a question of economics, which in turn is a function of the design pressure. The elements of the cylindrical or cubicle blast section are the same as those described in Section 7.2.1.

2. Compression Sphere

The nonblast-resistant structural system illustrated in Fig. 7-6 is particularly applicable to high pressure loading. As in the preceding case, the upstream entranceway structure is composed of cylinders or cubicles which are designed for 10 psi loading. The details of the compression sphere blast section are discussed in Section 7.2.1.

7.3 INPUT PARAMETERS FOR ENTRANCEWAY DESIGNS

7.3.1 Dimensional Elements

Chapter 3 lists the specific values which define traffic lane dimensions. In addition, Chapter 4 defines limiting ratios of cross section to length which are associated with blast attenuation in tunnels. Table 7-1 summarizes dimensional limitations which are necessary as input parameters to the sample design problems.

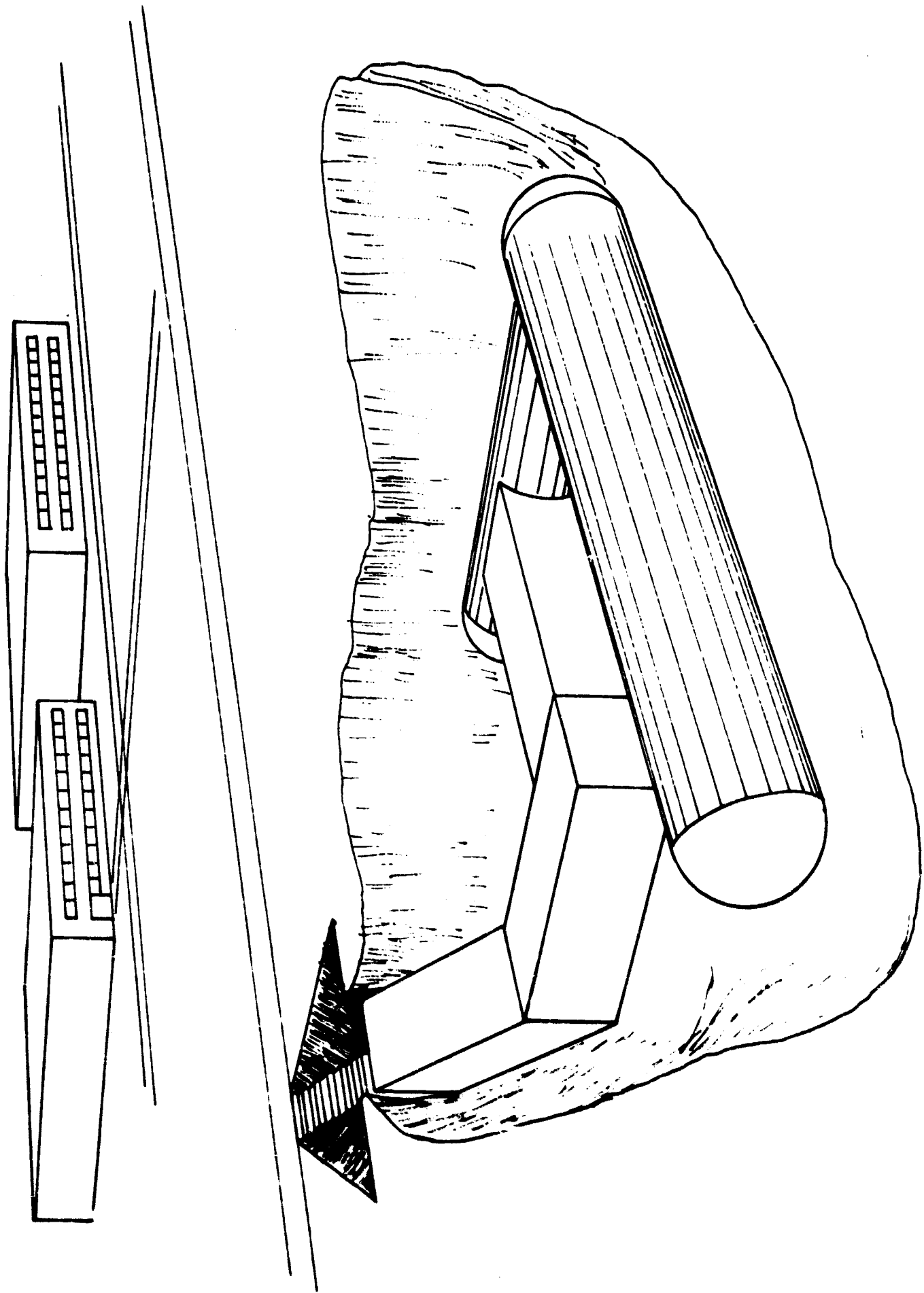


Fig. 7-5 ENTRANCEWAY CONFIGURATION WITH NONBLAST-RESISTANT CUBICLE

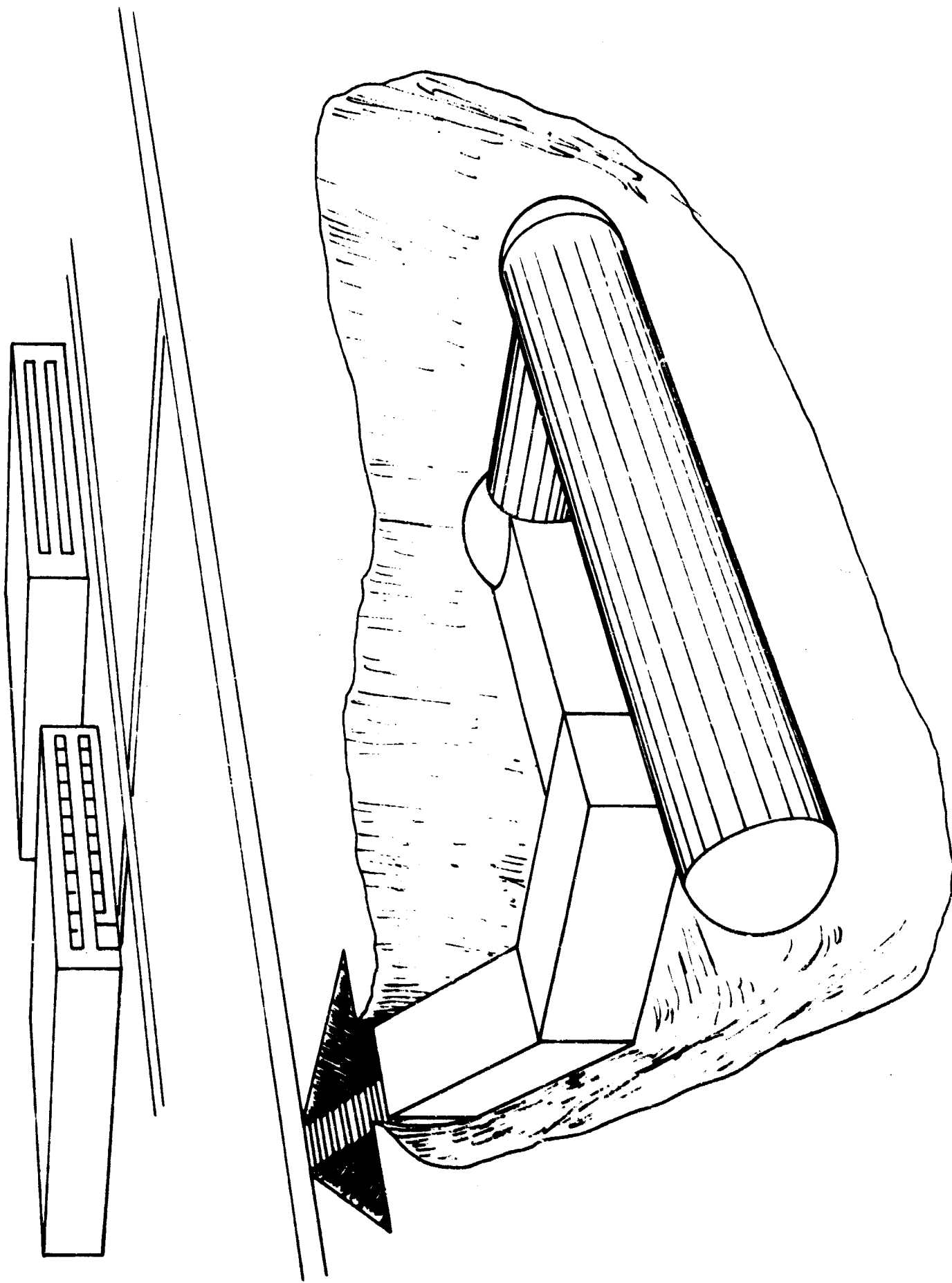


Fig. 7-6 ENTRANCEWAY CONFIGURATION WITH NONELAST-RESISTANT CUBICLE
AND COMPRESSION SPHERE

Table 7-1
MINIMUM DIMENSIONS FOR SELECTED ENTRANCEWAY ELEMENTS

	Cylinder			Cubicle		
	Plain End I. D.	Flared End* I. D.	Min. Blast Attenuation Length	Blast Sphere I. D.	Height Width	
					H	B
1 Lane	7'-6"	7'-6"	11'-3"	13'-0"	7'-0"	2'-6"
2 Lane	8'-0"	10'-6"	12'-0"	14'-0"	7'-0"	3'-8"
3 Lane	11'-0"	16'-0"	16'-0"	N. A.	8'-0"	7'-4"
					12'-0"	

* The flared-end design for the transition section is required if the blast door is to be wholly contained in the entrance structure in both the open and closed position for the compression sphere and cylinder designs. The plain end requires that a sleeve or pocket be constructed in the blast section to receive the open blast door.

The entranceway designs presented in this chapter are developed for specific optimum shelter configurations, as determined in other studies.^{1, 2} Table 7-2 presents features of these optimum shelters which are pertinent to the layout and radiation design of their associated entranceway structures.

Table 7-2

PARAMETERS OF OPTIMUM SHELTERS WHICH ARE PERTINENT
TO ENTRANCEWAY DESIGN

Capacity	Static Equivalent Design Pressure (psi)	Type *	Length (ft)	Width (ft)	Depth to Entrance Level (ft)	Effective Depth of Earth Cover (ft)
100 Man	10	1 St. Cubicle	40	23	12.1	3.5
	50	1 St. Cubicle	30	30	13.3	4.5
	100	1 St. Cubicle	30	30	15.0	5.5
	200	1 St. Cylinder	65	15	17.8	7.5
	325	1 St. Cylinder	65	15	20.3	10.0
500 Man	10	1 St. Cubicle	74	60	12.1	3.5
	50	1 St. Cubicle	74	60	13.3	4.5
	100	2 St. Cylinder	155	20	14.5	5.5
	200	2 St. Cylinder	155	20	16.5	7.5
	325	2 St. Cylinder	155	20	19.0	10.0
1000 Man	10	1 St. Cubicle	111	78	12.1	3.5
	50	1 St. Cubicle	96	90	13.3	4.5
	100	2 St. Cylinder	289	20	14.5	5.5
	200	2 St. Cylinder	289	20	16.5	7.5
	325	2 St. Cylinder	289	20	19.0	10.0

Note: The 10 psi level shelters are structural steel frames. All other shelters consist of reinforced concrete construction. "St." refers to "story"

7.3.2 Static Design Equivalent of Dynamic Blast Pressure

The relationship between dynamic pressures and static equivalent loads is explained in detail in Chapter 4. Entranceway trial designs will be developed in this chapter and, if they are to be compatible with the corresponding optimum shelter designs, they must be investigated for the same levels of static equivalent loading. Consequently, the dynamic pressure range of interest (10-200 psi) will be explored by examining five specific levels of static equivalent loading (10, 50, 100, 200, and 325 psi). These static equivalent design pressures q_E can be related to values of the peak overpressure p_{so} by means of the postulated structural ductility ratio and the plotted data of Fig. 4-1. In similar fashion, the design static loading q_I for interior pressures can be related to the peak intensity of the tunnel reflected pressure p_{ri} by Eq. (4-4) and Fig. 4-2. For an infinite-duration loading and assuming $\mu = 1.3$, Fig. 4-1 indicates that $p_{so}/q_E = 0.625$.

Table 7-3

RELATIONSHIPS BETWEEN VALUES OF STATIC EQUIVALENT LOAD AND LONG-DURATION DYNAMIC LOAD ($\mu = 1.3$)

Form of Loading	Static Equivalent External Load (q_E), psi	Ground-Transmitted Pressure or Peak Overpressure, psi ($p_{so}/q_E = 0.625$)
Ground-transmitted pressures or free-field peak overpressure	10	7
	50	32
	100	65
	200	125
	325	200

The static equivalent, q_I of the internal tunnel pressure loading, p_{ri} , must also be determined. As a first step, the design value of p_{so} is reduced by the tunnel effect (Fig. 4-2). This gives the value p_{to} , which can then be substituted into Eq. (4-4) to obtain the peak intensity of the interior reflected tunnel pressure, p_{ri} . We will again refer to Fig. 4-1, but will now assume that the ratio of the duration of p_{ri} to the natural period of the loaded element is ≈ 1.0 . Thus, with $\mu = 1.3$, we find that $p_{ri}/q_I = 0.77$. The various pressure relationships are finally summarized in Table 7-4.

Table 7-4

STATIC EQUIVALENT DESIGN PRESSURES

Static Equivalent (psi)			Dynamic Loading (psi) P_{to}	Reduced Reflected Pressure P_{ri}
External Load q_E	Internal Load q_I	Peak Overpressure P_{so}		
10	22	7	7	16.7
50	103	32	25	79.4
100	237	65	47	182.3
200	480	125	80	369.0
325	772	200	115	594.0

Conversion figures and equations are supplied in Chapter 4 for the more usual case where p_{so} is known. A solution for q_E and q_I for a particular value of μ is then desired.

7.3.3 Tension Cubicle Design and Cost Factors

The analysis and design of cubicles which are subjected to outwardly-directed reflected pressures on their interior faces are discussed in Section 6.2.1 and summarized in Eq. (6-1) and (6-2). Computer solutions of these equations are presented in Table 6-2 (a). In general, their particular solutions are functions of the six parameters, q , f_{dy} , f'_c , ϕ_L/ϕ_R , ϕ_R and D . However, for the cubicle sizes and range of pressures which are considered herein, solutions of Eq. (6-1) and (6-2) can be expressed more simply as a function of the three parameters q , ϕ_R and D . These solutions are presented in Fig. 7-7 and, using this figure, values of D and ϕ_R can be determined from Section 6.2.2.

7.3.4 Compression Cubicle Design and Cost Factors

The solutions of Eq. (6-1) and (6-2) for cubicles which are subjected to inwardly-directed pressures on their exterior faces cannot be expressed in such a simple form, since all six design parameters remain active. Computer solutions for the specific overpressures and cubicle sizes considered in this study are presented in Table 7-5. Unit costs and comparison with

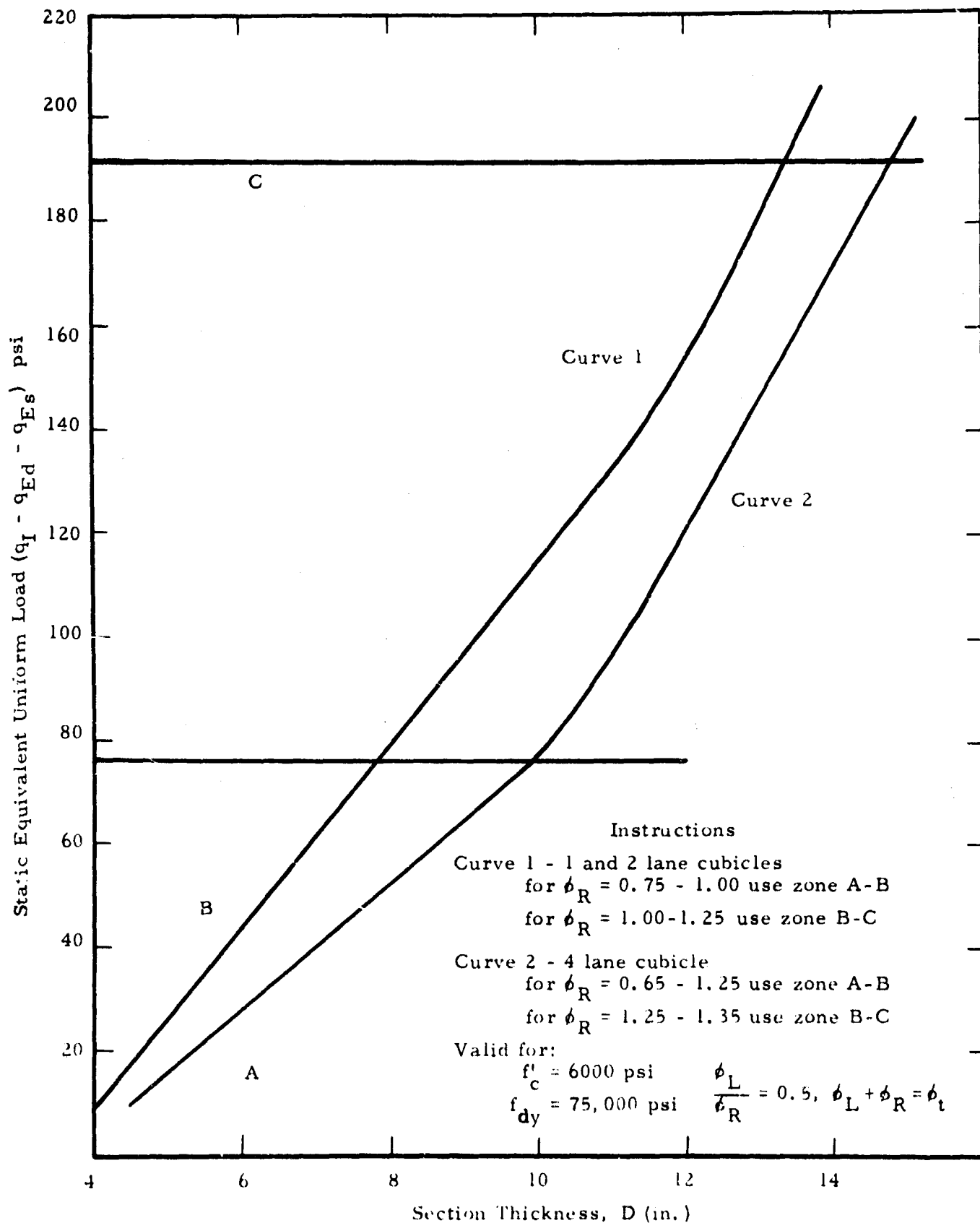


Fig. 7-7 DESIGN CHART FOR TENSION CUBICLE ROOF AND WALL SECTIONS

Table 7-5
COMPRESSION CUBICLE DESIGN AND COST PARAMETERS

Cubicle														Cylinder			
q psi	f' psi	f _{dy} psi	φ _R /φ _L	φ _L	D in.	C _t \$/sq ft	Structural Section	Composite Cost \$/ft of Cubicle	f' psi	f _{dy} psi	D in.	C _t \$/sq ft	Composite Cost \$/ft of Cylinder				
One Lane	10	2000 4000	1.00 5.75	0.25 0.35	4.0 4.0	1.55 1.65	Wall Roof	32.15	2000	60000	3.0	1.78	44.75				
	50	2000 2000	0.50 0.50	1.05 0.95	4.0 4.0	2.05 1.98	Wall Roof	41.35	2000	60000	3.0	1.78	44.75				
	100	2000 2000	0.75 1.00	0.95 0.75	4.0 5.0	2.08 2.04	Wall Roof	42.00	2000	60000	3.0	1.78	44.75				
	200	2000 3000	0.75 1.00	0.95 1.15	4.0 6.0	2.08 2.74	Wall Roof	46.45	3000	60000	3.0	1.80	45.25				
	325	3000 4000	1.00 1.00	1.25 1.25	4.0 8.0	2.30 3.31	Wall Roof	52.50	5000	60000	3.0	1.84	46.25				
Two Lanes	10	4000 4000	0.50 0.75	0.55 0.35	4.0 4.0	1.68 1.65	Wall Roof	37.80	2000	60000	3.0	1.78	47.50				
	50	2000 2000	0.50 0.50	1.05 0.95	4.0 4.0	2.05 1.98	Wall Roof	45.85	2000	60000	3.0	1.78	47.50				
	100	2000 2000	0.50 1.00	1.05 0.75	4.0 5.0	2.05 2.04	Wall Roof	46.40	2000	60000	3.0	1.78	47.50				
	200	2000 3000	1.00 1.00	0.85 1.15	5.0 6.0	2.22 2.74	Wall Roof	55.80	3000	60000	3.0	1.80	48.00				
	325	3000 4000	1.00 1.00	1.25 1.25	5.0 8.00	2.60 3.31	Wall Roof	66.20	5000	60000	3.0	1.84	48.00				
Four Lanes	10	4000 4000	0.50 0.75	0.65 0.55	4.00 4.00	1.71 1.73	Wall Roof	55.10	2000	60000	3.0	1.78	64.25				
	50	2000 2000	0.50 0.75	1.05 0.95	4.0 4.0	2.05 2.00	Wall Roof	64.80	2000	60000	3.0	1.78	64.25				
	100	2000 3000	1.00 0.75	0.75 1.25	5.0 4.0	2.21 2.19	Wall Roof	71.20	2000	60000	3.0	1.78	64.25				
	200	3000 3000	1.00 1.00	1.25 1.15	6.0 7.00	2.90 2.99	Wall Roof	96.20	4000	60000	3.0	1.82	65.75				
	325	4000 4000	1.00 1.00	1.35 1.25	8.0 9.00	3.52 3.64	Wall Roof	119.30	5000	60000	4.0	1.99	73.00				

comparable cylindrical design are presented therein for a finite number of design conditions.

7.3.5 Supplemental or Emergency Exits

Supplemental or emergency exits as described in Section 2 8.4 are deemed necessary for all shelters, whether serviced by blast or by non-blast resistant entranceways. A minimum of one supplemental exit will be supplied, regardless of entranceway type or shelter capacity. For those shelters which employ nonblast-resistant entranceways, the number of supplemental exits will be taken as equal to the number of entranceway traffic lanes. Shelters which use blast-resistant entranceways with capacities \geq 500 people will be provided with two supplemental exit structures.

7.4 BLAST-RESISTANT ENTRANCEWAY DESIGN

7.4.1 Compression Sphere (Sample Analysis and Cost Evaluation)

TRIAL DESIGN 7.4.1-325 A1

CONFIGURATION

One story sphere and cylinder (Fig. 7-8)

STRUCTURAL SYSTEM AND INPUT PARAMETERS (Fig. 7-1)

Transition Section -

Material: Prestressed concrete cylinder

Orientation: Makes ~ 39 deg angle with horizontal plane and is perpendicular to the long axis of the shelter

Dimension: I. D. 7 ft-6 in. ; length 13 ft-0 in. ; change in elevation between entrance and exit 8 ft-3 1/2 in.

Primary Design Load: $q_I = 772$ psi; $q_{Ed} = 325$ psi

Blast Section -

Material: Reinforced concrete sphere

Dimension: I. D. 13 ft-0 in. ; change in elevation between entrance and exit 4 ft-6 in.

Primary Design Load: $q_I = 772$ psi; $q_{Ed} = 325$ psi

Radiation Section - (R_1)

Material: Reinforced concrete cylinder

Orientation: \sim Horizontal, parallel to long axis of shelter

Dimension: I. D. 7 ft-6 in. ; length - 15 ft-0 in. ; change in elevation between entrance and exit 1 ft-6 in.

Primary Design Load: $q_{Ed} = 325$ psi

Radiation Section - (R_2)

Material: Reinforced concrete cylinder

Orientation: Horizontal, perpendicular to long axis of shelter

Dimension: I. D. 7 ft-6 in. ; length 15 ft-0 in. ; change in elevation between entrance and exit 1 ft-6 in.

Primary Design Load: $q_{Ed} = 325$ psi

Note: The dimensions of the two radiation sections are preliminary, and may require subsequent modification due to radiation design requirements.

Shelter -

Capacity: 100 Man (Table 7-2)

Primary Design Load: $q_{Ed} = 325$ psi

IIT RESEARCH INSTITUTE

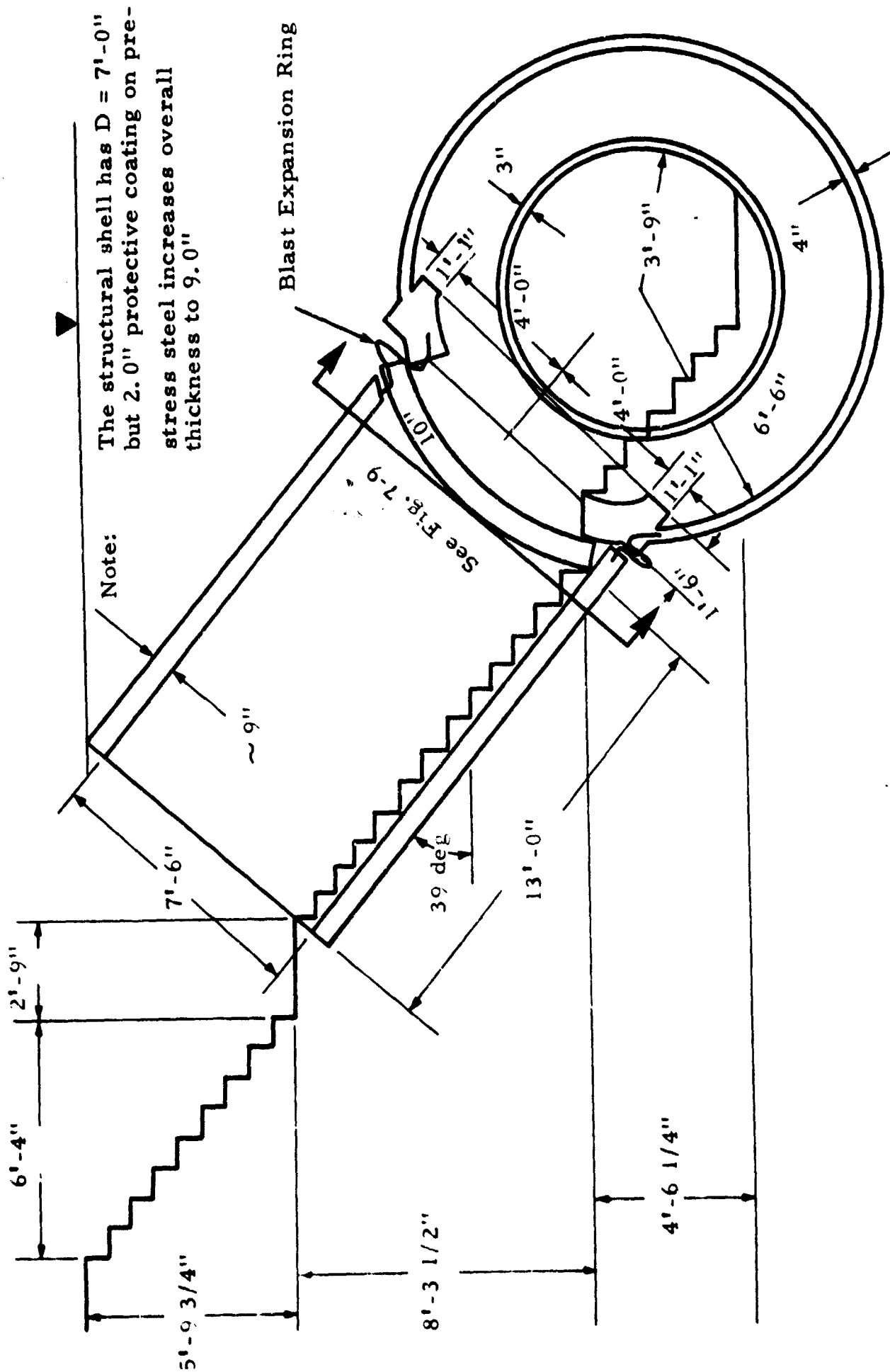


Fig. 7-8 SECTIONAL VIEW OF COMPRESSION SPHERE
(See Fig. 7-1 for layout)

1. Blast Analysis

(a) Transition Section:

Design of cylindrical shell, prestressed concrete

Take $D = 7.0$ in. ;

$$f'_c = 6000 \text{ psi}$$

$$\frac{6S_L}{D} = \frac{45.0}{7.0} = 6.4 < 10.0$$

Requires thick-wall analysis as outlined in Section 6.3 From Eq. (6-15)

$$q_{Ep} \leq 0.225 f'_c \left[1 - \left(\frac{S_L}{S_L + \frac{D}{6}} \right)^2 \right] - q_{Es} \quad (6-15)$$

Taking $q_{Es} \approx 0$ requires that

$$q_{Ep} \leq 0.225 \times 6000 \left[1 - \left(\frac{7.5}{8.66} \right)^2 \right] = 337 \text{ psi}$$

From Eq. (6-13)

$$q_{Ep} \geq \frac{q_I}{2} \left[1 + \left(\frac{S_L}{S_L + \frac{D}{6}} \right)^2 \right] - 1.5 \sqrt{f'_c} \left[1 - \left(\frac{S_L}{S_L + \frac{D}{6}} \right)^2 \right] - q_{Es} - q_{Ed} \quad (6-13)$$

$$q_{Ep} \geq \left[\frac{772}{2} (1 + 0.75) \right] - \left[1.5 \sqrt{6000} (1 - 0.75) \right] - 325$$

$$337 \geq (675 - 29.3 - 325) = 320.7 \therefore \text{OK}$$

From Eq. (6-17)

$$q_{Ep} \leq 0.85 f'_c \left[\frac{(S_L + D/6)^2 - S_L^2}{(S_L + D/6)^2 + S_L^2} \right] - q_{Es} - q_{Ed} \quad (6-17)$$

$$q_{Ep} > 0.85 \times 6000 \left(\frac{8.66^2 - 7.5^2}{8.66^2 + 7.5^2} \right) - 325$$

$$337 < 407 \quad \text{OK}$$

Use $D = 7.0$ in.

As a result of this analysis, a range of values $320.7 < q_{Ep} < 337.0$ is seen to be adequate for design. The upper limit of $q_{Ep} = 337$ psi

IIT RESEARCH INSTITUTE

will be used as the design parameter, since this will tend to reduce the tensile stresses in the shell during interior blast loading.

From Eq. (6-16) the effective prestressing force can be determined

$$T_{sp} = (6 S_L + D) q_{Ep} \quad (6-16)$$

$$T_{sp} = (45.0 + 7.0) = 17,500 \text{ lb/in.}$$

Assuming a 1/2 in. ϕ K 270 prestressing steel strand from Table 2-7, $F_{sp} = 23,150 \text{ lb/strand}$

$$L_{sp} = \frac{12 T_{sp}}{F_{sp}} \quad (6-18)$$

$$L_{sp} = \frac{12 \times 17,500}{23,150} = 9.1 \text{ ft/sq ft of shell}$$

(b) Cost Factors for Cylindrical Shell, Prestressed Concrete

From Section 6.22

Concrete

$$C_c = \frac{D}{12} X_c \quad (6-19)$$

$$C_c = \frac{7.0}{12} \times 130 = 0.76 \text{ \$/sq ft}$$

Reinforcing Steel

$$C_s = \frac{D \sum \phi_i}{1200} X_s \quad (6-20)$$

$$C_s = \frac{7.0 \times 0.6}{1200} \times 85.8 = 0.30 \text{ \$/sq ft}$$

Prestressing Steel

$$C_{sp} = L_{sp} X_p \quad (6-21)$$

$$C_{sp} = 9.1 \times 0.19 = 1.73 \text{ \$/sq ft}$$

Forms

$$C_f = X_f \quad (6-22)$$

$$C_f = 1.40 \text{ \$/sq ft}$$

Protective Coating

$$C_g = X_g \quad (6-23)$$

$$C_g = 0.30 \text{ \$/sq ft}$$

IIT RESEARCH INSTITUTE

Summary

$$C_t = C_c + C_s + C_{sp} + C_f + C_g \quad (6-24)$$

$$C_t = 0.76 + 0.30 + 1.73 + 1.40 + 0.30 = 4.49 \text{ \$/sq ft}$$

(c) Blast Section: Design of Entrance Support Ring (No. 1)

The inside diameter of the entrance ring is a function of the blast door layout. As shown in Fig. 7-9, the minimum inside support ring diameter for the one lane entranceway structure is 4 ft-0 in. In this design case, the blast door in both its open and its closed position can be contained entirely within the transition section. Some flaring of the 7 ft-6 in. diameter radius cylindrical shell will then be required to accommodate the corners of the blast door. We will assume that the entrance support ring has a thickness $b = 13.0$ in. and a depth $D = 18.0$ in. The maximum compression stress in the ring is then determined from Eq. (6-63).

$$f_t \bigg|_{r = \frac{S_L}{2}} = \frac{\left(\frac{-2 P_{L1}}{b \tan \psi_{01}} \right) (S_L + D/6)^2}{(S_L + D/6)^2 - S_L^2} \quad (6-63)$$

where

$$P_{L1} = 3 q_I S_L \sin \psi_{01} \quad (7-1)$$

In this instance

$$\sin \psi_{01} \approx \frac{S_L \text{ (transition section)}}{S_L \text{ (blast section)}} \quad (7-2)$$

$$\sin \psi_{01} = \frac{7.5}{13.0} = 0.576$$

$$P_{L1} = 3 \times 772 \times 13.0 \times 0.576 = 17,320 \text{ lb/in.}$$

As used in Eq. (6-63), $\tan \psi_{01}$ should be referenced to the center line of the entrance ring

$$\tan \psi_{01} = \frac{(S_L + b/12) \text{ (entrance ring)}}{\left[S_L^2 \text{ (blast sphere)} - (S_L + b/12)^2 \text{ (entrance ring)} \right]^{1/2}} \quad (7-3)$$

$$\tan \psi_{01} = \frac{9.083}{(169 - 9.083)^{1/2}} = 0.887$$

IIT RESEARCH INSTITUTE

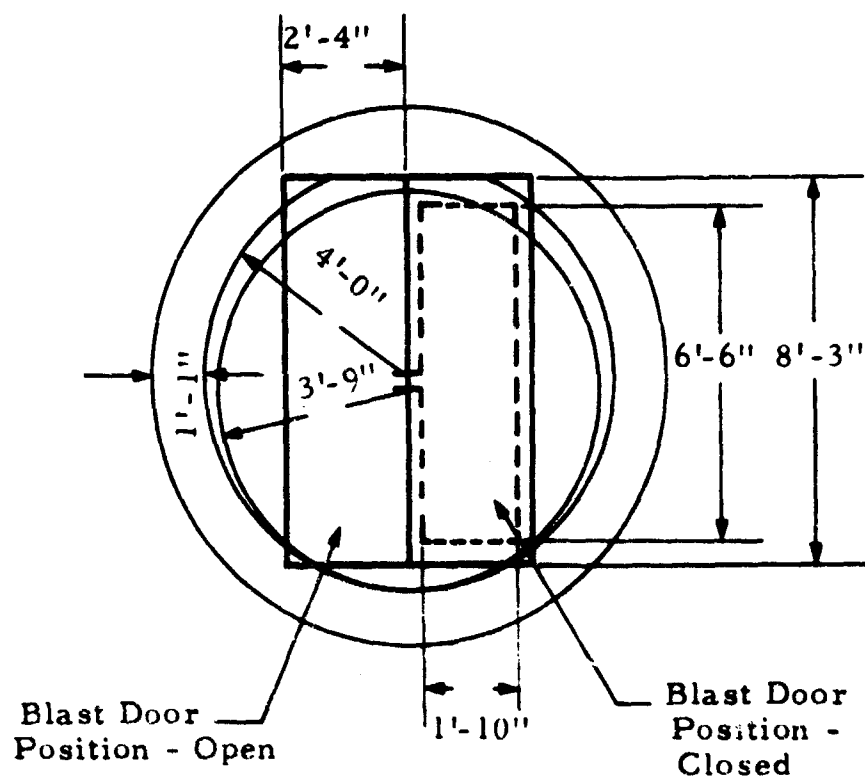


Fig. 7-9 DETAIL OF ENTRANCE RING
AND BLAST DOOR LAYOUT

From Eq. (6-63)

$$f_t = \frac{\left(\frac{-2 \times 17,320}{13.0 \times 0.887} \right) (8.0 + 3.0)^2}{(8.0 + 3.0)^2 - 8.0^2} = -6370 \text{ psi}$$

The limiting value of $f_{t(\max)}$ is obtained from Eq. (6-64)

$$-f_{t(\max)} = 0.85 f'_{dc} \quad (6-64)$$

$$-f_{t(\max)} = 6375 > 6370 \quad \text{OK}$$

∴ Use $b = 13.0 \text{ in.}$; $D = 18.0 \text{ in.}$

Assume a reversed loading magnitude of 25 percent of the primary loading.

From Eq. (6-65)

$$\phi_t = \frac{25 P_{L1} (6 S_L + D)}{b D f_{dy} \tan \psi_{01}} \quad (6-65)$$

$$\phi_t = \frac{25 \times 17,320 (6 \times 8.0 + 18.0)}{13.0 \times 18.0 \times 75,000 \times 0.887} = 1.85 \text{ percent}$$

The torsional moment is assumed as

$$M_t = P_{L1} \frac{b}{2} \quad (7-4)$$

$$M_t = 17,320 \times \frac{13.0}{2} = 112,500 \text{ in-lb}$$

From Eq. (6-66)

$$\phi_{vt} = \frac{200 M_t - 50 b^2 D (f'_{dc})^{2/3}}{b^2 D f_{dy}} \quad (6-66)$$

$$\phi_{vt} = \frac{(200 \times 112,500) - (50 \times 169 \times 18.0 \times 7500^{2/3})}{169 \times 18.0 \times 75,000}$$

Since the numerator is a negative quantity, no torsion steel is required.

(d) Cost Factors for Entrance Ring

Concrete

$$C_c = \frac{b D}{144} X_c \quad (6-67)$$

$$C_c = \frac{13.0 \times 18.0}{144} \times 1.30 = 2.11 \text{ \$/ft}$$

Steel

$$C_s = \frac{\phi_t b D}{14,400} X_s \quad (6-68)$$

$$C_s = \frac{1.85 \times 13.0 \times 18.0}{14,400} \times 100.5 = 3.02 \text{ \$/ft}$$

Tie Steel

$$C_{st} = \frac{\phi_{te} b D X_s}{14,400} \quad (6-69)$$

$$C_{st} = \frac{0.2 \times 13.0 \times 18.0}{14,400} = 85.8 = 0.28 \text{ \$/ft}$$

Forms

$$C_f = \left(\frac{b + D}{6} \right) X_f \quad (6-71)$$

$$C_f = \left(\frac{13.0 + 18.0}{6} \right) 1.00 = 5.17 \text{ \$/ft}$$

Summary

$$C_t = C_c + C_s + C_{st} + C_{vt} + C_f \quad (6-72)$$

$$C_t = 2.11 + 3.02 + 0.28 + 0.00 + 5.17 = 10.58 \text{ b/ft}$$

(e) Design of Spherical Shell, Reinforced Concrete

The design procedures for spherical shells are outlined in Section 6.5.1.

Assume $D = 4.00 \text{ in.}$; $f'_{dc} = 7500 \text{ psi}$, $f_{dy} = 60,000 \text{ psi}$

The quantity

$$\frac{P_{L1}}{q} = \frac{17,320}{325} = 53.4$$

The quantity

$$(3 S_L + D/2) = 39.0 + 2.0 = 41.0$$

thus

$$\frac{P_{L1}}{q} > (3 S_L + D/2)$$

∴ Use Eq. (6-43) to determine D_{max} of shell

$$D = \frac{P_L}{(0.85 f'_{dc} + 0.005 f_{dy}) \sin \gamma_{01}} \quad (6-47)$$

In this case, $\sin \psi_{01}$ is a function of the outside face of the entrance ring diameter.

$$\sin \psi_{01} = \frac{(S_L + b/6)}{S_L} \quad \begin{array}{l} \text{(entrance ring)} \\ \text{(blast section)} \end{array} \quad (7-5)$$

$$\sin \psi_{01} = \frac{(8.0 + 2.167)}{13.0} = 0.782$$

$$D = \frac{17,320}{(0.85 \times 7500 + 0.005 \times 60,000)} = 3.34 \text{ in.}$$

∴ Use $D = 4.00$ in.

From Eq. (6-42), the maximum requirement for tensile steel is

$$\phi_{tL(\max)} = \frac{\left[P_L / \sin \psi_{01} \right] - q_E (6 S_L + D)}{0.01 f_{dy}} \quad (6-46)$$

$$\phi_{tL(\max)} = \frac{17,320}{0.01 f_{dy} \times 0.782} - \frac{325 ((6 \times 13) + 4.0)}{0.01 f_{dy}} = -0.75$$

The negative result indicates that there is no tension in the shell and thus no tensile steel requirement.

(f) Cost Factors for Spherical Shell, Reinforced Concrete

$$C_c = \frac{D}{12} X_c \quad (6-50)$$

$$C_c = \frac{4.0}{12} \times 1.30 = 0.44 \text{ \$/sq ft}$$

Since there is no requirement for tensile steel

$$C_s = \frac{D \phi_t}{1200} X_s \quad (6-51b)$$

$$C_s = \frac{4.0}{1200} \times 1.0 \times 85.8 = 0.29 \text{ \$/sq ft}$$

$$C_f = X_f \quad (6-52)$$

$$C_f = 1.75 \text{ \$/sq ft}$$

Summary

$$C_t = C_c = C_c + C_s + C_f$$

$$C_t = 0.44 + 0.29 + 1.75 = 2.48 \text{ \$/sq ft}$$

Total Cost of Spherical Shell

$$C_T = \pi S_L^2 \cos\left(\frac{\psi_{01} + \psi_{02}}{2}\right) C_t \quad (6-53)$$

where ψ_{02} is determined in Section (g)

$$C_T = 3.14 \times 169 \cos\left(\frac{0.518\pi}{2} \text{ radians}\right) \times 2.48$$

$$C_T = 3.14 \times 169 \times 0.690 \times 2.48 = 908.00\$$$

(g) Design of Exit Ring (No. 2)

Use Eq. (6-73) to estimate design loads on the ring for

$$P_{L1/q} > (3 S_L + D/2) \sin \psi_{01}$$

$$-N_{\max} = \sum q_E (3 S_L + D/2) \left[1 - \frac{\sin^2 \psi_{01}}{\sin^2(\psi' - \psi_{02})} \right] - P_{L1} \left[\frac{\sin \psi_{01}}{\sin^2(\psi' - \psi_{02})} \right] \quad (6-77)$$

where

$$\psi' = 0.500\pi$$

$$\psi_{02} = \sin^{-1} \frac{(S_L + b/6)}{S_L} \quad \begin{array}{l} \text{(exit ring)} \\ \text{(blast sphere)} \end{array} \quad (7-6)$$

Assume $b = 6.0$ in. for exit ring

$$\psi_{02} = \sin^{-1} \frac{(8 + 1)}{13} = 0.24\pi \text{ radians}$$

$$\sin \psi_{01} = 0.782 \quad \text{Eq. (7-5)}$$

$$N_{\max} = -325 (41.0) \left[\frac{1 - 0.610}{\sin^2(0.500 - 0.242)\pi} \right] - 17,320 \left[\frac{0.782}{\sin^2(0.500 - 0.242)\pi} \right]$$

$$-N_{\max} = \left[-325 \times 41.0 \times \frac{0.390}{0.525} \right] - \left[17,320 \times \frac{0.782}{0.525} \right] = -35,720 \text{ lb}$$

Assume $f'_{dc} = 7500$ psi;

Required Exit Ring Area

$$A_{\text{ring}} = \frac{\cos \psi_{02}}{0.85 f'_{dc}} N_{\max} \quad (7-7)$$

$$A_{\text{ring}} = \frac{0.725}{0.85 \times 6375} \times 35,720 = 4.80 \text{ sq in.}$$

The minimum possible area, using a shell with $D = 4.0$ is

$$4.0 \times 4.0 = 16.0 > 4.80 \text{ sq in.}$$

Use a nominal exit ring

$$b = 4.0 \text{ in.}$$

$$D = 4.0 \text{ in.}$$

Revised: $\psi_{02} = \sin^{-1} \frac{(8 + 0.667)}{13.0} = 0.232\pi \text{ radians}$

Note: $(\psi_{02} + \psi_{01}) = (0.232 + 0.286)\pi = 0.518\pi$

This indicates there is some overlap of Rings No. 1 and 2 since the maximum angle possible between the outside edges is 0.500π . However, this overlap is permissible as long as it does not encroach on the inside face of either ring. As previously determined in Section (e), there are no tensile stresses in the shell.

(h) Cost Factors for Exit Ring(No. 2)

$$C_c = \frac{b D}{144} X_c \quad (6-67)$$

$$C_c = \frac{4.0 \times 4.0}{144} \times 1.30 = 0.15 \text{ \$/ft}$$

$$C_s = \frac{\phi_t b D}{14,400} X_s \quad (6-68)$$

$$C_s = \frac{0.5 \times 4.0 \times 4.0}{14,400} \times 85.8 = 0.05 \text{ \$/ft}$$

$$C_{st} = \frac{\phi_{te} b D}{14,400} X_s \quad (6-69)$$

$$C_{st} = \frac{0.2 \times 4.0 \times 4.0}{14,400} \times 85.8 = 0.02 \text{ \$/ft}$$

No torsional steel is required in this case, since the line of action of the membrane thrust can be made to act through the center of shear for the ring.

$$C_f = \frac{b + D}{6} X_f \quad (6-71)$$

$$C_f = \frac{(4.0 + 4.0)}{6} \times 1.00 = 1.33 \text{ \$/ft}$$

Summary

$$C_t = C_c + C_s + C_{st} + C_{ve} + C_f \quad (6-72)$$

$$C_t = 0.15 + 0.05 + 0.02 + 0.00 + 1.33 = 1.55 \text{ \$/ft}$$

(i) Design of Circular Slab for Blast Door Support

A discussion of the assumptions pertinent to the design of this element is found in Section 6.9.4.

$$d = \left[\frac{25.8 S_L}{289 + 0.00572 \phi_v f_{dy}} \right] \left[\frac{f_{dy}}{f'_c} \right]^{1/2} \quad (6-174)$$

where $S_L = 8.0$ ft, we will assume $\phi_v = 2.2$ percent; $f_{dy} = 75,000$ psi and $f'_c = 6000$ psi

$$d = \frac{201.0}{1229} \left(\frac{772 \times 75,000}{6000} \right)^{1/2} = 16.2 \text{ in.}$$

$$D = 16.2 + 1.5 = 17.7 \text{ in.} < \text{depth of entrance ring} \quad \text{OK}$$

$$\phi_c = \left[\frac{289 + 0.00572 \phi_v f_{dy}}{f_{dy}} \right]^2 f'_c \quad (6-173)$$

$$\phi_c = \left(\frac{2108}{75,000} \right)^2 \times 6.00 = 1.61 \text{ percent}$$

To preclude possible pure shear failure,

$$D < \frac{15 q_I S_L}{f'_c}$$

$$D = \frac{15 \times 772 \times 8.0}{6000} = 15.4 \text{ in.} < 18.0 \text{ in.} \quad \text{OK} \quad (7-8)$$

(j) Cost Factors of Circular Slab for Blast Door Support

$$A_{\text{slab}} = \frac{\pi}{4} S_{L(\text{ring})}^2 \cdot \left[L_{S(\text{slab})} \times L_{L(\text{slab})} \right] \quad (6-175)$$

$$A_{\text{slab}} = \frac{\pi}{4} \times 8.0^2 \times 6.5 \times 1.83 = 38.35 \text{ sq ft}$$

IIT RESEARCH INSTITUTE

Concrete

$$C_c = \frac{b D}{144} X_c \quad (6-176)$$

$$C_c = \frac{120 \times 18.0}{144} \times 1.30 = 1.95 \text{ \$/sq ft}$$

Flexural Steel

$$C_s = \frac{\phi_c D}{660} X_s \quad (6-177)$$

$$C_s = \frac{1.61 \times 18.0}{660} \times 85.8 = 3.78 \text{ \$/sq ft}$$

Shear Steel

$$C_v = \frac{\phi_v D}{1200} X_s \quad (6-178)$$

$$C_v = \frac{2.2 \times 18.0}{1200} \times 92.5 = 3.06 \text{ \$/sq ft}$$

Forms

$$C_f = X_f \quad (6-179)$$

$$C_f = 1.75$$

Summary

$$C_t = C_c + C_s + C_v + C_f \quad (6-180)$$

$$C_t = 1.95 + 3.78 + 3.06 + 1.75 = 10.54 \text{ \$/sq ft}$$

$$C_T = C_t A_{\text{slab}} \quad (6-181)$$

$$C_T = 10.54 \times 38.35 = \$405.00$$

(k) Design of Blast Door

Assume that a prestressed concrete door section will be used.

This choice ensures a homogeneous and elastic material, whose thickness will have a marked effect in reducing radiation streaming through the shelter.

From Section 6.7.3, assuming $D = 10.0$ in.

$$S_L/2 = 7.42 \quad L_S = 1.83 \text{ ft} \quad \mu = 0.0354 \quad K_{20} = 0.0111$$

$$\widehat{L}_L = 7.75 \text{ ft} \quad \lambda = L_S/\widehat{L}_L = 0.238 \quad K_{10} = 0.1235 \quad \lambda^2 = 0.0565$$

$$D = \left\{ \left[\frac{864 K_{10} q_I L_S^2 (1 - \lambda^2)^2}{0.45 f'_c + 3 \sqrt{f'_c}} \right] \left[\frac{(1 + \lambda^2)(1 + \nu \lambda^2) + 0.167 \lambda^2 \mu}{[(1 + \lambda^2)^4 + \mu] (1 + \nu \lambda^2)} \right] \right\}^{1/2}$$

IIT RESEARCH INSTITUTE

$$D = \left[\left(\frac{864 \times 0.1235 \times 772 \times 3.34 \times (1.12)}{(0.45 \times 6000) + 234} \right) \left(\frac{(1.112 \times 1.009) + 0.0003}{(1.238 + 0.035) + (1.009)} \right) \right]^{1/2} = 9.04 \text{ in.} \quad (6-119)$$

Use $D = 10.0 \text{ in.}$

Assuming $1/2 \phi 270 \text{ K}$ prestressing strand

$$L_{sp} = \frac{2.70 f'_c D}{F_{sp}} = \frac{2.70 \times 6000 \times 10.0}{23,150} = 7.0 \text{ ft/sq ft}$$

To determine the required percentage of longitudinal steel

$$\phi_{cL} = 17,800 K_{20} \left(\frac{q_I}{f_{dy}} \right) \left(\frac{L_S}{D} \right) \left[1 - \left(\frac{\mu}{(1 + \lambda^2)^4 + \mu} \right) \right] \quad (6-120)$$

$$\phi_{cL} = 17,800 \times 0.0111 \times \frac{772}{60,000} \times \frac{1.82}{10.0} \times \left[1 - \frac{0.0354}{(1 + 0.0316)^4 + 0.0354} \right]$$

$$\phi_{cL} = 0.452 > 0.225 \therefore \text{additional moment steel is required}$$

$$\phi_{cL} = 0.452 + 0.225 = 0.677 \text{ percent}$$

To preclude any possible pure shear failure,

$$D > 30 \frac{q_I L_S}{f'_c} \quad (6-123)$$

$$D = \frac{30 \times 772 \times 1.83}{6000} = 7.05 \text{ in} < 10.0 \text{ in.} \quad \text{OK}$$

(f) Cost Factors for Blast Door

Concrete

$$C_c = \frac{D}{12} X_c \quad (6-124)$$

$$C_c = \frac{10}{12} \times 1.30 = 1.08 \text{ \$/sq ft}$$

Reinforcing Steel

$$C_s = \frac{D \phi_{tL}}{1200} X_s \quad (6-125)$$

$$C_s = \frac{10 \times 0.677}{1200} \times 85.8 = 0.49 \text{ \$/sq ft}$$

Prestressing Steel

$$C_{sp} = L_{sp} X_p \quad (6-126)$$

$$C_{sp} = 7.0 \times 0.19 = 1.33 \text{ \$/sq ft}$$

Forms

$$C_f = X_f \quad (6-127)$$

$$C_f = 1.40 \text{ \$/sq ft}$$

Summary

$$C_t = C_c + C_s + C_{sp} + C_f \quad (6-128)$$

$$C_t = 1.08 + 0.49 + 1.33 + 1.40 = 4.30 \text{ \$/sq ft}$$

Total area of door includes 3.0 in. overhang on all sides

$$(L_S + 0.5) \times (\hat{L}_L + 0.5) = (2.33 \times 8.25) = 19.27 \text{ sq ft}$$

$$C_T = 4.30 \times 19.27 = 83\$$$

(m) Design of Support Structure Hardware for Blast Door

It is assumed that American Standard Channels will be used in supporting the blast door proper. The channel must have a web length between flanges in excess of 10.0 in. Assuming a 15.0 in. channel, the required web thickness is,

Bending

$$t_w = \frac{w}{f_y} \left(\frac{d_w}{2} \right)^2 \quad (6-131)$$

$$t_w = \frac{910}{50,000} \left(\frac{12.375}{2} \right)^2 = 0.695$$

Shear

$$t_w = \frac{w}{7.2 f_y} \quad (6-132)$$

$$t_w = \frac{910}{360,000} \text{ negligible}$$

Use 15 [50.0 with $t_w = 0.75 > 0.695 \therefore$ OK

Total length of channel required

$$4 (L_S + 0.5) + 2 (\hat{L}_L + 0.5) = (4 \times 2.33) + (2 \times 8.25) = 25.82 \text{ ft}$$

IIT RESEARCH INSTITUTE

(n) Cost Factors of Support Structure Hardware for Blast Door

Channels - From Table 2-2

$$X_s = 0.207 \text{ \$/lb for } f_y = 50,000 \text{ psi}$$

$$C_T = 50.0 \times 0.207 \times 25.82 = \$258.00$$

Roller Supports - From Section 2.8.2

$$C_T = 30 n_L D = 30 \times 1 \times 10.0 = \$300$$

Blast Door Latch - From Section 2.8.3

$$C_T = (25.00 + 10 D) n_L^{1/2}$$

$$C_T = (25.00 + 100.00) \times 1 = \$125.00$$

(o) Design of Cylindrical Shell

Radiation sections (R_1) and (R_2) are both located downstream from the blast door. As a consequence, they need only be designed for compressive earth loading. From Section 6.4.1, assuming $D = 3.0$ in.

$$f'_{dc} = 1.18 \left[q_{Ed} \left(\frac{6 S_L + D}{D} \right) - 0.01 \phi_t f_{dy} \right] \quad (6-27)$$

$$f'_{dc} = 1.18 (5200 - 300) = 5780 \text{ psi}$$

Use $f'_{dc} = 6250 > 5780$

(p) Cost Factors for Cylindrical Shell

Cost factors per linear foot of radiation section corridor can be taken from Table 7-5 or calculated in detail as follows:

Concrete

$$C_c = \frac{D}{12} X_c \quad (6-28)$$

$$C_c = \frac{3.0}{12} \times 1.21 = 0.31 \text{ \$/sq ft}$$

Steel

$$C_s = \frac{D \phi_t}{1200} X_s \quad (6-29)$$

Assuming 0.1 percent temperature steel in the longitudinal direction

$$C_s = \frac{3.0 \times 0.6}{1200} 85.8 = 0.13 \text{ \$/sq ft}$$

Forms

$$C_f = X_f \quad (6-30)$$

$$C_f = 1.40 \text{ \$/sq ft}$$

Summary

$$C_t = C_c + C_s + C_f \quad (6-31)$$

$$C_t = 0.31 + 0.13 + 1.40 = 1.84 \text{ \$/sq ft}$$

The cost per foot of corridor is

$$C_T = 1.84 \times 3.14 \times 8.0 = 46.25 \text{ \$/ft}$$

2. Radiation Analysis

The total radiation dose which is received by the shelter population is the cumulative total from the contributing factors outlined in Chapter 5.

(a) Prompt Radiation Overhead Shelter Contribution

Two possible weapon-burst orientations with respect to the shelter are investigated for prompt radiation effects. With respect to overhead contributions, a direct overhead burst results in maximum radiation dose rates. The maximum dosage as regards the entranceway contribution results from a weapon burst in line with the long axis of the entrance opening. Since the two cases cannot occur simultaneously for a single weapon burst, both are investigated to determine the critical condition. While it is possible that some weapon orientation other than the two studied may lead to higher dose rates for a particular case, it is felt that such rates would not differ significantly from the maximum of the two orientations which are studied.

As outlined in Section 5.3.2, use Fig. 5-1 to determine the solid angle fraction for the input parameters as listed for this shelter

Given: $B = 15.0 \text{ ft}$

Therefore: $e = \frac{15.0}{65.0} = 0.231$

$H_p = 65.0 \text{ ft}$

$n = \frac{2Z}{H_p} = \frac{2 \times 7.33}{65.0} = 0.226$

$*Z = 7.33 \text{ ft}$

and $\omega = 0.5 \text{ solid radians}$

* Note: The depth, Z is determined by taking the entrance depth listed in Table 7-2 for the particular shelter under consideration, and then subtracting the earth cover and the height of the detector from the floor (taken as 3.00 ft)

From Fig. 5-2 for overhead burst orientation ($\beta_B = 0$ deg; $\omega = 0.5$)

$$\text{Neutron } R_{f_e} = 0.80$$

$$\text{Gamma } R_{f_e} = 0.95$$

From Fig. 5-2 for entranceway burst orientation ($\beta_B = 50$ deg; $\omega = 0.5$)

$$\text{Neutron } R_{f_e} = 0.64$$

$$\text{Gamma } R_{f_e} = 0.50$$

From Fig. 5-4 for overhead burst orientation ($\beta_S = 90$ deg; $\rho_m = 1000$ psf) (ρ_m is effective mass density of radiation shielding in lb per sq ft)

$$\text{Gamma } R_{f_b} = 0.00005$$

For entranceway burst orientation $\beta_S = 40$ deg; $\rho_m = 1000$ psf)

$$\text{Gamma } R_{f_b} = 0.0000006$$

From Fig. 5-7

For overhead orientation ($\beta_S = 90$ deg; $\rho_m = 1000$ psf)

$$\text{Neutron } R_{f_b} = 0.000004$$

for entranceway orientation ($\beta_S = 40$ deg; $\rho_m = 1000$ psf)

$$\text{Neutron } R_{f_b} = 0.00000065$$

The free-field dose rate from Table 5-1

for overhead orientation ($\beta_B = 0$ deg; $\beta_S = 90$ deg; $W = 1$ MT; $p_{s0} = 200$ psi)

$$\text{Gamma Free-Field} = 1.45 \times 10^5 \text{ rads}$$

$$\text{Neutron Free-Field} = 2.27 \times 10^4 \text{ rads}$$

for entranceway orientation ($\beta_B = 50$ deg; $\beta_S = 40$ deg; $W = 1$ MT, $p_{s0} = 200$ psi)

IIT RESEARCH INSTITUTE

$$\text{Gamma Free-Field} = 4.58 \times 10^5 \text{ rads}$$

$$\text{Neutron Free-Field} = 1.29 \times 10^5 \text{ rads}$$

The prompt radiation dose received in the shelter through the roof can be expressed as follows

$$\begin{array}{lll} \text{(Table 5-1)} & \text{(Fig. 5-2)} & \text{(Fig. 5-4)} \\ \text{Gamma} = \text{free-field dose} \times \text{solid angle } R_{f_e} & \times \text{barrier } R_{f_b} & \\ \text{(Table 5-1)} & \text{(Fig. 5-2)} & \text{(Fig. 5-6)} \\ \text{Neutron} = \text{free-field dose} \times \text{solid angle } R_{f_e} & \times \text{barrier } R_{f_b} & \end{array}$$

for overhead orientation

$$\gamma = 1.45 \times 10^5 \times 0.95 \times 5 \times 10^{-5} = 6.82 \text{ rads}$$

$$N = 2.25 \times 10^4 \times 0.80 \times 4 \times 10^{-6} = 0.08 \text{ rads}$$

for entranceway orientation

$$\gamma = 4.58 \times 10^5 \times 0.50 \times 6 \times 10^{-7} = 0.14 \text{ rads}$$

$$N = 1.29 \times 10^5 \times 0.64 \times 6.5 \times 10^{-7} = 0.06 \text{ rads}$$

(b) Entranceway Contribution

As outlined in Section 5.8, use Eq. (5-5b) or Fig. 5-1 to determine solid angle fraction

- (1) Transition Section: Director No. 1 located at upstream face of blast door 3.0 ft above floor.

Entranceway Orientation

Given:

$$r_m = 3.75 \text{ ft} \quad \beta_z = \tan^{-1} \frac{r_m}{Z} = \tan^{-1} \frac{3.75}{13.0} = 16 \text{ deg}$$

$$Z = 13.0 \text{ ft} \quad \cos \beta_z = 0.953$$

$$\begin{aligned} \omega &= 1 - \cos \beta_z \\ \omega &= 1 - 0.953 = 0.047 \end{aligned} \quad (5-56)$$

Overhead Orientation

$$\begin{array}{ll} \text{Given:} & E_p = 7.5 \text{ ft} \\ & e = \frac{7.5}{10.0} = 0.75 \\ & H_p = 10.0 \text{ ft} \end{array}$$

IIT RESEARCH INSTITUTE

$$Z = 4.5 \text{ ft}$$

$$n = \frac{9.0}{10.0}$$

From Fig. 5-1

$$\omega = 0.32 \text{ solid radians}$$

(2) Blast Section: Detector No. 2 located in center of
blast sphere

Entranceway Orientation

$$r_m = 3.75 \text{ ft}$$

$$Z = 7.0 \text{ ft}$$

$$\beta_z = \tan^{-1} \frac{3.75}{7.0} = 28 \text{ deg}$$

$$\omega = 1.0 - 0.883 = 0.117 \text{ solid radians}$$

Overhead Orientation

Given:

$$r_m = 7.0 \text{ ft} \quad \beta_z = \tan^{-1} \frac{7.0}{4.0} = 80 \text{ deg}$$

$$Z = 4.0 \text{ ft} \quad \cos \beta_z = 0.174$$

$$\therefore \omega = 1.0 - 0.174 = 0.826 \text{ solid radians}$$

(3) Radiation Section (R_1): Detector No. 3 located at down-
stream end 3.0 ft above floor

Entranceway Orientation

Given:

$$r_m = 3.75 \text{ ft} \quad \beta_z = \tan^{-1} \frac{3.75}{22.0} = 10 \text{ deg}$$

$$Z = 22.0 \text{ ft} \quad \cos \beta_z = 0.985$$

$$\therefore \omega = 1.0 - 0.085 = 0.015 \text{ solid radians}$$

Overhead Orientation

Given:

$$B_p = 7.5 \text{ ft} \quad e = \frac{7.5}{15.0} = 0.5$$

$$H_p = 15.0 \text{ ft}$$

$$Z = 4.5 \text{ ft} \quad n = \frac{9.0}{15.0} = 0.60$$

From Fig. 5-1

$$\omega = 0.37 \text{ solid radians}$$

IIT RESEARCH INSTITUTE

(4) Radiation Section (R_2): Detector No. 4 located at downstream

end of radiation section at mouth of shelter 3.0 ft above floor

Entranceway Orientation

Given:

$$r_m = 3.75 \text{ ft} \quad \beta_z = \tan^{-1} \frac{3.75}{15.0} = 14 \text{ deg}$$

$$Z = 15.0 \text{ ft}$$

$$\cos \beta_z = 0.974$$

$$\therefore \omega = 1.0 - 0.974 = 0.026 \text{ solid radians}$$

Overhead Orientation

Same as Radiation Section (R_1), assuming an overhead burst orientation.

Detector No. 1

Entranceway Contribution ($\omega = 0.047$; $\beta_z = 50 \text{ deg}$)

(Table 5-1) (Fig. 5-2)

Gamma = free-field dose x solid angle R_{fe}

(Table 5-1) (Fig. 5-2)

Neutron = free-field dose x solid angle R_{fe}

$$\gamma = 1.45 \times 10^5 \times 0.06 = 8.7 \times 10^3 \text{ rads}$$

$$N = 2.27 \times 10^4 \times 0.10 = 2.27 \times 10^3 \text{ rads}$$

Overhead Contribution ($\omega = 0.32$; $\rho_m = 550 \text{ psf}$; $\beta_B = 0 \text{ deg}$; $\beta_S = 90 \text{ deg}$)

(Table 5-1) (Fig. 5-2) (Fig. 5-4)

Gamma = free-field dose x solid angle R_{fe} x earth barrier R_{fb}

(Table 5-1) (Fig. 5-2) (Fig. 5-7)

Neutron = free-field dose x solid angle R_{fe} x earth barrier R_{fb}

$$\gamma = 1.45 \times 10^5 \times 0.82 \times 0.005 = 5.95 \times 10^2 \text{ rads}$$

$$N = 2.27 \times 10^4 \times 0.67 \times 0.0011 = 1.68 \times 10 \text{ rads}$$

Total at Detector No. 1

$$\gamma = 8.7 \times 10^3 + 0.6 \times 10^3 = 9.3 \times 10^3 \text{ rads}$$

$$N = 2.27 \times 10^3 + 0.02 \times 10^3 = 2.29 \times 10^3 \text{ rads}$$

At Detector No. 2, recognizing that the radiation stream must pass through 10.0 in. concrete blast door

Entranceway Contribution ($\omega = 0.177$; $\rho_m = 12.5 \text{ psf}$; $\beta_B = 0 \text{ deg}$; $\beta_S = 90 \text{ deg}$)

Gamma = Detector No. 1 dose x solid angle R_{fe} x blast door barrier R_{fb}

Neutron = Detector No. 1 dose x solid angle R_{fe} x blast door barrier R_{fb}

$$\gamma = 9.3 \times 10^3 \times 0.68 \times 0.32 = 2.02 \times 10^3 \text{ rads}$$

$$N = 2.29 \times 10^3 \times 0.40 \times 0.30 = 2.75 \times 10^2 \text{ rads}$$

Overhead Contribution ($\gamma = 0.826$; $\rho_m = 975 \text{ psf}$; $\beta_B = 0 \text{ deg}$; $\beta_S = 90 \text{ deg}$)

Gamma = free-field dose x solid angle R_{fe} x earth barrier R_{fb}

Neutron = free-field dose x solid angle R_{fe} x earth barrier R_{fb}

$$\gamma = 1.45 \times 10^5 \times 0.98 \times 0.000066 = 0.01 \times 10^3$$

$$N = 2.27 \times 10^4 \times 0.04 \times 0.000054 = 0.001 \times 10^2$$

Total at Detector No. 2

$$\gamma = 2.02 \times 10^3 + 0.01 \times 10^3 = 2.03 \times 10^3$$

$$N = 2.75 \times 10^2$$

Detector No. 3

Entranceway Contribution ($\omega = 0.015$; $\beta_B = 0 \text{ deg}$)

The modified solid angle fraction due to corridor bends can be determined from Section 5.5.2

$$R_{f_{cl}} = 0.1 \omega_1 = \omega' \quad (5-12)$$

$$R_{f_{cl}} = 0.1 \times 0.015 = 0.0015$$

The entranceway wall attenuation of neutron flux is discussed in Section 5.5.2.

$$L_{1/2} = \frac{1}{2} K (H + B) \quad (5-9)$$

$$L_{1/2} = \frac{1}{2} 0.733 (7.5 + 7.5) = 5.5 \text{ ft}$$

$$n_{1/2} = \frac{L}{L_{1/2}} \quad (5-10)$$

$$n_{1/2} = \frac{15.0}{5.5} = 2.73$$

the reduction factor is expressed

$$R_{f_w} = \frac{1}{2^{n_{1/2}}} \quad (5-11)$$

$$R_{f_w} = \frac{1}{2^{2.73}} = 0.15$$

IIT RESEARCH INSTITUTE

Gamma = Detector No. 2 dose x solid angle R_{fe} ($\omega' = 0.0015$)

Neutron = Detector No. 2 dose x solid angle R_{fe} x wall attenuation R_{fw} ($\omega' = 0.0015$)

$$\gamma = 2.03 \times 10^3 \times 0.125 = 2.54 \times 10^2 \text{ rads}$$

$$N = 2.75 \times 10^2 \times 0.14 \times 0.15 = 5.78 \text{ rads}$$

Overhead Contribution ($\omega = 0.37$; $\rho_m = 1150$ psf; $\beta_B = 0$ deg; $\beta_S = 90$ deg)

Gamma = free-field dose x solid angle R_{fe} x earth barrier R_{fb}

Neutron = free-field dose x solid angle R_{fe} x earth barrier R_{fb}

$$\gamma = 1.45 \times 10^5 \times 0.88 \times 0.000011 = 1.40 \text{ rads}$$

$$N = 2.27 \times 10^4 = 0.71 \times 0.0000006 = \text{negligible}$$

Total at Detector No. 3

$$\gamma = 254 + 1.4 = 255.4 \text{ rads}$$

$$N = 5.78 \text{ rads}$$

Detector No. 4

Entranceway Contribution ($\omega = 0.026$; $\beta_B = 0$ deg)

$$R_{fc_2} = 0.5 \omega$$

(5-13)

$$R_{fc_2} = 0.5 \times 0.026 = 0.013$$

Gamma = Detector No. 3 dose x solid angle R_{fe}

Neutron = Detector No. 3 dose x solid angle R_{fe} x wall attenuation R_{fb}

$$\gamma = 255.4 \times 0.335 = 90.6 \text{ rads}$$

$$N = 5.78 \times 0.19 \times 0.15 = \underline{0.17 \text{ rads}}$$

$$\text{Total} \quad 90.8 \text{ rads}$$

Assuming an entranceway orientation of burst

Entranceway Contribution ($\omega = 0.047$; $\beta_B = 0$ deg)

Gamma = free-field dose x solid angle R_{fe}

Neutron = free-field dose x solid angle R_{fe}

$$\gamma = 4.58 \times 10^5 \times 0.55 = 2.55 \times 10^5 \text{ rads}$$

$$N = 1.29 \times 10^5 \times 0.27 = 3.48 \times 10^4 \text{ rads}$$

Overhead Contribution ($\omega = 0.32$; $\rho_m = 550 \text{ psf}$; $\beta_B = 50 \text{ deg}$; $\beta_S = 40 \text{ deg}$)

Gamma = free-field dose x solid angle R_{f_e} x earth barrier R_{f_b}

Neutron = free-field dose x solid angle R_{f_e} x earth barrier R_{f_b}

$$\gamma = 4.58 \times 10^5 \times 0.28 \times 0.00015 = 1.9 \times 10^4 \text{ rads}$$

$$N = 1.29 \times 10^5 \times 0.41 \times 0.00045 = 2.4 \times 10^4 \text{ rads}$$

The reduction factors for Detectors 2, 3 and 4 for the entranceway contribution are the same as for the overhead orientation case. The final radiation dose which is "seen" by Detector No. 4 for the overhead case can thus be determined from the ratios of the dose rates at Detector No. 1 for both cases, if the overhead contribution for the overhead orientation is disregarded.

At Detector No. 4

$$\gamma = \frac{2.55 \times 10^5}{0.93 \times 10^4} \times 90.6 = 2480 \text{ rads}$$

$$N = \frac{3.48 \times 10^4}{0.23 \times 10^4} \times 0.17 = 2.5 \text{ rads}$$

(c) Fallout Radiation

As in the case of prompt radiation, fallout radiation is received both from overhead sources and by streaming through the entranceway structure. As discussed in Chapter 5, the cumulative fallout radiation for the cases considered in this study, assuming a two week stay period as discussed in Chapter 5, can be taken as a constant 86,000 rads of gamma radiation. This is considered to be independent of weapon size or burst orientation.

The overhead contribution is determined from the solid angle fraction found in Fig. 5-1 together with Fig. 5-8, Case I, and Fig. 5-5, Case I.

Given:

$$B_p = 15.0 \text{ ft}$$

$$H_p = 65.0 \text{ ft}$$

$$Z = 7.33 \text{ ft}$$

Where:

$$e = \frac{B_p}{H_p} = \frac{15.0}{65.0} = 0.231$$

$$n = \frac{2Z}{H_p} = \frac{2 \times 7.33}{65.0} = 0.226$$

$$\therefore \omega = 0.5 \text{ solid radians}$$

From Fig. 5-8 ($\omega = 0.5$; Case I) and Fig. 5-5 ($\rho_m = 1000 \text{ psf}$; Case I)

$$\text{Solid angle } R_{f_e} = 0.125 \text{ and barrier shield } R_{f_b} \approx 2 \times 10^{-10}$$

Dose received in shelter from overhead fallout

$$\text{Fallout } \gamma = \text{free-field dose} \times \text{solid angle } R_{f_e} \times \text{barrier } R_{f_b}$$

$$\text{Fallout } \gamma = 8.6 \times 10^4 \times 0.125 \times 2 \times 10^{-10} = \text{negligible}$$

The entranceway contribution is based on the assumption that the free-field dose exists in the Transition Section immediately adjacent to the blast door. The fallout dosage "seen" by the detector in the blast section sphere is determined from Fig. 5-1, together with Fig. 5-8 and 5-5 for Case II. Propagation of the fallout radiation field beyond this detector and toward the shelter proper is assumed to take place in the same manner as for the prompt radiation.

From Part B (b) 2)

$$\omega = 0.117; \rho_m = 125 \text{ psf}$$

Dose received at Detector No. 2 in center of the blast sphere

From Fig. 5-8 Case II and Fig. 5-5, Case II

$$\text{Solid Angle } R_{f_e} = 0.127; \text{ barrier } R_{f_b} = 0.047$$

$$\text{Fallout } \gamma = 8.6 \times 10^4 \times 0.127 \times 0.047 = 514 \text{ rads}$$

The gamma dose at Detector No. 2 due to prompt radiation for the entranceway orientation case

$$2.55 \times 10^5 \times 0.68 \times 0.32 = 5.5 \times 10^4 \text{ rads}$$

The increase in total gamma dosage "seen" at Detector No. 4 in the shelter due to the addition of fallout radiation is in the proportion:

IIT RESEARCH INSTITUTE

$$\frac{0.0514 \times 10^4}{15.5 \times 10^4} = 0.00935$$

$$\text{Fallout } \gamma = 2480 \times 0.00935 = 23.0 \text{ rads}$$

Total Radiation Dose at Entrance of Shelter Proper

Prompt γ = 2480	Prompt N = 4.5 rads
Fallout γ = 23	
<hr style="width: 10%; margin: 0 auto;"/>	
Total	2503 rads

(d) Radiation Barrier Shielding Design

The worst-case radiation dosage for this example is in excess of the recommended dose rate of 40 rads total.²⁴ Reduction in the dosage through the entranceway structure can be effected by increasing the number and/or lengths of Radiation Sections or by placing barrier shielding at the entrance to the shelter proper. In general, the construction of barrier shielding is the simplest and less costly alternative.

Worst-case gamma dosage at entrance to shelter proper = 2503 rads

Radiation dosage through roof of shelter for this case = 0.2 rads

Allowable dosage through entranceway for this case = 40.0 - 0.2 = 39.8 rads

$$\text{Required } R_{fb} = \frac{39.8}{2503} = 0.0153$$

From Fig. 5-4 ($R_{fb} = 0.0153$, $\beta_S = 90$ deg)

$$p_m = 440 \text{ psf}$$

Assuming a reinforced concrete wall

$$\text{Required } D = \frac{440}{12.5} = 35.5 \text{ in.}$$

Use $D = 36.0$ in.

The barrier can be placed in the last radiation leg of the entranceway by flaring the section, or it can be placed in the shelter proper. In this instance, we will assume that the entranceway is flared and the radiation barrier shielding is placed in Radiation Section (R_2). The total area of barrier wall is now determined.

$$A = 2 \times 1/2 \times \pi \times 4.25^2 = 57.0 \text{ sq ft}$$

IIT RESEARCH INSTITUTE

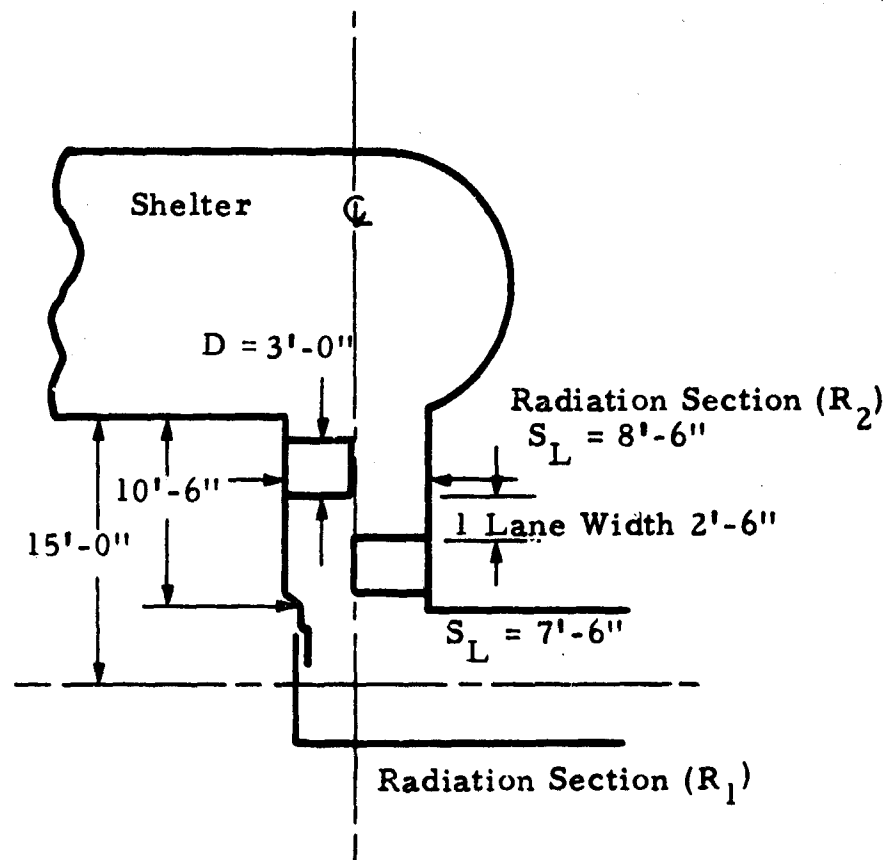


Fig. 7-10 PLAN VIEW OF RADIATION BARRIER SHIELD

(e) Radiation Barrier Shielding Cost Factor

Assuming $f'_c = 2000$ psi

Concrete
$$C_t = \frac{D}{12} X_c$$

$$C_c = \frac{36.0}{12} \times 1.00 = 3.00 \text{ \$/sq ft}$$

Steel

$$C_s = \frac{D \phi_t}{1200} X_s$$

$$C_s = \frac{36.0 \times 0.5 \times 78.8}{1200} = 1.18 \text{ \$/sq ft}$$

Forms

$$C_f = \frac{2 (A + 0.0833 D S_L)}{A} X_f$$

$$C_f = \frac{2 \times (57.0 + 3.0 \times 8.5)}{57.0} \times 1.00 = 2.90 \text{ \$/sq ft}$$

$$C_t = C_c + C_s + C_f = 3.00 + 1.18 + 2.90 = 7.08 \text{ \$/sq ft}$$

$$C_t = 7.08 \times 57.0 = 404N$$

It is apparent that either an increased number of radiation sections or the use of a radiation shield in the shelter proper will lead to considerably greater costs.

3. Total Cost

The cost factors for all structural elements developed on a blast resistance basis are given in 1. The total cost contribution as a result of radiation analyses is given in 2. There remains only the determination of excavation and open cut stair costs to develop the total entranceway cost factor.

(a) Excavation and Backfill

Whenever possible, the excavation required for the shelter proper will be utilized in construction of the entranceway. Assuming a 1:1 slope cut,

Average depth of Radiation Section (R_2) = 10.5 ft

$$\text{Volume} = \frac{z}{2} (A_1 + A_2) \quad (7-8)$$

where:

z = average depth of excavation

A_1 = gross area at bottom of excavation, $L_T \times B_T$,
where L_T = total length of entranceway section
in ft and B_T = total width of entranceway section in ft

A_2 = gross area determined by the intersection of
slope with existing ground surface, usually

$$A_2 = (L_T + 2z) \times (B_T + 2z)$$

From Fig. 7-1 and Table 7-2

Depth of existing excavation at side of shelter ≈ 21.0 ft

Existing depth of excavation 15.0 ft from side of shelter = 6.0 ft

Radiation Section (R_2)

Average depth of Radiation Section (R_2) = 10.5 ft

$$z = \frac{(19.5 - 21.0) + (19.5 - 6.0)}{2} = 6.0 \text{ ft}$$

$$\text{Vol} = \frac{6.0}{2} (15.0 \times 9.0) + (21.0 \times 21.0) = 1728 \text{ cu ft}$$

Radiation Section (R_1)

Depth of excavation, downstream end = 19.0 ft

Depth of excavation, upstream end = 6.0 ft

Average depth of Radiation Section (R_1) = 18.5 ft

$$z = \frac{(18.5 - 19.0) + (18.5 - 6.0)}{2} = 6.0 \text{ ft}$$

$$\text{Vol} = \frac{6.0}{2} (15.0 \times 8.0) + (21.0 \times 14.0) = 1242 \text{ cu ft}$$

Blast Section

Average depth of excavation = 12.0 ft

Average depth of Blast Section = 21.0 ft

$$z = (21.0 - 12.0) = 9.0 \text{ ft}$$

$$\text{Vol} = \frac{9.0}{2} (15.0 \times 15.0) + (24.0 \times 24.0) = 3600 \text{ cu ft}$$

Transition Section

Depth of excavation downstream end = 21.0 ft

Depth of excavation upstream end = 9.0 ft

$$z = \frac{(10 - 21.0) + (10 - 9.0)}{2} = -5.0 \therefore \text{fill required}$$

$$\text{Vol (of fill)} = \frac{5}{2} (9.0 \times 10.0) = 225 \text{ ft}$$

Entranceway Open Cut

Depth of excavation, downstream end = 9.0 ft

Depth of excavation, upstream end = 1.0 ft

Average depth of cut \simeq 3.0 ft

$$z = \frac{(3.0 - 9.0) + (3.0 - 1.0)}{2} = -2.0 \text{ ft}$$

$$\text{Vol (of fill)} = \frac{2}{2} (2.5 \times 6.5) = 16 \text{ cu ft}$$

Entrance Structure Volume

$$\text{Radiation Section } (R_1) = \pi \times 4.0^2 \times 15.0 = 755 \text{ cu ft}$$

$$\text{Radiation Section } (R_2) = \pi \times 4.0^2 \times 4.5 = 226 \text{ cu ft}$$

$$\text{Blast Section} = \frac{4}{3} \times \pi \times 7.0^3 = 1440 \text{ cu ft}$$

$$\text{Transition Section} = \pi \times 4.58^2 \times 13.3 = 896 \text{ cu ft}$$

$$\text{Open Cut } \frac{1}{4} \times (27.5 + 2.5) \times 6.0 = 50 \text{ cu ft}$$

Total	4002 cu ft
-------	------------

Total Volume of Excavation

$$\text{Radiation Section } (R_2) = 1728$$

$$\text{Radiation Section } (R_1) = 1242$$

$$\text{Blast Section} = 3600$$

$$\text{Transition Section} = -255$$

$$\text{Open Cut} = -16$$

Total	6699 cu ft
-------	------------

$$\text{Total Volume of Backfill} \quad 6699 - 4002 = 2697 \text{ cu ft}$$

(b) Open Cut Section

Slope surface area will require stabilization, assuming a 2:1 slope

$$8.5 \times 13.5 \times 1/2 \times 2 = 115.0 \text{ sq ft}$$

Assume slope stabilization consisting of 3 in. concrete slab or equivalent

$$C_f = 0.75 \text{ \$/sq ft}$$

$$C_T = 0.75 \times 115.0 = 87\$$$

Stair Costs from Section 2.2.9

$$C_T = 9 \text{ steps at } 18.00 \text{ \$/step} = 162\$$$

(c) Emergency Exit

The 100-man shelter serviced by a blast-resistant entranceway requires one emergency exit. From Table 7-2 the required length of emergency exit is assumed equal to the depth to entrance level. Unit cost from Section 2.8.4

$$C_T = \$4.00 \times 20.33 = 285\$$$

Total Cost

Open Cut Section

Side Slope Stabilization	0.75 x 115	= 87
Stairs	18.00 x 9	= 162

Transition Section

Prestressed Concrete Cylindrical Shell		
4.49 x 8.66 x π x 13.0		= 1590
Structural Steel Blast Exclusion Ring		
2.84 x 8.66 x π x 2.5		= 193
Stairs	18.00 x 13	= 236

Blast Section

Reinforced Concrete Spherical Shell		= 908
Reinforced Concrete Entrance Ring	10.58 x 8.5 x π	= 282
Reinforced Concrete Exit Ring	1.55 x 8.16 x π	= 40
Reinforced Concrete Blast Door Support Slab		= 405
Prestressed Concrete Door		= 83
Blast Door Support Channels		= 258
Blast Door Support Rollers		= 300
Blast Door Latch		= 125
Stairs	18.00 x 6	= 108

Radiation Section

Reinforced Concrete Cylindrical Shell	46.25 x 19.5	= 907
	1.86 x 9.0 x π x 10.5	= 552
Radiation Barrier Wall		404
Emergency Exit		285
Excavation	0.036 x 6699	242
Backfill	0.033 x 2697	90
Haul	0.026 x 3951	103

Total \$ 7360

7.4.2 Tension Cylinder (Sample Analysis and Cost Evaluation)

TRIAL DESIGN 7.4.2-200 B1

CONFIGURATION

One story cylinder (Fig. 7-11)

STRUCTURAL SYSTEM AND INPUT PARAMETERS

Reference Fig. 7-2

Transition Section -

Material: Prestressed concrete cylinder

Orientation: Makes ~ 39 deg angle with horizontal plane and is perpendicular to the long axis of the shelter

Dimension: I. D. 7 ft-6 in. ; length 13 ft-0 in. ; change in elevation between entrance and exit 8 ft-3 1/2 in.

Primary Design Loads: $q_I = 480$ psi; $q_{Ed} = 200$ psi

Blast Section -

Material: Prestressed concrete cylinder

Orientation: Horizontal; perpendicular to long axis of shelter

Dimension: I. D. 7 ft-6 in. ; overall length 18 ft-0 in. ; length of concrete shell 14 ft-9 in.

Primary Design Loads: $q_I = 480$ psi; $q_{Ed} = 200$ psi

Radiation Section (R_1) -

Material: Reinforced concrete cylinder

Orientation: \sim Horizontal; parallel to long axis of shelter

Dimension: I. D. 7 ft-6 in. ; length 15 ft-0 in. ; change in elevation 1 ft-6 in.

Primary Design Load: $q_{Ed} = 200$ psi

Radiation Section (R_2) -

Material: Reinforced concrete cylinder

Orientation: \sim Horizontal; perpendicular to long axis of shelter

Dimension: I. D. 7 ft-6 in. ; length 15 ft-0 in. ; change in elevation 1 ft-6 in.

Primary Design Load: $q_{Ed} = 200$ psi

Note: These dimensions may require subsequent modification due to radiation design requirements.

Shelter -

Capacity: 100 Man (Table 7-2)

Primary Design Load: $q_{Ed} = 200$ psi

1. Blast Analysis

(a) Transition and Blast Section:

Design of cylindrical shell, prestressed concrete

Shell Design

Assume $D = 4.5$ in. ; $f'_c = 6000$ psi

$$\frac{6 S_L}{D} = \frac{45.0}{4.5} = 10.0 = 10.0$$

Use thin-wall analysis as outlined in Sections 6.4.2 and 6.3. From Eq. (6-32)

$$q_{Ep(max)} = 0.45 f'_c \left(\frac{D}{6 S_L + D} \right) - q_{Es} \quad (6-32)$$

Taking $q_{Es} \sim 0$

$$q_{Ep(max)} \leq 0.450 \times 6000 \times \frac{4.5}{49.5} = 245 \text{ psi}$$

From Eq. (6-33) required

$$q_{Ep(min)} = \frac{q_I S_L - 0.5 D \sqrt{f'_c}}{S_L + D/6} - q_{Es} - q_{Ed} \quad (6-33)$$

$$q_{Ep} = \frac{(480 \times 7.5) - (2.25 \times 78)}{8.25} - 200 = 210 \text{ psi}$$

From Eq. (6-34), required

$$q_{Ep(max)} = 0.85 f'_c \left(\frac{D}{6 S_L + D} \right) - q_{Es} - q_{Ed} \quad (6-34)$$

$$q_{Ep(max)} = 0.85 \times 6000 \times \frac{4.5}{49.5} - 200 = 264 \text{ psi}$$

$$210 \leq 245 \leq 264 \therefore \text{OK}$$

\therefore Use $D = 4.5$ in.

As a result of this analysis, a range of values $210 < q_{Ep} < 245$ is seen to be adequate for design. The upper limit of $q_{Ep} = 245$ psi will be used as the design parameter, since this will tend to reduce the tensile stresses in the shell during interior blast loading.

The effective prestress force can be expressed as

$$T_{sp} = (45.0 + 4.5) 245 = 12,120 \text{ lb/in.} \quad (6-16)$$

Assuming a 1/2 in. ϕ K 270 prestressing steel strand from Table 2-7

$$F_{sp} = 23,150 \text{ lb/strand}$$

$$L_{sp} = \frac{12 \times 12,120}{23,150} = 6.28 \text{ ft/sq ft of shell} \quad (6-18)$$

The resulting pitch between wraps of prestress strand is

$$p_t = 12.0/6.28 = 1.91 \text{ in.}$$

(b) Transition-Blast Section:

Cost factors for cylindrical shell, prestressed concrete

Concrete

$$C_c = \frac{4.5}{12} \times 1.30 = 0.49 \text{ \$/sq ft} \quad (6-19)$$

Reinforcing Steel

$$C_s = \frac{4.5 \times 0.6}{1200} \times 85.8 = 0.24 \text{ \$/sq ft} \quad (6-20)$$

Prestressing Steel

$$C_{sp} = 6.28 \times 0.19 = 1.19 \text{ \$/sq ft} \quad (6-21)$$

Forms

$$C_f = 1.40 \text{ \$/sq ft} \quad (6-22)$$

Protective Covering

$$C_g = 0.30 \text{ \$/sq ft} \quad (6-23)$$

Summary

$$C_t = 0.49 + 0.24 + 1.19 + 1.40 + 0.30 = 3.62 \text{ \$/sq ft} \quad (6-24)$$

(c) Transition-Blast Section: Design of Elbow

In order to fit the Transition and Blast Sections as a continuous element, the top portions of both sections in the bend must be shorter than the bottom portions. To maintain a continuous wrap of prestress strand under uniform tension, it is necessary to reduce the pitch between wraps at the top of the shells. By so doing, these portions of the shells will be subjected to higher prestressing loads. In addition, since these bends are in the form of reentrant corners, a reinforced blast wave can be expected to form at this section.

Transition Section:

Take length of top bend = 2 ft-6 in. Then, from Fig. 7-11, the equivalent length of bottom bend = 5 ft-6 in.

Revised pitch is then

$$p_t = \frac{1.91}{\frac{5.5}{2.5}} = 0.870 \text{ in./in.}$$

and

$$T_{sp} = \frac{23,150}{0.870} = 26,800 \text{ lb/in.}$$

Since

$$T_{sp} = (6 S_L + D) q_{Ep} \quad (6-16)$$

Taking $D' = 12.0$ in at the top of bend, the average D over the section is

$$\left(\frac{12.0 + 4.5}{2} \right) = 8.25 \text{ in.}$$

and

$$q_{Ep} = \frac{T_{sp}}{(6S_L + D)} = \frac{26,800}{45.0 + 8.25} = 503 \text{ psi}$$

From Section 6.3.1, Eq. (6-15)

$$q_{Ep} \leq 0.225 \times 6000 \left[1 - \left(\frac{7.5}{9.50} \right)^2 \right] = 508 \text{ psi} \quad (6-15)$$

$$503 \leq 508 \therefore \text{OK}$$

From Eq. (6-17)

$$q_{Ep} \leq 0.85 \times 6000 \left(\frac{9.52 - 7.52}{9.52 + 7.52} \right) - 200 \leq 985 \text{ psi} \quad (6-17)$$

$$503 < 985 \therefore \text{OK}$$

Blast Section:

The same proportions hold for the blast section.

\therefore Use $D' = 12.0$ in. and length of top bend = 2 ft-6 in.

(d) Transition-Blast Section: Cost Factors for Elbow Section

Trial cost designs indicate that the cost of a straight cylinder section and bend is approximately the same as the straight section alone if the long or bottom length dimension is used in computing total cost. For this reason, the cost of the bend section is included in the cost factor determined in (b) of this example.

The Blast Section consists of a prestressed concrete horizontal cylinder with a crushable mild steel shield enclosing the downstream end. The blast door is supported by tension rings which are poured monolithically with the side of the cylinder.

(e) Blast Section: Design of Tension Ring; Prestressed Concrete

From Section 6.9.3

Assume prestressed concrete ring 14.0 in. x 15.0 in. in cross section

$$\text{Required } D = \frac{36 q_I S_{L \text{ ring}} (L_S + b/6)}{(0.45 f'_c + 3\sqrt{f'_c}) b} \quad (6-155)$$

$$D = \frac{36 \times 480 \times 8.75 \times 4.33}{(0.45 \times 6000 + 234) \times 1.50} = 14.65 \text{ in.} < 15.00 \therefore \text{OK}$$

$$L_{sp} = \frac{b T_{sp}}{F_{sp}} \quad (6-141)$$

$$L_{sp} = \frac{15.0 \times 0.45 \times 6000 \times 15.0}{23,150} = 26.30 \text{ strands}$$

Use 27 strands.

(f) Blast Section: Cost factors for Tension Ring

Concrete

$$C_c = \frac{15.0 \times 15.0}{144} \times 1.30 = 2.04 \text{ \$/ft} \quad (6-157)$$

Prestress Steel

$$C_{sp} = 27 \times 0.19 = 5.13 \text{ \$/ft} \quad (6-162)$$

Forms

$$C_f = \left(\frac{15.0 + 15.0}{6} \right) \times 1.00 = 5.00 \text{ \$/ft} \quad (6-159)$$

Summary

$$C_t = 2.04 + 5.13 + 5.00 = 12.17 \text{ \$/ft} \quad (6-163)$$

(g) Blast Section: Design of Beam Member Between Rings

Assume reinforced concrete beams with $b = 8.0 \text{ in.}$; $D = 10.0 \text{ in.}$;

$$\phi_v = 0.0 \text{ percent}$$

required

$$d = \left[\frac{36.5 L_S}{1045 + 0.0209 \phi_v f_{dy}} \right] \left[\frac{6 (q_I - q_{Es} - q_{Ed}) S_L f_{dy}}{f'_c} \right]^{1/2} \quad (6-165b)$$

$$d = \left[\frac{36.5 \times 1.83}{1045} \right] \left[\frac{6 \times (480 - 200) \times 7.5 \times 75,000}{8.0 \times 6000} \right]^{1/2} = 8.85 \text{ in.}$$

$$D = \frac{d}{0.9} = 9.85 \text{ in.}; 10.0 \text{ in.} \therefore \text{OK}$$

$$\phi_c = \left[\frac{1045 + 0.0209 \phi_v f_{dy}}{f'_c} \right]^2 \quad (6-135)$$

$$\phi_c = \left[\frac{1045}{75,000} \right]^2 \times 6000 = 1.40 \text{ percent}$$

(h) Blast Section: Cost Factors for Beam Member Between Rings

Concrete

$$C_c = \frac{8.0 \times 10.0}{144} \times 1.30 = 0.73 \text{ \$/ft} \quad (6-167)$$

Steel

$$C_s = \frac{1.40 \times 8.0 \times 10.0}{10,650} \times 85.8 = 0.91 \text{ \$/ft} \quad (6-168)$$

Forms

$$C_f = \left(\frac{8.0 + 10.0}{6} \right) 1.00 = 3.00 \text{ \$/ft} \quad (6-170)$$

Summary

$$C_t = 0.73 + 0.91 + 3.00 = 4.62 \text{ \$/ft} \quad (6-171)$$

(i) Blast Section: Design of Blast Door

The blast door is designed as a prestressed concrete shell segment. Assuming $D = 7.0$ in. results in

$$S_L/2 = 3.50 \text{ ft} \quad L = 1.83 \text{ ft} \quad \mu = 0.435 \quad K_{20} = 0.0090$$

$$\widehat{L}_L = 8.24 \text{ ft} \quad \lambda = L_S/\widehat{L}_L = 0.222 \quad K_{10} = 0.1242 \quad \lambda^2 = 0.0493$$

$$D = \left[\frac{864 \times 0.1242 \times 480 \times 1.10}{(0.45 \times 6000) + 234} \left(\frac{1.11}{1.65} \right) \right]^{1/2} = 6.55 \text{ in.} \quad (6-119)$$

$$D = 6.55 < 7.0 \therefore \text{OK}$$

From Section 6.7.3 assuming 1/2 ϕ 270 K prestressing strand

$$L_{sp} = \frac{2.70 f'_c D}{F_{sp}} = \frac{2.70 \times 6000 \times 7.0}{23,150} = 4.9 \text{ \$/sq ft}$$

To determine the required percentage of longitudinal steel

$$\phi_{cL} = 17,800 K_{20} \frac{q_I}{f_{dy}} \frac{L_S}{D} \left[1 - \frac{\mu}{(1 + \lambda^2)^4 + \mu} \right] \quad (6-120)$$

$$\phi_{cL} = 17,800 \times 0.0090 \times \frac{480 \times 1.83}{60,000 \times 7.0} \left(1 - \frac{0.435}{1.647} \right) = 0.244$$

$$\phi_{cL} = 0.244 > 0.225 \therefore \text{additional moment steel is required}$$

$$\phi_t = 0.244 + 0.225 = 0.469 \text{ percent}$$

Check for pure shear failure

$$D \geq \frac{30 q_I L_S}{f'_c} \quad (6-123)$$

$$D = \frac{30 \times 480 \times 1.83}{6000} = 4.40 < 7.0 \text{ in.} \therefore \text{OK}$$

(j) Blast Section: Cost Factors for Blast Door

Concrete

$$C_c = \frac{7.0}{12} \times 1.30 = 0.76 \text{ \$/sq ft} \quad (6-124)$$

Reinforcing Steel

$$C_s = \frac{7.0 \times 0.469 \times 85.8}{1200} = 0.24 \text{ \$/sq ft} \quad (6-125)$$

Prestressing Steel

$$C_{sp} = 4.9 \times 0.19 = 0.93 \text{ \$/sq ft} \quad (6-126)$$

Forms

$$C_f = 1.40 \text{ \$/sq ft} \quad (6-127)$$

Summary

$$C_t = 0.76 + 0.24 + 0.93 + 1.40 = 3.33 \text{ \$/sq ft} \quad (6-128)$$

Total area of door includes 3.0 in overlap on all sides

$$(L_S + 0.5) \times (\widehat{L}_L + 0.5) = (2.33 \times 8.74) = 20.40 \text{ sq ft} \quad (6-128)$$

$$C_T = 3.33 \times 20.40 = 68$$

IIT RESEARCH INSTITUTE

(k) Blast Section: Design of Support Structure Hardware for Blast Door

It is assumed that American Standard Channels will be used to support the blast door. A web length between flanges in excess of 7.0 in. is required. Try 9 in. channel

bending

$$t_w = \frac{765}{42,000} \frac{7.25^2}{2} = 0.239 \quad (6-131)$$

Use 9 [13.4

$$0.239 < 0.250 \therefore \text{OK}$$

Total length of channel required

$$4 (L_S + 0.5) + 2 (\widehat{L}_L + 0.5) = (4 \times 2.33) + (2 \times 8.74) = 26.80 \text{ ft}$$

(l) Blast Section: Cost Factors for Support Structure Hardware of Blast Door

(1) Channels

From Table 2-2, $X_s = 0.204$ \$/lb for $f_y = 42,000$ psi

$$C_T = 13.4 \times 0.204 \times 26.80 = 74 \$$$

(2) Roller Supports

From Section 2.8.2

$$C_T = 30 n_L \quad D = 30 \times 1 \times 7 = 210.00 \$$$

(3) Blast Door Latch

From Section 2.8.3

$$C_T = (25.00 + 10D) n_L^{1/2} = 25.00 + 70.00 = 95.00 \$$$

(m) Blast Section: Design and Cost Factors for Structural Steel Dome End

The dome end on the end of the blast cylinder serves as a crushable shield which can be driven into the earth by the blast wave in the section. It will thus be absorbing energy from the wave, while still having adequate flexibility to resist the subsequent earth pressure load without fracture.

Assume $f_{dy} = 60,000$ psi

$$f_{dy} t = 3 q_1 S_L$$

$$t = \frac{582 \times 22.5}{60,000} = \frac{13,100}{60,000} = 0.218 < 0.25$$

∴ Use 1/4 plate

From Table 2-3

$$C_t = X_s = 3.53 \text{ \$/sq ft}$$

(n) Blast Section : Design and Cost Factors for Structural Steel
Dome Support Ring

The lightest available wide flange shape which will allow a 1 ft-6 in. rattlespace is a 12 WF 27. From Table 2-2

$$C_t = 0.183 \times 27 = 4.94 \text{ \$/sq ft}$$

(o) Radiation Section: Design of Cylindrical Shell

Assuming the minimum $D = 3.0$ in. governs design

$$f'_{dc} = 1.18 \left[200 \left(\frac{45.0 + 3.0}{3.0} \right) - 300 \right] = 3300 \text{ psi} \quad (6.27)$$

Use $f'_{dc} = 3750 > 3300$ ∴ OK

(p) Radiation Section: Cost Factors for Cylindrical Shell

From Table 7-5

$$C_t = 45.25 \text{ \$/ft}$$

2. Radiation Analysis

(a) Prompt Radiation Overhead Shelter Contribution

As outlined in Section 5.3.2 and further detailed in Trial Design 7.4.1, use Fig. 5-1 to determine the solid angle fraction from the input parameters listed in Table 7-1 and Table 7-2. The dose received in the shelter is

From Fig. 5-1

$$\begin{aligned} \text{Given: } B_p &= 15.0 \text{ ft} & \therefore \omega &= 0.5 \text{ solid radians} \\ H_p &= 65 \text{ ft} \\ Z &= 7.25 \text{ ft} \end{aligned}$$

For overhead burst orientation ($\beta_B = 0$ deg; $\beta_S = 90$ deg; $\rho_m = 750$ psf;
 $W = 1$ MT, $\omega = 0.5$ solid radians, $p_{so} = 125$ psi)

(Table 5-1) (Fig. 5-2) (Fig. 5-4)

$$\gamma = 4.15 \times 10^4 \times 0.95 \times 6 \times 10^{-4} = 23.50 \text{ rads}$$

(Table 5-1) (Fig. 5-2) (Fig. 5-7)

$$N = 3.56 \times 10^3 \times 0.80 \times 9 \times 10^{-5} = 0.26 \text{ rads}$$

For entranceway burst orientation ($\beta_B = 50$ deg; $\beta_S = 40$ deg; $\rho_m = 750$ psf;

$W = 1$ MT, $\omega = 0.5$ solid radians, $p_{so} = 125$ psi)

(Table 5-1

Interpolation) (Fig. 5-2) (Fig. 5-4)

$$\gamma = 1.18 \times 10^5 \times 0.50 \times 1.3 \times 10^{-5} = 0.75 \text{ rads}$$

(Table 5-1

Interpolation) (Fig. 5-2) (Fig. 5-7)

$$N = 1.73 \times 10^4 \times 0.64 \times 3.5 \times 10^{-5} = 0.39 \text{ rads}$$

(b) Prompt Radiation Entranceway Contribution

As shown in Section 5.8 and Design Example 5.4.1, use Eq. (5-5b) or Fig. 5-1 to determine solid angle fraction. Assume an overhead weapon burst orientation.

(1) Transition Section - Detector No. 1 at bottom of stairs 3.0 ft above floor

(a) Entranceway contribution ($r_m = 3.75$; $Z = 13.0$ ft; \therefore
 $\beta_B = 50$ deg); $\omega = 0.047$ solid radians

(Table 5-1) (Fig. 5-2)

$$\gamma = 4.15 \times 10^4 \times 0.06 = 2.48 \times 10^3 \text{ rads}$$

(Table 5-2) (Fig. 5-2)

$$N = 3.56 \times 10^3 \times 0.10 = 3.56 \times 10^2 \text{ rads}$$

(b) Overhead contribution ($B_p = 7.5$ ft; $H_p = 10.0$ ft;
 $Z = 4.5$ ft;

$\therefore \omega = 0.32$ solid radians; $\rho_m = 375$ psf; $\beta_B = 0$ deg;

$\beta_S = 90$ deg)

$$\begin{aligned} & \text{(Table 5-1) (Fig. 5-2) (Fig. 5-4)} \\ \gamma &= 4.15 \times 10^4 \times 0.82 \times 0.03 = 1.02 \times 10^3 \text{ rads} \end{aligned}$$

$$\begin{aligned} & \text{(Table 5-1) (Fig. 5-2) (Fig. 5-7)} \\ N &= 3.56 \times 10^3 \times 0.67 \times 0.01 = 2.38 \times 10 \text{ rads} \end{aligned}$$

Total at Detector No. 1

$$\gamma = 2.48 \times 10^3 + 1.02 \times 10^3 = 3.50 \times 10^3 \text{ rads}$$

$$N = 3.56 \times 10^2 + 0.24 \times 10^2 = 3.80 \times 10^2 \text{ rads}$$

- (2) Blast Section - Detector No. 2 opposite blast door
3.0 ft above floor

- (a) Entranceway Contribution ($r_m = 3.75$ ft; $Z = 6.5$ ft;

$$\therefore \omega = 0.105 \text{ solid radians; } \beta_B = 0 \text{ deg)}$$

(At Detector No. 1) (Fig. 5-2)

$$\gamma = 3.50 \times 10^3 \times 0.68 = 2.38 \times 10^3 \text{ rads}$$

(At Detector No. 1) (Fig. 5-2)

$$N = 3.80 \times 10^2 \times 0.37 = 1.41 \times 10^2 \text{ rads}$$

- (b) Overhead Contribution ($B_p = 7.5$ ft; $H_p = 1.20$ ft;
 $Z = 4.5$ ft;

$$\therefore \omega = 0.37 \text{ solid radians; } \rho_m = 750 \text{ psf; } \beta_B = 0 \text{ deg;}$$

$$\beta_S = 90 \text{ deg)}$$

(Table 5-1) (Fig. 5-2) (Fig. 5-4)

$$\gamma = 4.15 \times 10^4 \times 0.88 \times 6.0 \times 10^{-1} = 0.02 \times 10^3 \text{ rads}$$

(Table 5-1) (Fig. 5-2) (Fig. 5-7)

$$N = 3.56 \times 10^3 \times 0.70 \times 0.09 \times 10^3 = 0.22 \text{ rads}$$

Total at Detector No. 2

$$\gamma = 2.40 \times 10^3 \text{ rads}$$

$$N = 1.41 \times 10^2 \text{ rads}$$

- (3) Radiation Section (R_1) - Detector No. 3 downstream
end of radiation section 3.0 ft above floor

- (a) Entranceway Contribution ($r_m = 3.75$ ft; $Z = 15.0$ ft;

IIIT RESEARCH INSTITUTE

$$R_{fc_1} = 0.1; R_{fw} = 0.15; \therefore \omega = 0.026 \text{ solid radians};$$

$$\beta_B = 0 \text{ deg}; \rho_m = 87.5 \text{ psf}; \beta_S = 90 \text{ deg}$$

(At Detector No. 2)(Fig. 5-2)(Fig. 5-4)

$$\gamma = 2.40 \times 10^3 \times 0.17 \times 0.55 = 2.24 \times 10^2 \text{ rads}$$

(At Detector No. 2) (Fig. 5-2) (Fig. 5-7) (R_{fw})

$$N = 1.41 \times 10^2 \times 0.11 \times 0.55 = 0.15 = 1.28 \text{ rads}$$

Note: Modified ω' for gamma radiation $\omega' = R_{fc_1}$; $\omega = 0.1 \times 0.026 = 0.0026$

(b) Overhead Contribution ($B_p = 7.5 \text{ ft}$; $H_p = 15.0 \text{ ft}$; $Z = 4.5 \text{ ft}$;

$$\therefore \omega = 0.37 \text{ solid radians}; \rho_m = 800 \text{ psf}; \beta_B = 0 \text{ deg}; \beta_S = 90 \text{ deg})$$

(Table 5-1) (Fig. 5-2) (Fig. 5-4)

$$\gamma = 4.15 \times 10^4 \times 0.88 \times 3.5 \times 10^{-4} = 1.28 \times 10 \text{ rads}$$

(Table 5-1) (Fig. 5-2) (Fig. 5-7)

$$N = 3.56 \times 10^3 \times 0.70 \times 0.05 \times 10^{-3} = 0.13 \text{ rads}$$

Total at Detector No. 3

$$\gamma = (2.24 \times 10^2 + 0.13 \times 10^2) = 2.37 \times 10^2 \text{ rads}$$

$$N = 1.28 + 0.13 = 1.41 \text{ rads}$$

(4) Radiation Section (R_2) - Detector No. 4 downstream
end of radiation section 3.0 ft above floor

(a) Entranceway Contribution ($r_m = 3.75 \text{ ft}$; $Z = 15.0 \text{ ft}$;

$$R_{fc_2} = 0.5; R_{fw} = 0.15;$$

$$\therefore \omega = 0.026; \omega' = 0.013; \beta_B = 0 \text{ deg})$$

(At Detector No. 3) (Fig. 5-2)

$$\gamma = 2.37 \times 10^2 \times 0.36 = 85.5 \text{ rads}$$

(At Detector No. 3) (Fig. 5-2) (R_{fw})

$$N = 1.41 \times 0.20 \times 0.15 = 0.04 \text{ rads}$$

(b) Overhead Contribution ($B_p = 7.5 \text{ ft}$; $H_p = 15.0 \text{ ft}$;
 $Z = 4.5 \text{ ft}$; $\therefore \omega = 0.37 \text{ solid radians}$; $\rho_m = 900 \text{ psf}$;

$$\beta_B = 0 \text{ deg}; \beta_S = 90 \text{ deg})$$

(Table 5-1) (Fig. 5-2) (Fig. 5-4)

$$\gamma = 4.15 \times 10^4 \times 0.88 \times 1.3 \times 10^{-4} = 4.75 \text{ rads}$$

IIT RESEARCH INSTITUTE

$$\begin{array}{ccccc} \text{(Table 5-1)} & \text{(Fig. 5-2)} & \text{(Fig. 5-7)} & & \\ N = 3.56 \times 10^3 & \times & 0.70 & \times & 0.014 \times 10^{-3} = 0.04 \text{ rads} \end{array}$$

Total at Detector No. 4 at shelter mouth

$$\gamma = 85.5 + 4.75 = 90.25 \text{ rads}$$

$$N = 0.04 + 0.04 = 0.08 \text{ rads}$$

Assuming an entranceway weapon burst orientation

(1) Transition Section - Detector No. 1

(a) Entranceway contribution ($\omega = 0.047$ solid radians,

$$\beta_B = 0 \text{ deg})$$

(Table 5-1
Interpolation) (Fig. 5-2)

$$\gamma = 1.18 \times 10^5 \times 0.55 = 6.50 \times 10^4 \text{ rads}$$

(Table 5-1
Interpolation) (Fig. 5-2)

$$N = 1.73 \times 10^4 \times 0.27 = 4.67 \times 10^3 \text{ rads}$$

(b) Overhead Contribution ($\omega = 0.32$ solid radians,

$$\rho_m = 375 \text{ psf}; \beta_B = 50 \text{ deg}; \beta_S = 40 \text{ deg})$$

$$\gamma = 1.18 \times 10^5 \times 0.33 \times 0.0018 = 7.02 \times 10 \text{ rads}$$

$$N = 1.73 \times 10^4 \times 0.44 \times 0.0040 = 3.40 \times 10 \text{ rads}$$

Total at Detector No. 1

$$\gamma = 6.50 \times 10^4 + 0.01 \times 10^4 = 6.51 \times 10^4 \text{ rads}$$

$$N = 4.67 \times 10^3 + 0.03 \times 10^3 = 4.70 \times 10^3 \text{ rads}$$

From Detector No. 1 to Detector No. 4, the reduction factors for the entranceway contribution are essentially the same for the entranceway orientated burst as for the overhead orientation. Neglecting the incremental contribution from the overhead at Detector No. 4, the radiation dose rate is determined directly from the R_f already determined for the overhead case. At Detector No. 4

Entranceway contribution

$$\gamma = \frac{6.51 \times 10^4}{0.35 \times 10^4} \times 85.5 = 1592 \text{ rads}$$

III RESEARCH INSTITUTE

$$N = \frac{4.70 \times 10^3}{0.38 \times 10^3} \times 0.08 = 1.0 \text{ rads}$$

(c) Fallout Radiation

As outlined in Section 5.7 and detailed in Design Example 7.4.1

(a) Fallout overhead shelter contribution

($\omega = 0.5$ solid radians; $\rho_m = 750$ psf; Case I)

$$\begin{array}{l} \text{(Free-field dose)} \quad \text{(Fig. 5-8)} \quad \text{(Fig. 5-5)} \\ \gamma = 8.6 \times 10^4 \times 0.13 \times 5 \times 10^{-8} = \text{negligible} \end{array}$$

(b) Fallout entranceway contribution

Dose rate at Detector No. 2 = 8.6×10^4 rads

At Detector No. 3 ($\omega = 0.026$ solid radians; $\rho_m = 75$ psf, Case II)

$$\begin{array}{l} \text{(Free-field dose)} \quad \text{(Fig. 5-8)} \quad \text{(Fig. 5-5)} \\ \gamma = 8.6 \times 10^4 \times 4.1 \times 10^{-2} \times 1.65 \times 10^{-1} = 5.80 \times 10^2 \text{ rads} \end{array}$$

Downstream from this detector, fallout radiation is treated in the same manner as prompt radiation. At Detector No. 3

The worst case prompt gamma radiation

$$\begin{array}{l} \text{(At Detector No. 1)} \quad \text{(Fig. 5-2)} \quad \text{(Fig. 5-2)} \quad \text{(Fig. 5-4)} \\ \gamma = 6.51 \times 10^4 \times 0.68 \times 0.17 \times 0.55 = 4.18 \times 10^3 \text{ rads} \end{array}$$

At Detector No. 4

$$\gamma = \frac{0.580 \times 10^3}{4.18 \times 10^3} \times 1592 = 221 \text{ rads}$$

Total worst case radiation dose at entrance of shelter proper

Prompt γ	= 1592	Prompt N	= 1.0 rads
Fallout γ	= 221		
Total	<hr/> 1813 rads		

(d) Radiation Barrier Shielding Design

Worst case γ dosage at shelter entrance = 1813 rads

Radiation dosage through shelter roof for this case =
1.14 rads

Allowable dose rate through entranceway for this
case = $40.0 - 1.14 = 38.86$ rads

$$\text{Required } R_{f_b} = \frac{38.86}{1813} = 0.0214$$

From Fig. 5-4 ($R_{f_b} = 0.0214$, $\beta_S = 90$ deg)

$$\rho_m = 400 \text{ psf}$$

Required

$$D = \frac{400}{12.5} = 32.0 \text{ in.}$$

Use $D = 32.0$ in.

Usually, in high overpressure ranges, the radiation worst-case is that of the entranceway orientated burst. Where this is not clearly the case, both the entranceway and overhead orientated burst should be investigated. See Design Example 7.4.4 Part B, Section (d) for detailed "worst case" determination.

As is discussed in Example 4.4.1 the barrier shielding is placed in Radiation Section (R_2) (see Fig. 5-7) with a flared diameter of 8.5 ft for a length of 9.83 ft.

Area of barrier wall

$$A = 2 \times 1/2 \times \pi 4.75^2 = 57.0 \text{ sq ft}$$

(e) Radiation Barrier Shielding Cost Factor

Assuming $f'_c = 2,000$ psi

Concrete

$$C_c = \frac{D}{12} \times X_c \frac{32.0}{12} \times 1.00 = 2.67 \text{ \$/sq ft}$$

Steel

$$C_s = \frac{D \phi_t X_s}{1200} = \frac{32.0 \times 0.5}{1200} \times 78.8 = 1.05 \text{ \$/sq ft}$$

Forms

$$C_f = \frac{2 (A + 0.0333 D S_L)}{A} X_f$$

$$C_f = 2 \times \frac{57.0 + 2.67 \times 8.5}{57.0} \times 1.00 = 2.80 \text{ \$/sq ft}$$

Summary

$$C_t = 2.67 + 1.05 + 2.80 = 6.52 \text{ \$/sq ft}$$

$$C_T = 6.52 \times 57.0 = 371 \text{ \$}$$

(f) Radiation Section - Flared Shell Cost Factor

$$f'_{dc} = 1.18 \left[200 \left(\frac{51.0 + 3.0}{3.0} \right) - 300 \right] = 3900 \text{ psi} \quad (6-27)$$

Use $f'_{dc} = 5000 > 3900 \text{ psi}$

Concrete

$$C_c = \frac{3.0}{12} \times 1.13 = 0.29 \text{ \$/sq ft} \quad (6-28)$$

Steel

$$C_s = \frac{3.0 \times 0.6}{1200} \times 85.3 = 0.13 \text{ \$/sq ft} \quad (6-29)$$

Forms

$$C_f = 1.40 \text{ \$/sq ft} \quad (6-30)$$

Summary

$$C_t = 0.29 + 0.13 + 1.40 = 1.82 \text{ \$/sq ft} \quad (6-31)$$

3. Total Cost

(a) Excavation and Backfill

Assuming an existing 1:1 slope cut excavation for the shelter, the volume of the additional excavation required can be determined from Eq. (7-8).

(1) For Radiation Section (R_2)

Depth of excavation at side of shelter $\approx 17.5 \text{ ft}$

Depth of excavation at upstream end of section = 2.5 ft

$$z = \frac{(17.5 - 17.5) + (17.5 - 2.5)}{2} = 7.5 \text{ ft}$$

$$\text{Vol} = \frac{7.5}{2} ((9.0 \times 15.0) + (23.5 \times 22.5)) = 2485 \text{ cu ft}$$

IIT RESEARCH INSTITUTE

(2) For Radiation Section (R_1)

Depth of excavation downstream end = 16.75 ft

Depth of excavation upstream end = 2.5 ft

Average depth of Radiation Section (R_1) = 16.00 ft

$$Z = \frac{(16.00 - 16.75) + (15.50 - 2.5)}{2} = 6.125 \text{ ft}$$

$$\text{Vol} = \frac{6.125}{2} ((8.0 \times 15.0) + (14.13 \times 15.0)) = 1040 \text{ cu ft}$$

(3) For Blast Section

Depth of excavation, downstream end = 11.5 ft

Depth of excavation, upstream end = 0.0 ft

Average depth of Blast Section = 15.50 ft

$$z = \frac{((15.50 - 11.5) + (15.50 - 0))}{2} = 9.75 \text{ ft}$$

$$\text{Vol} = \frac{9.75}{2} ((9.5 \times 18.0) + (18.5 \times 26.0)) = 3190 \text{ cu ft}$$

(4) For Transition Section

Depth of excavation, downstream end = 15.50 ft

Depth of excavation, upstream end = 5.50 ft

Average depth of Transition Section = 11.00 ft

$$Z = \frac{((11.00 - 15.50) + (11.00 - 5.50))}{2} = \frac{1.0}{2} = 0.5 \text{ ft}$$

$$\text{Vol} = \frac{0.5}{2} ((8.5 \times 10.0) + (9.0 \times 11.0)) = 50 \text{ cu ft}$$

(5) For Open Cut

Depth of excavation, downstream end = 5.50 ft

Depth of excavation, upstream end = 0.0 ft

Average depth of cut = 3.0 ft

$$Z = \frac{((3.0 - 5.5) + (3.0 - 0.0))}{2} = 0.25 \text{ ft}$$

Assuming 2:1 side slopes of open cut

$$\frac{0.25}{2} ((2.5 \times 9.0) + (3.0 \times 9.25)) = 10 \text{ cu ft}$$

Total volume of additional excavation

Radiation Section (R_2)	=	2485 cu ft
Radiation Section (R_1)	=	1040 cu ft
Blast Section	=	3190 cu ft
Transition Section	=	50 cu ft
Open Cut	=	10 cu ft
Total		<u>6775 cu ft</u>

Entrance Structure Volume

Radiation Section (R_2)	=	$\pi \times (4.5)^2 \times 10.0$	=	635 cu ft
Radiation Section (R_1)	=	$\pi \times (4.0)^2 \times 15.0$	=	754 cu ft
	=	$\pi \times (4.0)^2 \times 5.0$	=	252 cu ft
Blast Section	=	$\pi \times (4.25)^2 \times 18.0$	=	1025 cu ft
Transition Section	=	$\pi \times (4.25)^2 \times 13.0$	=	750 cu ft
Open Cut = $1/4 \times (27.5 + 2.5) \times 6.0$			=	<u>50 cu ft</u>
Total	=			3466 cu ft

Volume of Backfill

$$6775 - 3466 = 3309 \text{ cu ft}$$

(b) Open Cut Section

Slope surface area requiring stabilization, assuming a 2:1 slope

$$13.5 \times 8.5 \times 1/2 = 115 \text{ sq ft}$$

Assume slope stabilization will consist of 3 in. concrete slab or equivalent

$$C_f = 0.75 \text{ \$/sq ft}$$

$$C_T = 0.75 \times 115 = 87 \text{ \$}$$

Stair costs from Section 2.2.9

$$C_T = 9 \text{ steps at } 18.00 \text{ \$/step} = 162 \text{ \$}$$

(c) Emergency Exit

The 100 Man shelter serviced by a blast-resistant entrance-way requires one emergency exit. From Table 7-2, the required length of emergency exit is assumed equal to the depth to entrance level. Unit cost from Section 2.8.4

$$C_T = 14.00 \times 17.75 = 248 \text{ \$}$$

Total Cost

Surface Transition Section (Open Cut)

Side Slope Stabilization	=	87
Stairs 9 steps at 18 \$/step	=	162

Depth Transition Section

Prestressed Concrete Cylindrical Shell $3.62 \times 8.25 \times \pi \times 13.0$	=	1220
Stairs 13 steps at 18 \$/step	=	236

Blast Section

Prestressed Concrete Cylindrical Shell $3.62 \times 8.25 \times \pi \times 11.30$	=	1060
Prestressed Concrete Tension Rings $12.17 \times 8.75 \times \pi \times 2$	=	668
Concrete Frame Beams Between Rings $4.62 \times 1.82 \times 2$	=	17
Prestressed Concrete Blast Door	=	68
Blast Door Support Channels	=	74
Blast Door Roller Supports	=	210
Blast Door Latch	=	95
Structural Steel Dome End $3.53 \times 2 \times \pi \times (5.81)^2$	=	748
Structural Steel Dome End Support Ring $4.94 \times \pi \times 11.62$	=	181

Radiation Section

Reinforced Concrete Cylinder 45.25×20.16	=	913
$1.82 \times \pi \times 9.0 \times 9.84$	=	505
Radiation Barrier Wall	=	371

Emergency Exit	=	248
----------------	---	-----

Excavation	0.036 x 6775	=	244
Backfill	0.033 x 3309	=	109
Haul	0.026 x 3466	=	91

Total = \$ 7273

7.4.3 Compression Cylinder (Sample Analysis and Cost Evaluation)

TRIAL DESIGN 7.4.3 - 325 C2 Nonflare

CONFIGURATION

One story cylinder (Fig. 7-12)

STRUCTURAL SYSTEM AND INPUT PARAMETERS (Fig. 7-3)

Transition Section -

Material: Prestressed concrete cylinder

Orientation: Makes ~ 39 deg angle with horizontal plane and is perpendicular to the long axis of the shelter

Dimension: I. D. 8 ft-0 in.; length 13 ft-0 in.; change in elevation between entrance and exit 8 ft-3 1/2 in.

Primary Design Load: $q_I = 772$ psi; $q_{Ed} = 325$ psi

Blast Section -

Material: Reinforced concrete cylinder

Orientation: Parallel to long axis of shelter; horizontal change in elevation between entrance and exit 3 ft-3 in.

Dimension: I. D. 8 ft-6 in.; length 13 ft-0 in.; dome end I. D. 8 ft-6 in.; overall length 18 ft-0 in.

Primary Design Load: $q_{Ed} = 772$ psi

Radiation Section (R_1) -

Material: Reinforced concrete cylinder

Orientation: Parallel to long axis of shelter; horizontal; change in elevation between entrance and exit 0 ft-6 in.

Dimension: I. D. 8 ft-0 in.; length 16 ft-0 in.

Primary Design Load: $q_{Ed} = 325$ psi

Radiation Section (R_2) -

Material: Reinforced concrete cylinder

Orientation: Perpendicular to long axis of shelter; horizontal; change in length between entrance and exit 0 ft-6 in.

Dimension: I. D. 8 ft-0 in.; length 16 ft-0 in.

Primary Design Load: $q_{Ed} = 325$ psi

Note: These dimensions may require subsequent modification due to radiation design requirements.

Shelter -

Capacity: 500 Man (Table 7-2)

Primary Design Load: $q_{Ed} = 325$ psi

IIT RESEARCH INSTITUTE

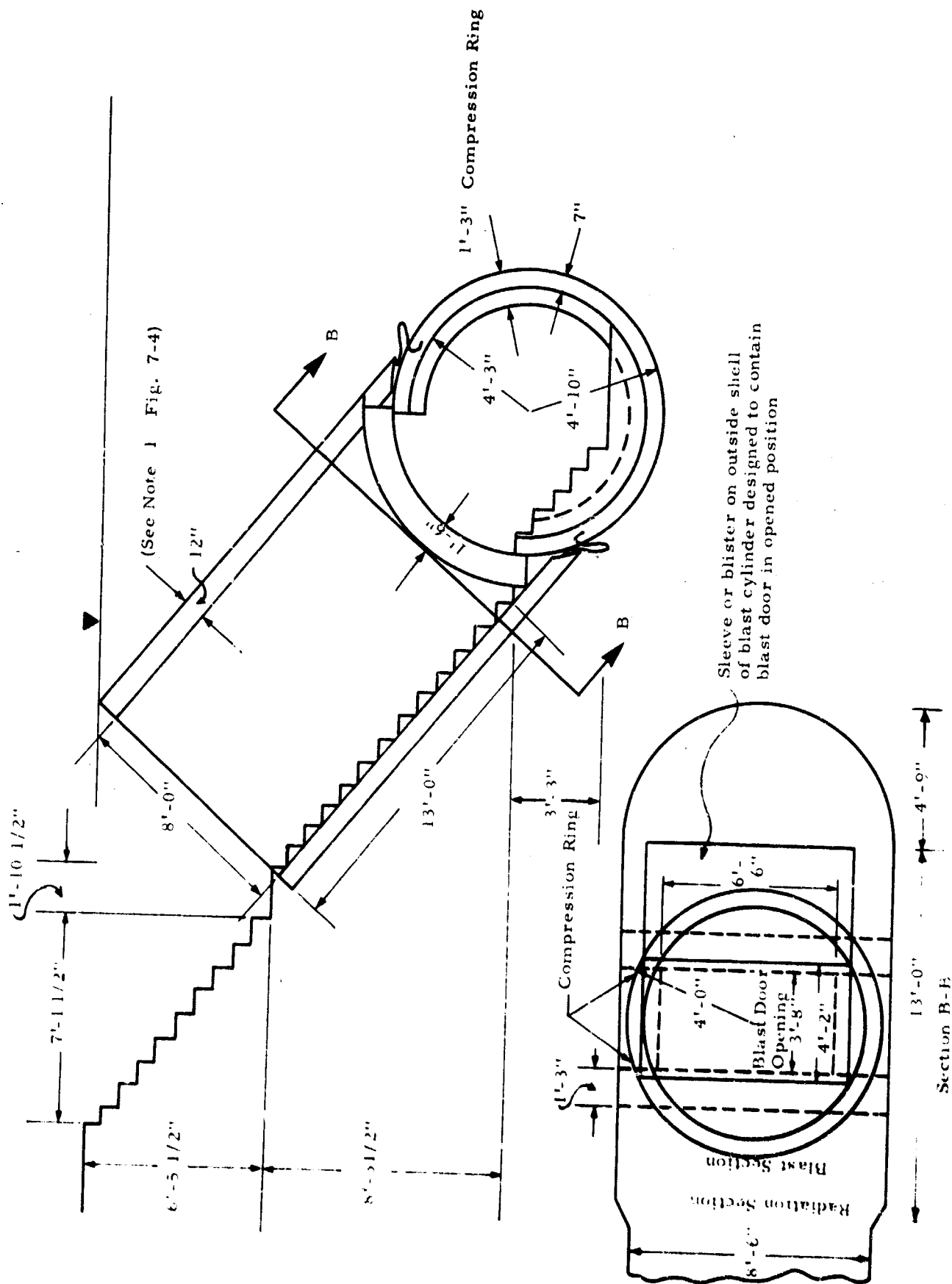


Fig. 7-12 SECTIONAL VIEW OF COMPRESSION CYLINDER

1. Blast Analysis

(a) Transition Section: Design of Cylindrical Shell, Prestressed Concrete

Assume $D = 8.0$ in.; $f'_c = 6000$ psi

$$\frac{6 S_L}{D} = \frac{48.0}{8.0} = 6.0 < 10.0$$

∴ requires thick wall analysis

From Section 6.3 as detailed in Trial Design 7.4.1 - 325 A1 (Part A(a))

From Eq.(6-15) From Eq.(6-13)

$$q_{Ep} = 359 \text{ psi} > q_{Ep} = 314.3 \text{ psi} \quad \therefore \text{OK}$$

From Eq. (6-17)

$$q_{Ep} = 457 \text{ psi} > 359 \text{ psi} \quad \therefore \text{OK}$$

∴ Use $D = 8.0$ in.

From Eq. (6-16)

$$T_{sp} = (48.0 + 8.0) 359 = 20,100 \text{ lb/in.} \quad (6-16)$$

Assuming a 1/2 in. ϕ K270 prestressing steel strand from Table 2-7

$$F_{sp} = 23,150 \text{ lb/strand}$$

$$L_{sp} = \frac{12 \times 20,100}{23,150} = 10.4 \text{ ft/sq ft of shell} \quad (6-18)$$

(b) Transition Section: Cost Factors for Cylindrical Shell, Prestressed Concrete

From Section 6.2.2

Concrete

$$C_c = \frac{8.0}{12} \times 1.30 = 0.87 \text{ \$/sq ft} \quad (6-19)$$

Steel

$$C_s = \frac{8.0 \times 0.6}{1200} \times 85.8 = 0.35 \text{ \$/sq ft} \quad (6-20)$$

Prestressing Steel

$$C_{sp} = 10.4 \times 0.19 = 1.98 \text{ \$/sq ft} \quad (6-21)$$

Forms

$$C_f = 1.40 \text{ \$/sq ft} \quad (6-22)$$

Protective Covering

$$C_g = 0.30 \text{ \$/sq ft} \quad (6-23)$$

Summary

$$C_t = 0.87 + 0.35 + 1.98 + 1.40 + 0.30 = 4.90 \text{ \$/sq ft} \quad (6-24)$$

(c) Blast Section: Design of Cylindrical Shell, Reinforced Concrete

Assume reinforced concrete $f'_{dc} = 7500 \text{ psi}$; $f_{dy} = 60,000 \text{ psi}$;
 $\phi_t = 0.5 \text{ percent}$; $D = 7.0 \text{ in.}$

$$\text{Required } D = \left[q_I \frac{(6 S_L + D)}{0.85 f'_{dc} + 0.01 \phi_t} \right] \quad (6-26)$$

$$D = \frac{772 (58.0)}{6638 + 300} = 6.45 \text{ in.} < 7.0$$

\therefore Use $D = 7.0 \text{ in.}$

(d) Blast Section: Cost Factors for Cylindrical Shell, Reinforced Concrete

$$C_c = \frac{7.0}{12} 1.30 = 0.76 \text{ \$/sq ft} \quad (6-28)$$

$$C_s = \frac{7.0 \times 0.6 \times 85.8}{1200} = 0.31 \text{ \$/sq ft} \quad (6-29)$$

$$C_f = 1.40 \text{ \$/sq ft} \quad (6-30)$$

$$C_t = 0.76 + 0.31 + 1.40 = 2.47 \text{ \$/sq ft} \quad (6-31)$$

(e) Blast Section: Design of Compression Ring, Reinforced Concrete

Assume $b = 15.0 \text{ in.}$; $D = 15.0 \text{ in.}$

$$D_{(\text{ring})} = \frac{36 q_I (L_S + b/6) S_{L(\text{cylinder})}}{0.85 b f'_{dc}} \quad (6-153)$$

$$D = \frac{36 \times 772 (6.16) \times 8.5}{0.85 \times 15 \times 7500} = 14.95 \text{ in.} < 15.0 \therefore \text{OK}$$

From Eq. (6-66) $\phi_{vt} < 0.0 \therefore$ No torsion steel required

(f) Blast Section: Cost Factors for Compression Ring,
Reinforced Concrete

Concrete

$$C_c = \frac{15.0 \times 15.0}{144} \times 1.30 = 2.03 \text{ \$/ft} \quad (6-157)$$

Steel

$$C_s = \frac{1.0 \times 15.0 \times 15.0}{14,400} \times 85.8 = 1.34 \text{ \$/ft} \quad (6-158)$$

Forms

$$C_f = \left(\frac{15.0 \times 15.0}{6} \right) \times 1.00 = 5.00 \text{ \$/ft} \quad (6-159)$$

Summary

$$C_t = 2.03 + 1.34 + 5.00 = 8.37 \text{ \$/ft} \quad (6-160)$$

(g) Blast Section: Design of Beam Member Between Rings

Assume reinforced concrete beam with $b = 10.0$ in.;

$D = 15.0$ in.; $\phi_v = 0.75$; $f_{dy} = 75,000$ psi; $f'_c = 6000$ psi

$$\text{Required } d = \left[\frac{36.5 L_s}{1045 + 0.0209 \phi_v f_{dy}} \right] \left[\frac{6 (q_{Es} + q_{Ed}) (S_L + \frac{D}{6} (\text{shell})) f_{dy}}{b f'_c} \right]^{1/2} \quad (6-165a)$$

$$d = \left(\frac{36.5 \times 3.66}{1045 + 1095} \right) \left(\frac{6 \times 325 (8.5 + 1.33) \times 75,000}{10 \times 6000} \right)^{1/2} = 13.42 \text{ in.}$$

$$D = \frac{13.42}{0.9} = 14.9 \text{ in.} < 15.0 \quad \therefore \text{ Use } D = 15.0 \text{ in.}$$

To determine moment steel

$$\phi_e = \left[\frac{1045 + 0.0209 \phi_v f_{dy}}{f_{dy}} \right]^2 f'_c \quad (6-135)$$

$$\phi_e = \left[\frac{1045 + 0.0209 \times 0.75 \times 75,000}{75,000} \right]^2 \times 60.00 = 5.17 \text{ percent}$$

(h) Blast Section: Cost Factors for Beam Member Between Rings

Concrete

$$C_c = \frac{10.0 \times 15.0}{144} \times 1.30 = 1.36 \text{ \$/ft} \quad (6-167)$$

Moment Steel

$$C_s = \frac{5.17 \times 10.0 \times 15.0}{10,650} \times 85.8 = 6.27 \text{ \$/sq ft} \quad (6-168)$$

Diagonal Tension Steel

$$C_v = \frac{0.75 \times 10.0 \times 15.0}{900} \left[0.196 \times 0.75 + 0.347 \right] \times 92.5 = 5.61 \text{ \$/ft} \quad (6-169)$$

Forms

$$C_f = \left(\frac{10 + 15}{6} \right) \times 1.00 = 4.17 \text{ \$/ft} \quad (6-170)$$

Summary

$$C_t = 1.36 + 6.27 + 5.61 + 4.17 = 17.41 \text{ \$/ft} \quad (6-171)$$

(i) Blast Section: Design of Reinforced Concrete Dome End

From Section 6.5.1, q_c must exceed q_I

Assuming $D = 4.0$ in.; $f'_{dc} = 7500$ psi; $f_{dy} = 60,000$ psi;

$\phi_t = 1.0$

$$q_c = \left[\frac{D}{6 S_L + D} \right] \left[1.70 f'_{dc} + 0.002 \phi_t f_{dy} \right] \quad (6-39)$$

$$q_c = \left[\frac{4.0}{6 \times 8.75 + 4.0} \right] \left[1.70 \times 7500 \times 0.002 \times 1.0 \times 60,000 \right] = 910 \text{ psi}$$

$910 > 772 \therefore \text{OK}$

(j) Blast Section: Cost Factors for Reinforced Concrete Dome End

Concrete

$$C_c = \frac{4.0}{12} \times 1.30 = 0.44 \text{ \$/sq ft} \quad (6-28)$$

Steel

$$C_s = \frac{4.0 \times 1.0}{1200} \times 85.8 = 0.29 \text{ \$/sq ft} \quad (6-29)$$

Forms

$$C_f = 1.75 \quad (6-30)$$

Summary

$$C_t = 0.44 + 0.29 + 1.75 = 2.48 \text{ \$/sq ft} \quad (6-31)$$

(k) Blast Section: Design of Prestressed Concrete Blast Door

The blast door is designed as a prestressed concrete shell segment. Assume $D = 18.0$ in.

$$\begin{aligned} \text{For: } S_L/2 &= 5.58 \text{ ft} & L_S &= 3.66 \text{ ft} & \mu &= 0.312 & K_{20} &= 0.025 \\ \widehat{L}_L &= 9.66 \text{ ft} & \lambda &= 0.380 & K_{10} &= 0.1127 & \lambda^2 &= 0.145 \end{aligned}$$

$$D = \left[\frac{86.4 \times 0.1127 \times 772 \times 13.4 \times 1.32}{[(0.45 \times 6000) + 234]} \left(\frac{1.39}{2.165} \right) \right]^{1/2} \quad (6-119)$$

$$D = 17.1 < 18.0 \quad \therefore \text{OK}$$

Assuming 1/2 ϕ 270 K prestressing strand

$$L_{sp} = \frac{270 f'_c D}{F_{sp}} = \frac{2.70 \times 6000 \times 18.0}{23,150} = 8.10 \text{ ft/sq ft}$$

The required percentage of longitudinal steel

$$\phi_{cL} = 17,800 \times 0.025 \times \frac{772 \times 3.66}{60,000 \times 18.0} \left[1 - \frac{0.380}{2,095} \right] = 0.095 \quad (6-120)$$

$$\phi_{cL} = 0.095 < 0.225$$

\therefore No additional steel required.

Check for pure shear failure

$$D = \frac{30 \times 772 \times 3.67}{6000} = 14.15 < 18.0 \quad \therefore \text{OK} \quad (6-123)$$

(2) Blast Section: Cost Factors for Blast Door

Concrete

$$C_c = \frac{18.0}{12} \times 1.30 = 1.95 \text{ \$/sq ft} \quad (6-124)$$

Reinforcing Steel

$$C_s = \frac{18.0 \times 0.45 \times 85.8}{1200} = 0.58 \text{ \$/sq ft} \quad (6-125)$$

Prestressing Steel

$$C_{sp} = 8.10 \times 0.19 = 1.54 \text{ \$/sq ft} \quad (6-126)$$

Forms

$$C_f = 1.40 \text{ \$/sq ft} \quad (6-127)$$

Summary

$$C_t = 1.95 + 0.58 + 1.54 + 1.40 = 5.47 \text{ \$/sq ft} \quad (6-128)$$

Total area of door, including 3.0 in. overlap on all sides

$$(L_S + 0.5) \times (\hat{L}_L + 0.5) = (4.16 \times 10.16) = 42.3 \text{ sq ft}$$

$$C_T = 5.47 \times 42.3 = 231 \text{ \$}$$

(m) Blast Section: Design of Blast Door Support Hardware

No Standard American channel can accommodate an 18.0 in. door width. Assume a built-up channel section, with a knee brace support at the center of the web which effectively reduces web space to $18.250/2 = 9.125$ in.

Bending

$$t_w = \frac{2170}{50,000} \left(\frac{9.125}{2} \right)^2 = 0.905 \text{ in. required}$$

Assume a built-up channel member

Flange $b = 4.0$ in.; Web $b = 18.250$ in.; cross-sectional area = 26.25 sq in.

Flange $t = 1.00$ in.; Web $t = 1.00$ in.; Weight = $3.4 \times 26.25 = 89.4$ lb/ft

The channel sections along the sides and top of the door could be somewhat reduced in section, since they do not carry the full weight of the door. However, it is assumed for cost purposes that the reduced cost of these sections is balanced by the knee brace cost.

Length of channel required

$$4 (L_S + 0.5) + 2 (\widehat{L}_L + 0.5) = 4 (4.16) + 2 (10.16) = 36.97 \text{ ft}$$

(n) Blast Section: Cost Factors for Blast Door Support Structure Hardware

(1) Channels

From Table 2-2 $X_s = 0.207$ \$/lb for $f_y = 50,000$ psi

$$C_T = 0.207 \times 89.4 \times 36.97 = 683 \text{ \$}$$

(2) Roller Supports

From Section 2.8.2

$$C_T = 30 \times 2 \times 18 = 1080 \text{ \$}$$

(3) Blast Door Latch

From Section 2.8.3

$$C_T = [25.00 + 180] \times (2)^{1/2} = 290 \text{ \$}$$

Note: A steel blast door of 10 J r 9 wide flange sections would also be suitable for ~ 10 percent additional cost of door and hardware.

(o) Radiation Section: Design of Reinforced Concrete Cylindrical Shell

Assuming minimum $D = 3.0$ governs design

$$f'_{dc} = 1.18 \left[325 \left(\frac{48.0 + 3.0}{3.0} \right) - 300 \right] = 6150 \text{ psi} \quad (6-27)$$

Use $f'_{dc} = 6250 > 6150 \text{ psi}$

(p) Radiation Section: Cost Factors for Cylindrical Shell

From Table 7-5

$$C_T = 51.70 \text{ \$/ft}$$

2. Radiation Analysis

(a) Prompt Radiation Overhead Shelter Contribution

As outlined in Section 5.3.2

For overhead burst orientation ($B_p = 20 \text{ ft}$; $H_p = 155 \text{ ft}$; $Z = 6.0 \text{ ft}$;

$\therefore \omega = 0.67 \text{ solid radians}$; $\beta_B = 0 \text{ deg}$; $\beta_S = 90 \text{ deg}$; $\rho_m = 1000 \text{ psf}$;

$W = 1 \text{ MT}$; $p_{so} = 200 \text{ psi}$)

$$\gamma = 1.45 \times 10^5 \times 0.96 \times 5 \times 10^{-5} = 6.95 \text{ rads}$$

$$N = 2.27 \times 10^4 \times 0.88 \times 0.04 \times 10^{-4} = 0.08 \text{ rads}$$

For entranceway burst orientation ($B_p = 20 \text{ ft}$; $H_p = 155 \text{ ft}$;

$Z = 6.0 \text{ ft}$; $\therefore \omega = 0.67 \text{ solid radians}$; $\beta_B = 50 \text{ deg}$;

$\beta_S = 40 \text{ deg}$; $\rho_m = 1000 \text{ psf}$; $W = 1 \text{ MT}$; $p_{so} = 200 \text{ psi}$)

$$\gamma = 4.58 \times 10^5 \times 0.55 \times 0.1 \times 10^{-5} = 0.25 \text{ rads}$$

$$N = 1.29 \times 10^5 \times 0.82 \times 0.15 \times 10^{-5} = 0.16 \text{ rads}$$

(b) Prompt Radiation Entranceway Contribution

For overhead burst orientation

(1) Transition Section - Detector No. 1 at bottom of stairs

3.0 ft above floor

Entranceway contribution ($r_m = 4.0 \text{ ft}$; $Z = 13.0 \text{ ft}$;

$\therefore \omega = 0.051$; $\beta_B = 50 \text{ deg}$)

IIT RESEARCH INSTITUTE

$$\gamma = 1.45 \times 10^5 \times 0.055 = 7.98 \times 10^3 \text{ rads}$$

$$N = 2.27 \times 10^4 \times 0.11 = 2.50 \times 10^3 \text{ rads}$$

Overhead contribution ($B_p = 8.0 \text{ ft}$; $H_p = 10.0 \text{ ft}$; $Z = 5.0 \text{ ft}$;

$$\therefore \omega = 0.34 \text{ solid radians}; \rho_m = 450 \text{ psf}; \beta_B = 0 \text{ deg}; \beta_S = 90 \text{ deg})$$

$$\gamma = 1.45 \times 10^5 \times 0.86 \times 0.0135 = 1.68 \times 10^3 \text{ rads}$$

$$N = 2.27 \times 10^4 \times 0.68 \times 0.004 = 6.18 \times 10 \text{ rads}$$

$$\text{Total: } \gamma = 7.98 + 1.68 = 9.66 \times 10^3 \text{ rads}$$

$$N = 2.50 + 0.06 = 2.56 \times 10^3 \text{ rads}$$

(2) Blast Section - Detector No. 2 Center of Blast Cylinder

Entranceway contribution ($r_m = 4.00 \text{ ft}$; $Z = 6.0 \text{ ft}$;

$$\therefore \omega = 0.180; \rho_m = 275 \text{ psf}; \beta_B = 0 \text{ deg}; \beta_S = 90 \text{ deg})$$

$$\gamma = 9.66 \times 10^3 \times 0.78 \times 0.14 = 1.06 \times 10^3 \text{ rads}$$

$$N = 2.56 \times 10^3 \times 0.52 \times 0.10 = 1.33 \times 10^2 \text{ rads}$$

Overhead contribution ($B_p = 8.25 \text{ ft}$; $H_p = 15.0 \text{ ft}$;
 $Z = 5.25$; $\therefore \omega = 0.35$; $\beta_B = 0 \text{ deg}$; $\beta_S = 90 \text{ deg}$; $\rho_m = 1100 \text{ psf}$)

$$\gamma = 1.45 \times 10^5 \times 0.86 \times 1.9 \times 10^{-5} = 2.37 \text{ rads}$$

$$N = 2.27 \times 10^4 \times 0.68 \times 4.0 \times 10^{-6} = \text{negligible}$$

$$\text{Total: } \gamma = 1.06 \times 10^3 \text{ rads}$$

$$N = 1.33 \times 10^2 \text{ rads}$$

(3) Radiation Section (R_1) - Detector No. 3 at downstream
 end 3.0 ft above floor

Entranceway contribution ($r_m = 4.00 \text{ ft}$; $Z = 23.0 \text{ ft}$;

$$\omega = 0.015; R_{fc_1} = 0.1; R_{fw} = 0.083; \omega' = 0.0015; \beta_B = 0 \text{ deg})$$

$$\gamma = 1.06 \times 10^3 \times 0.12 = 1.27 \times 10^2 \text{ rads}$$

$$N = 1.33 \times 10^2 \times 0.14 \times 0.083 = 1.55 \text{ rads}$$

IIT RESEARCH INSTITUTE

Overhead contribution ($B_p = 8.0$ ft; $H_p = 16.0$ ft;
 $Z = 5.0$ ft; $\therefore \omega = 0.35$; $\beta_B = 0$ deg; $\beta_S = 90$ deg; $\rho_m = 1175$ psf)

$$\gamma = 1.45 \times 10^5 \times 0.86 \times 1.0 \times 10^{-5} = 1.25 \text{ rads}$$

$$N = 2.27 \times 10^4 \times 0.68 \times 2.0 \times 10^{-6} = \text{negligible}$$

Total: $\gamma = 1.27 + 0.01 = 1.28 \times 10^2 \text{ rads}$

$$N = 1.55 \text{ rads}$$

(4) Radiation Section (R_2) - Detector No. 4 at downstream
 end 3.0 ft above floor

Entranceway contribution ($r_m = 4.00$ ft; $Z = 16.0$ ft;
 $\omega = 0.032$; $R_{fc_2} = 0.5$; $R_{fw} = 0.16$; $\therefore \omega' = 0.016$; $\beta_B = 0$ deg)

$$\gamma = 1.28 \times 10^2 \times 0.49 = 62.7 \text{ rads}$$

$$N = 1.55 \times 0.22 \times 0.16 = 0.055 \text{ rads}$$

Overhead contribution ($B_p = 8.0$ ft; $H_p = 16.0$ ft;
 $Z = 5.0$ ft; $\therefore \omega = 0.35$; $\beta_B = 0$ deg; $\beta_S = 90$ deg; $\rho_m = 1250$ psf)

$$\gamma = \sim 1.0 \text{ rad}$$

$$N = \text{negligible}$$

Total: $\gamma = 62.7 + 1 = 63.7 \text{ rads}$

$$N = 0.055 \text{ rads}$$

For Entranceway Weapon Burst Orientation

(1) At Detector No. 1

Entranceway contribution ($r_m = 4.0$ ft; $Z = 13.0$ ft;

$$\therefore \omega = 0.051$$
; $\beta_B = 0$ deg)

$$\gamma = 4.58 \times 10^5 \times 0.57 = 2.62 \times 10^5 \text{ rads}$$

$$N = 1.29 \times 10^5 \times 0.28 = 3.61 \times 10^4 \text{ rads}$$

Overhead contribution ($B_p = 8.0$ ft; $H_p = 10.0$ ft; $Z = 5.0$ ft;

$$\therefore \omega = 0.34$$
; $\beta_B = 50$ deg; $\beta_S = 40$ deg; $\rho_m = 450$ psf)

IIT RESEARCH INSTITUTE

$$\gamma = 4.58 \times 10^5 \times 0.5 \times 0.0006 = 138 \text{ rads}$$

$$N = 1.29 \times 10^5 \times 0.52 \times 0.0015 = 101 \text{ rads}$$

Total: $\gamma = 2.62 \times 10^5 \text{ rads}$

$$N = 3.61 + 0.01 = 3.62 \times 10^4 \text{ rads}$$

From Detector No. 1 to Detector No. 4, the reduction factors for the entrance-way contribution are essentially the same for the entranceway orientated burst as for the overhead orientation. Neglecting the incremental contribution from the overhead at Detector No. 4, the radiation dose is determined directly from the R_f already determined for the overhead case.

At Detector No. 4

Entranceway Contribution

$$\gamma = \frac{2.62 \times 10^5}{0.0966 \times 10^5} \times 62.7 = 1700 \text{ rads}$$

$$N = \frac{3.61 \times 10^4}{0.256 \times 10^4} \times 0.055 = 0.78 \text{ rads}$$

(c) Fallout Radiation

As outlined in Section 5.7 and detailed in Design Example

7.4.1

Fallout Overhead Shelter Contribution

$$(\omega = 0.67; \rho_m = 1000 \text{ psf; Case I})$$

$$\gamma = 8.6 \times 10^4 \times 0.2 \times 2 \times 10^{-10} = \text{negligible}$$

Fallout Entranceway Contribution

$$\text{At Detector No. 1 } \gamma \text{ dose rate} = 8.6 \times 10^4 \text{ rads}$$

$$\text{At Detector No. 2 } (\omega = 0.18; \rho_m = 225 \text{ psf; Case II})$$

$$\gamma = 8.6 \times 10^4 \times 0.15 \times 0.0055 = 71 \text{ rads}$$

Downstream from this detector fallout radiation is treated in the same manner as prompt radiation.

At Detector No. 4

$$\gamma = \frac{0.071 \times 10^3}{1.06 \times 10^3} \times 62.7 = 4.2 \text{ rads}$$

Total worst case radiation dose at entrance to shelter proper

$$\text{Prompt } \gamma = 1700 \quad \text{Prompt N} = 0.78 \text{ rads}$$

$$\text{Fallout } \gamma = 4$$

$$\text{Total} = 1704 \text{ rads}$$

Note: See Design Example 4.4.4, Part B, Section (d) if worst-case dose is not apparent by inspection.

(d) Radiation Barrier Shielding Design

Worst case γ dosage at shelter entrance = 1704 rads

Radiation dosage through shelter roof for this case =
0.41 rads

Allowable dosage through entranceway for this case =
40.0 - 0.41 = 39.59 rads

$$\text{Required } R_{fb} = \frac{39.59}{1704} = 0.0232$$

From Fig. 5-4 ($R_{fb} = 0.0232$; $\beta_S = 90 \text{ deg}$)

$$\rho_m = 320 \text{ psf}$$

$$\text{Required } D = \frac{320}{12.5} = 25.6 \text{ in.}$$

Use $D = 26.0 \text{ in.}$

As in Design Example 4.4.1 and 4.4.2, the barrier shielding is placed in Radiation Section (R_2) (Fig. 5-7) with a flared diameter of 10.0 ft for a length of 10.00 ft

Area of barrier wall

$$A = 2 \times 1/2 \times \pi \times 5.0^2 = 78.2 \text{ sq ft}$$

(e) Radiation Barrier Shielding Cost Factor

Assuming $f'_c = 2000 \text{ psi}$

Concrete

$$C_c = \frac{D}{12} \quad X_c = \frac{26.0}{12} \times 1.00 = 2.17 \text{ \$/sq ft}$$

IIT RESEARCH INSTITUTE

Steel

$$C_s = \frac{D \phi_t X_s}{1200} = \frac{26.0 \times 0.5 \times 78.8}{1200} = 0.86 \text{ \$/sq ft}$$

Forms

$$C_f = \frac{(A + 0.0833 D S_L)}{A} 2 X_f$$
$$C_f = \frac{2 \times (78.2 + (2.16 \times 10.0))}{78.2} \times 1.00 = 2.55 \text{ \$/sq ft}$$

Summary

$$C_t = 2.17 + 0.86 + 2.55 = 5.59 \text{ \$/sq ft}$$

$$C_T = 5.59 \times 78.2 = 437 \text{ \$}$$

(f) Radiation Section - Cost Factors for Flared Shell

$$f'_{dc} = 1.18 \left[325 \left(\frac{60.0 + 4.0}{4.0} - 300 \right) \right] = 5770 \text{ psi} \quad (6-27)$$

Use $f'_{dc} = 6250 > 5770 \text{ psi}$

Concrete

$$C_c = \frac{4.0}{12} \times 1.21 = 0.41 \text{ \$/sq ft} \quad (6-28)$$

Steel

$$C_s = \frac{4.0 \times 0.6 \times 85.8}{1200} = 0.18 \text{ \$/sq ft} \quad (6-29)$$

Forms

$$C_f = 1.40 \text{ \$/sq ft} \quad (6-30)$$

Summary

$$C_t = 0.41 + 0.18 + 1.40 = 1.99 \text{ \$/sq ft} \quad (6-31)$$

3. Total Cost

(a) Excavation and Backfill

Assuming an existing 1:1 slope cut excavation for the shelter, the volume of the additional excavation required can be determined from Eq. (7-8).

(1) For Radiation Section (R_2)

Depth of excavation at side of shelter = 22.0 ft

Depth of excavation at upstream end of Section = 6.0 ft

Average depth of Radiation Section (R_2) = 22.0 ft

$$z = \frac{(22.0 - 22.0) + (22.0 - 6.0)}{2} = 8.0 \text{ ft}$$

IIT RESEARCH INSTITUTE

$$\text{Vol} = \frac{8.0}{2} ((10.5 \times 16.0) + (26.5 \times 24.0)) = 3212 \text{ cu ft}$$

(2) For Radiation Section (R_1)

Depth of excavation at downstream end = 22.0 ft

Depth of excavation at upstream end = 6.0 ft

Average depth of Radiation Section (R_1) = 20.5 ft

$$z = \frac{(20.5 - 22.00) + (20.5 - 6.0)}{2} = 6.50 \text{ ft}$$

$$\text{Vol} = \frac{6.50}{2} ((8.5 \times 16.0) + (21.5 \times 22.5)) = 2015 \text{ cu ft}$$

(3) For Blast Section

Depth of excavation at downstream end = 20.5 ft

Depth of excavation at upstream end = 6.0 ft

Average depth of Blast Section = 20.5 ft

$$z = \frac{(20.5 - 20.5) + (20.5 - 6.0)}{2} = 7.25 \text{ ft}$$

$$\text{Vol} = \frac{725}{2} ((9.0 \times 18.0) + (23.5 \times 25.25)) = 2740 \text{ cu ft}$$

(4) For Transition Section

Depth of excavation, downstream end = 15.5 ft

Depth of excavation, upstream end = 5.5 ft

Average depth of Transition Section = 11.0 ft

$$z = \frac{(11.0 - 15.5) + (11.0 - 5.5)}{2} = 0.5 \text{ ft}$$

$$\text{Vol} = \frac{0.5}{2} ((8.5 \times 10.0) + (9.5 \times 11.0)) = 25 \text{ cu ft}$$

(5) For Open Cut

Depth of excavation, downstream end = 7.0 ft

Depth of excavation, upstream end = 0.0 ft

Average depth of cut = 3.5 ft

$$z = \frac{((3.5 - 7.0) + (3.5 - 0.0))}{2} = 0.0 \text{ ft}$$

$$\text{Vol} = 0.0 \text{ cu ft}$$

Total volume of additional excavation

Radiation Section (R_2)	=	3212 cu ft
Radiation Section (R_1)	=	2015 cu ft
Blast Section	=	2740 cu ft
Transition Section	=	25 cu ft
Open Cut	=	0 cu ft
		<hr/>
		7992 cu ft

Entrance structure volume

Radiation Section (R_2)	= $\pi \times (5.33)^2 \times 10.0$	=	893 cu ft
	$\pi \times (4.50)^2 \times 6.0$	=	381 cu ft
Radiation Section (R_1)	= $\pi \times (4.5)^2 \times 16.0$	=	1015 cu ft
Blast Section	= $\pi \times (4.83)^2 \times 18.0$	=	1320 cu ft
Transition Section	= $\pi \times (4.66)^2 \times 13.0$	=	885 cu ft
Open Cut	$1/4 \times (28.5 + 3.66) \times 6.5$	=	53 cu ft
			<hr/>
			4537 cu ft

Volume of Backfill $7992 - 4537 = 3455$ cu ft

(b) Open Cut Section

Slope surface area requiring stabilization assuming a 2:1 slope

$$15.0 \times 9.0 \times 1/2 \times 2 = 135 \text{ sq ft}$$

Assume slope stabilization consisting of 3 in. concrete slab or equivalent

$$C_f = 0.75 \text{ \$/sq ft}$$

$$C_T = 0.75 \times 135 = 102 \text{ \$}$$

Stair costs from Section 2.2.9

$$C_T = 10 \text{ steps at } 30 \text{ \$/step} = 180.00 \text{ \$}$$

(c) Emergency Exit

The 500 man shelter serviced by a blast-resistant entrance-way requires two emergency exits. From Table 7-2, the required length of emergency exit is assumed equal to the depth to entrance level. Unit cost from Section 2.8.4

$$C_T = 14.00 \times 19.00 = 266 \text{ \$}$$

Total Cost

Surface Transition Section (Open Cut)

Side Slope Stabilization	=	102
Stairs 10 steps at 30 \$/step	=	300

Depth Transition Section

Prestressed Concrete Cylindrical Shell 4.90 x 9.33 x π x 13.0	=	1867
Stairs 13 steps at 30 \$/step	=	390
Structural Steel Blast Expansion Ring 2.90 x 9.33 x π x 2.5	=	212

Blast Section

Reinforced Concrete Cylindrical Shell 2.37 x 9.33 x π x 9.23	=	668
Reinforced Concrete Compression Rings 8.37 x 8.50 x π x 2	=	447
Concrete Frame Beams Between Rings 17.41 x 3.66 x 2	=	128
Prestressed Concrete Blast Door	=	231
Blast Door Support Channels	=	683
Blast Door Roller Supports	=	1080
Blast Door Latch	=	290
Reinforced Concrete Door Sleeve	=	462
Reinforced Concrete Dome End 2.48 x 2 x π x (4.83) ²	=	363
Stairs 5 steps at 30 \$/step	=	150

Radiation Section

Reinforced Concrete Cylinder	51.70 x 22.00	=	1138
	1.99 x π x 10.66 x 10.00	=	666
Radiation Barrier Wall		=	437
Emergency Exit	2 x 266	=	532
Excavation	0.36 x 7992	=	288
Backfill	0.33 x 3455	=	113
Haul	0.26 x 4537	=	120

Total \$ 10,528

7.4.4 Tension Cubicle (Sample Analysis and Cost Evaluation)

TRIAL DESIGN 7.44 - 50 D4

CONFIGURATION

One story cubicle (Fig. 7-13)

STRUCTURAL SYSTEM AND INPUT PARAMETERS (Fig. 7-4)

Transition Section -

Material: Reinforced concrete cubicle

Orientation: Makes ~ 39 deg angle with horizontal plane and is perpendicular to long axis of the shelter

Dimension: H 8 ft-0 in.; B 7 ft-4 in.; length 11 ft -0 in.;
change in elevation between entrance and exit
7 ft-1 1/2 in.

Primary Design Loads: $q_I = 103$ psi; $q_{Ed} = 50$ psi

Blast Section -

Material: Reinforced concrete cubicle

Orientation: \sim Horizontal; perpendicular to long axis of shelter

Dimension: H 8 ft-0 in.; B 7 ft-4 in.; length 17 ft-6 in.

Primary Design Loads: $q_I = 103$ psi; $q_{Ed} = 50$ psi

Radiation Section (R_1) -

Material: Reinforced concrete cubicle

Orientation: \sim Horizontal, parallel to long axis of shelter

Dimensions: H 8 ft-0 in.; B 7 ft-4 in.; length 16 ft-0 in.

Primary Design Load: $q_{Ed} = 50$ psi

Radiation Section (R_2) -

Material: Reinforced concrete cubicle

Orientation: \sim Horizontal; perpendicular to long axis of shelter

Dimension: H 8 ft-0 in.; B 7 ft-4 in.; length 16 ft

Primary Design Load: $q_{Ed} = 50$ psi

Note: These dimensions may require subsequent modification due to radiation design requirements.

Shelter -

Capacity: 1000 Man (Table 7-2)

Primary Design Load: $q_{Ed} = 50$ psi

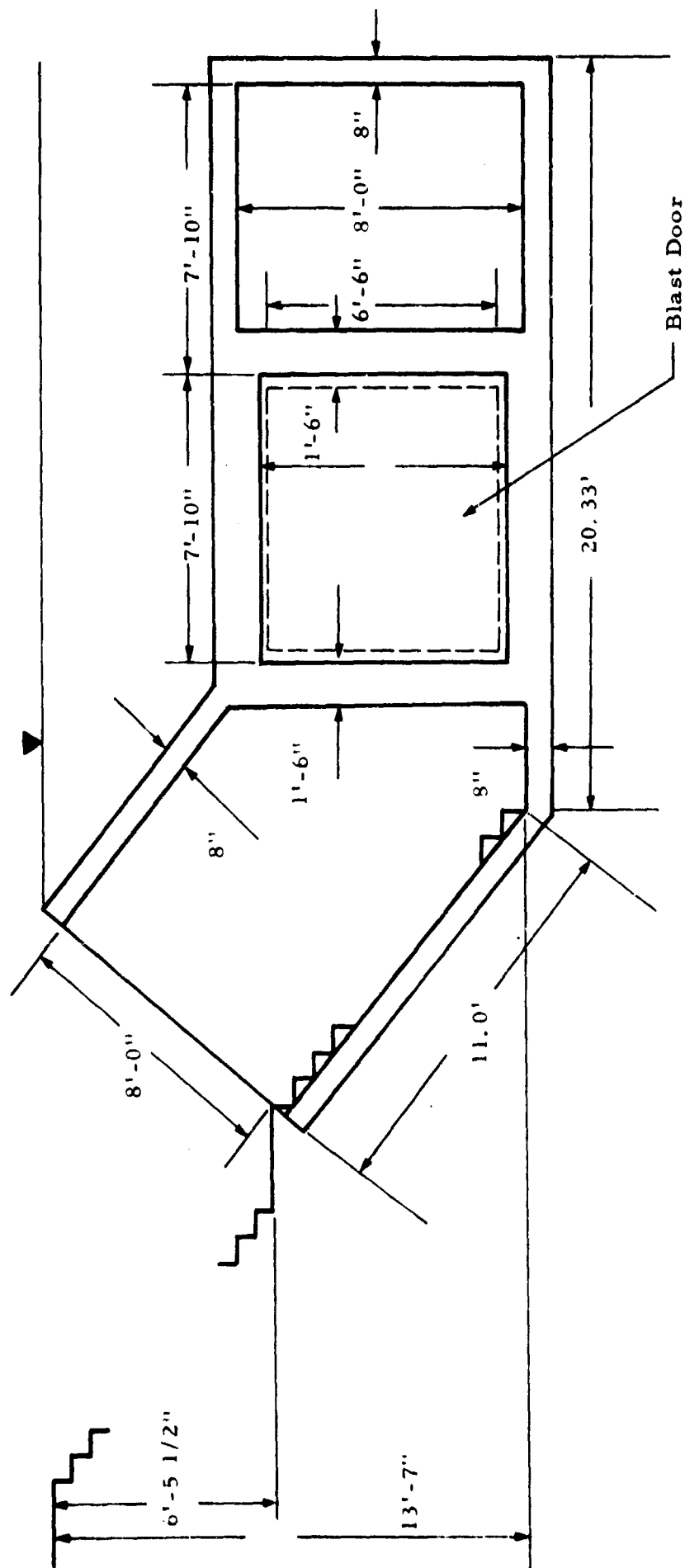


Fig. 7-13 SECTIONAL VIEW OF TENSION CUBICLE

1. Blast Analysis

(a) Transition Section: Design of Reinforced Concrete Slab

$$q_{\text{design}} = q_I - q_{Ed} - q_{Es}$$

Neglecting q_{Es}

$$q = 103 - 50 = 53 \text{ psi}$$

From Fig. 7-3 ($q = 53 \text{ psi}$; 4 lane entranceway, $f'_c = 6000 \text{ psi}$; $f_{dy} = 75,000 \text{ psi}$)

$$D = 8.0 \text{ in.}$$

Assume a linear variation of ϕ_R in zone A-B

$$\phi_R = 0.65 + \frac{43}{67} \times 0.60 = 1.05 \text{ percent}$$

$$d = 0.9D = 7.2 \text{ in.}$$

(b) Transition Section: Cost Factors for Reinforced Concrete Slab

From Section 6.2.2

Concrete

$$C_c = \frac{7.2}{10.8} \times 1.30 = 0.87 \text{ \$/sq ft} \quad (6-3)$$

Moment Steel

$$C_s = \frac{1.05 \times 7.2}{1200} \left[1.531 + 0.00334 \times \frac{75,000}{6000} \right] \times 85.8 = 1.06 \text{ \$/sq ft} \quad (6-4a)$$

Tie Steel

$$C_{st} = \frac{7.2 \times 0.2 \times 78.8}{10,800} = 0.11 \text{ \$/sq ft} \quad (6-5)$$

Forms

$$C_f = 1.00 \text{ \$/sq ft} \quad (6-6)$$

Summary

$$C_t = 0.87 + 1.06 + 0.11 + 1.00 = 3.04 \text{ \$/sq ft} \quad (6-7)$$

(c) Blast Section: Design of Reinforced Concrete Slab

Same as Section (a)

(d) Blast Section: Cost Factors for Reinforced Concrete Slab

Same as Section (b)

IIT RESEARCH INSTITUTE

(e) Blast Section: Design of Reinforced Concrete Blast Door
Support Frame Design

In this example, the short span of the door is in the vertical direction. The bulk of the blast door loading is thus carried by the horizontal framing members which run parallel to the long axis of the shelter. These members, in turn, frame into the vertical members which run along the vertical edges of the doorway. The actual distribution of the load which is carried by these vertical members is a function of relative displacements, and is beyond the scope of the simplified analysis used in this study. For the range of dimension parameters encountered in these examples, it is conservative to neglect two way action and to assume the same design requirements for the vertical and the horizontal members.

From Section 6.2.2, the design of the horizontal member is as follows:

$$\text{Required } d = \left[\frac{36.5}{1045 + 0.0209 \phi_v f_{dy}} \right] \left[\frac{q_I (6 L_S + b) f_{dy}}{6 f'_c} \right]^{1/2} \quad (6-136)$$

Assume $D = 18.0$ in.; $f'_c = 6000$ psi; $f_{dy} = 75,000$ psi; $\phi_v = 0.15$;

$$d = \left[\frac{36.5 \times 7.33}{1045 + 393} \right] \left[\frac{103 (6 \times 6.50 + 12.0) 75,000}{12.0 \times 6000} \right]^{1/2} = 15.45$$

$$D = \frac{15.45}{0.9} = 17.20 < 18.0 \therefore \text{OK} \quad \text{Use } D = 18.0 \text{ in.}$$

$$\phi_e = \left[\frac{1045 + 0.0209 \phi_v f_{dy}}{f_{dy}} \right]^2 f'_c \quad (6-135)$$

$$\phi_e = \left[\frac{1045 + 235}{75,000} \right]^2 \times 6000 = 1.75 \text{ percent}$$

$$\phi_{vt} = \frac{600 q_I b L_S - 70 b^2 D (f'_c)^{2/3}}{b^2 D f_{dy}} \quad (6-137)$$

$$\phi_{vt} = \frac{(600 \times 103 \times 12 \times 6.50) - (70 \times 144 \times 18 \times 330)}{144 \times 18.0 \times 60,000} < 0$$

∴ No ϕ_{vt} required

Design of horizontal tensile strut

$$\text{Required } D_{\text{strut}} = \frac{36 q_I (L_S + b/6) H}{(0.45 f'_c + 3 \sqrt{f'_c}) b_{\text{strut}}} \quad (6-140b)$$

In this instance replace L_S with L_L

$$D = \frac{36 \times 103 \times (7.33 + 2.0) 8.0}{(0.45 \times 6000 + 234) \times 12.0} = 7.87 \text{ in.}$$

Use $D = 8.0$ in.

$$T_{sp} = 0.45 f'_c D_{\text{strut}} \quad (6-140a)$$

$$T_{sp} = 21,600 \text{ lb}$$

$$L_{sp} = \frac{b T_{sp}}{F_{sp}} \quad (6-141)$$

Assuming 1/2 ϕ 270 K prestressing strand

$$L_{sp} = \frac{12.0 \times 21,600}{23,150} = 11.13 \text{ ft/ft}$$

(f) Blast Section: Cost Factors for Blast Door Support Frame,
Vertical and Horizontal Framing Members

Concrete

$$C_c = \frac{120 \times 18.0}{144} \times 1.30 = 1.50 \text{ \$/ft} \quad (6-143)$$

Moment Steel

$$C_s = \frac{1.75 \times 12.0 \times 18.0}{10,650} \times 85.8 = 3.12 \text{ \$/ft} \quad (6-144)$$

Shear Steel

$$C_v = \frac{0.15 \times 12.0 \times 18.0}{900} \left[0.196 \times 0.15 + 0.347 \right] \times 92.5 = 1.26 \text{ \$/ft} \quad (6-145)$$

Forms

$$C_f = \left(\frac{12.0 + 18.0}{6} \right) 1.00 = 5.00 \quad (6-146)$$

Summary

$$C_t = 1.50 + 3.12 + 1.26 + 5.00 = 10.88 \text{ \$/ft} \quad (6-147)$$

Horizontal Member (Tension Strut)

Concrete

$$C_c = \left(\frac{8.0 \times 12.0}{144} \right) \times 1.30 = 0.87 \text{ \$/ft} \quad (6-148)$$

Prestress Steel

$$C_{sp} = 11.13 \times 0.19 = 2.12 \text{ \$/ft} \quad (6-150)$$

Forms

$$C_f = \left(\frac{12.0 + 16.0}{12} \right) \times 1.00 = 2.50 \text{ \$/ft} \quad (6-151)$$

Summary

$$C_t = 0.87 + 2.12 + 2.50 = 5.49 \text{ \$/ft} \quad (6-152)$$

(g) Blast Section: Design of Prestressed Concrete Blast Door

Assume $f'_{dc} = 6000 \text{ psi}$; $\alpha = 6.5/7.33 = 0.890$; $1/\alpha = 1/12$

\therefore From Table 6-3, $K_{10} = 0.052$

$$\text{Required } D = L_S \left[\frac{864 q_I K_{10}}{0.45 f'_c + 3\sqrt{f'_c}} \right]^{1/2} \quad (6-91)$$

$$D = 6.50 \left[\frac{864 \times 103 \times 0.0520}{2700 + 234} \right]^{1/2} = 8.17 \text{ in.}$$

\therefore Use $D = 9.0 \text{ in.}$

$$L_{sp} = \frac{2.70 f'_c D}{F_{sp}} \quad (6-92)$$

Assuming $1/2 \phi 270 \text{ K}$ prestressing strand

$$L_{sp} = \frac{2.70 \times 6000 \times 9.0}{23,150} = 5.60 \text{ ft}$$

In this case, the bending moment in the long direction is approximately the same as for the short direction. Accordingly, prestressing steel is used in both directions.

$$\text{Effective } D = 6.50 \left[\frac{864 \times 103 \times 0.438}{2700 + 234} \right]^{1/2} = 6.75 \text{ in.}$$

$$L_{sp} = \frac{2.70 \times 6000 \times 6.75}{23,150} = 4.70 \text{ ft}$$

IIT RESEARCH INSTITUTE

Check for pure shear

$$\text{Required } D_{\text{shear}} \geq \frac{30 q L_S}{f'_c} \quad (6-96)$$

$$D = \frac{30 \times 103 \times 6.50}{6000} = 3.30 < 9.0 \text{ in. } \therefore \text{OK}$$

(f) Blast Section: Cost Factors for Blast Door

Concrete

$$C_c = \frac{9.0}{12} \times 1.30 = 0.98 \text{ \$/ft} \quad (6-97)$$

Prestress Steel

$$C_{sp} = (5.60 + 4.70) \times 0.19 = 1.96 \text{ \$/ft} \quad (6-99)$$

Forms

$$C_f = 1.00 \quad (6-100)$$

Summary

$$C_t = 0.98 + 1.96 + 1.00 = 3.94 \text{ \$/sq ft}$$

Total area of door includes 3.0 in. overlap on all sides

$$(L_S + 0.5) \times (L_L + 0.5) = (7.0 \times 7.83) = 54.80 \text{ sq ft}$$

$$C_T = 3.94 \times 54.80 = 216 \text{ \$}$$

(g) Blast Section: Design of Blast Door Support Structure

Hardware

Assume the use of American Standard Channels. Requirement for web length between flanges $d_w \geq 9.0$ in. Try 12 in. channel!

$$t_w = \frac{785}{42,000} \left(\frac{9.975}{2} \right)^2 = 0.455 \quad (6-131)$$

Use 12 [30 since $0.50 > 0.455$

Total length of channel required

$$4 (L_L + 0.5) + 2 (L_S + 0.5) = 4 (7.83) + 2 (7.0) = 45.4 \text{ ft}$$

(h) Blast Section: Cost Factors for Blast Door Support Structure Hardware

(1) Channels

From Table 2-2 $X_s = 0.207$ \$/lb for $f_y = 50,000$ psi

$$C_T = 30.0 \times 0.204 \times 45.4 = 278 \text{ \$}$$

(2) Roller Supports

From Section 2.8.2

$$C_T = 30 n_L \quad D = 30 \times 4 \times 9.0 = 1080 \text{ \$}$$

(3) Blast Door Latch

From Section 2.8.3

$$C_T = [25.00 + 10D] n_L^{1/2} = (25.00 + 90.00) \times 2 = 230 \text{ \$}$$

(i) Radiation Section: Design and Cost Factors for Compression Cubicle

From Table 7-5,

$$\text{Cost \$ / ft of cubicle} = 64.80 \text{ \$}$$

Although this is slightly more than the equivalent cylinder cost per foot, the cubicle is the less expensive of the two when excavation costs and overall lengths of section are determined.

2. Radiation Analysis

(a) Prompt Radiation Overhead Shelter Contribution

As outlined in Section 5.3.2

For overhead burst orientation ($B_p = 90$ ft; $H_p = 96$ ft;

$Z = 5.0$ ft; $\omega = 0.903$ solid radians; $\beta_B = 0$ deg; $\beta_S = 90$ deg; $\rho_m = 450$ psi;
 $W = 1$ MT; $p_{so} = 32$ psi)

$$\gamma = 865 \times 0.99 \times 0.014 = 12.0 \text{ rads}$$

$$N = 9.6 \times 0.99 \times 0.003 = \text{negligible}$$

MIT RESEARCH INSTITUTE

For entranceway burst orientation ($B_p = 90$ ft; $H_p = 96$ ft;
 $Z = 5.0$ ft; $\omega = 0.903$ solid radians; $\beta_B = 50$ deg; $\beta_S = 40$ deg; $\rho_m = 450$ psi;
 $W = 1$ MT; $p_{so} = 32$ psi)

$$\gamma = 1380 \times 0.94 \times 0.0008 = 1.03 \text{ rads}$$

$$N = 20.8 \times 0.95 \times 0.00015 = \text{negligible}$$

(b) Prompt Radiation Entranceway Contribution

For overhead burst orientation

(1) Transition Section - Detector No. 1 at bottom of stairs
 3.0 ft above floor

Entranceway Contribution ($B_p = 7.33$ ft; $H_p = 8.0$ ft;
 $Z = 9.0$ ft; $\therefore \omega = 0.10$ solid radians; $\beta_B = 50$ deg)

$$\gamma = 865 \times 0.10 = 86.5 \text{ rads}$$

$$N = 9.6 \times 0.19 = 1.83 \text{ rads}$$

Overhead Contribution ($B_p = 7.33$ ft; $H_p = 8.00$ ft;
 $Z = 5.0$ ft; $\therefore \omega = 0.25$ solid radians; $\rho_m = 250$ psf; $\beta_B = 0$ deg; $\beta_S = 90$ deg)

$$\gamma = 865 \times 0.82 \times 0.11 = 78 \text{ rads}$$

$$N = 9.6 \times 0.60 \times 0.06 = 0.01 \text{ rads}$$

Total

$$\gamma = 86.5 + 78.0 = 164.5 \text{ rads}$$

$$N = 1.83 + 0.01 = 1.84 \text{ rads}$$

It is obvious from these totals that neutron effects can be neglected.

(2) Blast Section - Detector No. 2 opposite center of blast
 door 3.0 ft above floor

Entranceway Contribution ($B_p = 7.33$ ft; $H_p = 8.0$ ft;
 $Z = 7.0$ ft; $\therefore \omega = 0.18$ solid radians; $\beta_B = 0$ deg)

$$\gamma = 164.5 \times 0.78 = 128.0 \text{ rads}$$

Overhead Contribution ($B_p = 7.33$; $H_p = 19.0$; $Z = 5.0$ ft;
 $\omega = 0.30$; $\beta_B = 0$ deg; $\beta_S = 90$ deg; $\rho_m = 500$ psf)

$$\gamma = 8.65 \times 0.84 \times 0.008 = 5.8 \text{ rads}$$

$$\text{Total } \gamma = 128.0 + 5.8 = 133.8 \text{ rads}$$

(3) Radiation Section (R_1) - Detector No. 3 at down-stream end 3.0 ft above floor

Entranceway Contribution ($B_p = 7.33$; $H_p = 8.0$ ft;
 $Z = 20.0$ ft; $\therefore \omega = 0.025$; $\beta_B = 90$ deg; $\beta_S = 0$ deg; $\rho_m = 112.5$ psf;
 $R_{fc_1} = 0.1$; $\therefore \omega' = 0.0025$)

$$\gamma = 133.8 \times 0.17 \times 0.40 = 9.1 \text{ rads}$$

Overhead Contribution ($B_p = 7.33$; $H_p = 16.0$ ft;
 $Z = 5.0$ ft; $\therefore \omega = 0.25$; $\beta_B = 0$ deg; $\beta_S = 90$ deg; $\rho_m = 500$ psf)

$$\gamma = 865 \times 0.80 \times 0.008 \times 5.54 \text{ rads}$$

$$\text{Total } \gamma = 9.1 + 5.54 = 14.64 \text{ rads}$$

(4) Radiation Section (R_2) - Detector No. 4 at down-stream end 3.0 ft above floor

Entranceway Contribution ($B_p = 7.33$; $H_p = 8.0$ ft;
 $Z = 16.0$ ft; $\therefore \omega = 0.035$; $\beta_B = 90$ deg; $R_{fc_2} = 0.5$; $\therefore \omega' = 0.017$)

$$\gamma = 14.64 \times 0.4 = 5.85 \text{ rads}$$

Overhead Contribution (Same as For Detector No.3)

$$\gamma = 5.54 \text{ rads}$$

$$\text{Total } \gamma = 5.85 + 5.54 = 11.39 \text{ rads}$$

For Entranceway Weapon Burst Orientation

(1) At Detector No. 1

Entranceway Contribution ($B_p = 7.33$ ft; $H_p = 8.0$ ft; $Z = 9.0$ ft;
 $\omega = 0.10$; $\beta_B = 0$ deg)

$$\gamma = 1380 \times 0.66 = 912 \text{ rads}$$

Overhead Contribution ($B_p = 7.33$ ft; $H_p = 8.00$ ft; $Z = 5.0$ ft;
 $\therefore \omega = 0.25$; $\rho_m = 250$ psf; $\beta_B = 50$ deg; $\beta_S = 40$ deg)

$$\gamma = 1380 \times 0.23 \times 0.015 = 4.75 \text{ rads}$$

$$\text{Total } \gamma = 912 + 4.75 = 916.75 \text{ rads}$$

(2) At Detector No. 2

Entranceway Contribution ($B_p = 7.33$ ft; $H_p = 8.0$ ft; $Z = 7.0$ ft;
 $\therefore \omega = 0.18$; $\beta_B = 0$ deg)

$$\gamma = 916.75 \times 0.78 = 715 \text{ rads}$$

Overhead Contribution ($B_p = 7.33$ ft; $H_p = 19.0$ ft; $Z = 5.0$ ft;
 $\therefore \omega = 0.30$; $\beta_B = 50$ deg; $\beta_S = 40$ deg; $\rho_m = 500$ psf)

$$\gamma = 1380 \times 0.84 \times 0.00023 = 0.27 \text{ rads}$$

The reduction factors for Detectors No. 3 and No. 4 are summarized:

Detector No. 3 - $R_{fe} = 0.17$; $R_{fb} = 0.40$; ($R_{fc_1} = 0.1$)

Detector No. 4 - $R_{fe} = 0.4$; ($R_{fc_2} = 0.5$)

Neglecting overhead contribution at Detector No. 3

At Detector No. 4

Entranceway Contribution

$$\gamma = 715 \times 0.17 \times 0.40 \times 0.4 = 19.5 \text{ rads}$$

Overhead Contribution ($B_p = 7.33$ ft; $H_p = 16.0$ ft; $Z = 5.0$ ft;
 $\therefore \omega = 0.25$; $\beta_B = 50$ deg; $\beta_S = 40$ deg; $\rho_m = 500$ psf)

$$\gamma = 1380 \times 0.80 \times 0.0023 = 0.26 \text{ rads}$$

$$\text{Total } \gamma = 19.5 + 0.3 = 19.8 \text{ rads}$$

(c) Fallout Radiation

As outlined in Section 5.7 and detailed in Design Example 7.4.1

Fallout Overhead Shelter Contribution ($\omega = 0.903$; $\rho_m = 450$

psf; Case I)

$$\gamma = 8.6 \times 10^4 \times 0.99 \times 0.00002 = 1.73 \text{ rads}$$

Fallout Entranceway Contribution

(1) At Detector No. 2 γ dose = 8.6×10^4 rads

(2) At Detector No. 3 ($\omega = 0.025$; $\rho_m = 112.5$ psf; Case II)

$$\gamma = 8.6 \times 10^4 \times 0.04 \times 0.066 = 227 \text{ rads}$$

Downstream from this detector, fallout radiation is treated in the same manner as prompt radiation.

(3) At Detector No. 4 ($\omega = 0.035$; $\beta_B = 90$ deg; $R_{fc1} = 0.1$;
 $\therefore \omega' = 0.0035$)

$$\gamma = 227 \times 0.2 = 45.4 \text{ rads}$$

(d) Worst Case Radiation Dose at Entrance to Shelter

(1) Overhead Burst Orientation

(a) Shelter Overhead Contribution

Prompt $\gamma = 12.00$ Prompt N = negligible

Fallout $\gamma = 1.73$

13.73 rads Total = 13.73 rads

Allowable dose through entranceway = $40.00 - 13.73 = 26.27$ rads

(b) Entranceway Contribution

Prompt $\gamma = 11.39$ Prompt N = negligible

Fallout $\gamma = 45.4$

56.79 rads Total = 56.79 rads

$$\text{Required } R_{fb} = \frac{26.27}{56.79} = 0.454$$

(2) Entranceway Burst Orientation

(a) Shelter Overhead Contribution

Prompt $\gamma = 1.03$ Prompt N = negligible

Fallout $\gamma = 1.73$

2.76 rads Total = 2.76 rads

IIT RESEARCH INSTITUTE

Allowable dose through entranceway = $40.00 - 2.76 = 37.34$ rads

(b) Entranceway Contribution

$$\begin{array}{rcl} \text{Prompt } \gamma & = & 19.8 \\ \text{Prompt } \gamma & = & 45.4 \\ \hline & & 65.2 \text{ rads} \end{array} \quad \begin{array}{l} \text{Prompt N = negligible} \\ \\ \text{Total} = 65.2 \text{ rads} \end{array}$$

∴ Worst case is overhead burst orientation ; $R_{f_b} = 0.454$

(e) Radiation Barrier Shielding Design

From Fig. 5-4 ($R_{f_b} = 0.454$; $\beta_s = 90$ deg)

$$\rho_m = 95 \text{ psf}$$

$$\text{Required } D = \frac{9.5}{12.5} = 7.6 \text{ in.}$$

Use $D = 8.0$ in.

Since the shelter is a one story cubicle whose configuration is similar to that of the entranceway, the barrier shielding wall is placed in the shelter proper. In this instance, particular advantage can be gained by using interior bearing walls of the shelter as barrier shielding.

Area of barrier wall

$$A = 8.0 \times 8.0 = 64.0 \text{ sq ft}$$

Required additional $D = 8.0 - 4.0 = 4.0$ in.

(f) Radiation Barrier Shielding Cost Factor

Assuming $f'_c = 2000$ psi

Concrete

$$C_c = \frac{D}{12} X_c = \frac{4.0}{12} \times 78.8 = 0.27 \text{ \$/sq ft}$$

Steel

$$C_s = \frac{D \phi_t X_s}{1200} = \frac{4.00 \times 0.5 \times 78.8}{1200} = 0.14 \text{ \$/sq ft}$$

Forms

$$C_f = (\text{Included in shelter costs})$$

Summary

$$C_t = 0.27 + 0.14 = 0.41 \text{ \$/sq ft}$$

$$C_T = 0.41 \times 64.0 = 27 \$$$

IIT RESEARCH INSTITUTE

3. Total Cost

(a) Excavation and Backfill

Assuming an existing 1:1 slope cut excavation for the shelter, the volume of the additional excavation required can be determined from Eq. (7-8).

(1) For Radiation Section (R_2)

Depth of excavation at side of shelter ≈ 14.0 ft

Depth of excavation at upstream end of section = 0.0 ft

Average depth of radiation section (R_2) = 14.0 ft

$$z = \frac{(14.0 - 14.0) + (14.0 - 0.0)}{2} = 7.0 \text{ ft}$$

$$\text{Vol} = \frac{7.0}{2} ((8.0 \times 16.0) + (22.0 \times 23.0)) = 2220 \text{ cu ft}$$

(2) For Radiation Section (R_1)

Depth of excavation at downstream end = 14.0 ft

Depth of excavation at upstream end = 0.0 ft

Average depth of radiation section (R_1) = 14.0 ft

$$z = \frac{(14.0 - 14.0) + (14.0 - 9.0)}{2} = 7.0 \text{ ft}$$

$$\text{Vol} = \frac{7.0}{2} ((8.0 \times 16.0) + (22.0 \times 23.0)) = 2220 \text{ cu ft}$$

(3) For Blast Section

Depth of excavation at downstream end = 10.0 ft

Depth of excavation at upstream end = 11.0 ft

Average depth of blast section = 14.0 ft

$$z = \frac{(14.0 - 11.0) + (14.0 - 10.0)}{2} = 3.5 \text{ ft}$$

$$\text{Vol} = \frac{3.5}{2} ((8.66 \times 17.5) + (15.66 \times 20.0)) = 795 \text{ cu ft}$$

(4) For Transition Section

Depth of excavation downstream end = 14.0 ft

Depth of excavation upstream end = 6.0 ft

Average depth of transition section = 10.75 ft

$$z = \frac{(10.75 - 14.0) + (10.75 - 6.0)}{2} = 0.75$$

$$\text{Vol} = \frac{0.75}{2} ((8.66 \times 8.00) + (10.16 \times 8.75)) = 60 \text{ cu ft}$$

(5) For Open Cut

Depth of excavation downstream end = 6.5 ft

Depth of excavation upstream end = 0.0 ft

Average depth of transition section = 3.25 ft

$$z = \frac{(3.25 - 6.5) + (3.25 - 0)}{2} = 0$$

$$\text{Vol} = 0 \text{ cu ft}$$

Total Volume of Additional Excavation

Radiation Section (R_2)	=	2220 cu ft
Radiation Section (R_1)	=	2220 cu ft
Blast Section	=	795 cu ft
Open Cut	=	0 cu ft
		<hr/>
		5235 cu ft

Entrance Structure Volume

Radiation Section (R_2)	=	8.00 x 8.66 x 16.0	=	1110 cu ft
Radiation Section (R_1)	=	8.00 x 8.66 x 16.0	=	1110 cu ft
Blast Section	=	8.66 x 9.33 x 17.5	=	1410 cu ft
Transition Section	=	8.66 x 9.33 x 11.0	=	890 cu ft
Open Cut	=	1/4 x (33.33 + 7.33) 6.5	=	65 cu ft
				<hr/>
				4585 cu ft

Volume of Backfill

$$5235 - 4595 = 740 \text{ cu ft}$$

IIT RESEARCH INSTITUTE

(b) Open Cut Section

Slope surface area requiring stabilization, assuming a 2:1
slope

$$15.0 \times 10.0 \times 1/2 \times 2 = 150 \text{ sq ft}$$

Assume slope stabilization consisting of 3 in. concrete slab
or equivalent

$$C_f = 0.75 \text{ \$/sq ft}$$

$$C_T = 0.75 \times 150 = 113 \text{ \$}$$

Stair costs from Section 2.2.9

$$C_T = 10 \text{ steps at } 35.00 \text{ \$/step} = 350.00 \text{ \$}$$

(c) Emergency Exit

The 1000 man shelter serviced by a blast-resistant entrance-way requires two emergency exits. From Table 7-2 the required length of emergency exit is assumed equal to the depth to entrance level. Unit cost from Section 2.8.4

$$C_T = 14.00 \times 13.33 = 187 \text{ \$}$$

Total Cost

Surface Transition Section (Open Cut)

Side Slope Stabilization	=	113
Stairs 10 steps at 35.00 \$/step	=	350

Depth Transition Section

Reinforced Concrete Cubicle 3.04 x 2 (8.66 + 8.00) x 11.00	=	1120
Stairs 11 steps at 35.00 \$/step	=	385

Blast Section

Reinforced Concrete Cubicle 3.04 x 2 (8.66 + 8.00) x 15.75	=	1595
Reinforced Concrete Blast Door Frame 10.88 x 31.33	=	341
Prestressed Concrete Tension Strut 5.49 x 29.33	=	161
Prestressed Concrete Blast Door	=	216
Blast Door Support Channels	=	278
Blast Door Roller Supports	=	1080
Blast Door Latch	=	230
Reinforced Concrete Cubicle End 3.04 x 8.66 x 9.33	=	246

Radiation Section

Reinforced Concrete Compression Cubicle 64.80 x 32.0	=	2080
Radiation Barrier Wall	=	27
Emergency Exit 187 x 2	=	374
Excavation 0.036 x 5235	=	188
Backfill 0.033 x 740	=	25
Haul 0.026 x 4585	=	119

\$ 9040

7.5 NONBLAST-RESISTANT ENTRANCEWAY DESIGN

7.5.1 Compression Cylinder (Sample Analysis and Cost Evaluation)

TRIAL DESIGN 7.5.1 - 325 E4

CONFIGURATION

One story cubicle and cylinder

STRUCTURAL SYSTEM AND INPUT PARAMETERS (Fig. 7-5)

Transition Section -

Material: Reinforced concrete cubicle

Orientation: Makes ~ 39 deg angle with horizontal plane and is perpendicular to long axis of the shelter

Dimension: H = 8 ft-0 in.; B = 7 ft-4 in.; length = 13 ft-0 in.; change in elevation between entrance and exit 8 ft-3 1/2 in.

Primary Design Load: $q_E = 10$ psi

Radiation Section (R_1) -

Material: Reinforced concrete cubicle

Orientation: \sim Horizontal and is perpendicular to long axis of the shelter

Dimensions: H = 8 ft-0 in.; B = 7 ft-4 in.; length = 16 ft-0 in.; change in elevation between entrance and exit 1 ft-6 in.

Primary Design Load: $q_E = 10$ psi

Radiation Section (R_2) -

Material: Reinforced concrete cubicle

Orientation: \sim Horizontal and is parallel to long axis of the shelter

Dimensions: H = 8 ft-0 in.; B = 7 ft-4 in.; length 16 ft-0 in.; change in elevation between entrance and exit 1 ft-6 in.

Primary Design Load: $q_E = 10$ psi

Note: These dimensions may require subsequent modification due to radiation design requirements.

Blast Section -

Material: Reinforced concrete cylinder

Orientation: \sim Horizontal and is perpendicular to long axis of the shelter

Dimensions: I. D. 13 ft-0 in.; length 20 ft-0 in.; change in elevation between entrance and exit ~ 1 ft-6 in.

Primary Design Load: $q_E = 772$ psi

Shelter -

Capacity: 1000 Man (Table 7-2)

Primary Design Load: $q_{Ed} = 325$ psi

1. Blast Analysis

(a) Transition and Radiation Section: Design and Cost Factors

From Table 7-5 ($q = 10$ psi, 4 lane)

(1) Wall

$$f'_c = 4000 \text{ psi}$$

$$\phi_L = 0.65$$

$$f_{dy} = 60,000 \text{ psi}$$

$$D = 4.0 \text{ in.}$$

$$\phi_R/\phi_L = 0.5$$

$$C_t = 1.71 \text{ \$/sq ft}$$

(2) Roof

$$f'_c = 4000 \text{ psi}$$

$$\phi_L = 0.55$$

$$f_{dy} = 75,000 \text{ psi}$$

$$D = 4.00 \text{ in.}$$

$$\phi_R/\phi_L = 0.75$$

$$C_t = 1.73 \text{ \$/sq ft}$$

$$C_T = 55.10 \text{ \$/ft of cubicle}$$

(b) Blast Section: Design of Reinforced Concrete Cylindrical Shell

Assume reinforced concrete $f'_{dc} = 7500$ psi; $f_{dy} = 60,000$ psi;

$$\phi_t = 0.5 \text{ percent; } D = 10 \text{ in.}$$

$$\text{Required } D = \frac{772 (6 \times 13.0 + 10.0)}{6638 + 300} = 9.8 \text{ in.} \quad (6-26)$$

\therefore Use $D = 10.0$ in.

(c) Blast Section: Cost Factors for Reinforced Concrete Cylindrical Shell

Concrete

$$C_c = \frac{10.0}{12} \times 1.30 = 1.09 \text{ \$/sq ft} \quad (6-28)$$

Steel

$$C_s = \frac{10.0}{1200} \times 0.6 \times 85.8 = 0.44 \text{ \$/sq ft} \quad (6-29)$$

Forms

$$C_f = 1.40 \text{ \$/sq ft} \quad (6-30)$$

Summary

$$C_t = 1.09 + 0.44 + 1.40 = 2.93 \text{ \$/sq ft}$$

IIT RESEARCH INSTITUTE

(d) Blast Section: Design of Reinforced Concrete Compression Ring

Assume $b = 30.0$ in. ; $D = 24.0$ in.

$$\text{Required } D_{(\text{ring})} = \frac{36 \times 772 \times (12.33) \times 13.0}{0.85 \times 30.0 \times 7500} = 23.35 \text{ in.} \quad (6-153)$$

Use $D = 24.0$ in.

From Eq. (6-66), $\phi_{vt} < 0$ \therefore no torsion steel required

(e) Blast Section: Cost Factors for Reinforced Concrete Compression Ring

Concrete

$$C_c = \frac{30.0 \times 34.0}{144} \times 1.30 = 6.50 \text{ \$/ft} \quad (6-157)$$

Steel

$$C_s = \frac{1.0 \times 30.0 \times 24.0}{14,400} \times 85.8 = 4.29 \text{ \$/ft} \quad (6-158)$$

Forms

$$C_f = \frac{30.0 + 24.0 \times 1.00}{6} = 9.00 \text{ \$/ft} \quad (6-159)$$

Summary

$$C_t = 6.50 + 4.29 + 9.00 = 19.79 \text{ \$/ft} \quad (6-160)$$

(f) Blast Section: Design of Beam Member Between Rings

Assume reinforced concrete beam with $b = 18.0$ in. ; $D = 24$ in. ;

$\phi_v = 0.45$; $f_{dy} = 75,000$ psi; $f'_c = 6000$ psi.

$$\text{Required } d = \left[\frac{36.5 \times 7.33}{1045 + 707} \right] \left[\frac{6 \times 325 (13.0 + 1.66) \times 75,000}{18 \times 6000} \right]^{1/2} = 21.6 \text{ in.} \quad (6-165a)$$

$$D = \frac{21.6}{0.9} = 24.0 \text{ in.} \quad \therefore \text{Use } D = 24.0 \text{ in.}$$

To determine moment steel

$$\phi_e = \left[\frac{1045 + 707}{75,000} \right]^2 \times 6000 = 3.24 \text{ percent} \quad (6-135)$$

(g) Blast Section: Cost Factors for Beam Member Between Rings

Concrete

$$C_c = \frac{18.0 \times 24.0}{144} = 3.90 \text{ \$/ft} \quad (6-167)$$

Moment Steel

$$C_s = \frac{3.24 \times 18.0 \times 24.0}{10,650} \times 85.8 = 11.30 \text{ \$/ft} \quad (6-168)$$

Shear Steel

$$C_v = \frac{0.45 \times 18.0 \times 24.0}{900} \left[0.196 \times 0.45 + 0.347 \right] \times 92.5 = 86.7 \text{ (6-169)} \\ \$/\text{ft}$$

Forms

$$C_f = \left(\frac{18.00 + 24.00}{6} \right) \times 1.00 = 7.00 \text{ \$/ft} \quad (6-170)$$

Summary

$$C_t = 3.90 + 11.30 + 8.67 + 7.00 = 30.87 \text{ \$/ft} \quad (6-171)$$

(h) Blast Section: Design of Reinforced Concrete Dome End

From Section 6.5.1, q_c must exceed q_I

Assume $D = 5.00$ in.; $f'_{dc} = 7500$ psi; $f_{dy} = 60,000$ psi;

$\phi_t = 1.0$ percent

$$q_c = \frac{5.0}{(6 \times 12.00) + 5.0} \left[1.70 \times 7500 + 0.002 \times 1.0 \times 60,000 \right] = 897 \text{ psi (6-39)}$$

$892 > 772 \therefore \text{OK}$

(i) Blast Section: Cost Factors for Reinforced Concrete Dome End

Concrete

$$C_c = \frac{5.0}{12} \times 1.30 = 0.55 \text{ \$/sq ft} \quad (6-28)$$

Steel

$$C_s = \frac{5.0 \times 1.0}{1200} \times 85.8 = 0.43 \text{ \$/sq ft} \quad (6-29)$$

Forms

$$C_f = 1.75 \text{ \$/sq ft} \quad (6-30)$$

Summary

$$C_t = 0.55 + 0.43 + 1.75 = 2.73 \text{ \$/sq ft}$$

(j) Blast Section: Design of Blast Door

The practical limits, both in terms of thickness dimensions and in terms of cost, were reached in the two-lane capacity Design Example 7.4.3. Assume a blast door design which utilizes wide flange rolled shapes to span the short dimension of the doorway. Curved cover plates will be welded to the wide flange sections to carry the long span loads.

Assume gross depth of section = 12.00 in.

Effective height of door at compression ring I. D. = 6.5 ft.

($S_L = 10.66$ ft)

Effective door height at middle surface of blast door = 9.52 ft

($S_L = 15.66$ ft), \widehat{L}_L of blast door middle surface = 10.25 ft.

IIT RESEARCH INSTITUTE

For $S_L/2 = 7.83 \text{ ft}$ $L_S = 7.33 \text{ ft}$ $\mu = 4.80$ $K_{20} = 0.0517$

$\hat{L}_L = 10.25 \text{ ft}$ $\lambda = 7.33/10.25 = 0.715$ $K_{10} = 0.0756$ $\lambda^2 = 0.512$

Equivalent solid plate D required

$$D = \left[\frac{864 \times 0.0756 \times 772 \times 53.8 \times 2.38}{60,000} \left(\frac{(2.38 \times 1.156) + 0.410}{(5.22 + 4.80) \times 1.153} \right) \right]^2 \quad (6-129)$$

$$D \left(\frac{864 \times 0.0756 \times 7.72 \times 53.8 \times 0.647}{60,000} \right)^{1/2} = 5.4 \text{ in.}$$

Equivalent section modulus required

$$S = \frac{(5.4)^2}{6} = 4.87 \text{ cu in./in.}$$

Try 12I 35.0 $S = 7.2 > 4.87$ \therefore OK for moment (6-122)

Shear requirement $V = 6q_I L_S = 6 \times 772 \times 7.33 = 34,000 \text{ psi/in.}$

Web section required, assuming

$$f_{dv} = 0.6 f_{dy} = 0.6 \times 60,000 = 36,000 \text{ psi}$$

$$\therefore \text{Required } A_v = \frac{V}{f_{dv}} = \frac{34,000}{36,000} = 0.945 \text{ sq in./in.}$$

For 12I 35.0 on 5.078 in. centers

$$A_v = 0.428 \times 12.0 \times \frac{1}{5.078} = 1.01 \text{ sq in./in.}$$

$$1.01 > 0.95 \therefore \text{OK}$$

In \hat{L}_L direction the equivalent solid plate D required

Assuming $f_{dy} = 44,000 \text{ psi}$

$$D = \left[\frac{864 \times K_{20} q_I L_S^2 (1 + \lambda^2)^2}{f_{(max)}} \left(\frac{(1 + \lambda^2)^2 (1 + \nu \lambda^2) + 0.167\mu}{[(1 + \lambda^2)^4 + \mu] (1 + \nu \lambda^2)} \right) \right]^{1/2} \quad (7-10)$$

$$D = \left[\frac{864 \times 0.0517 \times 772 \times 53.8 \times 2.38}{44,000} \left(\frac{(2.38 \times 1.156) + 0.802}{(5.22 + 4.80) \times 1.153} \right) \right]^{1/2}$$

$$D = \left(\frac{864 \times 0.0517 \times 772 \times 53.8 \times 2.38 \times 0.732}{44,000} \right)^{1/2} = 5.47 \text{ in.}$$

Equivalent section modulus required

$$S = \frac{(5.47)^2}{6} = 5.00 \text{ cu in.}$$

IIT RESEARCH INSTITUTE

Assuming 1/2 plate

$$S = 2 \frac{Ad}{2} = 2 \times 0.5 \times 6.0 = 6.0$$

$$6.0 > 5.0 \therefore \text{OK}$$

Total depth of section = $12.00 + 2 \times 0.5 = 13.00$ in.

(k) Blast Section: Cost Factors for Blast Door

Minimum width

$$\hat{L}_L + 0.5 = 10.25 + 0.5 = 10.75 \text{ ft}$$

$$\text{No. of sections} = \frac{12 (\hat{L}_L + 0.5)}{b} = \frac{12 \times 10.75}{5.078} = 25.5$$

\therefore 26 required

Length of sections

$$(L_S + 0.5) = 7.83 \text{ ft}$$

Total length of sections

$$26 \times 7.83 = 203.5 \text{ ft}$$

Cost of rolled shapes (12 I 35)

$$C_t = 0.207 \times 35.0 \times 203.5 = 1475 \$$$

Cost of plates

$$C_t = 2 \times 6.08 \times 10.75 \times 7.83 = 1025 \$$$

Cost of concrete filler

$$C_c = \frac{\text{web length}}{12} \quad X_c = \frac{9.75}{12} \times 1.00 = 0.82 \$/\text{sq ft}$$

$$C_c = 0.82 \times 10.75 \times 7.83 = 69 \$$$

Total Cost of Blast Door

$$C_T = 1475 + 1025 + 69 = 2569 \$$$

(l) Blast Section: Design of Blast Door Support Structure Hardware

Assume that American Standard Channels will be used to support the blast door. A web length between flanges in excess of 13.0 in. is then required. Try 18 in. channel, check bending

$$t_w = \frac{1750}{50,000} \left(\frac{15.375}{2} \right)^2 = 2.09 \text{ sq in.}$$

IIT RESEARCH INSTITUTE

Assume a knee bracket is employed which reduces effective space to 7.68 in.

$$t_w = \frac{1750}{42,000} \left(\frac{7.68}{2} \right)^2 = 0.615$$

Use 18 [51.9; $t_w = 0.625 > 0.615 \therefore$ OK

Total Length of Channel required

$$4 (L_S + 0.5) + 2 (\hat{L}_L + 0.5) = 4 \times 7.83 + 2 \times 10.75 = 52.83 \text{ ft}$$

(m) Blast Section: Cost Factors for Blast Door Support Structure Hardware

(1) Channels

From Table 2-2, $X_s = 0.204 \text{ \$/lb}$ $f_y = 42,000 \text{ psi}$

$$C_T = 51.9 \times 0.204 \times 52.83 = 560 \text{ \$}$$

(2) Knee Brace

$$C_T = 50.00 \text{ \$}$$

(3) Roller Supports

From Section 2.8.2,

$$C_T = [50.00 + (30 \times 13.0)] \times 4 = 1760 \text{ \$}$$

(4) Blast Door Latch

From Section 2.8.3

$$C_T = [50.00 + (10 \times 13.0)] \times 2 = 360 \text{ \$}$$

(n) Blast Section: Cost Factors for Blast Door Sleeve

Concrete

$$C_c = \frac{30}{12} \times 1.30 = 0.33 \text{ \$/sq ft}$$

Steel

$$C_s = \frac{3.0}{12} \times 0.6 \times 85.8 = 0.13 \text{ \$/sq ft}$$

Forms

$$C_f = 1.40 \text{ \$/sq ft}$$

Summary

$$C_t = 0.33 + 0.13 + 1.40 = 1.86 \text{ \$/sq ft}$$

$$C_T = 1.86 \times 13.00 \times 9.00 = 218 \text{ \$}$$

2. Radiation Analysis

(a) Prompt Radiation Overhead Shelter Contribution

As outlined in Section 5.3.2

For overhead burst orientation ($B_p = 20$ ft; $H_p = 289$ ft; $Z = 6.0$ ft;
 $\therefore \omega = 0.66$ solid radians; $\beta_B = 0$ deg; $\beta_S = 90$ deg; $\rho_m = 1000$ psf; $W = 1$ MT;
 $p_{so} = 200$ psi)

$$\chi = 1.45 \times 10^5 \times 0.95 \times 5 \times 10^5 = 6.90 \text{ rads}$$

$$N = 2.27 \times 10^4 \times 0.88 \times 0.04 \times 10^{-4} = 0.08 \text{ rads}$$

For entranceway burst orientation ($B_p = 20$ ft; $H_p = 289$ ft;
 $Z = 6.0$ ft; $\therefore \omega = 0.66$ solid radians; $\beta_B = 50$ deg; $\beta_S = 40$ deg; $\rho_m = 1000$ psf;
 $W = 1$ MT; $p_{so} = 200$ psi)

$$\chi = 4.58 \times 10^5 \times 0.53 \times 0.1 \times 10^{-5} = 0.25 \text{ rads}$$

$$N = 1.29 \times 10^5 \times 0.81 \times 0.15 \times 10^{-5} = 0.16 \text{ rads}$$

(b) Prompt Radiation Entranceway Contribution

For overhead burst orientation

(1) Transition Section - Detector No. 1 at bottom of stairs

3.0 ft above floor

Entranceway Contribution ($B_p = 7.33$ ft; $H_p = 8.00$ ft;
 $Z = 13.0$ ft; $\therefore \omega = 0.054$; $\beta_B = 50$ deg)

$$\chi = 1.45 \times 10^5 \times 0.06 = 8.70 \times 10^3 \text{ rads}$$

$$N = 2.27 \times 10^4 \times 0.12 = 2.72 \times 10^3 \text{ rads}$$

Overhead Contribution ($B_p = 7.33$ ft; $H_p = 10.0$ ft; $Z = 5.0$ ft;
 $\therefore \omega = 0.28$; $\rho_m = 350$ psf; $\beta_B = 0$ deg; $\beta_S = 90$ deg)

$$\chi = 1.45 \times 10^5 \times 0.84 \times 0.04 = 4.87 \times 10^3 \text{ rads}$$

$$N = 2.27 \times 10^4 \times 0.65 \times 0.016 = 2.38 \times 10^2 \text{ rads}$$

Total

$$\chi = 8.70 + 4.87 = 1.357 \times 10^4 \text{ rads}$$

$$N = 2.72 + 0.24 = 2.96 \times 10^3 \text{ rads}$$

(2) Radiation Section (a) - Detector No. 2 downstream end of section 3.0 ft above floor

Entranceway Contribution ($B_p = 7.33$ ft; $H_p = 8.00$ ft;

$Z = 16.0$ ft; $\therefore \omega = 0.037$ solid radians; $\beta_B = 0$ deg)

$$\chi = 1.357 \times 10^4 \times 0.52 = 7.2 \times 10^3 \text{ rads}$$

$$N = 2.96 \times 10^3 \times 0.28 = 8.28 \times 10^2 \text{ rads}$$

Overhead Contribution ($B_p = 7.33$; $H_p = 16.0$ ft; $Z = 5.0$ ft;

$\therefore \omega = 0.50$; $\rho_m = 775$ psf; $\beta_B = 0$ deg; $\beta_S = 90$ deg)

$$\chi = 1.45 \times 10^5 \times 0.92 \times 47 \times 10^{-5} = 62.8 \text{ rads}$$

$$N = 2.27 \times 10^4 \times 0.82 \times 0.65 \times 10^{-4} = 1.21 \text{ rads}$$

Total $\chi = 7.12 + 0.06 = 7.18 \times 10^3 \text{ rads}$

$$N = 8.28 + 0.01 = 8.29 \times 10^2 \text{ rads}$$

(3) Radiation Section (R_2) - Detector No. 3 downstream end of section 3.0 ft above floor

Entranceway Contribution ($B_p = 7.33$; $H_p = 8.0$ ft;

$Z = 16.0$ ft; $\therefore \omega = 0.037$; $\beta_B = 0$ deg; $R_{c1} = 0.1$; $\therefore \omega' = 0.0037$;

$R_{fw} = 0.14$)

$$\chi = 7.18 \times 10^3 \times 0.21 = 1.51 \times 10^3 \text{ rads}$$

$$N = 8.29 \times 10^2 \times 0.24 \times 0.14 = 2.78 \text{ rads}$$

Overhead Contribution ($B_p = 7.33$; $H_p = 16.0$ ft; $Z = 5.0$ ft;

$\therefore \omega = 0.50$; $\rho_m = 925$ psf; $\beta_B = 0$ deg; $\beta_S = 90$ deg)

$$\chi = 1.45 \times 10^5 \times 0.92 \times 11 \times 10^{-5} = 14.7 \text{ rads}$$

$$N = 2.27 \times 10^4 \times 0.82 \times 0.1 \times 10^{-4} = 0.186 \text{ rads}$$

Total $\chi = 1.51 + 0.01 = 1.52 \times 10^3 \text{ rads}$

$$N = 2.78 + 0.19 = 2.99 \text{ rads}$$

(4) Blast Section - Detector No. 4 opposite blast door 3.0 ft above floor

Entranceway Contribution ($B_p = 7.33$; $H_p = 8.0$ ft;

$$\therefore \omega = 0.12; \rho_m = 175; \beta_B = 0 \text{ deg}; \beta_S = 90 \text{ deg})$$

$$\gamma = 1.52 \times 10^3 \times 0.7 \times 0.23 = 245 \text{ rads}$$

$$N = 2.99 \times 0.48 \times 0.195 = 0.27 \text{ rads}$$

Overhead Contribution - (Included at Detector No. 4)

$$\text{Total } \gamma = 2.45 \text{ rads}$$

$$N = 0.27 \text{ rads}$$

(5) Blast Section - Detector No. 5 downstream end of blast section at entrance of shelter proper 3.0 ft above floor

Entranceway Contribution ($r_m = 5.5$ ft; $Z = 11.0$ ft;

$$\therefore \omega = 0.175; R_{fc_2} = 0.5; \therefore w' = 0.088; R_{fw} = 0.253)$$

$$\gamma = 245 \times 0.64 = 156.5 \text{ rads}$$

$$N = 0.27 \times 0.50 \times 0.253 = 0.034 \text{ rads}$$

Overhead Contribution ($B_p = 11.0$ ft; $H_p = 19.0$ ft;

$$Z = 5.0 \text{ ft}; \therefore \omega = 0.45; \rho_m = 950 \text{ psf}; \beta_B = 0 \text{ deg}; \beta_S = 90 \text{ deg})$$

$$\gamma = 1.45 \times 10^5 \times 0.90 \times 8.5 \times 10^{-5} = 11.0 \text{ rads}$$

$$N = 2.27 \times 10^4 \times 0.80 \times 0.075 \times 10^{-4} = 0.140 \text{ rads}$$

$$\text{Total } \gamma = 156.5 + 11.0 = 167.5 \text{ rads}$$

$$N = 0.034 + 0.140 = 0.174 \text{ rads}$$

For Entranceway Burst Orientation

(1) At Detector No. 1

Entranceway Contribution ($B_p = 7.33$ ft; $H_p = 8.00$ ft; $Z = 130$ ft;

$$\therefore \omega = 0.054; \beta_B = 0 \text{ deg})$$

$$\gamma = 4.58 \times 10^5 \times 0.56 = 2.57 \times 10^5 \text{ rads}$$

$$N = 1.29 \times 10^5 \times 0.29 = 3.74 \times 10^4 \text{ rads}$$

Overhead Contribution ($B_p = 7.33$ ft; $H_p = 10.0$ ft; $Z = 5.0$ ft;

$$\therefore \omega = 0.28; \rho_m = 350 \text{ psf}; \beta_B = 50 \text{ deg}; \beta_S = 40 \text{ deg}$$

$$\gamma = 4.58 \times 10^5 \times 0.25 \times 0.0025 = 2.86 \times 10^2 \text{ rads}$$

$$N = 1.29 \times 10^5 \times 0.46 \times 0.006 = 3.56 \times 10^2 \text{ rads}$$

$$\text{Total } \gamma = 2.57 \times 10^5 \text{ rads}$$

$$N = 3.47 + 0.04 = 3.78 \times 10^4 \text{ rads}$$

Assume reduction factors are the same as in the overhead contribution burst and neglect overhead contribution

$$\gamma = 2.57 \times 10^5 \times 0.52 \times 0.21 \times 0.7 \times 0.23 \times 0.64 = 2.89 \times 10^3 \text{ rads}$$

$$N = 3.78 \times 10^4 \times 0.28 \times 0.24 \times 0.14 \times 0.48 \times 0.195 \times 0.253 = 4.21 \text{ rads}$$

$$\text{Total } \gamma = 2890 \text{ rads}$$

$$N = 4.21 \text{ rads}$$

(b) Fallout Radiation

The collapse of the Transition and Radiation Sections will negate any fallout radiation effect, except through the shelter roof.

Fallout Overhead Shelter Contribution ($\omega = 0.66$; $\rho_m = 1000$ psf; Case I)

$$\gamma = 8.6 \times 10^4 \times 0.2 \times 2 \times 10^{-10} = \text{negligible}$$

$$\text{Worst case radiation dose at shelter entrance} = 2890 + 4.21 = 2894 \text{ rads}$$

$$\text{Radiation dose through shelter roof for this case} = 0.41 \text{ rads}$$

$$\text{Allowable dosage through entranceway for this case} = 40.0 - 0.41 = 39.59 \text{ rads}$$

$$\text{Required } R_{f_b} = \frac{39.59}{2894} = 0.0137$$

From Fig. 5-4 ($R_{f_b} = 0.0137$; $\beta_S = 90 \text{ deg}$)

$$\rho_m = 455 \text{ psf}$$

$$D = \frac{455}{12.5} = 36.4 \text{ in.}$$

Try $D = 41.0$ in.

The barrier shielding is placed in redesigned Radiation Section (R_2). (See Fig. 7-14)

III RESEARCH INSTITUTE

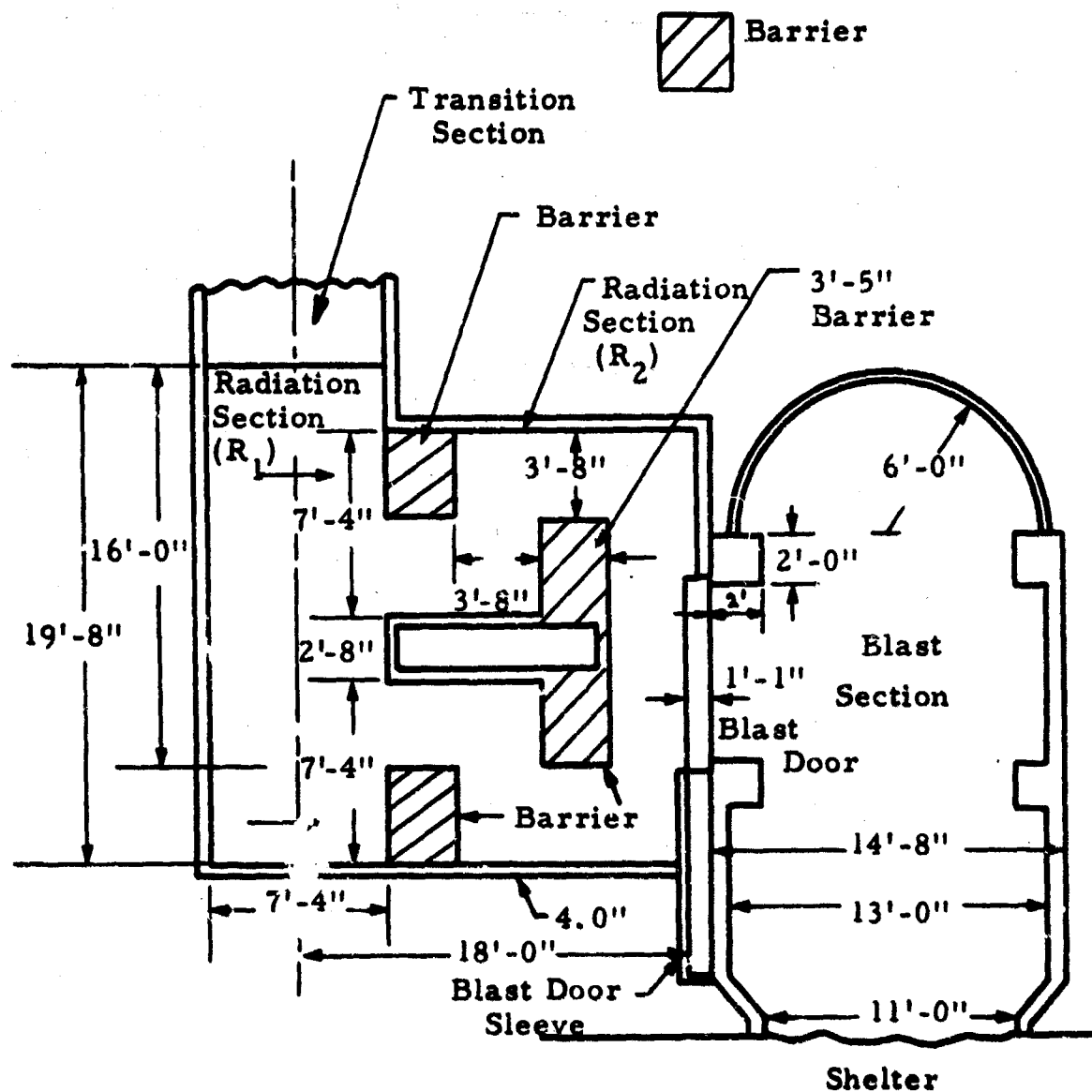


Fig. 7-14 PLAN VIEW OF REVISED ENTRANCEWAY LAYOUT, NONBLAST-RESISTANT CUBICLE AND CYLINDER

(d) Radiation Entranceway Contribution Based on Redesigned Radiation Section (R_2)

Note: In the other design example presented in this chapter, the limited layout changes did not require any radiation reanalysis.

For Entranceway Burst Orientation

(1) Dosage at upstream entrance of Radiation Section (R_2) is taken as the same as Detector No. 1

$$\gamma = 4.58 \times 10^5 \times 0.56 = 2.57 \times 10^5 \text{ rads}$$

$$N = 1.29 \times 10^5 \times 0.29 = 3.74 \times 10^4 \text{ rads}$$

(2) Dosage at downstream entrance of Radiation Section (R_2) taken as the same as Detector No. 2

$$\gamma = 2.57 \times 10^5 \times 0.52 = 1.34 \times 10^5 \text{ rads}$$

$$N = 3.78 \times 10^4 \times 0.28 = 1.06 \times 10^4 \text{ rads}$$

(3) Dosage at Detector No. 3 located upstream side of blast door 3.0 ft above floor

Through upstream entrance ($B_p = 7.33 \text{ ft}$; $H_p = 8.0 \text{ ft}$; $Z = 18.0 \text{ ft}$; $\omega = 0.018$; $\rho_m = 460 \text{ psf}$; $\beta_B = 0 \text{ deg}$; $\beta_S = 90 \text{ deg}$; $R_{c1} = 0.1$;

$$\therefore \omega' = 0.0018; R_{fw} = 0.10)$$

$$\gamma = 2.57 \times 10^5 \times 0.14 \times 0.0074 = 2.56 \times 10^2 \text{ rads}$$

$$N = 3.78 \times 10^4 \times 0.16 \times 0.10 \times 0.002 = 1.2 \text{ rads}$$

Through downstream entrance ($\omega = 0.018$; $\rho_m = 460 \text{ psf}$;

$$\beta_B = 0 \text{ deg}; \beta_S = 90 \text{ deg}; R_{c1} = 0.1; \therefore \omega' = 0.0018; R_{fw} = 0.10)$$

$$\gamma = 1.34 \times 10^5 \times 0.14 \times 0.0074 = 1.39 \times 10^2 \text{ rads}$$

$$N = 1.06 \times 10^4 \times 0.16 \times 0.10 \times 0.002 = 0.3 \text{ rads}$$

$$\text{Total } \gamma = 2.50 + 1.39 = 3.89 \times 10^2 \text{ rads}$$

$$N = 1.2 + 0.3 = 1.5 \text{ rads}$$

(4) At Detector No. 4 ($\omega = 0.12$; $\rho_m = 175$ psi; $\beta_B = 0$ deg; $\beta_S = 90$ deg)

$$\gamma = 3.89 \times 10^2 \times 0.7 \times 0.23 = 62.6 \text{ rads}$$

$$N = 5.75 \times 0.48 \times 0.195 = 0.54 \text{ rads}$$

(5) At Detector No. 5 ($r_m = 5.5$ ft; $Z = 14.0$ ft; $\omega = 0.067$;

$$R_{fc_2} = 0.5; \therefore \omega' = 0.034; R_{fw} = 0.22; \beta_B = 0 \text{ deg; } \beta_S = 90 \text{ deg}$$

$$\gamma = 62.6 \times 0.5 = 31.3 \text{ rads}$$

$$N = 0.54 \times 0.33 \times 0.22 = 0.039 \text{ rads}$$

Total

$$\gamma = 31.3 + 0.41 = 31.71 \text{ rads}$$

$$N = 0.4 \text{ rads}$$

$$\text{Total Radiation} = 31.75 < 40.0 \\ \therefore \text{OK}$$

Note: Consider that radiation streaming around the barrier shielding, striking the blast door at a ~ 30 deg in plane angle, will result in R_f approximately equal to the R_{fb} determined.

(e) Radiation Barrier: Shielding Cost Factor

Total area of barrier wall

$$A = 8 (3.66 \times 8.0) + (3.42 \times 8.0) = 344 \text{ sq ft}$$

Projected area of barrier wall

$$A = 4 (3.66 \times 8.0) = 117.33 \text{ sq ft}$$

Assuming $f'_c = 2000$ psi

Concrete

$$C_c = \frac{D}{12} X_c = \frac{41.0}{12} \times 1.00 = 3.41 \text{ \$/sq ft}$$

Steel

$$C_s = \frac{D \phi_t X_s}{1200} = \frac{41.0 \times 0.5 \times 78.8}{1200} = 1.34 \text{ \$/sq ft}$$

Forms

$$C_f = \frac{344}{117.33} \times 1.00 = 2.93 \text{ \$/sq ft}$$

Summary

$$C_t = 3.41 + 1.34 + 2.93 = 7.68 \text{ \$/sq ft}$$

$$C_T = 7.68 \times 117.33 = 900 \text{ \$}$$

(f) Radiation Section (R_2) Revised Design and Cost Factor

The two legs of Radiation Section (R_2) could be designed as an integral unit, but design and cost data would not differ appreciably from the assumption of two standard four lane sections from Table 7-5.

3. Total Cost

(a) Excavation and Backfill

Assuming an existing 1:1 slope cut excavation for the shelter the volume of the additional excavation required can be determined from Eq. (7-8).

(1) For Blast Section

Depth of excavation at side of shelter = 22.0 ft

Depth of excavation at upstream end of section = 0.0 ft

Average depth of blast section = 22.0 ft

$$z = \left(\frac{(22.0 - 22.0) + (22.0 - 0.0)}{2} \right) = 11.0 \text{ ft}$$

$$\text{Vol} = \frac{11.0}{2} ((14.66 \times 26.0) + (36.66 + 37.0)) = 9550 \text{ cu ft}$$

(2) For Radiation Section (R_2)

Depth of excavation, downstream end = 22.0 ft

Depth of excavation, upstream end = 4.0 ft

Average depth of radiation section (R_2) = 17.0 ft

$$z = \left(\frac{(17.0 - 22.0) + (17.0 - 0.0)}{2} \right) = 6.0 \text{ ft}$$

$$\text{Vol} = \frac{6.0}{2} ((18.0 \times 18.0) + (24.0 \times 24.0)) = 2700 \text{ cu ft}$$

(3) For Radiation Section (R_1)

Depth of excavation, downstream end = 16.0 ft

Depth of excavation, upstream end = 0.0 ft

Average depth of radiation section (R_1) = 16.0 ft

$$z = \left(\frac{(16.0 - 16.0) + (16.0 - 0)}{2} \right) = 8.0 \text{ ft}$$

$$\text{Vol} = \frac{8.0}{2} ((4.0 \times 16.0) + (12.0 \times 24.0)) = 1408 \text{ cu ft}$$

(4) For Transition Section

Depth of excavation, downstream end = 15.0 ft

Depth of excavation, upstream end = 5.0 ft

Average depth of transition section = 11.0 ft

$$z = \left(\frac{(11.0 - 15.0) + (11.00 - 5.0)}{2} \right) = 1.0 \text{ ft}$$

$$\text{Vol} = \frac{1.0}{2} ((8.0 \times 10.0) + (10.0 \times 11.0)) = 95 \text{ cu ft}$$

(5) For Open Cut

Depth of excavation, downstream end = 6.5 ft

Depth of excavation, upstream end = 0.0 ft

Average depth of transition section = 3.25 ft

$$z = \left(\frac{(3.25 - 6.5) + (3.25 - 0)}{2} \right) = 0$$

$$\text{Vol} = 0 \text{ cu ft}$$

Total Volume of Additional Excavation

Blast Section	=	9550
Radiation Section (R_2)	=	2700
Radiation Section (R_1)	=	1408
Transition Section	=	95
Open Cut	=	0
		<hr/>
		13,753 cu ft

Entrance Structure Volume

Blast Section	=	$\pi \times 7.33^2 \times 23.0$	=	3880
Radiation Section (R_2)	=	$8.66 \times 18.0 \times 18.0$	=	2810
Radiation Section (R_1)	=	$8.66 \times 4.0 \times 20.0$	=	693
Transition Section	=	$8.66 \times 8.00 \times 13.0$	=	900
Open Cut	=	$1/4 (33.33 + 7.33) 6.5$	=	65
				<hr/>
				8348 cu ft

Volume of Backfill

$$13753 - 8348 = 5405 \text{ cu ft}$$

(b) Open Cut Section

From TRIAL DESIGN 7.4.4

Slope Stabilization $C_T = 113 \$$

Stairs $C_T = 350 \$$

(c) Emergency Exit

The 1000 man shelter serviced by a nonblast-resistant entranceway requires the same number of emergency exits as entranceway traffic lanes (250 man/lane). This results in a total requirement for four exits and, from Table 7-2, the required length of emergency exit is assumed equal to the depth to entrance level. Unit cost from Section 2.8.4

$$C_T = 14.00 \times 19.00 = 268 \$$$

Total Cost

Surface Transition Section (Open Cut)

Slide Slope Stabilization	=	113
Stair 10 steps at 35.00 \$/step	=	350

Depth Transition Section

Reinforced concrete cubicle 55.10 x 13.0	=	717
Stairs 13 steps at 35.00 \$/step	=	455

Radiation Section (R_1)

Reinforced concrete cubicle 55.10 x 19.00	=	1045
---	---	------

Radiation Section (R_1)

Reinforced concrete cubicle 55.10 x 2 x 14.33	=	1580
---	---	------

Blast Section

Reinforced concrete cylindrical shell 2.93 x 14.66 x 8.83	=	1125
--	---	------

Reinforced concrete spherical dome shell 2.73 x π x 2 x 6.42 ²	=	705
--	---	-----

Reinforced concrete compression ring 19.79 x π x 2 x 14.66	=	1820
---	---	------

Reinforced concrete beam frame 30.87 x 7.33 x 2	=	453
--	---	-----

Steel Rolled Shape Blast Door	=	2569
-------------------------------	---	------

Blast Door Support Channel	=	610
----------------------------	---	-----

Blast Door Roller Supports	=	1760
----------------------------	---	------

Blast Door Latch	=	360
------------------	---	-----

Blast Door Sleeve	=	218
-------------------	---	-----

Emergency Exit 268 x 4	=	1072
------------------------	---	------

Excavation 0.036 x 13753	=	495
--------------------------	---	-----

Backfill 0.033 x 5405	=	179
-----------------------	---	-----

Haul 0.026 x 8348	=	217
-------------------	---	-----

\$ 15,833

7.5.2 Compression Sphere (Sample Analysis and Cost Evaluation)

TRIAL DESIGN 7.5.2 - 325 F1

CONFIGURATION

One story cubicle and sphere

STRUCTURAL SYSTEM AND INPUT PARAMETERS (Fig. 7-6)

Transition Section -

Material: Reinforced Concrete Cubicle

Orientation: Makes ~ 39 deg angle with horizontal plane and is perpendicular to long axis of the shelter

Dimension: H = 7 ft-0 in.; B = 2 ft-6 in.; length = 11 ft-0 in.;
change in elevation between entrance and exit =
8 ft- 3 1/2 in.

Primary Design Load: $q_E = 10$ psi

Radiation Section (R_1) -

Material: Reinforced concrete cubicle

Orientation: Horizontal and is perpendicular to long axis of the shelter

Dimension: H = 7 ft-0 in.; B = 2 ft-6 in.; length = 14 ft -0 in.;
change in elevation between entrance and exit =
1 ft-6 in.

Primary Design Load: $q_E = 10$ psi

Radiation Section (R_2) -

Material: Reinforced concrete cubicle

Orientation: Horizontal and is parallel to long axis of the shelter

Dimension: H = 7 ft-0 in.; B = 2 ft-6 in.; length = 14 ft-0 in.;
change in elevation between entrance and exit =
1 ft-6 in.

Primary Design Load: $q_E = 10$ psi

Blast Section -

Material: Reinforced concrete sphere

Orientation: \sim Horizontal

Dimensions: I. D. 13 ft-0 in.

Primary Design Load: 772 psi

Connecting Cylinder-

Material: Reinforced concrete cylinder

Orientation: \sim Horizontal

Dimension: I. D. 7 ft-0 in.; length 4 ft-0 in.

Primary Design Load: $q_{Ed} = 325$ psi

Note: These dimensions may require subsequent modification due to radiation design requirements.

Shelter -

Capacity: 100 man (Table 7-2)

Primary Design Load: $q_{Ed} = 325$ psi

1. Blast Analysis

(a) Transition and Radiation Section: Design and Cost Factors

From Table 7-5 ($q = 10$ psi; 1 Lane)

(1) Wall

$$\begin{array}{ll} f'_c = 2000 & \phi_L = 0.25 \\ f_{dy} = 60,000 & D = 4.0 \text{ in.} \\ \phi_R/\phi_L = 1.00 & C_t = 1.55 \text{ \$/sq ft} \end{array}$$

(2) Roof

$$\begin{array}{ll} f'_c = 4000 \text{ psi} & \phi_L = 0.35 \\ f_{dy} = 75,000 \text{ psi} & D = 4.0 \text{ in.} \\ \phi_R/\phi_L = 0.75 & C_t = 1.65 \text{ \$/sq ft} \end{array}$$

$$C_T = 32.15 \text{ \$/ft of cubicle}$$

(b) Blast Section: Design and Cost Factors for Reinforced Concrete Sphere

The same design presented in Design Example 7.4.1 is used in this case, since the overall dimension requirements and loadings are essentially the same. See Design Example 7.4.1, Part A (c)-(m) for details.

(c) Blast Section: Design and Cost Factors for Shelter Connecting Section

Since the spherical surface of the blast section is difficult to match with the shelter cylindrical surface, use a 4.0 ft long cylindrical connecting section which is similar in design to Radiation Section (R_1) of Design Example 7.4.1.

2. Radiation Analysis

(a) Prompt Radiation Overhead Shelter Contribution

From example 7.4.1 Part B

Overhead burst orientation

$$\gamma = 6.82 \text{ rads} \quad N = 0.08 \text{ rads}$$

IIT RESEARCH INSTITUTE

Entranceway burst orientation

$$\gamma = 0.14 \text{ rads} \quad N = 0.06 \text{ rads}$$

(b) Prompt Radiation Entranceway Contribution

For Overhead Burst Orientation

(1) Transition Section - Detector No. 1 at bottom of stairs

3.0 ft above door

Entranceway contribution ($B_p = 2.5 \text{ ft}$; $H_p = 7.0 \text{ ft}$;

$Z = 13.0 \text{ ft}$; $\therefore \omega = 0.014 \text{ solid radians}$; $\beta_B = 50 \text{ deg}$)

$$\gamma = 1.45 \times 10^5 \times 0.018 = 2.62 \times 10^3 \text{ rads}$$

$$N = 2.27 \times 10^4 \times 0.025 = 7.85 \times 10^2 \text{ rads}$$

Overhead contribution ($B_p = 2.5 \text{ ft}$; $H_p = 10.0 \text{ ft}$;

$Z = 4.0 \text{ ft}$; $\therefore \omega = 0.15$; $\rho_m = 400 \text{ psf}$; $\beta_B = 0 \text{ deg}$; $\beta_S = 90 \text{ deg}$)

$$\gamma = 1.45 \times 10^5 \times 0.74 \times 0.023 = 2.47 \times 10^3 \text{ rads}$$

$$N = 2.27 \times 10^4 \times 0.48 \times 0.0075 = 8.17 \times 10 \text{ rads}$$

$$\text{Total} \quad \gamma = 2.67 + 2.47 = 5.14 \times 10^3 \text{ rads}$$

$$N = 7.85 + 0.82 = 8.67 \times 10^2 \text{ rads}$$

(2) Radiation Section (R_1) - Detector No. 2 downstream end

of section 3.0 ft above floor

Entranceway contribution ($B_p = 2.5 \text{ ft}$; $H_p = 7.0 \text{ ft}$;

$Z = 14.0 \text{ ft}$; $\therefore \omega = 0.01$; $\beta_B = 0 \text{ deg}$)

$$\gamma = 5.14 \times 10^3 \times 0.33 = 1.71 \times 10^3 \text{ rads}$$

$$N = 8.67 \times 10^2 \times 0.11 = 9.55 \times 10 \text{ rads}$$

Overhead contribution ($B_p = 2.5 \text{ ft}$; $H_p = 14.0 \text{ ft}$;

$Z = 4.0 \text{ ft}$; $\therefore \omega = 0.17$; $\rho_m = 825 \text{ psf}$; $\beta_B = 0$; $\beta_S = 90$)

$$\gamma = 1.45 \times 10^5 \times 0.76 \times 0.0003 = 3.31 \times 10 \text{ rads}$$

$$N = 2.27 \times 10^4 \times 0.50 \times 0.000037 = 0.42 \text{ rads}$$

$$\text{Total} \quad \gamma = 1.71 + 0.03 = 1.74 \times 10^3 \text{ rads}$$

$$N = 9.55 + 0.04 = 9.59 \times 10 \text{ rads}$$

MIT RESEARCH INSTITUTE

(3) Radiation Section (R_2) - Detector No. 3 downstream end of section 3.0 ft above floor

Entranceway contribution ($B_p = 2.25$ ft; $H_p = 7.0$ ft; $Z = 14.0$ ft; $\omega = 0.01$; $R_{c1} = -.1$; $\therefore \omega' = 0.001$; $R_{fw} = 0.07$; $\beta_B = 0$ deg)

$$\gamma = 1.74 \times 10^3 \times 0.10 = 1.74 \times 10^2 \text{ rads}$$

$$N = 9.59 \times 10 \times 0.11 \times 0.07 = 0.67 \text{ rads}$$

Overhead contribution ($B_p = 2.5$; $H_p = 14.0$ ft; $Z = 4.0$ ft; $\omega = 0.17$; $\rho_m = 950$ psf; $\beta_B = 0$ deg; $\beta_S = 90$ deg)

$$\gamma = 1.45 \times 10^5 \times 0.76 \times 0.00008 = 8.8 \text{ rads}$$

$$N = 2.27 \times 10^4 \times 0.50 \times 0.08 \times 10^{-4} = 0.09 \text{ rads}$$

Total

$$\gamma = 1.74 + 0.09 = 1.83 \times 10^2 \text{ rads}$$

$$N = 0.67 + 0.09 = 0.76 \text{ rads}$$

(4) Blast Section - Detector No. 4 opposite blast door in center of sphere

Entranceway contribution ($B_p = 2.5$; $H_p = 7.0$ ft; $Z = 8.0$ ft; $\omega = 0.045$; $\rho_m = 125$ psf; $\beta_B = 0$ deg; $\beta_S = 90$ deg)

$$= 1.83 \times 10^2 \times 0.5 \times 0.35 = 32.0 \text{ rads}$$

$$N = 0.76 \times 0.23 \times 0.35 = 0.06 \text{ rads}$$

Overhead contribution ($r_m = 6.5$ ft; $Z = 8.0$ ft; $\omega = 0.232$;

$\rho_m = 850$ psf; $\beta_B = 0$ deg; $\beta_S = 90$ deg)

$$= 1.45 \times 10^5 \times 0.80 \times 0.00023 = 26.8 \text{ rads}$$

$$N = 2.27 \times 10^4 \times 0.57 \times 0.000026 = 0.33 \text{ rads}$$

Total

$$= 32.0 + 26.8 = 58.8 \text{ rads}$$

$$N = 0.06 + 0.33 = 0.39 \text{ rads}$$

(5) Entrance to Shelter - Detector No. 5 at shelter entrance 3.0 ft above floor

Entranceway contribution ($r_m = 4.0$; $Z = 8.0$ ft; $\therefore \omega = 0.105$; $R_{fc2} = 0.5$; $\therefore \omega' = 0.053$; $\beta_B = 0$ deg)

III RESEARCH INSTITUTE

$$\gamma = 58.8 \times 0.54 = 31.3 \text{ rads}$$

$$N = 0.39 \times 0.40 = 0.15 \text{ rads}$$

Overhead Contribution (Included at Detector No. 4)

$$\text{Total } \gamma = 31.3 \text{ rads}$$

$$N = 0.15 \text{ rads}$$

For Entranceway Burst Orientation

1. At Detector No. 1

Entranceway contribution ($B_p = 2.5 \text{ ft}$; $H_p = 7.0 \text{ ft}$; $Z = 13.0 \text{ ft}$;

$$\therefore \omega = 0.014; \beta_B = 0 \text{ deg})$$

$$\gamma = 4.58 \times 10^5 \times 0.37 = 1.69 \times 10^5 \text{ rads}$$

$$N = 1.29 \times 10^5 \times 0.14 = 1.805 \times 10^4 \text{ rads}$$

Overhead Contribution ($B_p = 2.5 \text{ ft}$; $H_p = 10.0 \text{ ft}$; $Z = 4.0 \text{ ft}$;

$$\therefore \omega = 0.15; \rho_m = 400 \text{ psf}; \beta_B = 50 \text{ deg}; \beta_S = 40 \text{ deg})$$

$$\gamma = 4.58 \times 10^5 \times 0.74 \times 0.001 = 3.39 \times 10^2 \text{ rads}$$

$$N = 1.29 \times 10^5 \times 0.48 \times 0.0032 = 1.98 \times 10^2 \text{ rads}$$

Total

$$\gamma = 1.69 + 0.003 = 1.69 \times 10^5 \text{ rads}$$

$$N = 1.805 + 0.020 = 1.825 \times 10^4 \text{ rads}$$

Assume reduction factors are the same beyond this point as in the overhead burst orientation, and neglect overhead contribution

$$\gamma = 1.69 \times 10^5 \times 0.33 \times 0.10 \times (0.50 \times 0.35) \times 0.54 = 499.0 \text{ rads}$$

$$N = 1.825 \times 10^4 \times 0.11 \times (0.11 \times 0.07) \times (0.23 \times 0.35) \times 0.40 = 0.50 \text{ rads}$$

(c) Fallout Radiation

The collapse of the Transition and Radiation Sections will eliminate any fallout radiation streaming through the entranceway, and the effect through the shelter roof is negligible.

(d) Radiation Barrier Shielding: Design and Cost Factors

Worst case radiation dose at shelter entrance = 499.0 +
0.50 = 499.5 rads

Radiation dose through shelter roof for this case = 0.41 rads

Allowable dosage through entranceway for this case = 40.0 -
0.41 = 39.59 rads

$$\text{Required } R_{f_b} = \frac{39.59}{499.5} = 0.793$$

From Fig. 5-4 ($R_{f_b} = 0.793$, $\beta_S = 90$ deg)

$$\rho_m = 240 \text{ psf}$$

$$D = \frac{240}{12.5} = 19.2 \text{ in.} \quad \text{Use } D = 20.0 \text{ in.}$$

The additional barrier shielding in this case can be best placed in the connecting cylinder between the blast sphere section and shelter. See Fig. 7-15 for details. The addition of radiation barrier walls requires the redesign of the connecting blast cylinder. From Table 7-5 ($q_E = 325$; 2 Lanes)

$$f'_c = 5000 \text{ psi} \quad C_t = 1.84 \text{ \$/sq ft}$$

$$f_{dy} = 6000 \text{ psi} \quad C_T = 48.00 \text{ \$/ft of cylinder}$$

$$D = 3.0 \text{ in.}$$

Area of barrier wall

$$A = Z \times 1/2 \times \pi \times 4.0^2 = 50.3 \text{ sq ft}$$

Assuming $f'_c = 2000$ psi

Concrete

$$C_c = \frac{D}{12} X_c = \frac{20.0}{12} \times 1.00 = 1.67 \text{ \$/sq ft}$$

Steel

$$C_s = \frac{D \phi_t X_a}{1200} = \frac{20.0 \times 0.5 \times 78.8}{1200} = 0.66 \text{ \$/sq ft}$$

Forms

$$C_f = \left(Z \frac{[A + 0.0833 D S_L]}{A} \right) X_f$$

$$C_f = \frac{2 \times (50.3 + (1.66 \times 8.0))}{50.3} \times 1.00 = 2.53 \text{ \$/sq ft}$$

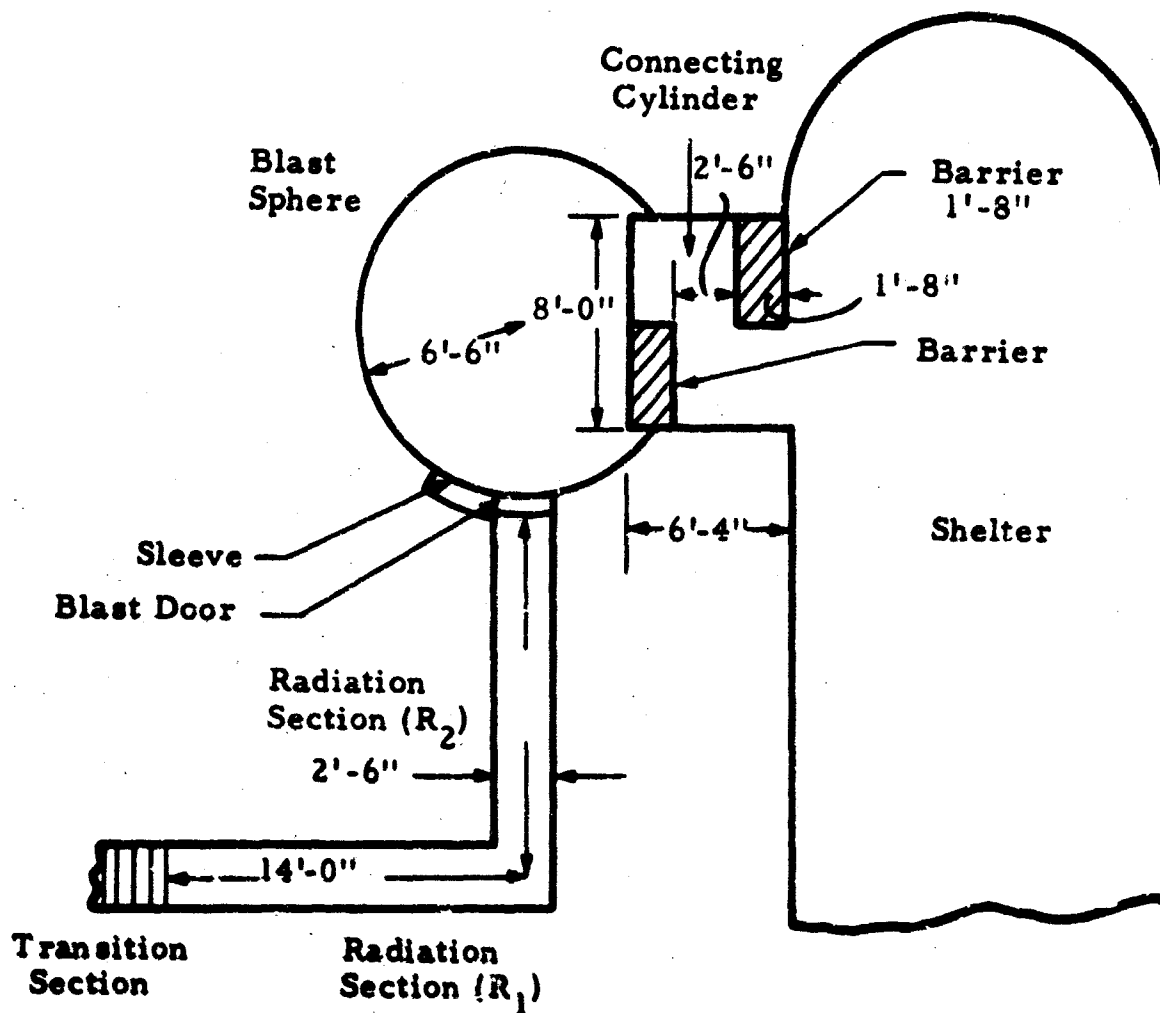


**Fig. 7-15 PLAN VIEW OF REVISED ENTRANCEWAY LAYOUT,
NONBLAST-RESISTANT COMPRESSION SPHERE**

Summary

$$C_t = 1.67 + 0.66 + 2.53 = 4.86 \text{ \$/sq ft}$$

$$C_T = 4.86 \times 50.3 = 245 \text{ \$}$$

3. Total Cost

(a) Excavation and Backfill

Assume an existing 1:1 slope cut excavation for the shelter.
The volume of the additional excavation required can then be determined from Eq. (7-8).

(1) For Connecting Cylinder

Depth of excavation at side of shelter = 22.0 ft

Depth of excavation at upstream end of section = 16.0 ft

Average depth of section = 22.0 ft

$$z = \left(\frac{(22.0 - 22.0) + (22.0 - 16.0)}{2} \right) = 3.0 \text{ ft}$$

$$\text{Vol} = \frac{3.0}{2} ((8.5 \times 6.33) + (14.5 \times 9.33)) = 290 \text{ cu ft}$$

(2) For Blast Section

Depth of excavation, downstream end = 22.0 ft

Depth of excavation, upstream end = 9.0 ft

Average depth of blast section = 23.0 ft

$$z = \left(\frac{(23.0 - 22.0) + (23.0 - 9.0)}{2} \right) = 15.0 \text{ ft}$$

$$\text{Vol} = \frac{15.0}{2} ((14.0 \times 14.0) + (44.0 \times 29.0)) = 11,080 \text{ cu ft}$$

(3) For Radiation Section (R_2)

Depth of excavation, downstream end = 23.0 ft

Depth of excavation, upstream end = 9.0 ft

Average depth of radiation section (R_2) = 16.0 ft

$$z = \left(\frac{(16.00 - 23.0) + (23.0 - 9.0)}{2} \right) = 0$$

$$\text{Vol} = 0$$

(4) For Radiation Section (R_1)

Depth of excavation, downstream end = 15.0 ft

Depth of excavation, upstream end = 12.0 ft

Average depth of radiation section (R_1) = 14.5 ft

$$z = \left(\frac{(14.5 - 15.0) + (14.5 - 12.0)}{2} \right) = 1.0$$

$$\text{Vol} = \frac{1.0}{2} ((3.0 \times 14.0) + (5.0 \times 15.0)) = 59 \text{ cu ft}$$

(5) For Transition Section

Depth of excavation, downstream end = 14.0 ft

Depth of excavation, upstream end = 4.0 ft

Average depth of transition section = 10.0 ft

$$z = \left(\frac{(10.0 - 14.0) + (10.0 - 4.0)}{2} \right) = 1.0 \text{ ft}$$

$$\text{Vol} = \frac{1.0}{2} ((3.0 \times 10.0) + (5.0 \times 11.0)) = 43 \text{ cu ft}$$

(6) For Open Cut

Depth of excavation, downstream end = 6.5 ft

Depth of excavation, upstream end = 0.0 ft

Average depth of open cut = 3.25 ft

$$z = \left(\frac{(3.25 - 6.5) + (3.25 - 0)}{2} \right) = 0$$

$$\text{Vol} = 0 \text{ cu ft}$$

Total Volume of Additional Excavation

Connecting Cylinder	=	290
Blast Section	=	11,080
Radiation Section (R_2)	=	0
Radiation Section (R_1)	=	59
Transition Section	=	43
Open Cut	=	0
		<hr/>
		11,472 cu ft

Entrance Structure Volume

Connecting Section	=	$\pi \times 4.25^2 \times 6.33$	=	359
Blast Section	=	$4/3 \times \pi \times 6.75^3$	=	1,290
Radiation Section (R_2)	=	$3.33 \times 7.66 \times 14.0$	=	1,125
Radiation Section (R_1)	=	$3.33 \times 7.66 \times 14.0$	=	1,125
Transition Section	=	$3.33 \times 7.66 \times 13.0$	=	1,045
Open Cut	=	$1/4 (27.5 + 2.5) \times 6.0$	=	45
				<hr/>
				5,139 cu ft

Volume of Backfill

$$11,472 - 5,139 = 6,333 \text{ cu ft}$$

(b) Open Cut Section

From Trial Design 7.4.1

$$\text{Slope } C_T = 87 \$$$

$$\text{Stairs 9 steps at 18.00} = 162.00 \$$$

(c) Emergency Exit

The exit requirement for 100 man shelter is the same for both blast and nonblast-resistant entranceway systems. From Design Example 7.4.1,

$$C_T = 14.00 \times 20.33 = 285$$

Total Cost

Open Cut Section

Side Slope Stabilization	=	87
Stairs	=	162

Transition Section

Reinforced Concrete Cubicle	32.15 x 13.0	=	418
Stairs	18.00 x 13.00	=	234

Radiation Section (R_2)

Reinforced Concrete Cubicle	32.15 x 14.0	=	450
-----------------------------	--------------	---	-----

Radiation Section (R_1)

Reinforced Concrete Cubicle	32.15 x 14.0	=	450
-----------------------------	--------------	---	-----

Blast Section

From Design Example 7.4.1	=	2,510
Blast Door Sleeve	=	77

Connecting Cylinder

Reinforced Concrete Cylinder	48.00 x 6.33	=	302
Radiation Barrier Wall		=	245

Emergency Exit

Excavation	0.036 x 11,472	=	413
Backfill	0.033 x 6,333	=	209
Haul	0.026 x 5,139	=	134

Total = \$ 5,985

CHAPTER 8

OPTIMUM ENTRANCEWAY DESIGN

8.1 INTRODUCTION

8.1.1 Optimization Techniques

A cost function which is to be optimized (minimized) can be represented conceptually as a hypersurface in n -dimensional space, where n is the number of design variables in the cost function. If the function is relatively well-behaved in the region of interest, in that there exists a minimum or a point of zero slope in all directions, this point can be found by solving n simultaneous equations. These equations are generated by determining the partial derivatives of the cost function with respect to each design variable, and then equating each such partial derivative to zero. This procedure, which is simple in its concepts, is designated as the direct or Lagrangian method. Unfortunately, it is often impossible to apply in practice, since it is usually not known in advance whether or not the cost function is well-behaved (i. e., one, none or many relative minima) within the region of interest. Even if this behavior condition is met, there can be major difficulties in obtaining the solution of a group of nonlinear simultaneous equations. This is a problem class which, in many cases, defies solution.

Another method of determining the optimum parameters of a cost function is known as the gradient technique. Here the negative gradients to contours of equal cost are found, thus determining a direction of travel for subsequent cost analysis. This process, which insures lower-cost design, continues until a minimum is reached or a side constraint is encountered. The procedure greatly reduces the number of cost points which must be surveyed, but its application usually requires the use of a large digital computer. Systematic methods for progressive movement along constraints to the acceptable region of design are required, as are means for dealing with relative minima within the region. In general, the gradient technique must be tailored to a specific problem. This task, in itself, often becomes a major research project.

IIT RESEARCH INSTITUTE

The simplest optimization method, and one of those employed in this study, is the n-dimensional search technique. This procedure surveys a number of preselected coordinates in the cost space, and then selects the set of coordinates or design variables which yield the least cost. The method requires a good deal of engineering judgment in the initial selection of coordinates which are to be searched. While it does not yield absolute minimum values, it can frequently supply approximations which are entirely acceptable for practical applications. The method can make effective use of a digital computer when extreme accuracy is not deemed essential, the number of design points to be surveyed is > 5000 and the analysis cycle is limited to a few seconds. Obviously, as a practical matter, there is a tradeoff between the number of design points and the length of the analysis cycle. A manual search for the cost optimum becomes feasible only when the number of points to be searched is small and the design cycle requires complex judgment decisions.

Two n-dimensional searches were employed during the course of this study. A computer program was used to develop minimum costs for the compression and tension cubicles, introducing six design variables as discussed in Section 7.3. The development of Fig. 7-7 and of Table 7-5 is based on approximately 2000 trial designs using this program. In addition, the cost curves which are supplied for the four blast-resistant and the two nonblast-resistant entranceway systems were obtained by combining the results of a manual solution and an optimum search of 64 trial designs similar to the trial design examples given in Section 7.4 and 7.5.

8.1.2 Cost Allocation by Functional Area

For both blast and nonblast-resistant structures, the total cost of the entranceway systems can be subdivided into three basic areas. It is then found that the percentage of total entranceway cost which is represented by each of these areas will remain fairly constant for all entranceway configurations and for all pressure ranges. The first of these cost areas, which results from the basic requirement for blast protection, accounts for 55 to 60 percent of the total entranceway cost. System components will include the transition and blast sections as well as the blast door, door hardware and door support items. A second cost area can be correlated with ionizing

radiation protection, and represents some 22 to 27 percent of the total cost. Included items in this category are the radiation sections themselves plus any supplementary barrier shielding. Finally, the remaining 15 to 20 percent of the total entranceway cost can be allocated to site preparation, including excavation and slope stabilization, and to such necessary functional elements as stairs and emergency exits.

8.2 MATERIALS

Almost exclusive use is made of prestressed and reinforced concrete structural elements. Previous studies^{1,2} have indicated that reinforced concrete is normally the most economical material for the basic buried shelter, assuming that dynamic pressures are at a significant level ($p_{so} > 25$ psi), and a similar trend can be expected for the entranceway elements. Framed buried shelters of steel and timber were found to merit consideration at lower levels of loading, but this relationship is not equally valid when the entranceway is examined. Large stress reversals in the entranceway elements must be anticipated, as explained earlier, and these lead to difficulties in fabricating the joints of framed steel and timber components. As a consequence, we have excluded the explicit consideration of steel and timber materials for optimum cost entranceways. At the same time, it is believed that the use of these materials in entranceway designs for dynamic pressure ranges of less than 25 psi will result in costs which are not appreciably greater than those indicated in this study.

Structural steel plate is used in design applications where large plastic deformation is permitted or where structural integrity between elements is desired without the transferral of large bending stresses. Structural steel shapes are used in functional applications, such as the support channels for the blast door, and in instances where weight or dimensional limitations requires the substitution of structural steel for a reinforced concrete member.

Prestressed concrete elements are used extensively in the blast-resistant portions of the entranceway, since this composite material has the capability of carrying both tension and compression loading in a stress reversal cycle.

8.3 MINIMUM-STRUCTURAL-COST ENTRANCEWAYS

The findings of this study are summarized by plotting in-place structural cost as a function of design pressure. The resulting plots are shown in Fig. 8-1 and 8-2. These permit easy recognition of the influence of entranceway capacity, type and structural system on the estimated in-place structural cost associated with structural loading.

In general, the tension cubicle represents the least-cost entranceway design in the low pressure loading range ($p_{s0} < 25$ psi), while the compression cylinder dominates in the middle and high overpressure ranges. The actual cross-over point between the cubicle and cylinder seems to be dependent on the requirements for entranceway capacity. In most cases, the compression sphere costs closely parallel the compression cylinder costs.

Figure 8-3 is based on blast-resistant entranceway costs, and shows the percentage savings which can be obtained by substituting the optimum nonblast-resistant entranceway system for the optimum blast-resistant facility. Savings of 10 to 30 percent are thus shown to be possible, depending on lane capacity and the overpressure level which is considered.

The optimum shelter designs have already been listed (Table 7-2). With this information, together with the data presented in Fig. 8-1, 8-2, and 8-3, the optimum shelter entranceway system can be matched with the corresponding optimum shelter for a particular shelter capacity and design pressure. Figure 8-4 presents the cost per sheltered occupant of the optimum entranceway system for least-structural-cost shelters of 100-500 and 1000 man capacity.^{1, 2} with entranceway cost shown as a function of the design overpressure. The data presented in Fig. 8-4 can thus be added directly to the optimum shelter costs from Fig. 6-3 of Ref. 2. In this way, a rapid estimate can be obtained of the total structural costs for a proposed buried shelter. In preparing Fig. 8-4, the combination of entranceway lane designs which is used with each particular shelter is based on a rated traffic capacity of 250 persons per lane. A 1000 man shelter capacity would thus require four one-lane entranceway structures or two two-lane entranceways. In developing the cost data presented in Fig. 8-4, it is further postulated that shelter systems with capacities greater than 500 persons will require

III RESEARCH INSTITUTE

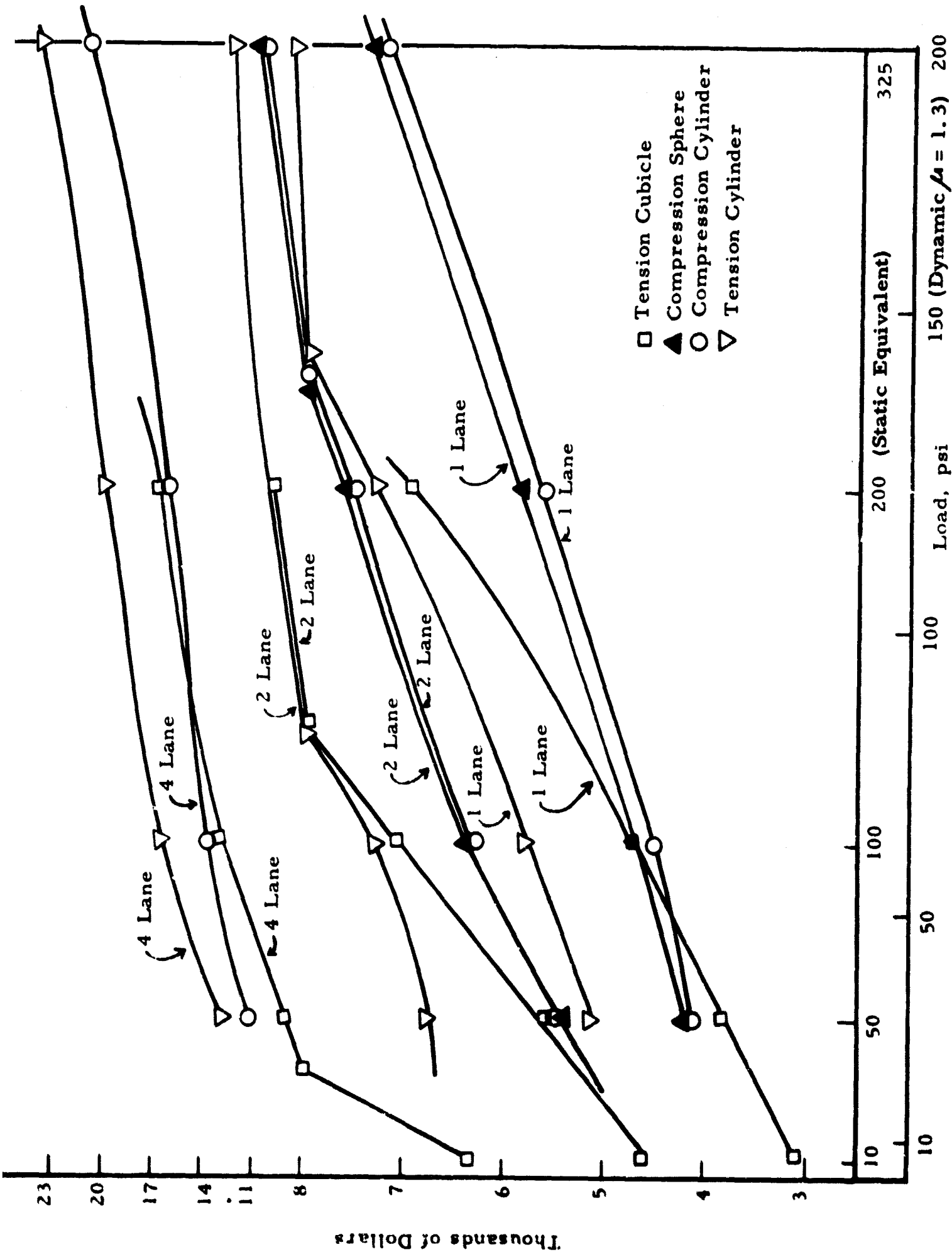


Fig. 8-1 IN-PLACE COST FOR BLAST-RESISTANT ENTRANCEWAYS

150 (Dynamic $\mu = 1.3$) 200

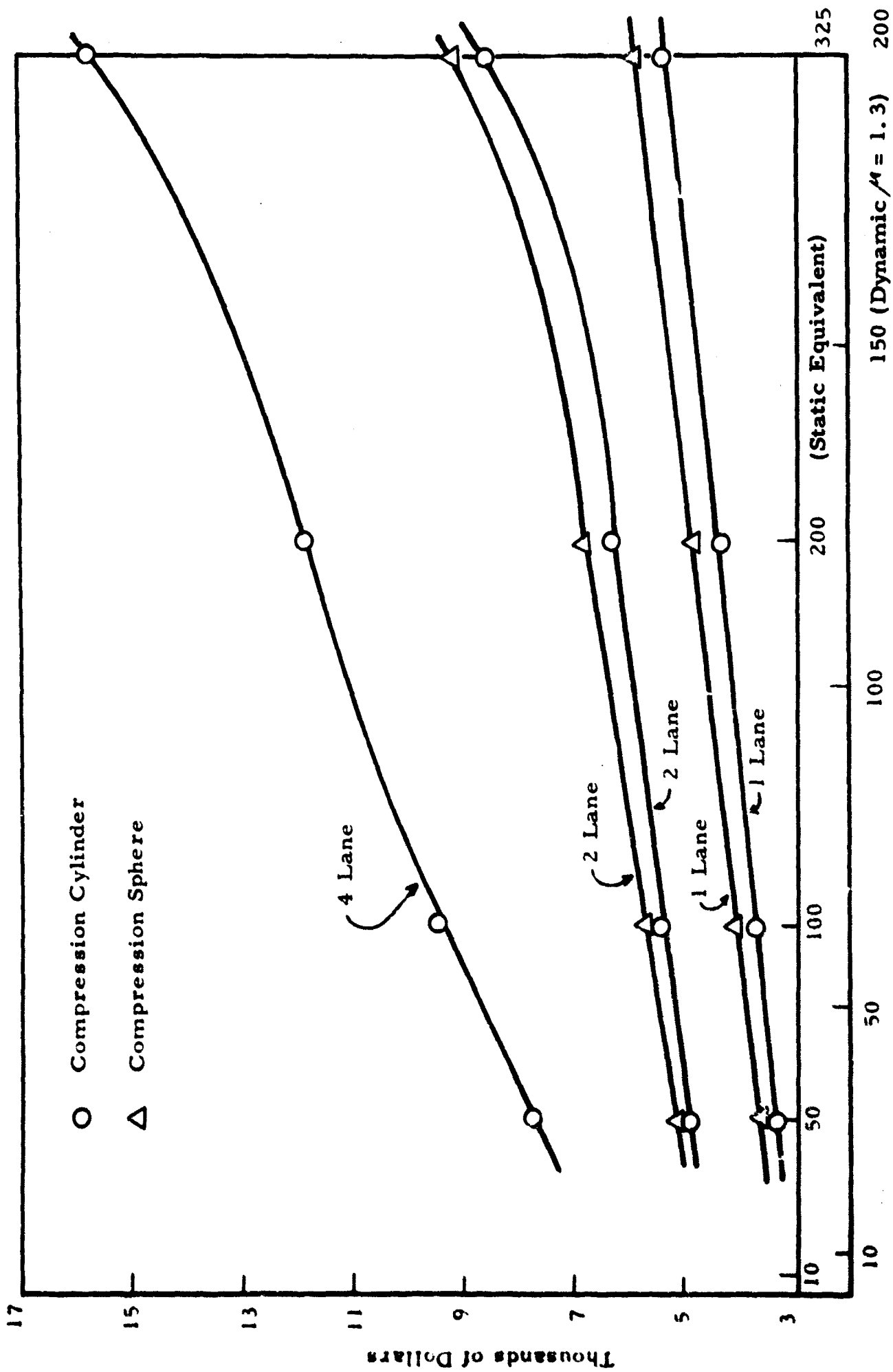


Fig. 8-2 IN-PLACE COST FOR NONBLAST-RESISTANT ENTRANCEWAYS

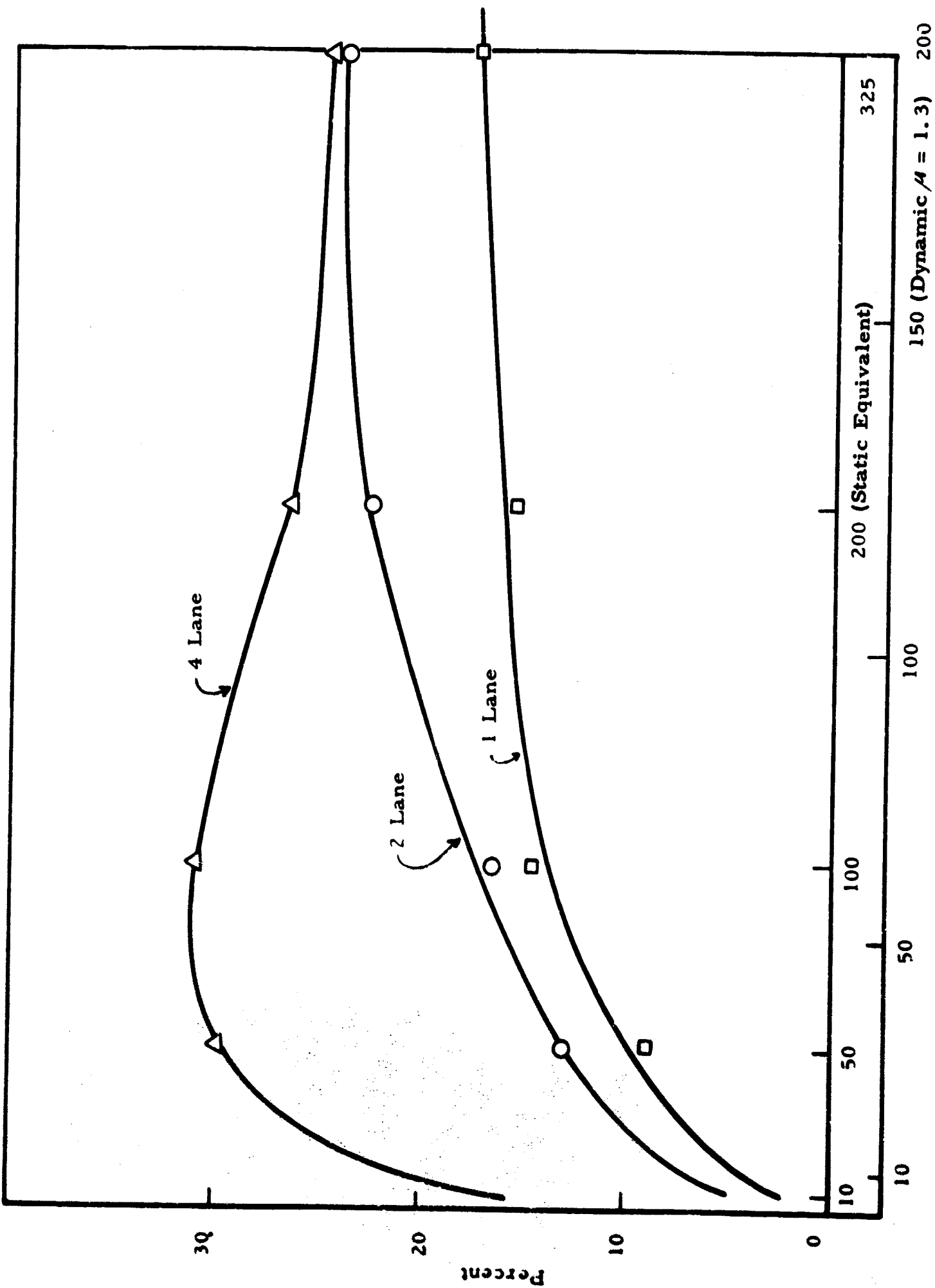


Fig. 8-3 PERCENTAGE COST ADVANTAGE, NONBLAST VERSUS BLAST RESISTANT ENTRANCEWAYS

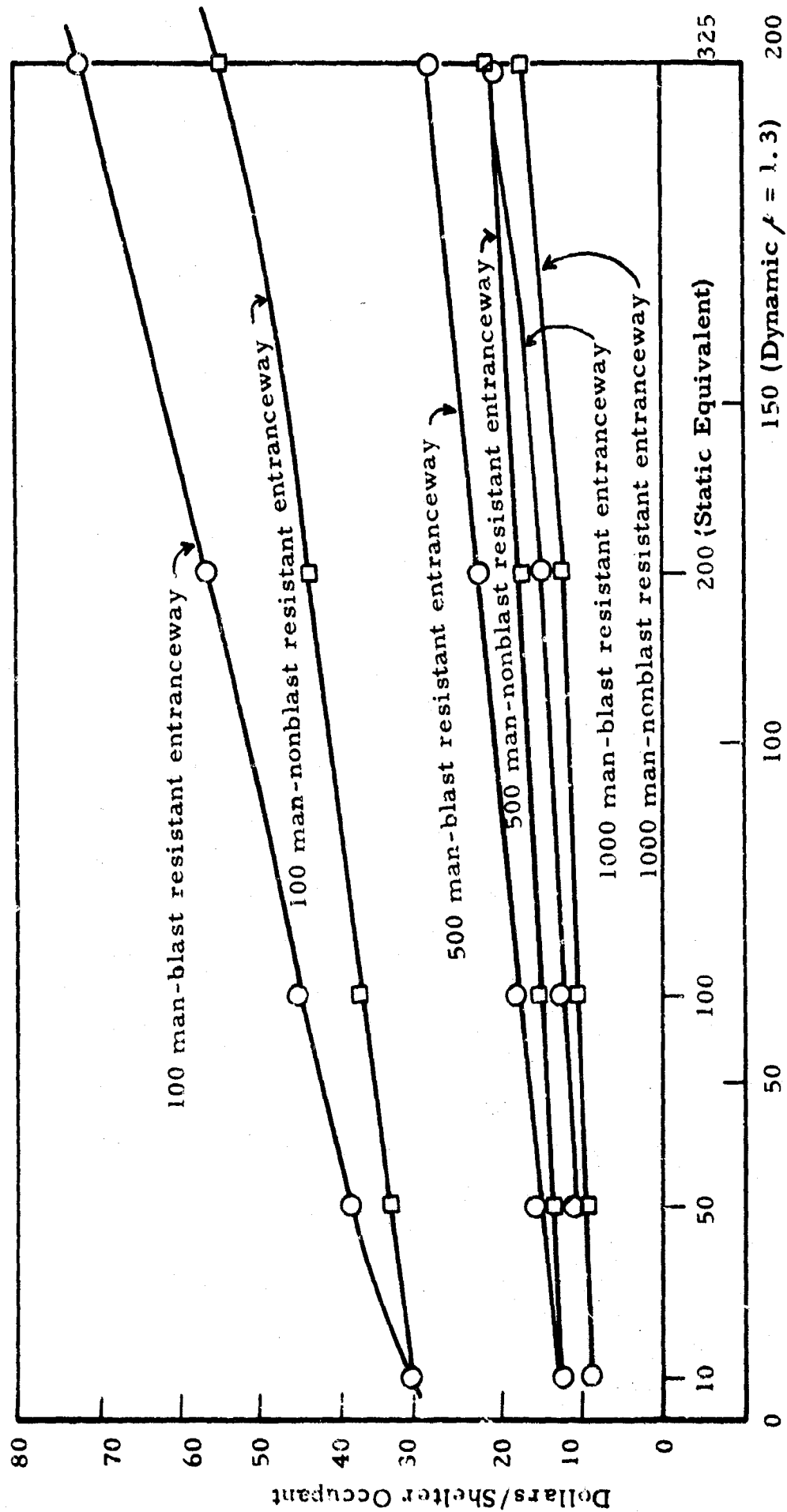


Fig. 8-4 MINIMUM IN-PLACE ENTRANCEWAY STRUCTURAL COSTS

a minimum of two separate entranceways in addition to any emergency exits which may be provided.

8.4 CONCLUSIONS

The results of this study indicate that entrance systems which are adequate for buried shelters of 100-500 and 1000 man capacities and for overpressure ranges of 10 to 200 psi can be provided at an additional cost of between 25 to 40 percent of the structural cost of the basic shelter. It has been further determined that an a priori knowledge of the shelter which is to be serviced is necessary input if optimum entranceway designs are to be realized. As was found to be true in the case of the basic shelter structures,^{1, 2} but to an even greater degree, an increase in the design capacity of the entranceway is seen to decrease the system cost per entrant. Of the entranceway lane capacities studied in detail, the optimum two-lane system can accommodate traffic at approximately 30 percent less cost than can an equivalent one-lane system. A two-lane system is slightly less expensive (< 5 percent) than an equivalent four-lane system in the higher overpressure range ($p_{so} > 50$ psi), but the reverse is true in the lower overpressure design region.

8.5 RECOMMENDATIONS FOR FURTHER STUDY

This report, together with the related earlier studies,^{1, 2} form the basis for the preliminary evaluation of the capacity requirements, structural protection and radiation attenuation systems which are necessary for buried shelters of 100, 500 and 1000 man capacities in the 10-200 psi dynamic overpressure range. Obviously, there is a need for prooftesting models or prototypes based on the designs developed in these studies, in order to verify the postulated gross structural behavior of many of the structural elements. In addition, it now appears appropriate to test the relative merits of applying more sophisticated analyses in optimization studies of blast-resistant structures.

All structural designs or analyses require some simplifying assumptions in order to reconcile the anticipated service conditions with the current state of the pertinent technological knowledge. In the field of blast-resistant underground structures, there has been a considerable research effort

IIT RESEARCH INSTITUTE

devoted to the structural response to dynamic loading, the soil-structure interaction and the elastic and plastic stability of the various structural elements. The less-sophisticated methods of analysis, which employ a simplified equivalent static loading and which largely ignore questions of stability and soil-structure interaction, are often criticized as inadequate representations of the actual loading and structural response. Further research in these areas will undoubtedly be useful in gaining a more thorough knowledge of the dynamic response of such structures. At the same time, it is not clear that more sophisticated analyses will result in designs which, from the economic standpoint, will more nearly approach the optimum. Some thought might now be given to analyzing the same structure by means of two methods, one similar to that employed herein and a second which would apply rigorous analytical and cost optimization techniques. By this process, some quantitative appraisal could be made of the expectation of achieving further significant design and cost improvement for the fully-buried shelter.

BIBLIOGRAPHY

1. Havers, J. A., "Structural Materials for Hardened Personnel Shelters," Contract OCD-PS-62-66, Subtask 1151A, Prepared for the Department of Defense, Office of Civil Defense, by the IIT Research Institute, Chicago, Illinois, December 1963.
2. Havers, J. A. and Lukes, J. J., "Structural Cost Studies for Hardened Shelters," Contract OCD-PS-64-50, Subtask 1152E, Prepared for the Department of Defense, Office of Civil Defense, IIT Research Institute, Chicago, Illinois, January 1965.
3. _____, "Design of Entrance Systems," Prepared for U. S. Naval Civil Engineering Laboratory, Port Hueneme, California, by Armour Research Foundation, Chicago, Illinois, December 1959.
4. Newmark, N. M., "Design of Openings for Buried Shelters," Prepared under Contract No. DA-22-079-eng-225, OCD Subtask 1122A, U. S. Army Engineer Waterways Experiment Station, Corps of Engineers, Vicksburg, Mississippi, July 1963 (with corrections dated June 1964).
5. Merritt, J. L. and Newmark, N. M., "Design of Underground Structures to Resist Nuclear Blast," Vol. 2, Final Report, Contract No. DA-29-129-eng-312, University of Illinois for Office of Chief of Engineers, U. S. Army, Washington, D. C., April 1958.
6. Glasstone, S. (Editor), "The Effects of Nuclear Weapons," Prepared by the U. S. Department of Defense, published by the U. S. Atomic Energy Commission, Superintendent of Documents, Washington, D. C., April 1962.
7. Godfrey, R. S. (Editor), "Building Construction Cost Data," 1962, R. S. Means Company, Duxbury, Massachusetts, 1962.
8. _____, "Engineering News-Record," (Quarterly summaries of construction costs), McGraw Hill Book Company, Inc., 1962-63.
9. Pulver, H. E., "Construction Estimates and Costs," 3rd Edition, McGraw Hill Book Company, Inc., 1960.
10. Peurifoy, R. L., "Estimating Construction Costs," 2nd Edition, McGraw Hill Book Company, Inc., 1958.
11. _____, "Manual of Steel Construction," 6th Edition, American Institute of Steel Construction, New York, 1963.
12. Manjoine, M. J., "Influence of Rate of Strain and Temperature on Yield Stress of Mild Steel," Journal of Applied Mechanics, Vol. 11, No. 4, December 1944.

IIT RESEARCH INSTITUTE

BIBLIOGRAPHY (Cont'd)

13. Fry, L. H., "Speed in Tension Testing and Its Influence of Yield Point Values," ASTM Proceedings, Vol. 40, 1940.
14. Norris, C. H., Hansen, R. J., et al, "Structural Design for Dynamic Loads," McGraw Hill Book Company, Inc., 1959.
15. Newmark, Hansen and Associates, "Protective Construction Review Guide," Vol. 1, Contract No. SD-52-prepared by the Office of the Assistant Secretary of Defense, Washington, D. C., June 1961.
16. Newmark, N. M. and Hiltiwanger, J. D., "Principles and Practices for Design of Hardened Structures," Contract No. AF29 (601)-2390, Project No. 1080, Task No. 10802, University of Illinois for Research Directorate, Air Force Special Weapons Center, Kirtland Air Force Base, New Mexico, December 1962.
17. _____, "High Strength Steel Concrete Reinforcing Base," American Iron and Steel Institute. New York, 1961.
18. _____, "Tension Materials for Prestressed Concrete," Construction Materials Division, John A. Roebling's Sons Division, The Colorado Fuel and Iron Corporation, Trenton, New Jersey, 1957.
19. _____, "Stressteel Post-Tensioning," Stressteel Corporation, Wilkes-Barre, Pennsylvania. 1963.
20. _____, "Building Code Requirements for Reinforced Concrete," ACI 318-63.
21. Walstein, D., "Properties of Concrete at High Rates of Loading," Symposium on Impact Testing, ASTM Special Technical Publication No. 76, 1938.
22. _____, National Fire Codes, Vol. 4. Building Construction and Facilities, National Fire Protection Association, Boston, Massachusetts 1963-64.
23. "Design of Structures to Resist Nuclear Weapons Effects," ASCE Manual of Engineering Practice No. 42, American Society of Civil Engineers, New York, New York, 1961.
24. _____, "Design of Structures to Resist the Effects of Atomic Weapons," Corps of Engineers, E. M. 1110-345-413 through 421, Superintendent of Documents, Washington, D. C.
25. Richie, R. H. and Hurst, G. D., "Penetration of Weapon Radiation: Application to the Hiroshima-Nagasaki Studies," Health Physics, Vol. 4, March 1959.

BIBLIOGRAPHY (Cont'd)

26. French, R. L. and Wells, M. B., "Calculations of the Spatial Energy and Angular Distributions of Weapons Radiation," Proceedings of NRDL-OCD Shielding Symposium, Report No. 110, U. S. Naval Radiological Defense Laboratory, San Francisco, 1960.
27. Kirn, F. S., Kennedy, R. J., and Wychaff, H. O., Radiology 63, 94, 1954.
28. Chilton, A. B., "Progress in Radiation Shielding Research for Prospective Shelters," Technical Note N-385, U. S. Naval Civil Engineering Laboratory, Port Hueneme, California, June 1960.
29. Spielberg, D. and Duneer, A., "Dose Attenuation by Soils and Concrete for Broad, Parallel-Beam Neutron Sources," AN-108, Prepared for U. S. Naval Civil Engineering Research and Evaluation Laboratory by Associated Nucleonics, Inc., Garden City, New York, May 1958.
30. _____, "Design and Review of Structures for Protection from Fallout Gamma Radiation, Office of Civil Defense, Revised 1 October 1961.
31. Terrell, C. W. and Jerri, A. J., "Radiation Streaming in Shelter Entranceways," Armour Research Foundation Report ARF 1158401-5, July 1961.
32. Seely, F. B. and Smith, J. O., "Advanced Mechanics of Materials," 2nd Edition, John Wiley and Sons, Inc., New York, 1952.
33. Roark, R. J., "Formulas for Stress and Strain," 3rd Edition, McGraw Hill and Company, Inc., New York, 1954.
34. Flugge, W., "Stresses in Shells," Springer, Verlag, Germany, 1960.
35. Vlasov, V. Z., "General Theory of Shells and Its Applications in Engineering," NASA Technical Translation, NASA TT F-99, National Aeronautics and Space Administration, Washington, 1954.
36. Timoshenko, S., "Theory of Plates and Shells," McGraw Hill Book Company, Inc., New York, 1960.
37. Cowan, H. J., "Design of Beams Subject to Torsion Related to the New Australian Code," Proceedings of the American Concrete Institute, Vol. 56, p. 591-618, January 1960.
38. Jones, L. L., "Ultimate Load Analysis of Reinforced and Prestressed Concrete Structures," John Wiley and Sons, Inc., New York, 1962.
39. Wood, R. H., "Plastic and Elastic Design of Slabs and Plates," Ronald Press Company, New York, 1961.

Unclassified

Security Classification

DOCUMENT CONTROL DATA - R&D

(Security classification of title, body of abstract and indexing annotation must be entered when the overall report is classified)

1. ORIGINATING ACTIVITY (Corporate author) IIT Research Institute 10 W. 35th Street Chicago, Illinois 60616		2a. REPORT SECURITY CLASSIFICATION Unclassified	
		2b. GROUP (Not applicable)	
3. REPORT TITLE ENTRANCEWAYS AND EXITS FOR BLAST-RESISTANT FULLY-BURIED PERSONNEL SHELTERS			
4. DESCRIPTIVE NOTES (Type of report and inclusive dates) FINAL REPORT (3)			
5. AUTHOR(S) (Last name, first name, initial) Stevenson, John D. Havers, John A.			
6. REPORT DATE September 1965		7a. TOTAL NO. OF PAGES 335	7b. NO. OF REFS 39
8a. CONTRACT OR GRANT NO. OCD-PS-64-50 Subtask 1152E		9a. ORIGINATOR'S REPORT NUMBER(S) M6064(3)	
b. PROJECT NO. M6064			
c.		9b. OTHER REPORT NO(S) (Any other numbers that may be assigned this report)	
d.			
10. AVAILABILITY/LIMITATION NOTICES Distribution of this document is unlimited.			
11. SUPPLEMENTARY NOTES		12. SPONSORING MILITARY ACTIVITY Office of Civil Defense Dept. of the ARMY OSA	
13. ABSTRACT <p>The work reported in this study is a continuation of the Total Shelter Design Optimization series which, under OCD sponsorship, is currently in progress at the IIT Research Institute. These studies have developed the design requirements and identified in-place costs for single-purpose, fully-buried personnel shelters of 100, 500, and 1000-man capacities. The attack environment, for analytical purposes, is described by a megaton (W = 1 to 100 MT) nuclear explosion and by side-on surface overpressures of 10 to 200 psi. Reports issued to date in this series have included the following:</p> <ol style="list-style-type: none">(1) "Structural Materials for Hardened Personnel Shelters," by John A. Havers, Contract No. OCD-PS-62-66, Subtask 1151-A, IIT Research Institute, December 1963.(2) "Structural Cost Studies for Hardened Shelters," by John A. Havers and Jerry J. Lukes, Contract No. OCD-PS-64-50, Subtask 1152-E, IIT Research Institute, January 1965.(3) "Entranceways and Exits for Blast-Resistant Fully-Buried Personnel Shelters," by John D. Stevenson, and John A. Havers, Contract No. OCD-PS-64-50, Subtask 1152-E, IIT Research Institute, May 1965(draft).(4) "An Investigation of Minimal Equipment Needs in Personnel Shelters," by John A. Havers, Claire B. Monk, Jr. and Erich H. Koeller, Contract No. OCD-PS-64-50, Subtask 1216-A, May 1965 (draft). <p>By combining the findings of these separate studies, it is possible to perform rapid evaluations of specific attack environments, composite performance requirements, alternative analytical solutions and estimated in-place costs as a basis for the preliminary design of this particular type of shelter. It is found that structural per-occupant costs are strongly related to the design capacity of the shelter, and exhibit a decrease as the shelter capacity is increased. The structural costs are also found to increase with increasing levels of design overpressure, although this latter correlation becomes decidedly weaker as the overpressure level is increased.</p>			

14. KEY WORDS	LINK A		LINK B		LINK C	
	ROLE	WT	ROLE	WT	ROLE	WT

INSTRUCTIONS

1. **ORIGINATING ACTIVITY:** Enter the name and address of the contractor, subcontractor, grantee, Department of Defense activity or other organization (*corporate author*) issuing the report.

2a. **REPORT SECURITY CLASSIFICATION:** Enter the overall security classification of the report. Indicate whether "Restricted Data" is included. Marking is to be in accordance with appropriate security regulations.

2b. **GROUP:** Automatic downgrading is specified in DoD Directive 5200.10 and Armed Forces Industrial Manual. Enter the group number. Also, when applicable, show that optional markings have been used for Group 3 and Group 4 as authorized.

3. **REPORT TITLE:** Enter the complete report title in all capital letters. Titles in all cases should be unclassified. If a meaningful title cannot be selected without classification, show title classification in all capitals in parenthesis immediately following the title.

4. **DESCRIPTIVE NOTES:** If appropriate, enter the type of report, e.g., interim, progress, summary, annual, or final. Give the inclusive dates when a specific reporting period is covered.

5. **AUTHOR(S):** Enter the name(s) of author(s) as shown on or in the report. Enter last name, first name, middle initial. If military, show rank and branch of service. The name of the principal author is an absolute minimum requirement.

6. **REPORT DATE:** Enter the date of the report as day, month, year, or month, year. If more than one date appears on the report, use date of publication.

7a. **TOTAL NUMBER OF PAGES:** The total page count should follow normal pagination procedures, i.e., enter the number of pages containing information.

7b. **NUMBER OF REFERENCES:** Enter the total number of references cited in the report.

8a. **CONTRACT OR GRANT NUMBER:** If appropriate, enter the applicable number of the contract or grant under which the report was written.

8b, 8c, & 8d. **PROJECT NUMBER:** Enter the appropriate military department identification, such as project number, subproject number, system numbers, task number, etc.

9a. **ORIGINATOR'S REPORT NUMBER(S):** Enter the official report number by which the document will be identified and controlled by the originating activity. This number must be unique to this report.

9b. **OTHER REPORT NUMBER(S):** If the report has been assigned any other report numbers (*either by the originator or by the sponsor*), also enter this number(s).

10. **AVAILABILITY/LIMITATION NOTICES:** Enter any limitations on further dissemination of the report, other than those imposed by security classification, using standard statements such as:

- (1) "Qualified requesters may obtain copies of this report from DDC."
- (2) "Foreign announcement and dissemination of this report by DDC is not authorized."
- (3) "U. S. Government agencies may obtain copies of this report directly from DDC. Other qualified DDC users shall request through _____."
- (4) "U. S. military agencies may obtain copies of this report directly from DDC. Other qualified users shall request through _____."
- (5) "All distribution of this report is controlled. Qualified DDC users shall request through _____."

If the report has been furnished to the Office of Technical Services, Department of Commerce, for sale to the public, indicate this fact and enter the price, if known.

11. **SUPPLEMENTARY NOTES:** Use for additional explanatory notes.

12. **SPONSORING MILITARY ACTIVITY:** Enter the name of the departmental project office or laboratory sponsoring (*paying for*) the research and development. Include address.

13. **ABSTRACT:** Enter an abstract giving a brief and factual summary of the document indicative of the report, even though it may also appear elsewhere in the body of the technical report. If additional space is required, a continuation sheet shall be attached.

It is highly desirable that the abstract of classified reports be unclassified. Each paragraph of the abstract shall end with an indication of the military security classification of the information in the paragraph, represented as (TS), (S), (C), or (U).

There is no limitation on the length of the abstract. However, the suggested length is from 150 to 225 words.

14. **KEY WORDS:** Key words are technically meaningful terms or short phrases that characterize a report and may be used as index entries for cataloging the report. Key words must be selected so that no security classification is required. Identifiers, such as equipment model designation, trade name, military project code name, geographic location, may be used as key words but will be followed by an indication of technical context. The assignment of links, rules, and weights is optional.